BEST AVAILABLE IMAGES

Defective images within this document are accurate representations of the original documents submitted by the applicant.

Defects in the images may include (but are not limited to):

- BLACK BORDERS
- TEXT CUT OFF AT TOP, BOTTOM OR SIDES
- FADED TEXT
- ILLEGIBLE TEXT
- SKEWED/SLANTED IMAGES
- COLORED PHOTOS
- BLACK OR VERY BLACK AND WHITE DARK PHOTOS
- GRAY SCALE DOCUMENTS

IMAGES ARE BEST AVAILABLE COPY.

As rescanning documents *will not* correct images, please do not report the images to the Image Problem Mailbox.

0021-972X/97/$03.00/0
Journal of Clinical Endocrinology and Metabolism

Vol. 82, No. 5
Printed in U.S.A.

Cytochrome P450 1A2 Is a Hepatic Autoantigen in Autoimmune Polyglandular Syndrome Type 1*

MARIA GRAZIA CLEMENTE, PETRA OBERMAYER-STRAUB, ANTONELLA MELONI, CHRISTIAN P. STRASSBURG, VINCENZO ARANGINO, ROBERT H. TUKEY, STEFANO DE VIRGILIIS, AND MICHAEL P. MANNS

Department of Gastroenterology and Hepatology (M.G.C., P.O.-S., C.P.S., M.P.M.), Hannover Medical School, 30625 Hannover, Germany; Institute of Clinica e Biologia dell'eta evolutiva (M.G.C., A.M., S.D.V.), Universita degli Studi di Cagliari, Cagliari, Italy 09121; Patologia Medica II (V.A.), Universita degli Studi di Cagliari, Cagliari, Italy; and University of California at San Diego Cancer Center (R.H.T.), Department of Medicine and Pharmacology, San Diego, La Jolla, California 92093

ABSTRACT

Autoantibodies directed against proteins of the adrenal cortex and the liver were studied in 88 subjects of Sardinian descent, namely six patients with autoimmune polyendocrine syndrome type 1 (APS1), 22 relatives of APS1 patients, 40 controls with other autoimmune diseases, and 20 healthy controls. Indirect immunofluorescence, using tissue sections of the adrenal cortex, revealed a cytoplasmatic staining pattern in 4 of 6 patients with APS1. Western blotting with adrenal mitochondria identified autoantigens of 54 kDa and 57 kDa. Western blotting with placental mitochondria revealed a 54-kDa autoantigen. The 54-kDa protein was recognized by 4 of 6 patients with APS1 both in placental and adrenal tissue, whereas the 57-kDa protein was detected only by one serum. Using recombinant preparations of cytochrome P450 proteins, the autoantigens were identified as P450 scc and P450 c17.

One of six APS1 patients suffered from chronic hepatitis. In this patient, immunofluorescence revealed a centrolobular liver and a proximal renal tubule staining pattern. Western blots using microsomal preparations of human liver revealed a protein band of 52 kDa. The autoantigen was identified as cytochrome P450 1A2 by use of recombinant protein preparations. P450 1A2 represents the first hepatic autoantigen reported in APS1. P450 1A2 usually is not detected by sera of patients with isolated autoimmune liver disease and might be a hepatic marker autoantigen for patients with APS1. (*J Clin Endocrinol Metab* 82: 1353–1361, 1997)

AUTOIMMUNE polyendocrine syndrome type 1 (APS1) is a rare autosomal recessive disorder characterized by a variable combination of disease components (1–3). The first clinical manifestation of APS1 usually occurs in childhood, and progressively new components appear throughout life, the majority (63%) of the patients suffering from three to five of them (2). The most frequent components in APS1 are chronic mucocutaneous candidiasis, hypoparathyroidism, adrenocortical failure, and gonadal failure in females (2, 3). Hepatitis is a serious, but less frequent, disease component (1–3). Defects in immunoregulation were suggested to play a role in the disease mechanism, and the presence of organ-specific autoantibodies was demonstrated repeatedly (4–12; also see Ref. 14)

Recently, progress was made in the study of APS1-related Addison's disease, which affects more than 60% of APS1 patients (1–3). Adrenal autoantigens in APS1 are cytochromes P450 c17, P450 scc, and P450 c21, which are all enzymes involved in steroidogenesis (5–13). P450 c21 is reported to be present in the adrenal cortex; expression of P450 c17 is found in adrenal tissue and steroid-producing cells of testis and ovary; and P450 scc is expressed in adrenals, gonads, and placenta (8). It was shown previously that autoantibodies directed against the adrenal cortex alone correlate with a high risk of adrenocortical failure, and antibodies directed against steroidal cells in females, in addition, correlate with a high risk of ovarian failure (14).

Chronic hepatitis is a serious disease component present in 10–18% of patients with APS1 (1–3), and occasional deaths related to hepatitis are reported in APS1 (2, 15). However, hepatitis as a disease component of APS1 still is poorly investigated. Autoantibodies associated with autoimmune hepatitis as part of APS1 were not described before, and the corresponding antigens accordingly remained unidentified.

Here we report the characterization of six patients with APS1 and confirm P450 scc and P450 c17 as adrenal autoantigens in APS1 in patients from Sardinia. We present the first characterization of hepatic autoantibodies in patients with APS1 and the molecular identification of a hepatic autoantigen in APS 1. The molecular target, cytochrome P450 1A2, is different from the targets of LKM1 and LKM3 autoantibodies that are found in autoimmune hepatitis type 2. Potential diagnostic consequences of this finding are discussed.

Subjects and Methods

Patients

We studied six patients with APS1 (Table 1). Patient 1 suffered from liver disease. Patient 1 is female and lacks markers for hepatitis B, C, and

Received November 21, 1995. Revision received May 9, 1996. Rerevision received December 20, 1996. Accepted January 31, 1997.

Address all correspondence and requests for reprints to: Prof. M. P. Manns, Department of Gastroenterology and Hepatology, Hannover Medical School Carl-Neuberg Strasse 30625 Hannover, Germany.

* This work was supported by Grant SFB 244 of the Deutsche Forschungsgemeinschaft and USPHS Grant GM-49135 (to R.H.T.).

D viruses and HIV. Serum ceruloplasmin and α-1 antitrypsin levels are normal. She presented at the clinic at the age of 6 yr with acute hepatitis that subsequently turned chronic. Four years after the onset of hepatitis, she developed adrenal failure and chronic mucocutaneous candidiasis. A percutaneous liver biopsy revealed the histologic picture of chronic active hepatitis.

We also studied sera of 22 first-degree relatives of APS1 patients, of 40 patients with other autoimmune diseases (namely 1 with isolated Addison's disease, 10 with Hashimoto disease, 10 with insulin-dependent diabetes mellitus (IDDM), 3 with IDDM and celiac disease, 4 with autoimmune hepatitis type 1 and type 2, 10 with chronic hepatitis C virus, 1 with primary billiary cirrhosis, 1 with systemic lupus erythematosus) and of 20 healthy controls (Table 2). All subjects were of Sardinian descent. As shown in Fig. 1, the 6 APS1 patients belong to 5 different families. In family 3 and in family 5, 1 sister affected by APS1 died of acute adrenal failure (at 8 yr old and 15 yr old, respectively). None of the other 22 relatives had evidence of an autoimmune disorder.

Materials

Human liver tissue was obtained during liver transplantation from a patient's liver that was removed because of hepatocellular carcinoma. The tissue otherwise would have been discarded.

For the immunofluorescence studies, a goat antihuman IgM, IgG, IgA polyclonal FITC-conjugated antiserum was used (Dianova, Hamburg, Germany). The antibody used for Western blots was an alkaline phosphatase conjugated anti-IgG, IgA, and IgM antiserum (Dianova). The complementary DNA (cDNA) construct pBS/1A2, used for subcloning the cDNA of P450 1A2, was provided by one of us (R. H. Tukey, UC San Diego). The cDNA constructs, pUC18-scc and PUC 18-c17, containing the cDNAs of P450 scc and P450 c17, were a kind gift of Walter Miller, UC San Francisco (16, 17). The DH5α FIQ cells were from GIBCO-BRL (Eggenstein, Germany).

Nitro blue tetrazolium chloride/5-bromo-chloro-3 indolyl phosphate substrates and isopropylthiogalactoside (IPTG) for bacterial induction were from Promega (Madison, WI). Vectors for the expression of bacterial proteins were from the pQE 30 series of Quiagen (Hilden, Ger-

TABLE 1. Disease components and analytical results of six patients with APS1

Patients	Disease components in APS1	IF Adrenals (Human)	WB Adrenal mitoch. (Human)	WB Placental mitoch. (Human)	WB P450 scc	WB P450 c17	IF Liver (Rat)	IF Kidney (Rat)	WB Liver micros. (Human)	WB P4501A2
Patient 1	M. candidiasis Addison's disease (11) Chronic hepatitis (15) Pernicious anemia	1:40	54 kD	54 kD	+		1:1000	1:320	52 kD	+
Patient 2	M. candidiasis Hypoparathyroidism Addison's disease (8)	1:1000	54 kD 57 kD	54 kD	+	+				
Patient 3	Hypoparathyroidism									
Patient 4	M. candidiasis Hypoparathyroidism Addison's disease (7) Fat malabsorption Polyneuropathy	1:1000	54 kD	54 kD	+					
Patient 5	M. candidiasis Hypoparathyroidism Addison's disease (19) Pernicious anemia	1:40	54 kD	54 kD	+					
Patient 6	M. candidiasis Hypoparathyroidism Addison's disease (7)									

Listed in parentheses in the column of disease components is the time interval between the first occurrence of chronic active hepatitis or Addison's disease and the time point of blood sampling. M. candidiasis, mucocutaneous candidiasis; IF, indirect immunofluorescence; WB, Western blot.

TABLE 2. Diseases and analytical results of the control subjects

	Addison's disease	IDDM	IDDM & celiac disease	Hashimoto's disease	AIH	HCV	PBC	SLE	APS1 Relatives	Healthy controls
No. subjects	1	10	3	10	4	10	1	1	22	20
IF/WB human adrenals										
IF rat liver/kidney										
LKM					2	2				
SMA (F-actin)					2					
ANA				8	1	5		1		
AMA							1			
WB human liver microsomes:										
LKM (50 kDa)					1	2				
LKM (50 kDa + 68 kDa)					1					
WB—P450 c17										
WB—P450 scc										
WB – P450 1A2										

IDDM, Insulin-dependent diabetes mellitus; AIH, autoimmune hepatitis; HCV, hepatitis C virus; PBC, primary biliary cirrhosis; SLE, systemic lupus erythematosus; IF, indirect immunofluorescence; WB, Western blot; LKM, liver kidney microsomal autoantibodies; SMA, smooth muscle antibodies; ANA, antinuclear antibodies; AMA, antimitochondrial antibodies.

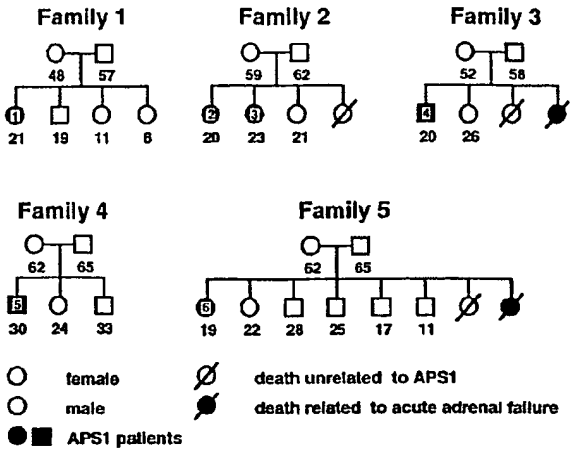

FIG. 1. Families of the APS1 patients studied. The *number below* each *symbol* indicates the age in years. *Numbers in a black square* or *circle* indicate the number for this APS1 patient used in this paper. The dead relatives of APS1 patients are not included in this study.

many). Restriction enzymes were purchased from New England Biolabs (Schwalbach/Taunus, Germany), and the sequencing kit was from Pharmacia (Freiburg, Germany). All other chemicals used were of the highest degree available and purchased from Sigma (Heidelberg, Germany).

Methods

Indirect immunofluorescence. Frozen sections of rat liver and kidney and of human adrenals were incubated at room temperature for 30 min with patient sera at dilutions of 1:40, 1:80, 1:160, 1:320, 1:640, and 1:1280 in phosphate buffered saline (PBS). The sections were washed twice in PBS and incubated with a goat antihuman anti-IgM, IgA, and IgG FITC-conjugated antiserum at a dilution of 1:100 in PBS for 30 min at room temperature. The sections were washed twice in PBS and embedded in 90% vol/vol glycerol in PBS. For analysis of the results, we used an Olympus IMT2 microscope (Olympus, Hamburg, Germany) fitted with an Olympus SC 35 type 12 camera.

Antigen preparations. One gram of frozen tissue was homogenized with 20 strokes of a homogenisator in 3 mL ice-cold solution of 0.25 mol/L sucrose containing 0.1 mmol/L phenylmethylsulfonylfluoride. Cellular debris and nuclei were removed by centrifugation (Sigma SK15 centrifuge, 1000 × *g*, 4 C, 15 min). The supernatant was fractionated by centrifugation (Sigma SK15 centrifuge, 3000 × *g*, 4 C, 15 min) into a mitochondrial pellet and the supernatant containing microsomes and the soluble liver proteins.

Mitochondrial preparation. For mitochondrial preparations, the pellet was resuspended in the sucrose solution, and the mitochondria were washed three times, as described above. The washed pellet was frozen on dry ice and stored at −80 C. The resulting fraction is enriched in mitochondria.

Microsomal preparation. The supernatant containing microsomes and soluble liver proteins was subjected to ultracentrifugation (Beckman ultracentrifuge, TLA 100 rotor, 100,000 × *g*, 4 C, 1 h). The supernatant was discarded, and the microsomal pellet was resuspended in 0.5 ml sucrose solution. The subcellular fractions were frozen on dry ice and stored at −80 C. The resulting preparation is enriched in microsomal proteins.

Western blotting. Fifty micrograms of tissue antigens and bacterial extracts containing recombinant proteins were separated on a 10% polyacrylamide gel and transferred to nitrocellulose (18, 19). The blots were blocked in PBS containing 0.1% Tween 20 and 5% nonfat dry milk and incubated for 1 h with a 1:100 dilution of the patient's or control sera in PBS-Tween. The blots were then washed three times for 10 min with PBS-Tween and incubated for 1 h with a 1:1000 dilution of an alkaline phosphatase conjugated antihuman IgM, IgA, IgG antiserum in PBS-Tween. After washing three times with PBS-Tween and two times in alkaline phosphatase buffer, the blots were developed using the nitro blue tetrazolium chloride/5-bromo-chloro-3 indolyl phosphate detection system (20).

Cloning and expression of recombinant cytochromes P450s. The primers used for amplification and modification of cytochromes P450 according to Waterman (21) had the following sequences: P450 scc-primers: 5' GTGAGGTACCGCTCTGTTATTAGCAGTTTTTCTGTCAGTCCTGGTCAAAGGCTAC 3' and 5' GCTCAAGCTTTGATCACTGCTGGGTTGCTTC 3'; P450 c17-primers: 5' GTGAGGTACCGCTCTGTTATTAGCAGTTTTTCTGCTTACCCTAGCTTATTTGTTT 3' and 5' GCTCAAGCTTTGATCACTGCTGGGTTGCTTC 3'; P450 1A2-primers: 5' GTGAGGTACCGCTCTGTTATTAGCAGTTTTTCTGTTCTGCCTGGTATTCTGGGTG 3' and 5' GCTCAAGCTTCAATTGATGGAGAACG 3'.

The cDNAs were amplified by the Vent polymerase according to the manufacturers recommendations (New England Biolabs) (Fig. 2A). Denaturation was performed for 1 min at 94 C, annealing for 2 min at 62 C, and the elongation for 3 min at 72 C. Twenty cycles were applied for the amplification of the cDNA, with a final elongation step of 7 min. After PCR, the modified cDNAs were purified by the Quiagen PCR-purification kit, digested with *Hind*III and *Kpn*I, and inserted into the respective restriction sites of the pQE 30 vector. All constructs were confirmed by several restriction digests and by sequence analysis of the N- and C-termini, using the T7 sequencing kit, according to the manufacturer's recommendations. For expression of the recombinant cytochrome P450 proteins, all cDNA-expression vectors were transfected into DH5αFIQ cells. The expression of the recombinant proteins was induced by the addition of IPTG to a final concentration of 2 mmol/L for 3 h after the cells were grown to late-log phase. The cells were harvested by centrifugation, lysed in SDS-sample buffer, and the proteins were analyzed by SDS-PAGE and Western blotting. The expression of cytochrome P450 1A2 was further confirmed by Western blotting using a polyclonal rabbit antihuman P4501A2 antibody that was a kind gift from Prof. P. Beaune of the University of Paris.

Absorption studies. For absorption experiments, all sera were incubated with total proteins from *Escherichia coli* (*E. coli*) cells, carrying the expression vector alone or expressing the recombinant cytochromes P450 c17, P450 scc, or P450 1A2, according to the method described by Uibo *et al.* (8). Experiments of indirect immunofluorescence and immunoblotting (of human adrenal, human liver antigen preparations, and recombinant P450 enzymes) were performed with nonadsorbed and absorbed sera.

Results

Indirect immunofluorescence on human adrenal sections

Indirect immunofluorescence studies of the sera were performed on cryosections of human adrenal tissue (Table 1). Four of six APS1 sera detected tissue antigens in all three layers (zona glomerulosa, the zona fasciculata, and the zona reticularis) of the human adrenal cortex. None of the 82 other sera, including the serum from a patient with idiopathic Addison's disease, recognized adrenal antigens.

Immunoblotting with human adrenal antigens

To further characterize the adrenal autoantigens involved, we prepared mitochondrial subfractions of human adrenal and placental tissues. Western blotting, with patient sera 1, 2, 4, and 5, revealed a protein band at 54 kDa in both tissues (Fig. 3, A and B). In addition to the 54-kDa protein, patient serum no. 2 recognized a second band at 57 kDa in adrenal but not in placental tissue. In contrast, none of the sera from the patients' first-degree relatives, from patients with other autoimmune diseases, or from healthy controls showed pro-

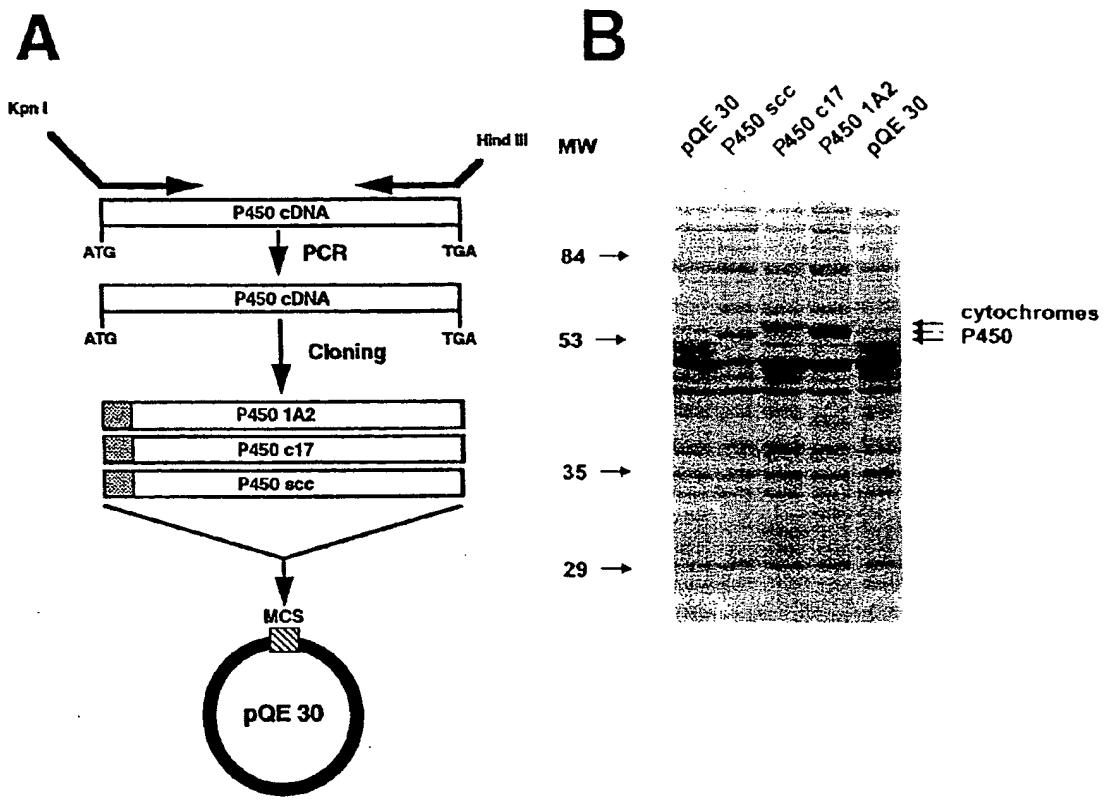

FIG. 2. Expression of recombinant cytochromes P450 scc, P450 c17, and P450 1A2 in *E. coli*. A, Construction of the expression vectors; B, the figure shows a typical result after Coomassie Blue staining of *E. coli* lysates expressing cytochromes P450 1A2, P450 scc, and P450 c17. *Arrows* on the *left* indicate the position of the molecular weight standards, *arrows* on the *right* mark the positions of the recombinant cytochrome P450 proteins.

tein bands at the levels of 54 or 57 kDa (Fig. 3, A and B, Table 2). Also, the serum of the patient with isolated Addison's disease failed to recognize any of these autoantigens. This result is in accordance with the working hypothesis that the autoantigenes recognized in immunofluorescence are the 54-kDa and 57-kDa protein bands found in Western blotting.

Immunoblotting with recombinant cytochromes P450 scc and P450 c17

Bacterial lysates of clones expressing cytochromes P450 scc and P450 c17 were used to test for the presence of autoantibodies directed against these two proteins. Sera 1, 2, 4, and 5, which also reacted with the 54-kDa adrenal and placental autoantigens, recognized the recombinant P450 scc (Fig. 3C). Serum 2, which in addition detected a 57-kDa adrenal antigen, recognized P450 c17 (Fig. 3D). In contrast, none of 82 sera from the patients' first-degree relatives, patients with other autoimmune diseases, and healthy controls recognized P450 scc or P450 c17 (Fig. 3, C and D and Table 2).

Control experiments with lysates from bacteria expressing the empty pQE vector were performed with all patient and control sera, demonstrating the specificity of the reaction by the absence of the specific 54-kDa and 57-kDa bands (data not shown).

Absorption studies were performed with recombinant preparations of P450 scc and P450 c17 (data not shown). As expected, recombinant P450 scc absorbed the bands at 54 kDa and P450 c17 the band at 57 kDa, in Western blots with human adrenal mitochondria, demonstrating the identity of the molecular targets. Interestingly, using P450 scc for absorption, no other signal was left in blots with patient sera 1, 4, and 5, whereas only the 57-kDa band remained in blots using serum 2.

Also, the signals in immunofluorescence could be absorbed by the recombinant preparations of P450 scc and P450 c17, if P450 scc were used for sera 1, 4, and 5 and a combination of P450 scc and P450 c17 was used for patient serum 2 (data not shown). These results clearly demonstrate that the immunofluorescence is caused by autoantibodies directed against cytochromes P450 scc and P450 c17. They further show that no autoantibodies directed against cytochrome P450 c21 are present that would not have been absorbed by the recombinant antigens.

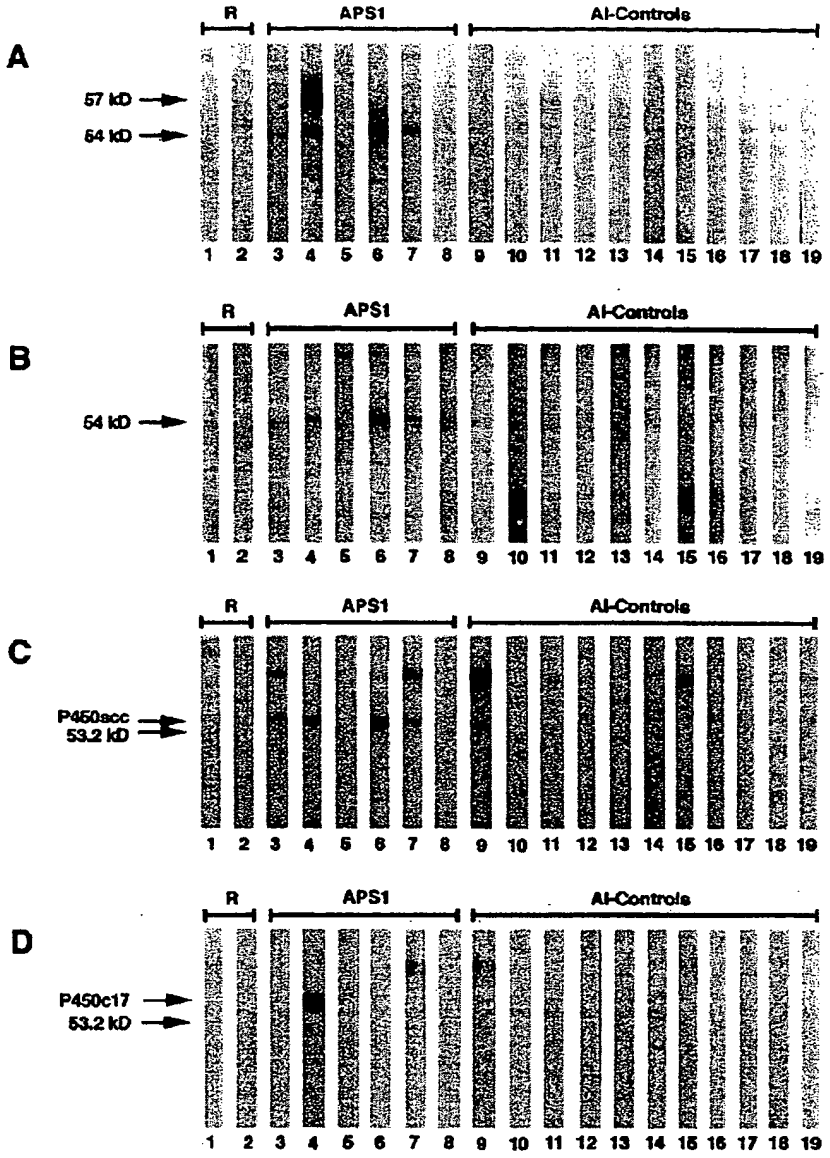

FIG. 3. Western blots with adrenal antigens, placental antigens, and recombinant cytochromes P450 scc and P450 c17. A, Western blots with mitochondrial antigens of human adrenals; B, Western blots with mitochondrial antigens of human placenta; C, Western blots with P450 scc expressed in *E. coli*; D, Western blots with P450 c17 expressed in *E. coli*; Lanes 1 and 2, first-degree APS1 patients' relatives; lanes 3–8, APS1 patients 1–6; lane 9, patient with isolated Addison's disease; lanes 10–12, patients with Hashimoto disease; lane 13, LKM1-positive patient with autoimmune hepatitis; lane 14, LKM1-positive patient with hepatitis C virus; lane 15, patient with primary biliary cirrhosis; lanes 16–18, patients with IDDM and celiac disease; lane 19, patient with systemic lupus eythematosus.

Indirect immunofluorescence on rat liver and kidney sections

To investigate the hepatic autoantigens involved in chronic autoimmune hepatitis associated with APS1, indirect immunofluorescence was performed (Tables 1 and 2). Six out of 88 sera tested revealed immunostaining of liver and kidney sections. These sera were the serum of patient 1, who suffered from chronic hepatitis and APS1, two sera from patients with LKM-1 positive autoimmune hepatitis, two sera from patients with LKM-1 positive hepatitis C, and one serum from a patient with primary biliary cirrhosis, who was positive for antimitochondrial antibodies. The staining pattern of the serum of patient 1 (Fig. 4) was characterized by a predominant staining of the perivenous hepatocytes (titer > 1:1000) and of the proximal renal tubules (titer 1:320). This pattern differs from the homogeneous staining pattern found in patients with isolated autoimmune hepatitis, suggesting that the serum of patient 2 recognizes an autoantigen that is different from LKM1 (anticytochrome P450 2D6) and LKM3 (anti-UDP-glucuronosyltransferase) autoantigenes that were described earlier to be targets for autoimmunity in patients with autoimmune and virus hepatitis (22, 23).

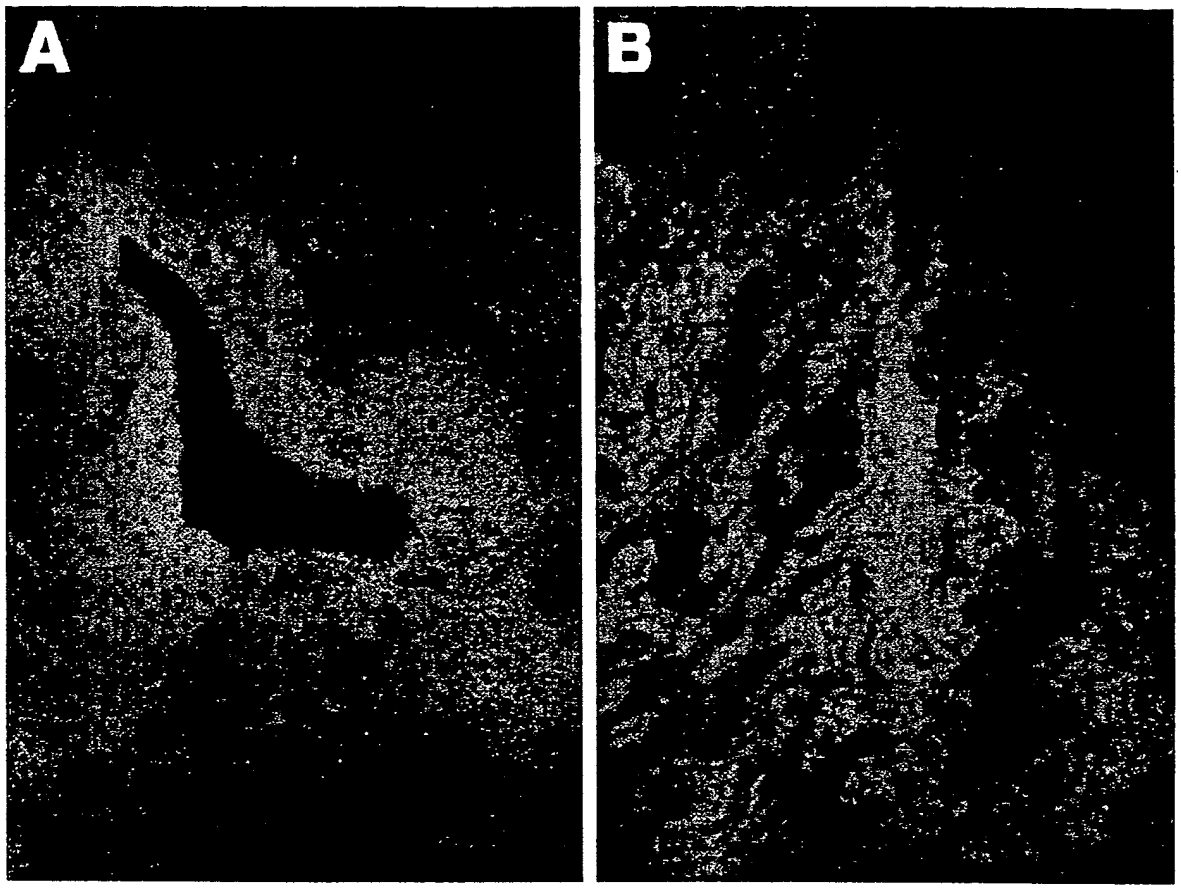

FIG. 4. Indirect immunofluorescence of rat liver and rat kidney sections. Patient serum 2 was diluted 1:320 in PBS, and indirect immunofluorescence was performed on cryosections on rat liver (A) and rat kidney (B). For immunostaining, a goat antihuman anti-IgM, IgA, and IgG FTC-conjugated antiserum was used at a dilution of 1:100.

Immunoblotting with human liver antigens

To further characterize the hepatic antigens involved, the microsomal fraction of human liver tissue was handled under nonreducing conditions and tested by immunoblotting. As shown in Fig. 5A, a protein band of approximately 52 kDa was detected by the serum of patient 1. Bands of 50 kDa and 68 kDa were detected by the LKM1-positive patients, the 50-kDa band representing an autoantibody directed against cytochrome P450 2D6 (22). The patient with PBC shows a band at about 70 kDa, which is caused by a high-titer antimitochondrial antibody produced by this patient.

Immunoblotting with P450 1A2

To identify the hepatic autoantigen recognized by patient 1, we expressed cytochrome P450 1A2 in *E. coli* (Fig. 2). Preparations of the recombinant cytochrome P450 1A2 were used in Western blotting experiments. All of the 88 sera were tested; however, only the serum of patient 1 was positive (Fig. 5B). This result demonstrates that P450 1A2 is an autoantigen in autoimmune hepatitis associated with APS1. To demonstrate the specificity of the reaction, a Western blot of serum 1 was performed, using *E. coli* extracts of clones carrying the empty vector alone, in parallel with preparations containing recombinant P450 1A2. No band appeared in the control extract, whereas a clear signal was visible in the lane containing P450 1A2 (Fig. 5C).

P450 1A2 is expressed in liver, but not in kidney, and therefore, antibodies directed against P450 1A2 were described before as LM autoantibody in patients with dihydralazine-induced hepatitis (24). There are two potential explanations for the renal immunofluorescence pattern. The first explanation consists of a cross-reaction of the autoantibody with a kidney antigen. A cross-reaction also would explain why the signal is only detected at lower serum dilutions. The second explanation is the presence of an unrelated second autoantibody present at a lower titer. To distinguish between these possibilities, absorption studies were performed.

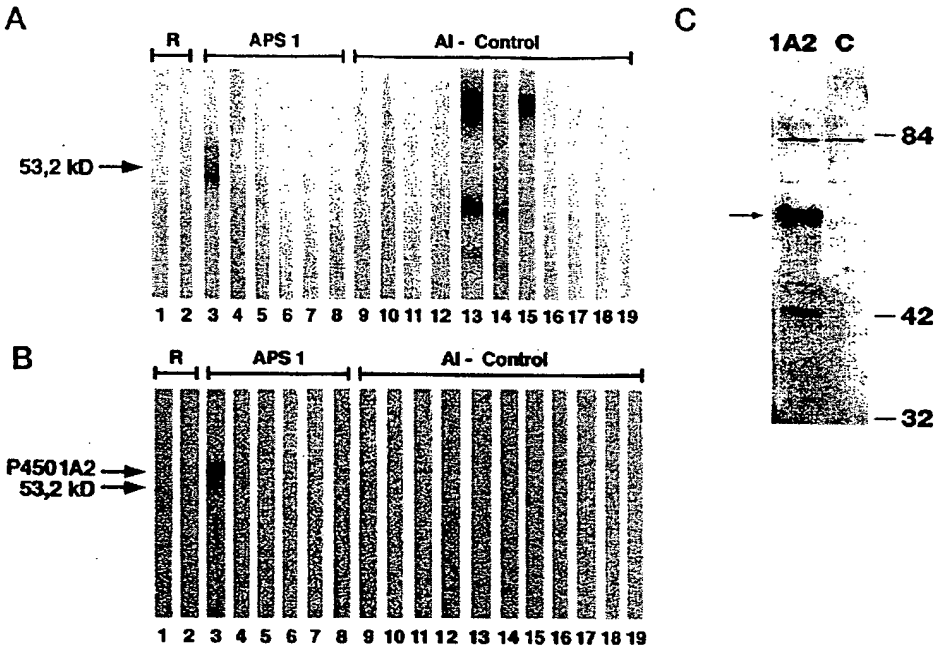

FIG. 5. Western blotting of microsomal antigens of human liver and recombinant P450 1A2. The numbering of patient sera is the same as in Fig. 3, A–C. A, Western blotting of microsomal antigens of human liver; B, Western blotting of a recombinant preparation of P450 1A2. The *arrow* on the *left* indicates the position of the recombinant cytochrome P450 1A2. C, Lysates from cells induced by IPTG carrying the empty vector (control) and expression vector for cytochrome P450 1A2 were analyzed by Western blot using the serum of patient 1, who is suffering fom APS1-related autoimmune hepatitis. The *arrow* on the *left* indicates the position of the recombinant cytochrome P450 1A2, the *arrows* on the *right* indicate the molecular mass in kDa.

Absorption studies

After absorption with preparations of recombinant P450 1A2, the immunofluorescence studies shown in Fig. 4 were repeated (data not shown). In three independent experiments, the immunofluorescence disappeared in liver and in kidney. In control experiments performed with LKM1 positive control sera, the immunofluorescence patterns persisted after absorption with the recombinant P450 1A2.

Figure 6A shows a result after Western blotting with liver microsomes. The serum of patient 1 revealed a clear signal at 52 kDa in a Western blot with liver microsomes before absorption (Fig. 6A, lane 1) the signal almost completely disappeared after absorption with P450 1A2 (Fig. 6A, lane 2). The third lane of Fig. 6A shows that the signals of an LKM1-positive serum that are not related to P450 1A2 persist after absorption with P450 1A2. Figure 6B shows a result after Western blotting using recombinant P450 1A2.

Based on these results, we conclude that the 52-kDa band detected in Western blotting experiments with liver microsomes is caused by an autoantibody directed against P450 1A2. The fact that the immunostaining of kidney sections that was found at lower serum dilutions could be absorbed sug-

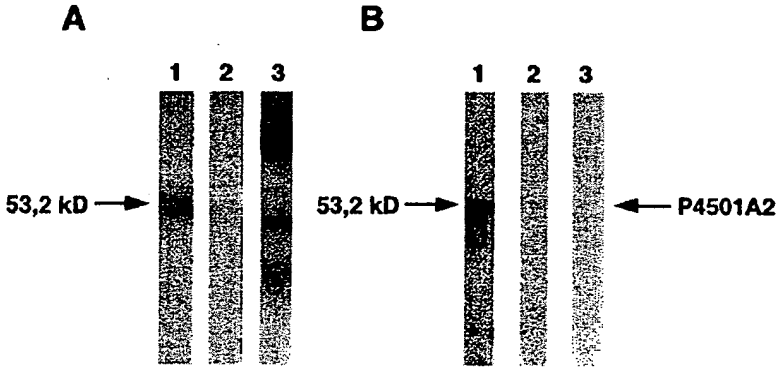

FIG. 6. Absorption experiments with recombinant P450 1A2. A, Immunoblotting using liver microsomes; B, immunoblotting using recombinant P450 1A2; Lane 1, serum of patient 1 before absorption with cytochrome P450 1A2; lane 2, serum of patient 1 after absorption with cytochrome P450 1A2; lane 3, LKM1-positive control serum after absorption with P4501A2.

gests that the autoantibody directed against P450 1A2 shows some cross-reactivity with renal autoantigens.

Discussion

APS1 is characterized by the progressive manifestation of a multitude of endocrine and nonendocrine disease components (1, 2, 3). Frequent disease components, Addison's disease, and premature ovarian failure in females are linked to the presence of adrenal and steroidal cell autoantibodies (9, 14, 25–27). Autoantigens detected by these autoantibodies in APS1 patients are P450 c21, P450 scc, and P450 c17 (5–12). In our study, four of six Sardinian patients with APS1 recognized cytochrome P450 scc, and one patient's serum detected cytochrome P450 c17. This result is in accordance with studies showing that autoantibodies directed against cytochrome P450 scc are produced with a high frequency in Scandinavian patients with APS1 (7, 8, 12); however, other investigators failed to detect autoantibodies directed against P450 scc (10). Differing results also are reported concerning the frequency of detection of P450 c17. Whereas Krohn and his colleges reported the presence of P450 c17 autoantibodies in a substantial fraction of their patients (5, 8, 9), others failed to detect reactivity directed against cytochrome P450 c17 (7, 10, 12). In our study, we confirm that cytochrome P450 c17 is recognized by sera from patients with APS1, albeit at a lower frequency than P450 scc. The identification of the autoantigens was based on apparent molecular weight in SDS-PAGE and on the use of recombinant preparations expressed in *E. coli* (Fig. 3, A–D). There also is some disagreement as to whether P450 c21 is an autoantigen in APS1. Although Uibo *et al.* (8) report P450 c21 being an autoantigen in 15/50 patients with APS1, Winqvist *et al.* (7, 12) failed to detect this autoantibody in APS1. In our group of six patients with APS1, we also did not detect other adrenal autoantigens than P450 scc and P450 c17.

The most important aspect of this paper, however, is the detection and identification of a hepatic autoantigen in patients with APS1. Ten to eighteen percent of APS1 patients develop chronic hepatitis (1–3), and occasionally, patients are reported to have died within only a few days from hepatitis, which occurred unexpectedly and without signs of prewarning (2, 15). However, in contrast to the wealth of information collected by the researchers working on adrenal and gonadal failure in APS1, very little is known about hepatitis as a disease component in APS1. Here we report for the first time the characterization of hepatic autoantigens and the identification of cytochrome P450 1A2 as hepatic autoantigen in APS1. The identification of the autoantigen was facilitated by an immunofluorescence pattern that was different from the patterns resulting from LKM1 and LKM3 autoantibodies. When Western blots were performed with rat microsomes, we failed to detect a specific protein recognized by the antiserum (data not shown). However, using human liver microsomes, a protein band of 52 kDa appeared. This is in accordance with observations published by P. Beaune and his colleges (24), who identified cytochrome P450 1A2 as hepatic autoantigen in dihydralazine hepatitis. In addition, control experiments with intestinal microsomes were performed (data not shown), demonstrating by the absence of the 52-kDa signal that an organ specific autoantigen is detected by the serum of patient 1. To prove that cytochrome P450 1A2 also is an autoantigen in APS1, P450 1A2 was expressed in *E. coli*. The serum not only specifically recognized cytochrome P450 1A2 in Western blot experiments, but absorption with recombinant P450 1A2 resulted in a complete disappearance of the immunofluorescence pattern and the reactivity in Western blots with human liver microsomes. At lower dilutions of the serum, immunofluorescence also was detected in kidney sections, in spite of the fact that P450 1A2 is not expressed in kidney. This result seems to be caused by a cross-reaction of the antibody, because the renal immunofluorescence also could be absorbed with the recombinant cytochrome P450 1A2.

Cytochrome P450 1A2 was described earlier by our group as autoantigen in an unusual case of autoimmune hepatitis (28, 29). This patient suffered from vitiligo, alopecia, and nail dystrophy and had a brother who had died from Addison's disease at the age of 8 yr. We now believe that in accordance with the criteria for diagnosis of APS1 from Neufeld (1), this patient also suffered from APS1. Adding the present patient to that previous one, we now have two patients on record suffering from autoimmune hepatitis in APS1 with cytochrome P450 1A2 as hepatic autoantigen.

Extensive control studies were performed. A total of 40 patient sera with other autoimmune diseases and 22 first-degree relatives of the patients were tested for autoantibodies directed against hepatic antigens and cytochrome P450 1A2. However, only patient serum 1 and 4 sera from patients with other liver diseases reacted with human hepatic microsomes (Fig. 5, Tables 1, 2). When extracts of expression clones containing the recombinant P450 1A2 were used, reaction of only patient serum 1 was detected, showing that the detection of the hepatic autoantibodies and P450 1A2 did not represent false positive results caused by elevated IgG-levels that are typical for patients with autoimmune diseases. Most patients with autoimmune hepatitis type 2 recognize P450 2D6, and about 10% recognize UGT 1 proteins. Of 15 German patients with autoimmune hepatitis type 2, none was found to recognize cytochrome P450 1A2 (data not shown). Determination of the exact molecular target of autoimmunity in patients with autoimmune hepatitis could help to distinguish patients with autoimmune hepatitis-2 from patients with hepatitis in APS1. The later patients should be closely monitored for the development of further disease manifestations.

Acknowledgments

We thank Prof. W. Miller for providing the cDNAs for P450 scc and P450 c17. We also thank Dr. B. Lüttig, S. Loges, and E. Schmidt for their help in the indirect immunofluorescence studies of the patient sera used in this work.

References

1. Neufeld M, Maclaren N, Blizzard R. 1980 Autoimmune polyglandular syndromes. Pediatr Ann. 9:154–162.
2. Ahonen P, Myllärniemi S, Sipilä I, Perheentupa J. 1990 Clinical variation of autoimmune polyendocrinopathy-candidiasis-ectodermal dystrophy (APECED) in a series of 68 patients. N Engl J Med. 322:1829–1836.
3. Riley WJ. 1992 Autoimmune polyglandular syndromes. Horm Res. [Suppl 38]2:9–15.
4. Arulantham K, Dwyer JM, Genel M. 1979 Evidence for defective immuno-

regulation in the syndrome of familial candidiasis endocrinopathy. N Engl J Med. 300:164–168.
5. Krohn K, Uibo R, Aavik E, Peterson P, Savilahti K. 1992 Identification by molecular cloning of an autoantigen associated with Addison's disease as steroid 17α-hydroxylase. Lancet. 339:770–773.
6. Winqvist O, Karlsson FA, Kämpe O. 1992 21-hydroxylase, a major autoantigen in idiopathic Addison's disease. Lancet. 339:1559–1562.
7. Winqvist O, Gustafsson J, Rorsman F, Karlsson F, Kampe O. 1994 Two different cytochrome P450 enzymes are the adrenal antigens in autoimmune polyendocrine syndrome type 1 and Addison's disease. J Clin Invest. 92:2377–2385.
8. Uibo R, Aavik E, Peterson P, Perheentupa J, Aranko S, Pelkonen R, Krohn K. 1994 Autoantibodies to cytochrome P450 enzymes P450 scc, P450 c17 and P450 c21 in autoimmune polyglandular diseases types I and II and in isolated Addison's disease. J Clin Endocrinol Metab. 78:323–328.
9. Uibo R, Perheentupa J, Ovod V, Krohn KJE. 1994 Characterization of adrenal autoantigens recognized by serta from patients with autoimmune polyglandular syndrome (APS) type 1. J Autoimmun. 7:399–411.
10. Song YH, Connor EL, Muir A, et al. 1994 Autoantibody epitope mapping in autoimmune Addison's disease. J Clin Endocrinol Metab. 78:1108–1112.
11. Peterson P, Krohn JE. 1994 Mapping of B cell epitopes on steroid 17a-hydroxylase, an autoantigen in autoimmune polyglandular syndrome type I. Clin Exp Immunol. 98:104–109.
12. Winqvist O, Gebre-Mehedin G, Gustafsson J, et al. 1995 Identification of the main gonadal autoantigens in patients with adrenal insufficiency and associated ovarian failure. J Clin Endocrinol Metabol. 80:1717–1723.
13. Nebert DW, Gonzalez FJ. 1987 P450 genes: structure, evolution, and regulation. Annu Rev Biochem. 56:945–993.
14. Ahonen P, Miettinen A, Perheentupa J. 1987 Adrenal and steroidal cell antibodies in patients with autoimmune polyglandular disease type I and risk of adrenocortical and ovarian failure. J Clin Endocrinol Metab. 64:494–500.
15. Michele TM, Fleckenstein J, Sgrignoli AR, Tuluvath PJ. 1994 Chronic active hepatitis in the type I polyglandular autoimmune syndrome. Postgrad Med J. 70:128–131.
16. Chung BC, Matteson KJ, Voutilainen R, Mohandas TK, Miller WL. 1986 Human cholesterol side-chain cleavage enzyme P450 scc; cDNA cloning, assignment of the gene to chromosome 15 and expression in the placenta. Proc Natl Acad Sci USA. 83:8962–8966.
17. Chung BC, Picardo-Leonard J, Haniu H, et al. 1987 Cytochrome P450 c17 (steroid 17 hydroxylase-17,20 lyase): cloning of human adrenal and testis cDNAs indicates the same gene is expressed in both tissues. Proc Natl Acad Sci USA. 84:407–411.
18. Laemmli UK. 1970 Cleavage of structural proteins during the assembly of the head of bacteriophage T4. Nature. 227:680–685.
19. Towbin HT, Staehelin T, Gordon J. 1979 Electrophoretic transfer of proteins from polyacrylamide gels to nitrocellulose sheets: procedure and some application. Proc Natl Acad Sci USA 76:4350–4354.
20. Sambrook J, Fritsch EF, Maniatis T. 1989 Molecular cloning. A laboratory manual. 2nd ed. New York: Cold Spring Harbor Laboratory Press; 18.67–18.74.
21. Barnes HJ, Arlotto MP, Waterman MR. 1991 Expression and enzymatic activity of recombinant cytochrome P450 c17 hydroxylase in *E. coli*. Proc Natl Acad Sci USA. 88:5597–5601.
22. Manns MP, Griffin KJ, Sullivan KF, Johnson EF. 1991 LKM1 autoantibodies recognize a short linear sequence in P450 IID6, a cytochrome P450 monooxygenase. J Clin Invest. 88:1370–1378.
23. Philipp T, Durazzo M, Trautwein C, et al. 1994 Recognition of uridine-diphosphate-glucuronosyl-transferases by LKM3 antibodies in chronic hepatitis D. Lancet. 344:578–581.
24. Bourdi M, Larrey D, Nataf J, et al. 1991 Anti-liver endoplasmatic reticulum autoantibodies are directed against human cytochrome P450 1A2. J Clin Invest. 85:1967–1973.
25. Irvine WJ, Chan MMW, Scarth L. 1969 The further characterization of autoantibodies reactive with extra-adrenal steroid-producing cells in patients with adrenal disorders. Clin Exp Immunol. 4:489–503.
26. Elder M, Maclaren N, Riley W. 1981 Gonadal autoantibodies in patients with hypogonadism and/or Addison's disease. J Clin Endocrinol Metab. 52:1137–1142.
27. Betterle C, Rossi A, Pria SD, et al. 1993 Premature ovarian failure: autoimmunity and natural history. Clin Endocrinol (Oxf). 389:35–43.
28. Sacher M, Blumel P, Thaler H, Manns M. 1990 Chronic active hepatitis associated with vitiligo, nail dystrophy, alopecia and a new variant of LKM antibodies. J Hepatol. 10:364–369.
29. Manns MP, Griffin KJ, Quattrochi L, et al. 1990 Identification of cytochrome P450 1A2 as a human autoantigen. Arch Biochem Biophys. 280:229–232.

0026-895X/96/030573-10$3.00/0

MOLECULAR PHARMACOLOGY, 50:573-582 (1996).

Cytochrome P450 2E1 Is a Cell Surface Autoantigen in Halothane Hepatitis

ERIK ELIASSON and J. GERALD KENNA

Department of Pharmacology and Toxicology, Imperial College School of Medicine at St. Mary's, London W2 1PG, UK

Received March 14, 1996; Accepted May 29, 1996

SUMMARY

Recent studies have shown that cytochrome P450 2E1 (CYP2E1) is a major catalyst of formation of trifluoroacetylated proteins, which have been implicated as target antigens in the mechanism of halothane hepatitis. In the present investigation, trifluoroacetylated CYP2E1 was detected immunochemically in livers of rats treated with halothane. Furthermore, high levels of autoantibodies that recognized purified rat CYP2E1 but not purified rat CYP3A were detected by enzyme-linked immunosorbent assay in 14 of 20 (70%) sera from patients with halothane hepatitis. Only very low levels of such antibodies were detected in sera from healthy controls, from patients anesthetized with halothane without developing hepatitis, or from patients with other liver diseases. The intracellular distribution of CF_3CO-adducts was studied in highly differentiated FGC4 rat hepatoma cell cultures. High levels of adducts were found after 22-hr culture in the presence of halothane, and their generation was dependent on the expression of CYP2E1. Adducts were predominantly located in the endoplasmic reticulum but also, to a minor extent, on the cell surface, as detected by immunofluorescence. A very similar distribution was found for CYP2E1 in FGC4 cells, and immunoprecipitation experiments performed in cultures of FGC4-related Fao hepatoma cells suggest that surface immunoreactivity originates from a small fraction of intact CYP2E1 apoprotein. Human CYP2E1, expressed in V79 cells after cDNA transfection, was also detected to a minor extent in the plasma membrane, whereas no immunofluorescence was evident in parental V79 cells. It is suggested that immune responses to cell surface CYP2E1 could be involved in the pathogenesis of halothane hepatitis.

The anesthetic halothane (2-bromo-2-chloro-1,1,1-trifluoroethane) is associated with a severe and sometimes fatal hepatitis in approximately one in several thousand anesthetized patients and also with a mild form of liver injury that occurs in ~25% of patients (1). The great majority of patients (>80%) who develop the severe form of liver injury, termed halothane hepatitis, have been exposed to halothane on two or more occasions, and these patients frequently exhibit rash, arthralgia, eosinophilia, and a variety of autoantibodies, which are characteristics of immune-mediated drug hepatotoxicity (1). Furthermore, a series of investigations have directly implicated immune responses to novel antigens, halothane metabolite-modified protein adducts, in the mechanism of liver injury.

Initial investigations showed that patients with halothane hepatitis exhibited cellular and humoral immune sensitization to novel antigens expressed in livers of halothane-dosed rabbits. In particular, antibodies that recognized the novel antigens were shown to be highly specific for patients with halothane hepatitis and could not be detected in various control groups, including halothane-anesthetized individuals who do not develop halothane hepatitis, patients anesthetized with halothane who develop liver injury attributable to other causes (2), and patients with the mild form of halothane-induced liver dysfunction (1). The novel halothane-induced antigens have been detected on the surface of isolated rabbit hepatocytes, and it has been shown that such hepatocytes are susceptible to antibody-mediated cytotoxic killing by normal human lymphocytes *in vitro* (2). This suggests that the antibodies could be responsible for and/or contribute to liver injury in patients *in vivo*.

Halothane is oxidized by hepatic P450 to the highly reac-

Portions of this work were presented at meetings of the British Toxicological Society and the International Society for the Study of Xenobiotics and have been published in abstract form [*Hum. Exp. Toxicol.* 14:755 (1995); *ISSX Proc.* 8:229 (1995)].

E.E. was Visiting Research Fellow from the Department of Medical Biochemistry and Biophysics, Karolinska Institutet, Stockholm, Sweden, and was supported by the Swedish Medical Society, Magnus Bergvalls Stiftelse, the Swedish Society for Medical Research 1994, and a Wellcome/Swedish Medical Research Council Travelling Fellowship (1995).

ABBREVIATIONS: SDS, sodium dodecyl sulfate; PAGE, polyacrylamide gel electrophoresis; ELISA, enzyme-linked immunosorbent assay; IP, immunoprecipitation; ER, endoplasmic reticulum; PM, plasma membrane; P450 or CYP, cytochrome P450; HRP, horseradish peroxidase; PDI, protein disulfide isomerase; FITC, fluorescein isothiocyanate; DAS, diallylsulfide; PBS, phosphate-buffered saline; BSA, bovine serum albumin; FBS, fetal bovine serum; TBS, Tris-buffered saline; PMSF, phenylmethylsulfonyl fluoride; PEST, penicillin/streptomycin; RT, room temperature; HEPES, 4-(2-hydroxyethyl)-1-piperazineethanesulfonic acid.

tive metabolite trifluoroacetylchloride, which either reacts with water to yield trifluoroacetate or binds covalently to hepatic proteins and lipids to produce trifluoroacetyl adducts (CF_3CO adducts) (3). The novel antigens recognized by antibodies from patients with halothane hepatitis have been shown to comprise a range of CF_3CO-protein adducts, which are expressed in livers of halothane-exposed rabbits, rats, and humans and are concentrated in the liver microsomal fraction (1). Studies performed using the technique of SDS-PAGE and immunoblotting (4, 5) have identified at least eight distinct CF_3CO-modified polypeptide antigens, of which all except one are derived from the lumen of the ER (4–6). In addition, a second group of antigens was identified recently that could be detected by ELISA but not by immunoblotting (7). It seems that these comprise one or more CF_3CO-modified integral membrane proteins of the ER and that the epitopes recognized by the antibodies of patients are conformational (7).

Studies undertaken *in vivo* in rats and *in vitro* in rat and human liver microsomes have shown that the P450 isozyme primarily responsible for generation of the CF_3CO adducts detectable by immunoblotting is CYP2E1 (8).[1] The major CF_3CO adduct(s) formed *in vitro* exhibited a subunit molecular mass of 55 kDa, and so could constitute CYP2E1 adducts.[1] In the current report, we demonstrate expression of CF_3CO-CYP2E1 adducts in livers of rats treated with halothane *in vivo* and the presence of autoantibodies to CYP2E1 in sera from patients with halothane hepatitis. In addition, by the use of cell model systems that express CYP2E1, we demonstrate expression of a fraction of cellular CYP2E1 and CF_3CO adducts on the cell surface. These findings indicate that CYP2E1 is a cell surface autoantigen in halothane hepatitis and suggest that this enzyme plays a dual role in the mechanism of liver injury.

Materials and Methods

Chemicals

BSA (fraction V), casein (Hammarsten grade), DAS, dithio-bis-(propionic-*N*-hydroxysuccinimide ester, protein A/Sepharose CL-4B, iodoacetamide, PMSF, Nonidet P-40 (octylphenoxy polyethoxy ethanol), Tween 20 (polyoxy ethylenesorbitan monolaurate), Triton X-100 (*t*-octylphenoxy polyethoxy ethanol), *o*-phenylenediamine, and streptavidin-agarose were purchased from Sigma Chemical (Poole, UK). Halothane was purchased from Aldrich Chemical (Gillingham, UK) and distilled to eliminate thymol (a stabilizer). Imidazole was obtained from BDH Chemicals (Merck, Lutterworth, UK). Chlormethiazole was from Astra Arcus AB (Södertälje, Sweden) and was provided by Prof. Magnus Ingelman-Sundberg (Karolinska Institutet, Stockholm, Sweden). SDS and EDTA were obtained from Koch-Light (Haverhill, UK). Protein A-HRP, acrylamide/bis (40%), polymerization initiators, and molecular mass standards were from BioRad Lab (Hemel Hempstead, UK). Ham's F12 medium [including 0.86 mg of ($ZnSO_4 \times 7H_20$)/liter], Dulbecco's modified Eagle's medium (including 4500 mg of glucose/liter), fetal bovine serum, PEST (5000 IU of penicillin/ml, 5000 μg of streptomycin/ml), geneticin sulfate (G-418), and Dulbecco's PBS were from GIBCO BRL (Life Technologies, Paisley, UK). Biotinylation reagent and Sephadex G-25 was included in a protein biotinylation module from Amersham Life Sciences (Amersham, UK). Enhanced chemiluminescent HRP substrates were also obtained from Amersham Life Sciences or from Pierce & Warriner (Chester, UK). Vectashield anti-bleach was from Vector Lab (Bretton, UK).

Purified Enzymes

CYP2E1 and P450 reductase were purified to homogeneity from livers of starved and acetone-treated male Sprague-Dawley rats in the laboratory of Prof. M. Ingelman-Sundberg (Karolinska Institutet, Stockholm, Sweden) according to a published protocol (9). Purified rat CYP3A (PCNb) was a gift from Prof. J. R. Halpert (University of Arizona, Tucson, AZ) and was purified as described previously (10).

Sera

Human sera were obtained from healthy individuals (25 sera), patients anesthetized with halothane on multiple occasions who did not develop hepatitis (six sera), patients with halothane hepatitis (20 sera), patients with primary biliary cirrhosis (seven sera), or patients with other liver disorders [i.e., chronic autoimmune hepatitis (six sera), alcoholic liver disease (four sera), and chronic viral hepatitis C (seven sera)]. Rabbit anti-CF_3CO adduct antiserum, which was produced as described in detail elsewhere (11), has been shown to recognize specifically CF_3CO-modified rat and human liver proteins in immunoblots and ELISA (5).[1] Polyclonal goat anti-human IgG/HRP or anti-rabbit IgG/HRP conjugate was from Tago Immunochemicals (Serotech, Kidlington, UK). Polyclonal goat anti-rabbit IgG/FITC conjugate was from Sigma. Polyclonal rabbit anti-CYP2E1 antiserum, raised against rat liver CYP2E1 (9) but also recognizing human CYP2E1 (12), was a gift from Magnus Ingelman-Sundberg (Stockholm, Sweden). Antiserum to PDI was obtained from a rabbit that had been immunized with rat PDI, purified essentially as described previously (13). This antiserum was shown by immunoblotting to recognize purified rat PDI (subunit molecular mass, 57 kDa) and to recognize a single 57-kDa polypeptide expressed in rat liver microsomes (results not shown).

Animals

Male Sprague-Dawley rats (200–250 g) were administered halothane (10 mmol/kg) in a single dose by intraperitoneal injection of a 21.5% (v/v) solution in sesame oil. Control rats received sesame oil only. After the indicated time intervals (see Fig. 4), rats were killed, and the livers were removed, homogenized, and subjected to differential centrifugation to obtain isolated liver microsomes (5).

Cell Cultures

FGC4 rat hepatoma cells (14) were obtained from Dr. M. Weiss (Institute Pasteur, Paris, France). These cells originated from a H4IIEC3 clone of the Reuber H35 rat hepatoma (14). Batches of FGC4 cells (2×10^6/ml) were kept frozen at −70° in 1.5 ml of Ham's F12 medium, including 25% (v/v) fetal bovine serum, 16% (v/v) dimethylsulfoxide, and 2% (v/v) PEST. Before each experiment, cells were quickly thawed at +37°, diluted into 15 ml of Ham's F12 medium [including 5% (v/v) fetal bovine serum and 2% (v/v) PEST], and cultured in 75-cm^2 plastic flasks (Corning; Costar, Cambridge, MA, or Falcon; Becton & Dickinson, Parsippany, NJ) in humidified atmosphere with 5% CO_2 at 37°. Medium was renewed after 24 hr and every second day thereafter. Rat hepatoma Fao cells (15), originating from the same H4IIEC3 clone as FGC4, were obtained from M. Ingelman-Sundberg and cultured under the same conditions as FGC4 cells. V79MZ Chinese hamster cells were provided by Prof. J. Doehmer (Technische Universität München, Munich, Germany). These cells exhibited a stable expression of human CYP2E1 after transfection with an simian virus 40 early promoter-controlled expression vector, which included human CYP2E1 cDNA (12). Both the transfected, CYP2E1-expressing V79MZh2E1 cells and the non-transfected, parental V79MZ cells were cultured in Dulbecco's mod-

[1] E. Eliasson, H. Hume-Smith, I. Gardner, I. de Waziers, P. Beaune, and J. G. Kenna. Cytochrome P450 2E1-dependent generation of trifluoroacetyl protein adducts recognized by antibodies from patients with halothane hepatitis. Submitted for publication.

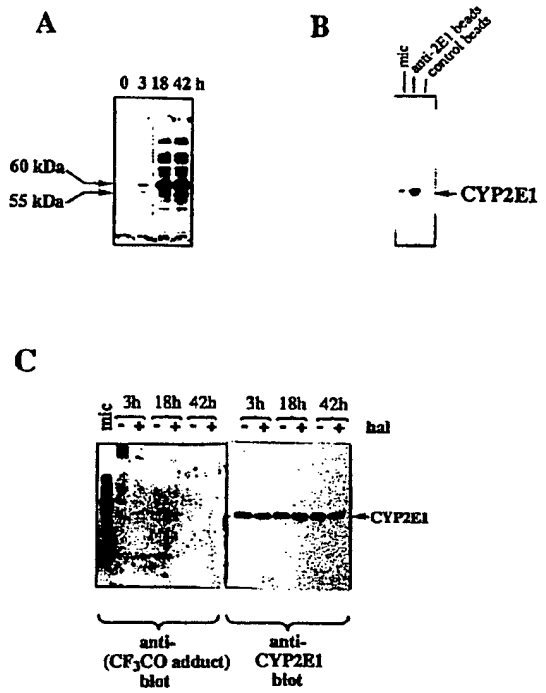

Fig. 1. Identification of CF_3CO-modified CYP2E1 in livers of rats treated with halothane. Microsomes were prepared from pooled livers of groups of four rats given an intraperitoneal dose of either halothane (10 mmol/kg) or sesame oil and killed after 3, 18, or 42 hr. A, Time-dependent formation of CF_3CO adducts. Liver microsomal proteins, corresponding to 5 μg/lane, were resolved by SDS-PAGE (8.5% gels) under reducing conditions, and immunoblots were developed using an anti-CF_3CO adduct rabbit antiserum, with final detection by peroxidase-generated chemiluminescence. B, IP of CYP2E1. Rabbit IgG specific for CYP2E1 or nonimmune IgG was cross-linked to protein A/Sepharose beads and used for precipitation of CYP2E1 from solubilized liver microsomes. Precipitates were subjected to SDS-PAGE (anti-2E1 beads and control beads, respectively), as were intact rat liver microsomes (*mic*) and CYP2E1 was detected by immunoblotting. C, Detection of CF_3CO-CYP2E1 formed in rat liver *in vivo*. CYP2E1 was immunoprecipitated from the various liver microsomes using the anti-2E1 beads; then, immunoprecipitates were resolved by SDS-PAGE (10% gels), and immunoblots were probed using anti-CYP2E1 antiserum (right) or anti-CF_3CO adduct antiserum (*left*), as was a reference sample of liver microsomes from halothane-treated animal (*mic*; 18 hr time point). Similar results were obtained in three separate experiments.

ified Eagle's medium (4500 mg/liter glucose), including 10% fetal bovine serum and 2% PEST, but geneticin sulfate (G-418, 200 μg/ml) was also included in the V79MZh2E1 cultures.

Formation of CF_3CO Adducts in FGC4 Cells

Within 5 weeks after initial thawing and reseeding, FGC4 cells were challenged with imidazole (0.5 mM, 2 days) or chlormethiazole (20 μM, 2 days) and thereafter washed twice in PBS and incubated in fresh medium for 60 min. Medium was exchanged once again, and flasks were closed air-tight with the use of silicone stoppers and parafilm. Halothane (5 μl of a 1:10 dilution in methanol) was injected through the stopper onto a strip of filter paper positioned inside the cell flask (16). This dose of halothane has been shown in a previous investigation to result in maximal generation of CF_3CO adducts in primary cultures of rat hepatocytes and has been estimated to give a final halothane concentration of ~20 μM in the culture medium (16). After the indicated incubation time (Figs. 4 and 5) at 37°, cells were washed three times in cold PBS and scraped off the plastic into Eppendorff tubes. The cells were pelleted by low-speed centrifugation and frozen in 100 μl of PBS at −20° before preparation of microsomes.

Isolation of Microsomes

Cell microsomes were isolated essentially as described previously (17) with minor modifications. The FGC4 samples (~5 × 10^6 cells) were thawed and sonicated in 1 ml of ice-cold 0.25 M sucrose, 1 mM EDTA, and 50 mM HEPES, pH 7.4. The homogenate was centrifuged at 10,000 × *g* for 10 min at +5°, and the resulting supernatant was ultracentrifuged at 109,000 × *g* for 60 min at +4° with a Beckman Optima TL ultracentrifuge with a TLA45 rotor (Beckman Instruments, Columbia, MD). Microsomal pellets were homogenized with a tight-fitting pestle in 200 μl of ice-cold centrifugation buffer. Protein concentration was determined according to the Lowry method using BSA as standard.

SDS-PAGE and Immunoblotting

Microsomal aliquots, corresponding to 150 μg (FGC4 cells) or 15 μg (rat liver), were diluted to 75 μl in water, mixed with 75 μl of SDS sample buffer [0.125 M Tris-HCl, ph 6.8, including 8% SDS (w/v), 20% glycerol (v/v), 0.002% bromphenol blue (w/v)] containing dithiotreitol (10 mg/ml), and boiled for 3 min. Thereafter, aliquots (specified in figure legends) were resolved by SDS-PAGE (using BioRad minigels with 8.5% or 10% acrylamide in the resolving gel) and transferred to nitrocellulose sheets. The sheets were incubated for 90 min at RT (20–25°) in blocking solution consisting of TBS, Tween 20 [0.05% (v/v)], fat-free dry milk [5% (w/v)], and fetal bovine serum [2% (v/v)]. Anti-CF_3CO protein antiserum was used at a 1:5000 dilution in blocking buffer and incubated for 3 hr or overnight at RT, after which blots were washed with 1% milk/TBS-Tween and incubated with goat anti-rabbit IgG/HRP conjugate at 1:5000 dilution in 1% milk/TBS-Tween for 2 hr. Primary antibody incubations with anti-CYP2E1 antiserum were performed using a 1:5000 dilution in 1% milk/TBS-Tween for 90 min at RT, followed by a thorough wash in TBS-Tween and incubation at RT for 90 min with protein A-HRP (1:3000) in 1% milk/TBS-Tween. Thereafter, sheets were washed again in TBS-Tween, and antibody reactivity was visualized using enhanced chemiluminescence HRP substrates and Hyperfilm (Amersham Life Sciences). The intensity of immunoblot signals was determined using a Molecular Dynamics scanner (Sunnyvale, CA) and ImageQuant software. The apparent molecular masses of protein adducts were estimated by comparison of their electrophoretic mobilities with those of molecular mass standards.

ELISA

Aliquots of PBS (96 μl) were added to wells of polystyrene microtiter plates (Immulon 4; Dynatech Lab, Billinghurst, UK). Subsequently, 5-μl aliquots of purified rat CYP2E1, which previously had been diluted to a final concentration of 1.8 pmol of CYP2E1/5 μl in 0.2% (w/v) sodium cholate, 50 mM HEPES, pH 7.4, were added to the wells (yielding a final protein concentration of ~1 μg/ml). Control wells received the same volumes of PBS and cholate dilutent buffer. Plates were incubated for 16 hr at +5°; then wells were washed four times in washing buffer [TBS, casein (0.5% (w/v), 0.02% (w/v) thimerosal] using a Titertek SA/12 Microplate washer (Flow Lab, ICN Biomedical, Thame, UK) at RT. Human sera (100 μl, diluted 1:100 in washing buffer) were added to the wells and plates were incubated for 3 hr at +4°. After another wash step, 100 μl of anti-human IgG/HRP conjugate (dilution 1:1000 or 1:3000 in washing buffer) was added to the wells, and plates were incubated for 2 hr at +4°. After a final wash (four times with washing buffer, then twice with TBS alone), bound HRP activity was determined by reaction with *o*-phenylenediamine (7) and determinations of absorbance at 490 nm (performed using a Titertek Multiskan Plus MkII Plate Reader; Flow Lab). The same protocol was used in ELISA studies of antibody binding to rat CYP3A and purified P450 reductase.

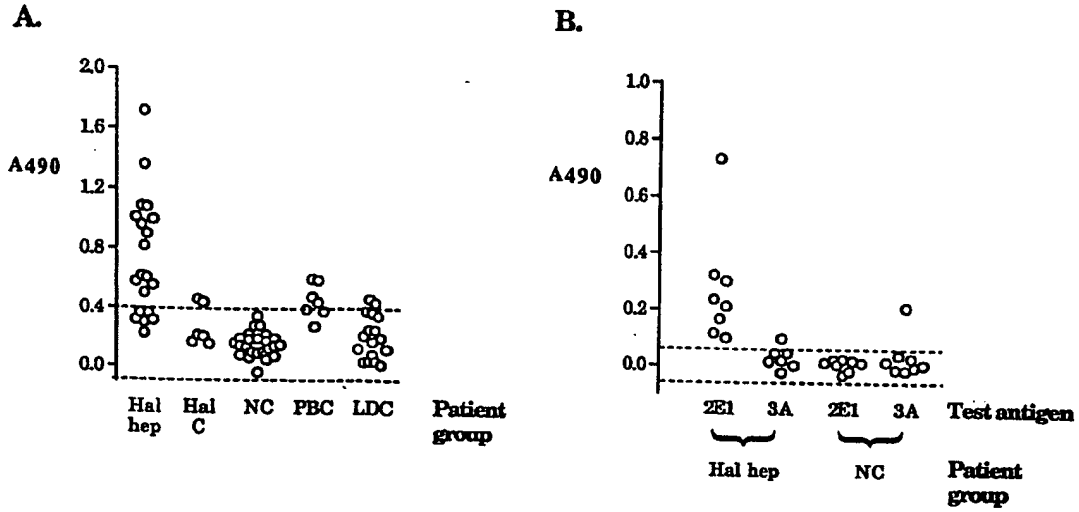

Fig. 2. Expression of anti-CYP2E1 antibodies in the sera of patients with halothane hepatitis. Binding of human antibodies (serum dilution 1:100) to purified rat CYP2E1 (A) or rat CYP2E1 and rat CYP3A (B) was investigated by ELISA. The dilutions of secondary antibody (goat anti-human IgG/HRP conjugate) were 1:1000 for A and 1:3000 for B. Sera were from patients with halothane hepatitis (*Hal hep*, 20 sera), patients undergoing multiple halothane anesthesia without hepatitis (*Hal C*, six sera), healthy controls (*NC*, 25 sera), patients with primary biliary cirrhosis (*PBC*, seven sera), or patients with other liver disorders (*LDC*, 17 sera). The background reactivity of each serum against wells coated with PBS was subtracted from each presented value. The analysis was repeated twice, with similar results.

Immunofluorescence

FGC4 cells were reseeded in 3 ml of complete F12 medium (described above) in Slide-Flasks (Nunc, Roskilde, Denmark) and grown to 40–50% confluency. The medium was replaced, and FGC4 cells were incubated with or without halothane, as described above. The cells were washed (2 × 5 min) in PBS and fixed in 2.5 ml of 5% (v/v) formaldehyde in PBS for 25 min at RT. After another wash in PBS, cells were treated by slow shaking for 20 min at RT in PBS, with or without 0.2% (v/v) Triton X-100, and then incubated without shaking for 15 hr at +5° with 10% (v/v) FBS in PBS. Subsequently, the Slide-Flasks were washed briefly in PBS and incubated (gentle shaking) for 3 hr at RT with 1 ml of primary antibody solution [either anti-CYP2E1 antiserum, diluted 1:2000 in 3% (w/v) BSA in PBS, or nonimmune rabbit antiserum or anti-CF_3CO adduct antiserum, diluted 1:400 in 1% (w/v) BSA in PBS]. Cell specimens were then washed in 3 ml of 3% (w/v) BSA (3 × 10 min) and incubated with goat anti-rabbit IgG/FITC conjugate [diluted 1:200 in 0.8 ml of 3% (w/v) BSA in PBS] for 1.5 hr at RT. Finally, specimens were washed in BSA/PBS (3 × 10 min) and once in H_2O, before being mounted in Vectashield anti-bleach under a glass coverslip. The specimens were analyzed by immunofluorescence microscopy using a Zeiss Axioskop and photographed using a Nikon UFX-DX camera, with the same exposure time for all samples. The same immunofluorescence protocol was used for V79 cells. Confocal microscopy was performed using a BioRad MRC600 with a krypton/argon laser.

IP of CYP2E1 from Liver Microsomes

Coupling of IgG to insoluble beads. Protein A/Sepharose CL-4B beads (80 mg) were equilibrated in 1 ml of IP buffer [0.15 M NaCl, 0.2% (v/v) Nonidet P-40, 1 mM EDTA, 50 mM HEPES, pH 7.4], including 2% (w/v) BSA, to yield a 20% (v/v) suspension. This was incubated with 4 mg of anti-CYP2E1 IgG (9) or 200 μl of nonimmune rabbit serum by shaking on ice for 2 hr. Beads were pelleted and washed once in IP buffer/BSA and twice in PBS and then incubated with 1.5 ml of dithio-bis(propionic-*N*-hydroxysuccinimide ester (1 mM in PBS) for 45 min during shaking on ice. Beads were washed three times with glycine (2 mM) in PBS and stored in this buffer at +5°.

IP of CYP2E1. Liver microsomes (300 μg) were solubilized in 1 ml of ice-cold IP buffer including 0.5% (w/v) BSA, 1% (w/v) deoxycholate, 1 mM PMSF, and 1 mM iodoacetamide and then incubated with 75 μl of a 10% (v/v) suspension of IgG beads for 2.5 hr on ice, with continuous shaking. The beads were pelleted by centrifugation and washed three times in solubilization buffer and then three times in IP buffer. Beads were boiled for 15 min in 100 μl of SDS sample buffer without DTT and then analyzed by SDS-PAGE and immunoblotting. Sample loading was 10 μl/well, and immunoblotting was performed using either anti-CYP2E1 or anti-CF_3CO adduct antiserum.

IP of CYP2E1 from Hepatoma Cells

Biotinylation of IgG. Anti-CYP2E1 IgG (2.5 mg) was biotinylated in 2.5 ml of sodium bicarbonate buffer (40 mM, pH 8.6) using 60 μl of biotinylation reagent from Amersham Life Sciences, according to the manufacturer's recommendation. The biotinylated IgG was separated from free biotin on a Sephadex G-25 column, resulting in an approximate protein concentration of 0.8 mg/ml in PBS.

Precipitation of CYP2E1. Fao cells were grown to 90% confluency under the conditions described above for FGC4 cells and then washed in PBS at RT (3 × 5 ml) and cooled to +5° in 10 ml of PBS containing 5% (v/v) FBS. This buffer was replaced with a further 10 ml of FBS in PBS, with or without digitonin (50 μg/ml). Biotinylated anti-CYP2E1 IgG was added (approximate concentration, 4 or 16 μg/ml), and incubation was conducted for 75 min at +5°, with very gentle agitation. Cell integrity, or permeabilization of cells in the presence of digitonin, was verified in separate flasks by investigation of trypan blue uptake. Essentially all of digitonin-treated cells (>99%) took up trypan blue, compared with <0.5% of cells incubated in PBS. The antibody solution was then discarded, and cells were washed once in 10 ml of PBS containing 10% (v/v) FBS, once in 20 ml of PBS supplemented with 5% FBS, and once in 20 ml of PBS. Cells were lysed by shaking on ice for 15 min in 2.5 ml of 1% Nonidet P-40, 0.15 M NaCl, 50 mM Tris, pH 7.8, including 1 mM EDTA, 1 mM PMSF, and 1 mM iodoacetamide. The lysate was further disrupted by vortex mixing, incubation on ice for 20 min, and then centrifugation at 2500 × *g* for 5 min. The supernatant was incubated on ice for 2 hr with streptavidin-agarose (60-μl beads, pre-equilibrated in lysis buffer), and then CYP2E1 bound to biotinylated IgG was pelleted by

centrifugation. The agarose pellet was washed in lysis buffer (3 × 1 ml) and once in PBS before boiling in SDS sample buffer (60 μl), without DTT, for 5 min. Aliquots (20 μl of each sample) were subjected to SDS-PAGE and immunoblotted with anti-CYP2E1 antiserum.

Results

Identification of CF_3CO-modified CYP2E1 in livers of halothane-treated rats. Liver microsomes were isolated from rats killed at 3, 18, or 42 hr after an *in vivo* dose of halothane (10 mmol/kg, in sesame oil) and from rats killed at the same time intervals after administration of the vehicle alone. Initially, formation of microsomal CF_3CO adducts was evaluated by immunoblotting, using a specific anti-CF_3CO adduct rabbit antiserum. Although only a very low of expression of two adducts (55 and 60 kDa) was evident at 3 hr after administration of halothane (Fig. 1A), much higher levels of many different CF_3CO adducts were detected after 18 hr and after 42 hr (Fig. 1A). Subsequently, IP experiments were undertaken using anti-CYP2E1 IgG antibodies coupled to insoluble beads (see Materials and Methods) to investigate expression of CF_3CO-modified CYP2E1. This procedure resulted in efficient precipitation of CYP2E1 from detergent-solubilized microsomes (Fig. 1B). Analyses of the immunoprecipitates by immunoblotting with anti-CF_3CO adduct serum revealed the presence of CF_3CO-modified CYP2E1 in livers of halothane-dosed rats but not in livers of control rats (Fig. 1C, *left*). Expression of CF_3CO-CYP2E1 could be detected in livers at 3 hr after halothane and was maximal at 18 hr (Fig. 1C). In contrast to the expression of the majority of other CF_3CO adducts (Fig. 1A), no CF_3CO-CYP2E1 was detectable after 42 hr. No significant differences between the expression of CYP2E1 apoprotein in the liver microsomes from halothane-treated and control rats were noted (Fig. 1C, *right*).

Autoantibodies to CYP2E1 in sera of patients with halothane hepatitis. The finding that CYP2E1 was modified by reactive metabolites of halothane raised the possibility that the protein could evoke an immune response in halothane hepatitis. To investigate this, purified rat CYP2E1 was used as test antigen in ELISA studies. Only low levels of antibody binding were detected using a control group of 25 sera from healthy blood donors (Fig. 2A). In contrast, levels of antibody binding that exceeded the normal range (defined as the mean plus three standard deviations of the values obtained for the healthy blood donors) were detected in 14 of 20 (70%) sera from patients with halothane hepatitis (Fig. 2A, *Hal hep*). Testing of six sera from patients who had received multiple halothane anesthesia without sustaining liver injury revealed that four were negative for CYP2E1, whereas two gave results that were very slightly above the normal range (Fig. 2A, *Hal C*). Negative results were also obtained with 16 of 18 sera from patients with various liver diseases unrelated to halothane (chronic autoimmune hepatitis, viral hepatitis, and alcoholic hepatitis), whereas two were found very weakly positive (Fig. 2A, *LDC*). A low anti-CYP2E1 reactivity could be detected in four of seven sera from patients with primary biliary cirrhosis (Fig. 2A, *PBC*). However, it is notable that the levels of antibody binding to CYP2E1 were markedly higher for 9 of the 20 sera from patients with halothane hepatitis than for any of the various control sera (Fig. 2A). Further ELISA studies, undertaken using 10 of the sera from patients with halothane hepatitis that contained elevated levels of antibodies to CYP2E1, revealed that the sera did not contain antibodies to purified rat CYP3A (Fig. 2B) or purified rat NADPH-dependent P450 reductase (data not shown).

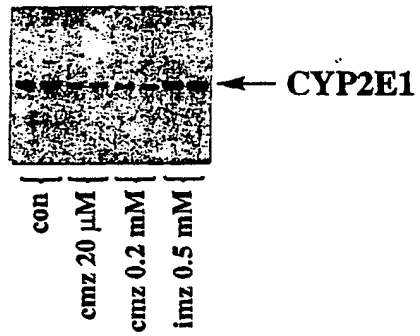

Fig. 3. Regulation of expression of CYP2E1 in FGC4 rat hepatoma cells. FGC4 cells were grown in the absence or presence of imidazole (*imz*) or chlormethiazole (*cmz*) for 2 days. Cells were harvested and microsomal CYP2E1 levels were analyzed by SDS-PAGE and immunoblotting with anti-CYP2E1 antiserum (loading 15 μg of microsomal protein/well). *con*, control.

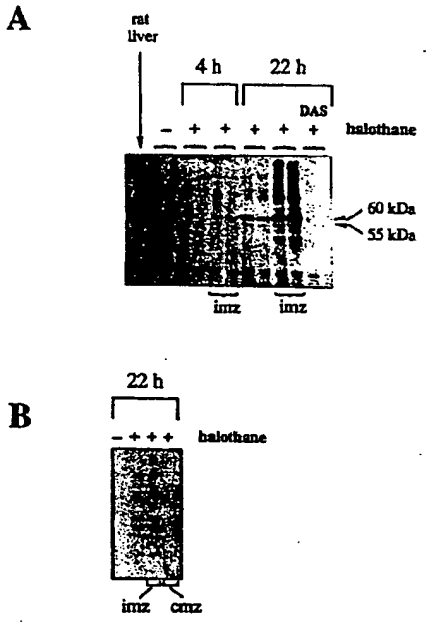

Fig. 4. Formation of microsomal CF_3CO adducts in FGC4 cells. A, Cell cultures were pretreated with or without imidazole, washed, and incubated with or without halothane. Some cells were preincubated for 1 hr with DAS (1 mM) before the addition of halothane. After 4 or 22 hr, cells were harvested in PBS, and formation of microsomal CF_3CO-protein adducts was detected by SDS-PAGE (10% gel, 40 μg of microsomal protein/well) and immunoblotting with anti-CF_3CO adduct antiserum. B, Formation of CF_3CO adducts in FGC4 cells pretreated with or without imidazole or chlormethiazole and then incubated with halothane for 22 hr. Microsomal proteins were resolved using an 8.5% gel and then developed as described above. The results were replicated two or three times.

Expression of CYP2E1 and CF_3CO adducts in FGC4 cells. The highly differentiated FGC4 rat hepatoma cell line (14) was used as a model system to study the expression of

CYP2E1 in relation to the intracellular formation of CF_3CO adducts. The basal level of CYP2E1 expression in FGC4 hepatoma cells was estimated, by immunoblotting, to be ~1-2 pmol/mg of microsomal protein. Treatment of cell cultures with the CYP2E1-stabilizer imidazole [0.5 mM, (17)] for 2 days caused a 3-fold increase in CYP2E1 expression (293 ± 126% of untreated control cells, three experiments). In contrast, the expression of CYP2E1 decreased to 25 ± 3% (three experiments) after 2 days in the presence of chlormethiazole (20 μM) (Fig. 3). As shown in Fig. 1A, CF_3CO-modified microsomal proteins were formed when FGC4 cells were pretreated with or without imidazole or chlormethiazole and thereafter incubated with halothane for 4 or 22 hr at 37°. Formation of the adducts was more rapid and extensive after pretreatment of the cells with imidazole. In these cells, only two distinct adducts (55 and 60 kDa) were detectable after 4 hr, whereas many other adducts had been formed after 22 hr (Fig. 4A). The addition of the CYP2E1-selective inhibitor DAS (18) (1 mM) to the cell cultures completely blocked adduct formation (Fig. 4A), as did pretreatment of cells with chlormethiazole (Fig. 4B).

The subcellular locations of CF_3CO adducts and CYP2E1 in FGC4 cells. Studies in which expression of CF_3CO adducts in halothane-treated FGC4 cells was investigated by indirect immunofluorescence, using the anti-CF_3CO adduct antiserum, revealed no significant expression of adducts after 4 hr (Fig. 5A), whereas intense immunofluorescence was evident after 22 hr (Fig. 5B). The fluorescence was distributed in a granular pattern throughout the cytoplasm in permeabilized cells, whereas no reactivity was seen in the area corresponding to the cell nuclei (Fig. 5, B and E), which was easily identified in phase-contrast microscopy (data not shown). A very similar picture was seen when specimens were probed for the expression of PDI, an abundant ER enzyme (Fig. 6D). However, studies of adduct expression in intact cells resulted in detection of a more diffuse immunofluorescence, which was concentrated at the edges of the cell (Fig. 5, C and F). This corresponds to the pattern expected for the plasma membrane (18a). Essentially no fluorescence was detected in cells incubated without halothane (Fig. 5D) or in cells developed using preimmune serum (data not shown).

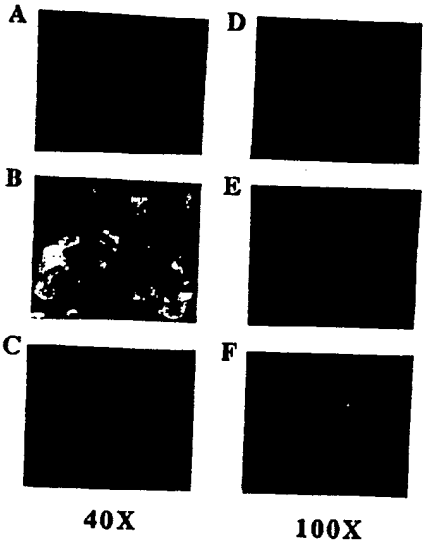

Fig. 5. Subcellular location of CF_3CO adducts in FGC4 cells. Cells were grown on Slide-Flasks and pretreated with imidazole for 2 days before washing and incubation with halothane. After 4 or 22 hr, cells were fixed in 5% formaldehyde, washed in PBS (C and F) or PBS/Triton X-100 (A, B, D, and E), and then blocked in 10% FBS and incubated with anti-CF_3CO adduct serum [1:400 in 1% (w/v) BSA/PBS] followed by anti-rabbit IgG/FITC (1:200 in 3% BSA/PBS) before analysis by immunofluorescence microscopy. A, Four hours with halothane (permeabilized cells), 40× magnification; B, 22 hr with halothane (permeabilized cells), 40×; C, 22 hr with halothane (nonpermeabilized cells), 40×; D, 22 hr without halothane (permeabilized cells), 100×; E, 22 hr with halothane (permeabilized cells), 100×; and F, 22 hr with halothane (nonpermeabilized cells), 100×.

Investigations of the cellular distribution of CYP2E1, which were undertaken using the anti-CYP2E1 antiserum, yielded a very similar pattern of results. In these studies, cells were visualized by conventional fluorescence microscopy (Fig. 6, A–C) and also by confocal microscopy (Fig. 6, D and E). In the permeabilized cells, immunofluorescence was distributed in a granular pattern all throughout the cytoplasm, whereas no fluorescence was detected in the cell nuclei (Fig. 6, B and D). Immunoreactivity was also detected to a minor extent on the surface of nonpermeabilized cells (Fig. 6, C and E). No significant fluorescence was detected in cell samples incubated without the anti-CYP2E1 antiserum (Fig. 6A).

The subcellular location of human CYP2E1 in transfected V79 cells. As a control for the specificity of the anti-CYP2E1 antibody reaction and to investigate whether human CYP2E1 is expressed on the cell surface, experiments were performed using V79 Chinese hamster fibroblast cells transfected with human CYP2E1-cDNA, which stably express human CYP2E1 (12). Immunofluorescence analysis of the transfected V79 cells after membrane permeabilization by detergent revealed that human CYP2E1 was distributed in a pattern corresponding to the ER (Fig. 7A). Immunofluorescence was also detected along the edges of cells without pretreatment with detergent (Fig. 7B). No signal was detected when nontransfected, parental V79 cells were permeabilized and incubated with the anti-CYP2E1 serum (Fig. 7C) or when immunofluorescence studies of either parental or transfected V79 cells were performed using nonimmune serum (data not shown).

Identification of intact CYP2E1 apoprotein on the surface of Fao cells. IP studies were undertaken to evaluate whether the anti-CYP2E1 reactivity evident on the surface of cultured cells corresponded to intact CYP2E1 or proteolytic fragments of the protein. Cultures of an FGC4-related cell line, Fao (15), which has a higher expression of CYP2E1 than FGC4 cells, were incubated with biotinylated anti-CYP2E1 IgG. Incubations were performed using intact cells and cells that had been permeabilized using digitonin. Subsequently, cells were washed extensively and lysed with detergent; then, the biotinylated IgG was precipitated using streptavidin-agarose beads. The precipitates were subjected to SDS-PAGE and immunoblotted using anti-CYP2E1 antiserum. This procedure showed that the CYP2E1 immunoprecipitated from the surface of nonpermeabilized cells exhibited an identical electrophoretic mobility to the intact CYP2E1 apoprotein immunoprecipitated from digitonin-permeabilized cells (Fig. 8). Furthermore, it was evident that only a very small fraction of the total cellular contents of CYP2E1 was expressed on the surface. Control experiments confirmed that no

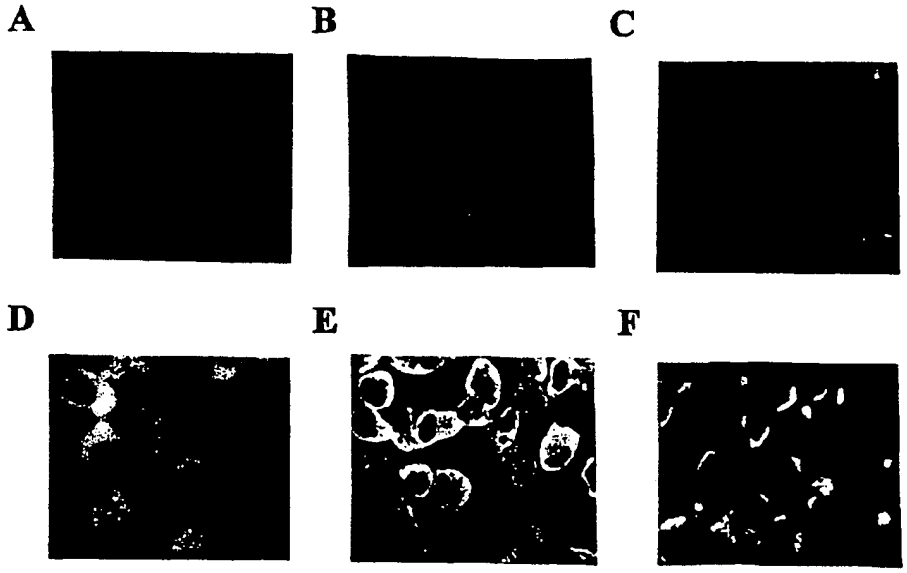

Fig. 6. Subcellular location of rat CYP2E1 in FGC4 cells. FGC4 cells were grown to 60–70% confluency in Slide-Flasks. Thereafter, cells were fixed in formaldehyde and either permeabilized by detergent or left intact, as described in Materials and Methods, and then incubated with anti-CYP2E1 antiserum (diluted 1:2000) or anti-PDI antiserum (1:2000) and, finally, FITC-coupled goat anti-rabbit IgG. The results on CYP2E1 distribution have been replicated at least five times, whereas the PDI control was performed twice. A, FITC-goat anti-rabbit IgG only (permeabilized cells), 100× magnification; B, anti-CYP2E1 antiserum (permeabilized cells), 100×; C, anti-CYP2E1 antiserum (nonpermeabilized cells), 100×; D, anti-PDI antiserum (permeabilized cells), 63×; E, confocal microscopy, anti-CYP2E1 (permeabilized cells), 40×; and F, confocal microscopy, anti-CYP2E1 (nonpermeabilized cells), 40×.

CYP2E1 was precipitated when solubilized rat liver microsomes were incubated with streptavidin-agarose in the absence of anti-CYP2E1 antibodies (data not shown).

Discussion

Identification of CF_3CO-modified CYP2E1. The IP studies of liver microsomes revealed that CF_3CO modification of CYP2E1 occurs relatively rapidly (within 3 hr) after intraperitoneal administration of a single dose of halothane to rats (Fig. 1C). The relatively rapid appearance of CF_3CO-CYP2E1, compared with other CF_3CO adducts, is consistent with the demonstration that CYP2E1 is a major catalyst of protein trifluroacetylation *in vitro* in rat and human liver microsomes[1] and *in vivo* in the rat (8). Furthermore, in agreement with previous studies (8), a 55-kDa adduct that most probably corresponds to CF_3CO-CYP2E1 was one of only two modified proteins detected at the 3-hr time point (Fig. 1A). It should also be noted that high levels of 55-kDa CF_3CO adducts have been detected after incubation of both rat and human liver microsomes with halothane *in vitro* (5, 6).[1]

It is unclear why significantly higher levels of CF_3CO-CYP2E1 were detected at 18 hr after administration of halothane than after 3 hr (Fig. 1C). One possible explanation is concentration-dependent inhibition of P450-dependent bioactivation of halothane at the early time point (16, 19).[1] Covalent modification of CYP2E1, either by cAMP-dependent phosphorylation (20) or by heme alkylation caused by reactive metabolites of carbon tetrachloride (21), has been shown to result in denaturation of the enzyme and subsequent rapid degradation. Presumably, this explains why in contrast to the many other CF_3CO adducts detectable after 18 hr, CF_3CO-modified CYP2E1 was not detectable at 42 hr (Fig. 1C).

CYP2E1 as an autoantigen in halothane hepatitis. Markedly elevated levels of antibodies that recognized rat liver CYP2E1 were detected in a high proportion (70%) of the sera from patients with halothane hepatitis, whereas only low levels of such antibodies were present in a range of control sera (Fig. 2). It is conceivable that a higher number of patient sera might recognize the human form of CYP2E1. By analogy, antibodies that recognized a purified rat liver microsomal carboxylesterase were detected by ELISA in only 2 of 10 sera from patients with halothane hepatitis (20%) (22), whereas the corresponding human enzyme, which exhibited 77% amino acid sequence identity, was recognized by 17 of 20 sera (85%) (23). Rat and human CYP2E1 are 78% homologues at the amino acid level (24), and the substrate specificities of the two forms are highly similar. However, a few minor structural differences do exist, mainly distributed on surface of the CYP2E1 molecule, as predicted by comparison with the known three-dimensional structure of bacterial CYP102 (24a). For example, it is possible that surface-located Asp92, Asp96, Pro259, and Pro262, all present only in the human enzyme, represent part of epitopes to which autoantibody binding could be reduced in ELISA assays with the rat CYP2E1 enzyme.

Sera from patients with halothane hepatitis have been shown to contain elevated levels of antibodies to numerous hepatic protein antigens other than CYP2E1 and microsomal carboxylesterase. These include protein disulfide isomerase (57 kDa), a 58-kDa protein of unknown function; calreticulin (63 kDa); ERp72 (80 kDa); and the stress proteins BiP/GRP78 (82 kDa) and endoplasmin/GRP94 (100 kDa) (reviewed in Refs. 1 and 22). Initially, immunoblotting studies revealed that the the antibodies of patients recognized unique CF_3CO-modified epitopes expressed on the adduct-modified forms of the proteins (5). However, ELISA studies undertaken using purified non-CF_3CO-modified forms of several of the proteins subsequently showed that the predominant antibody responses detectable in the sera of patients are directed against non-CF_3CO-modified epitopes, which presumably are conformational because they are not detectable by immunoblotting (1, 13, 22). It is probable that the antibody response to unmodified epitopes arises because CF_3CO adduct formation causes a specific loss of immunological tolerance and that a similar adduct-induced loss of immunological tolerance underlies the anti-CYP2E1 autoantibody response demonstrated in the present investigation. A

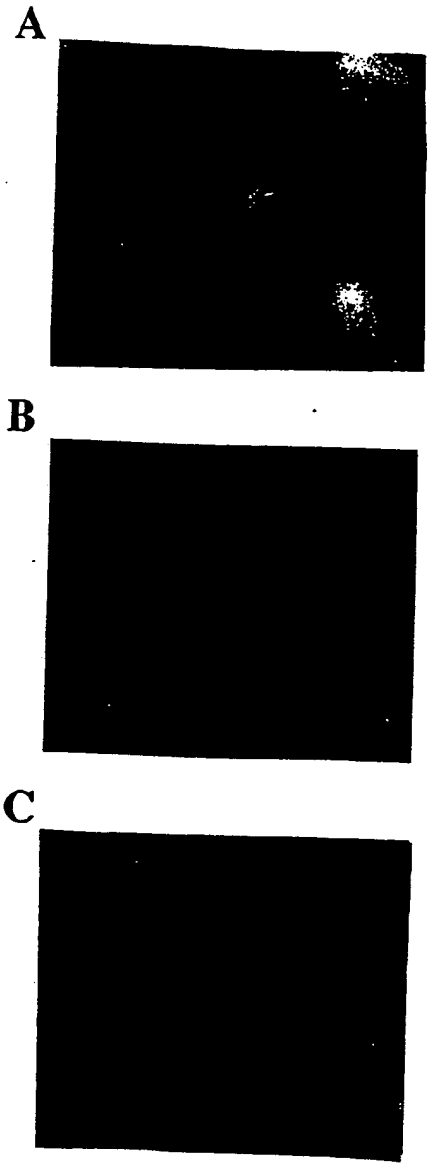

Fig. 7. Subcellular location of human CYP2E1 in V79 cells transfected with human CYP2E1-cDNA. V79 cells stably expressing human CYP2E1, or parental V79 cells, were grown to 40% confluency and fixed, washed in PBS (B) or PBS/Triton X-100 (A and C), blocked in FBS, incubated with anti-CYP2E1 antiserum and anti-rabbit IgG/FITC, and then analyzed by immunofluorescence microscopy. A, Human CYP2E1-cDNA-transfected V79 cells (permeabilized), 100× magnification; B, human CYP2E1-cDNA-transfected V79 cells (nonpermeabilized), 100×; and C, parental V79 cells (permeabilized), 100×.

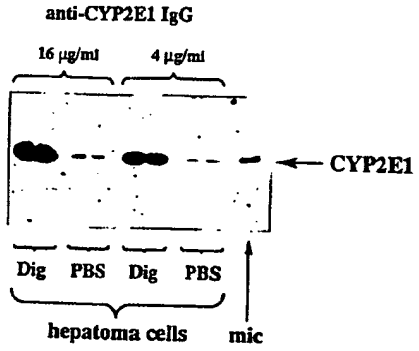

Fig. 8. IP of CYP2E1 from the surface of Fao hepatoma cells. Fao hepatoma cell cultures were permeabilized by digitonin (*Dig*) or left intact in PBS and then incubated at +5° with biotinylated anti-CYP2E1 IgG in the presence of bovine serum. Thereafter, cell cultures were washed extensively and lysed in a detergent-containing buffer including protease inhibitors. The lysate was incubated with streptavidin-agarose, which was precipitated by centrifugation and thoroughly washed in lysis buffer. Streptavidin-adsorbed proteins were eluted by boiling in SDS sample buffer, resolved by SDS-PAGE, and immunoblotted using anti-CYP2E1 antiserum. A reference sample of rat liver microsomes (*mic*; 2 μg) was also included in the electrophoresis. The results presented are duplicate precipitations from each culture. Similar results were obtained in two independent experiments.

nonspecific loss of immunological tolerance toward hepatic proteins seems unlikely because significant autoreactivity against another P450 (CYP3A) (Fig. 2) or against NADPH-dependent P450 reductase was not detected.

A specific loss of tolerance toward native CYP2E1, as a consequence of CF_3CO-CYP2E1 adduct formation, would be analogous with two other examples of drug-induced hepatitis, namely, hepatitis caused by tienilic acid and by dihydralazine. In both cases, P450 isozyme-specific metabolism of the causative agent to reactive metabolites that bind covalently to the same P450s was demonstrated, as was the presence in the sera of patients of autoantibodies that recognized the relevant P450s (CYP2C9 and CYP1A2) (25, 26). Furthermore, it was reported that anti-CYP3A antibodies are expressed in sera of patients who develop hypersensitivity reactions to carbamazepine, a CYP3A substrate (27). Overall, these findings prompted the speculation that autoimmune responses to P450s could be a common process underlying many allergic drug reactions. Clearly, the present findings are consistent with this hypothesis.

CYP2E1 is the first example of an integral membrane protein that has been shown to be recognized by antibodies from patients with halothane hepatitis. The other protein antigens identified to date are believed to be concentrated in the lumen of the endoplasmic reticulum and are either soluble or peripheral membrane proteins (6). A group of halothane-induced liver antigens was described recently that is recognized by antibodies from patients with halothane hepatitis in a conformation-dependent manner (7). It seems likely that a part of this group of microsomal neoantigens, shown to be integral membrane proteins (7), constitutes CF_3CO-CYP2E1 adducts.

Cell model systems for investigation of expression of CF_3CO adducts. Cultured FGC4 rat hepatoma cells provided a very useful model system for investigation of formation and trafficking of CF_3CO adducts. The FGC4 cell is highly differentiated and constitutively expresses liver-specific proteins, including albumin, phosphoenolpyruvate carboxykinase, alcohol dehydrogenase, and the P450 isozymes CYP2B (14) and CYP2E1 (28). Regulation of CYP2E1 expression in these cells shows several similarities with primary hepatocytes and with regulatory mechanisms operative *in vivo*. Thus, the cellular level of CYP2E1 is increased by imidazole (Fig. 3) and by ethanol (28), which is most probably explained by a specific ligand-dependent stabilization of the CYP2E1 holoenzyme (17). Chlormethiazole has been recog-

nized previously as a specific inhibitor of CYP2E1 expression *in vivo* during starvation of rats (29), and run-off analysis with isolated nuclei from livers of starved rats indicated that this effect was mediated at the level of transcription of the CYP2E1 gene (29). The results presented here (Fig. 3) confirm that chlormethiazole is acting directly on the liver cell and that starvation is not a prerequisite for its inhibitory action on CYP2E1 expression.

The pattern of adducts formed *in vitro* in the FGC4 cells was very similar to that detected *in vivo* in livers of halothane-treated rats. In particular, the preferential targets for CF_3CO-modification in FGC4 cells and *in vivo* seemed to be the same at early time points after halothane administration [i.e., 55- and 60-kDa proteins (compare Fig. 4A and Fig. 1A)]. Furthermore, because imidazole pretreatment of cells enhanced adduct formation, whereas chlormethiazole dramatically inhibited adduct formation (Fig. 4, A and B), it seems clear that adduct formation was dependent on the level of CYP2E1. Furthermore, an almost-complete block of adduct formation was mediated by DAS, a specific inhibitor of CYP2E1 catalysis (18). Although it cannot be excluded that some of this inhibition is due to a direct reaction between DAS and the reactive halothane metabolites, CYP2E1-dependent generation of CF_3CO adducts in FGC4 cells is consistent with the recent finding that CF_3CO adduct formation *in vitro*, in isolated rat and human liver microsomes, correlated with the microsomal content and activity of CYP2E1.[1] It is also consistent with earlier studies of adduct formation *in vivo* in livers of rats treated with halothane after pretreatment with various P450 isozyme-selective inducers (8).

Expression of CF_3CO adducts and CYP2E1 on the cell surface. Clearly, the vast majority of CF_3CO adducts and CYP2E1 were expressed intracellularly, in a morphological pattern corresponding to the ER (Fig. 5). This is consistent with the known organellar location of P450s (30), with biochemical studies that have shown that CF_3CO adducts are concentrated in microsomal fractions prepared from rabbit and rat liver (4, 5) and with the finding that the major CF_3CO adducts are modified forms of proteins believed to reside in the lumen of the ER (6). In addition, a small but significant fraction of both total cellular CF_3CO adducts and CYP2E1 were detected on the cell surface.

Earlier investigations of cell surface expression of these molecules were undertaken using cells isolated by mechanical disruption or collagenase digestion of livers. These have yielded conflicting results, which could have been affected by cell surface modification, due either to proteolysis or to incorporation of intracellular debris released from damaged cells. Immunofluorescence studies have suggested that antibodies from patients with halothane hepatitis recognize neoantigens expressed on the surface of hepatocytes isolated from livers of halothane-treated rabbits (2), whereas studies performed using anti-CF_3CO adduct antisera have indicated that such adducts are expressed on hepatocytes from rats treated with halothane *in vivo* (11) and on the surface of isolated human hepatocytes that were exposed to halothane *in vitro* (31). Similarly, CYP2E1, other P450 isozymes, and P450 reductase were found on the surface of hepatocytes isolated from rat and human liver (18a, 33). However, no expression of hepatocyte surface-located CF_3CO adducts were detected when hepatocytes isolated from livers of halothane-treated mice were analyzed by fluorescence activated flow cytometry (35). Furthermore, no CYP2B or CYP2D could be detected on the cell surface using electron microscopy (30, 36).

The investigations of the cellular location of CYP2E1 addressed two further important issues. First, studies of transfected and untransfected V79 cells (Fig. 7) verified that the cell surface immunoreactivity recognized by the anti-CYP2E1 antiserum was attributable to CYP2E1 and indicated that the cell surface form of the protein originates from the wild-type human CYP2E1 mRNA, and not a splicing variant. Second, the IP studies (Fig. 8) revealed that the cell surface immunoreactivity was due to the presence of intact CYP2E1 apoprotein, and not to any detectable proteolytic fragments. Although quantitative interpretations of the IP data should be made with great caution, the results suggest that maximally a small percentage, probably less, of the cellular contents of CYP2E1 can become expressed on the surface of the hepatoma cells studied. This implies that although there is an uncharacterized mechanism of efficient retention of P450 in the ER, leakage of P450 molecules into the secretory pathway (34) can occur. Furthermore, some epitopes of CYP2E1 must be oriented extracellularly to be recognized by antibodies on the surface of intact cells. It is interesting to note that this is inconsistent with the current models of the membrane topology of P450s in the ER, which predict that very little of the molecule is exposed on the luminal side of the lipid bilayer (37).

The role of CYP2E1 in halothane hepatitis. Our results suggest that CYP2E1 could play a dual role in halothane hepatitis: first, as a major catalyst of formation of CF_3CO-protein adducts, which elicit immune responses in susceptible patients,[1] and, second, as a cell surface target antigen that is recognized by the antibodies of patients and potentially by other immune effector mechanisms. CYP2E1 could be an especially important target antigen because it is an integral membrane protein that will be bound tightly to the cell surface. In contrast, the other CF_3CO adducts identified to date are soluble or peripheral membrane proteins that if exported from the lumen of the ER to the cell surface, could well be poorly retained and/or released from the cell. CYP2E1 is an abundant and inducible hepatic enzyme that has been shown to bioactivate many xenobiotics other than halothane (including various other volatile anesthetics and structurally related compounds) (38). In the future, it may prove to also be involved in allergic reactions to other compounds.

Acknowledgments

We are very grateful to Prof. M. Ingelman-Sundberg (Karolinska Institutet, Stockholm, Sweden) for the generous provision of purified rat CYP2E1, rabbit antiserum against CYP2E1, purified P450 reductase, and chlormethiazole. We also thank Prof. J. R. Halpert (Tucson, AZ) for the purified rat CYP3A, Prof. J. Doehmer (Munich, Germany) for the V79 cells expressing human CYP2E1, and Dr. M. Weiss (Paris, France) for provision of rat hepatoma cells.

References

1. Kenna, J. G., and J. M. Neuberger. Immunopathogenesis and treatment of halothane hepatitis. *Clin. Immunother.* 3:108-124 (1995).
2. Vergani, D., G. Mieli-Vergani, A. Alberti, J. Neuberger, A. L. W. F. Eddleston, M. Davis, and R. Williams. Antibodies to the surface of halothane-altered rabbit hepatocytes in patients with severe halothane-associated hepatitis. *N. Engl. J. Med.* 303:66-71 (1980).
3. Gandolfi, A. J., R. D. White, I. G. Sipes, and L. R. Pohl. Bioactivation and

covalent binding of halothane *in vitro*: studies with [^{3}H] and [^{14}C] halothane. *J. Pharmacol. Exp. Ther.* 214:721-725 (1980).
4. Kenna, J. G., J. Neuberger, and R. Williams. Identification by immunoblotting of three halothane-induced liver microsomal polypeptide antigens recognized by antibodies in sera from patients with halothane hepatitis. *J. Pharmacol. Exp. Ther.* 242:733-740 (1987).
5. Kenna, J. G., H. Satoh, D. D. Christ, and L. R. Pohl. Metabolic basis for a drug hypersensitivity: antibodies in sera from patients with halothane hepatitis recognize liver neoantigens that contain the trifluoroacetyl group derived from halothane. *J. Pharmacol. Exp. Ther.* 245:1103-1109 (1988).
6. Kenna, J. G., J. L. Martin, and L. R. Pohl. The topography of trifluoroacetylated protein antigens in liver microsomal fractions from halothane treated rats. *Biochem. Pharmacol.* 44:821-829 (1992).
7. Knight, T. L., K. M. Scatchard, F. N. A. M. van Pelt, and J. G. Kenna. Sera from patients with halothane hepatitis contain antibodies to halothane-induced liver antigens which are not detectable by immunoblotting. *J. Pharmacol. Exp. Ther.* 270:1325-1333 (1994).
8. Kenna, J. G., J. L. Martin, H. Satoh, and L. R. Pohl. Factors affecting the expression of trifluoroacetylated liver microsomal protein neoantigens in rats treated with halothane. *Drug Metab. Dispos.* 18:788-793 (1990).
9. Johansson, I., G. Ekström, B. Scholte, D. Puzycki, H. Jörnvall, and M. Ingelman-Sundberg. Ethanol-, fasting-, and acetone-inducible cytochromes P.-450 in rat liver: regulation and characteristics of enzymes belonging to the IIB and IIE gene subfamilies. *Biochemistry* 27 :1925-1934 (1988).
10. Halpert, J. R. Multiplicity of steroid-inducible cytochromes P-450 in rat liver microsomes. *Arch. Biochem. Biophys.* 263:59-68 (1988).
11. Satoh, H., Y. Fukida, D. K. Anderson, V. J. Ferrans, J. R. Gilette, and L. R. Pohl. Immunological studies on the mechanism of halothane-induced hepatotoxicity: immuno-histochemical evidence of trifluoroacetylated hepatocytes. *J. Pharmacol. Exp. Ther.* 233:857-862 (1985).
12. Schmalix, W. A., M. Barrenscheen, R. Landsiedel, C. Jansowski, G. Eisenbrand, F. J. Gonzalez, E. Eliasson, M. Ingelman-Sundberg, M. Perchermeier, F. Wiebel, H. Greim, and J. Doehmer. Stable expression of human cytochrome P450 2E1 in V79 Chinese hamster cells. *Eur. J. Pharmacol.* 293:123-131 (1995).
13. Martin, J. L., J. G. Kenna, B. M. Martin, D. Thomassen, G. F. Reed, and L. R. Pohl. Halothane hepatitis patients have serum antibodies that react with protein disulfide isomerase. *Hepatology* 18:858-863 (1993).
14. Angrand, P.-O., S. Kallenbach, M. C. Weiss, and J.-P. Rousset. An exogenous albumin promotor can become silent in dedifferentiated hepatoma variants as well as intertypic hybrids. *Cell Growth Diff.* 1:519-526 (1990).
15. de Waziers, I., J. Bouguet, P. H. Beaune, F. J. Gonzalez, B. Ketterer, and R. Barouki. Effects of ethanol, dexamethasone and RU 486 on expression of cytochromes P450 2B, 2E, 3A and glutathione transferase in a rat hepatoma cell line (Fao). *Pharmacogenetics* 2:12-18 (1992).
16. van Pelt, F. N. A. M., and J. G. Kenna. Formation of trifluoroacetylated protein antigens in cultured rat hepatocytes exposed to halothane *in vitro*. *Biochem. Pharmacol.* 48:461-471 (1994).
17. Eliasson, E., I. Johansson, and M. Ingelman-Sundberg. Ligand-dependent maintenance of ethanol-inducible cytochrome P-450 in primary rat hepatocyte cell cultures. *Biochem. Biophys. Res. Commun.* 150: 436-443 (1988).
18. Brady, J. F., D. Li, H. Ishizaki, and C. S. Yang. Effect of diallyl sulfide on rat liver microsomal nitrosamine metabolism and other monooxygenase activities. *Cancer Res.* 48:5937-5940 (1988).
18a. Loeper, J., V. Descatoire, M. Maurice, P. Beaune, J. Belghiti, D. Houssin, F. Ballet, G. Feldmann, F. P. Guengerich, and D. Pessayre. Cytochromes P-450 in human hepatocyte plasma membrane: recognition by several autoantibodies. *Gastroenterology* 104:203-216 (1993).
19. Lind, R. C., and A. J. Gandolfi. Concentration-dependent inhibition of halothane biotransformation in the guinea pig. *Drug Metab. Dispos.* 21:386-389 (1993).
20. Eliasson, E., I. Johansson, and M. Ingelman-Sundberg. Substrate-, hormone-, and cAMP-regulated cytochrome P450 degradation: *Proc. Natl. Acad. Sci. USA* 87:3225-3229 (1990).
21. Tierney, D. J., A. L. Haas, and D. R. Koop. Degradation of cytochrome P450 2E1: selective loss after labilization of the enzyme. *Arch. Biochem. Biophys.* 293:9-16 (1992).
22. Pohl, L. R., D. Thomassen, N. R. Pumford, L. E. Butler, H. Satoh, V. J. Ferrans, A. Perrone, B. M. Martin, and J. L. Martin. Hapten carrier conjugates associated with halothane hepatitis, in *Biological Reactive Intermediates IV* (C. Witmer, R. Snyder, and D. Jollow, eds.). Plenum Press, New York, 111-120 (1990).
23. Smith, G. C. M., J. G. Kenna, D. Harrison, D. Tew, and C. R. Wolf. Autoantibodies to hepatic carboxylesterase in halothane hepatitis. *Lancet* 342:963-964 (1993).
24. Song, B. J., H. V. Gelboin, S. S. Park, C. S. Yang, and F. J. Gonzalez. Complementary DNA, and protein sequences of ethanol-inducible rat and human cytochrome P-450s: transcriptional and post-transcriptional regulation of the rat enzyme. *J. Biol. Chem.* 261:16689-16697 (1986).
24a. Hasemann, C. A., R. G. Kurumbail, S. S. Boddupalli, J. A. Peterson, and J. Deisenhofer. Structure and function of cytochromes P450: a comparative analysis of three crystal structures. *Structure* 2:41–62 (1995).
25. Lecoeur, S., E. Bonierbale, D. Challine, J.-C. Gautier, P. Valadon, P. M. Dansette, R. Catinot, F. Ballet, D. Mansuy, and P. H. Beaune. Specificity of *in vitro* covalent binding of tienilic acid metabolites to human liver microsomes in relationship to the type of hepatotoxicity: comparison with two directly hepatotoxic drugs. *Chem. Res. Toxicol.* 7:434-442 (1994).
26. Leeder, J. S., A. Gaedigk, X. Lu, and V. A. Cook. Epitope mapping studies with human anti-cytochrome P450 3A antibodies. *Mol. Pharmacol.* 49: 234-243 (1996).
27. Bourdi, M., M. Tinel, P. H. Beaune, and D. Pessayre. Interactions of dihydralazine with cytochromes P450 1A: a possible explanation for the appearance of anti-P450 1A2 autoantibodies. *Mol. Pharmacol.* 45:1287-1295 (1994).
28. McGehee, R. E., Jr., M. J. J. Ronis, R. M. Cowherd, M. Ingelman-Sundberg, and T. M. Badger. Characterization of cytochrome 450 2E1 induction in a rat hepatoma FGC-4 cell model by ethanol. *Biochem. Pharmacol.* 48:1823-1833 (1994).
29. Hu, Y., V. Mishin, I. Johansson, C. von Bahr, A. Cross, M. J. J. Ronis, T. M. Badger, and M. Ingelman-Sundberg. Chlormethiazole as an efficient inhibitor of cytochrome P450 2E1 expression in rat liver. *J. Pharmacol. Exp. Ther.* 269:1286-1291 (1994).
30. Brands, R., M. D. Snider, Y. Hino, S. S. Park, H. V. Gelboin, and J. E. Rothman. Retention of membrane proteins by the endoplasmic reticulum. *J. Cell Biol.* 101:1724-1732 (1985).
31. Ilyin, G. P., M. Rissel, Y. Malledant, M. Tanguy, and A. Guillouzo. Human hepatocytes express trifluoroacetylated neoantigens after *in vitro* exposure to halothane. *Biochem. Pharmacol.* 48:561-567 (1994).
32. Deleted in proof.
33. Wu, D., and A. I. Cederbaum. Presence of functionally active cytochrome P-450IIE1 in the plasma membrane of rat hepatocytes. *Hepatology* 16: 515-524 (1992).
34. Robin, M.-A., M. Maratrat, J. Loeper, A.-M. Durand-Schneider, M. Tinel, F. Ballet, P. Beaune, G. Feldmann, and D. Pessayre. Cytochrome P4502B follows a vesicular route to the plasma membrane in cultured rat hepatocytes. *Gastroenterology* 108:1110-1123 (1995).
35. Heijink, E., F. De Matteis, A. H. Gibbs, A. Davies, and I. N. H. White. Metabolic activation of halothane to neoantigens in C57B1/10 mice: immunochemical studies. *Eur. J. Pharmacol.* 248:15-25 (1993).
36. Yamamoto, A. M., C. Mura, C. De Lemos-Chiarandini, R. Kriahnamoorthy, and F. Alvarez. Cytochrome P450IID6 recognized by LKM1 antibody is not exposed on the surface of hepatocytes. *Clin. Exp. Immunol.* 92:381-390 (1993).
37. Black, S. D. Membrane topology of the mammalian P450 cytochromes. *FASEB J.* 6:680-685 (1992).
38. Terelius, Y., K. O. Lindros, E. Albano, and M. Ingelman-Sundberg. Isozyme-specificity of cytochrome P450-mediated hepatotoxicity, in *Frontiers of Biotransformation* (H. Rein and K. Ruckpaul, eds.). Vol 8. Akademic Verlag, Berlin, 187-232 (1992).

Send reprint requests to: Dr. Erik Eliasson, Division of Molecular Toxicology, Department of Environmental Medicine, Karolinska Institutet, S-171 77 Stockholm, Sweden. E-mail: erieli@ki.se

Identification of tryptophan hydroxylase as an intestinal autoantigen

Olov Ekwall, Håkan Hedstrand, Lars Grimelius, Jan Haavik, Jaakko Perheentupa, Jan Gustafsson, Eystein Husebye, Olle Kämpe, Fredrik Rorsman

Summary

Background Autoimmune polyendocrine syndrome type 1 (APS1) is an autosomal recessive disorder with both endocrine and non-endocrine features. Periodic gastrointestinal dysfunction occurs in 25–30% of APS1 patients. We aimed to identify an intestinal autoantigen.

Methods A human duodenal cDNA library was immunoscreened with serum samples from APS1 patients. A positive clone was identified and used for in-vitro transcription and translation, followed by immunoprecipitation with serum samples from 80 APS1 patients from Norway, Finland, and Sweden. Sections of normal and APS1-affected small intestine were immunostained with serum from APS1 patients and specific antibodies. An enzyme-inhibition assay was used to characterise the autoantibodies.

Findings We isolated a cDNA clone coding for tryptophan hydroxylase. 48% (38/80) of APS1 patients had antibodies to tryptophan hydroxylase, whereas no reactivity to this antigen was detected in patients with other autoimmune diseases (n=372) or healthy blood donors (n=70). 89% (17/19) of APS1 patients with gastrointestinal dysfunction were positive for antibodies to tryptophan hydroxylase, compared with 34% (21/61) of patients with no gastrointestinal dysfunction (p<0·0001). Serum from antibody-positive APS1 patients specifically immunostained tryptophan-hydroxylase-containing enterochromaffin cells in normal duodenal mucosa. No serotonin-containing cells were seen in duodenal biopsy samples from APS1 patients. Serum from antibody-positive APS1 patients almost completely inhibited activity of tryptophan hydroxylase.

Interpretation Tryptophan hydroxylase is an endogenous intestinal autoantigen in APS1, and there is an association between antibodies to the antigen and gastrointestinal dysfunction. Analysis of antibodies to tryptophan hydroxylase may be a valuable diagnostic tool to predict and monitor gastrointestinal dysfunction in APS1.

Lancet 1998; **352**: 279–83
See Commentary page 255

Departments of Internal Medicine (O Ekwall MD, H Hedstrand MD, O Kämpe MD, F Rorsman MD), **Pathology** (Prof L Grimelius MD), **and Pediatrics** (J Gustafsson MD), **University Hospital, Uppsala University, Uppsala, Sweden; Department of Biochemistry and Molecular Biology** (Prof J Haavik MD) **and Medical Department B** (E Husebye MD), **University of Bergen, Bergen, Norway; and Hospital for Children and Adolescents, University of Helsinki, Helsinki, Finland** (Prof J Perheentupa MD)

Correspondence to: Dr Olov Ekwall, Department of Internal Medicine, University Hospital, Uppsala University, S-751 85 Uppsala, Sweden

(e-mail: olov.ekwall@medicin.uu.se)

Introduction

Autoimmune polyendocrine syndrome type 1 (APS1; otherwise known as autoimmune polyendocrinopathy, candidosis, ectodermal dystrophy) is a monogenic, autosomal, recessively inherited disorder. The gene that causes this disorder, autoimmune regulator (*AIRE*), has been identified.[1,2] A diagnosis of APS1 requires two of the following features: mucocutaneous candidosis, adrenocortical insufficiency, and hypoparathyroidism.[3] Other common features are failure of gonad function, chronic active hepatitis, alopecia, vitiligo, insulin-dependent diabetes mellitus, and gastrointestinal dysfunction.[4] Autoantibodies to tissue-specific key enzymes are common in APS1.[5-10]

The intestinal dysfunction that affects 25–30% of APS1 patients is characterised by periodic, therapy-resistant steatorrhoea, watery diarrhoea, or constipation. These gastrointestinal disorders interfere with the pharmacological treatment of other elements of APS1. The links between the gastrointestinal symptoms and the other elements of APS1 are unclear, except that hypocalcaemia is known to exacerbate diarrhoea.[11] There is no consistent evidence that dysfunction of the exocrine pancreas[12] or intestinal lymphangiectasis[13] is the cause of the intestinal dysfunction. Organ-specific autoantibodies against many organs have been identified in APS1 patients. We aimed to identify an intestinal autoantigen that could be correlated with symptoms of gastrointestinal dysfunction in APS1 patients.

Patients and methods

Patients

Serum samples were taken from eight Swedish patients, nine Norwegian patients (table 1), and 63 Finnish patients with APS1; the clinical characteristics of the Swedish and Finnish patients have been described elsewhere.[4,10] We also tested serum samples from 224 patients with isolated insulin-dependent diabetes mellitus, 51 with Graves' disease, 31 with Hashimoto's thyroiditis, and 66 with Addison's disease. 70 healthy Swedish blood donors were used as controls. Duodenal biopsy samples from two Swedish APS1 patients with severe gastrointestinal dysfunction were used for immunostaining. The local ethics committee approved our methods, and all experiments were done in accordance with the Helsinki Declaration.

Methods

We used a commercial λGT11 cDNA library constructed from human duodenum (Clontec, Palo Alto, CA, USA) for immunoscreening (as described elsewhere[5]) of APS1 patients' (n=7) serum samples, diluted 1 in 3000. The positive cDNA clones were amplified by PCR with vector primers flanking the insert (KEBO, Solna, Sweden). The products were separated by agarose-gel electrophoresis, and purified with a Jetsorb purification kit (Genomed, Triangle Park, NC, USA). The DNA was quantified and then sequenced with internal primers (KEBO), a dye-terminator-sequencing kit (Perkin Elmer, Foster City, CA, USA), and a DNA sequencer (version 310 or 373A, Applied Biosystems, Foster City, CA, USA).

The cDNA clone that encoded tryptophan hydroxylase

Characteristic	Patient								
	1	2	3	4*	5*	6*	7	8	9
Sex	F	F	M	F	F	F	M	F	M
Year of birth	1957	1958	1948	1990	1986	1981	1990	1967	1962
Intestinal dysfunction	+	−	−	−	−	−	−	−	−
Insulin-dependent diabetes mellitus	−	−	−	−	−	−	−	−	−
Adrenal insufficiency	+	+	+	+	+	+	+	+	+
Hypoparathyroidism	+	+	+	+	−	−	+	+	+
Alopecia	−	−	+	−	−	−	−	+	−
Vitiligo	−	−	+	−	−	+	−	−	−
Pernicious anaemia	−	−	−	−	−	+	−	−	−
Gonad failure	+	+	−	−	−	−	−	+	−

*These patients are sisters.

Table 1: **Clinical characteristics of Norwegian APS1 patients**

(EC.1.14.16.4) was then subcloned into the pSP64-polyA vector (Promega, Madison, WI, USA) to allow optimum in-vitro translation and transcription. We used primers (KEBO) designed to amplify the 1335 bp coding portion of the cDNA and add a 23 bp upstream sequence (CGCAAGCTTGGATCCAATTCACC: A Falorni, personal communication), with the aim of improving transcription and introducing appropriate restriction enzyme sites. After ligation into the *HindIII/XbaI* site of the pSP64-polyA vector, the sequence was analysed to make sure it was correct.

The pSP64-polyA/tryptophan hydroxylase clone was transcribed and translated in vitro with a TNT-SP6 coupled reticulocyte-lysate system (Promega). The size of the radioactive product was measured by means of sodium dodecyl sulphate/polyacrylamide-gel electrophoresis (BioRad, Richmond, CA, USA). Immunoprecipitation was done,[14] and the results were expressed as:

$$\text{Tryptophan hydroxylase antibody index} = \frac{\text{cpm sample} - \text{cpm negative control}}{(\text{cpm positive control} - \text{cpm negative control})} \times 100$$

Each sample was tested three times. One APS1 patient known to have a high titre of antibodies to tryptophan hydroxylase was used as a positive control, and one of the blood donors was used as a negative control. The upper normal limit of the tryptophan hydroxylase antibody index was 14—the mean value for the blood donors plus four SD. Values above this cut-off were taken to indicate the presence of autoantibodies to tryptophan hydroxylase.

Tissue samples from normal human small intestine and duodenal biopsy samples from two APS1 patients were fixed in 10% buffered formalin and processed routinely to paraffin. 5 µm sections were immunostained by the avidin-biotin technique.[15] This method gives better results than immunofluorescence staining of unfixed tissue samples, presumably because of the large amounts of mucins and proteolytic enzymes in intestinal tissue. To assess colocalisation, consecutive intestinal sections made by the mirror technique were immunostained. Before immunostaining, the sections were stored in a citrate buffer at pH 6·0, heated in a microwave oven at 750 W for two periods of 5 min, then left in the buffer at room temperature for 15 min. The sections were then treated with 3% aqueous hydrogen peroxide in a phosphate buffer at pH 7·4 for 15 min so that endogenous peroxide activity was inhibited. We used serum samples from APS1 patients, a specific serotonin antibody (code number YC5/45, Medicorp, Montreal, Canada), and an antiserum to tryptophan hydroxylase (Chemicon, Temecula, CA, USA) as primary antibodies at a dilution of 1 in 100. Control stains omitted the primary antibody or replaced it with serum from a healthy blood donor at a dilution of one in ten.

Activity of tryptophan hydroxylase was measured by radioenzymatic assay,[16] which used 25 µmol/L tritium-labelled L-tryptophan and 0·5 µmol/L 6*R*-tetrahydrobiopterin as substrates. We used 4 µL reticulocyte lysate as the source of tryptophan hydroxylase. The final assay volume of 100 µL contained 0–10 µL patient's serum. The mixture was incubated at 30°C in pH 7·0 buffer for 10 min. A second assay, which used high-performance liquid chromatography with fluorimetric detection, gave similar results (data not shown). Gel chromatography on a Sephacryl-200 column (Pharmacia, Uppsala, Sweden) of tryptophan hydroxylase produced in vitro showed that a substantial fraction migrated as a tetramer complex (data not shown).

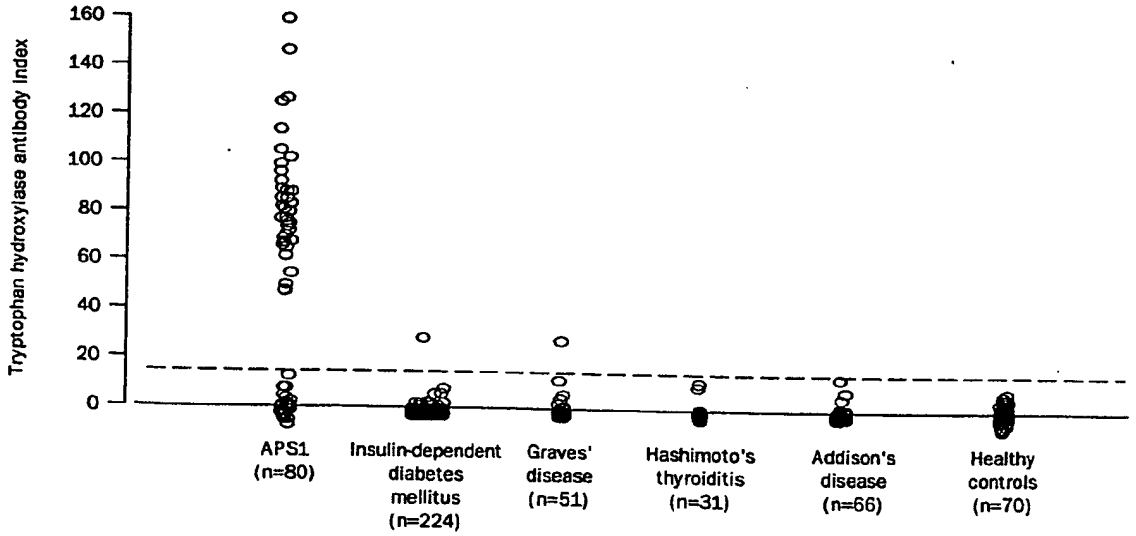

Figure 1: **Immunoreactivity to tryptophan hydroxylase of serum samples from 80 APS1 patients, controls, and patients with other autoimmune endocrine diseases**

Broken line indicates cut-off value for positive result, mean value of negative controls plus 4 SD.

Clinical disorder	Number with disorder/ total	Number with antibodies to tryptophan hydroxylase/total		p*
		With disorder	Without disorder	
Intestinal dysfunction	19/80 (24%)	17/19 (89%)	21/61 (34%)	<0·0001
Insulin-dependent diabetes mellitus	9/80 (11%)	4/9 (44%)	34/71 (48%)	>0·99
Adrenal insufficiency	66/80 (83%)	34/66 (52%)	4/14 (29%)	0·15
Hypoparathyroidism	65/80 (81%)	30/65 (46%)	8/15 (53%)	0·78
Alopecia	26/80 (32%)	11/26 (42%)	27/54 (50%)	0·63
Vitiligo	17/80 (21%)	12/17 (71%)	26/63 (41%)	0·054
Pernicious anaemia	16/80 (20%)	7/16 (44%)	31/64 (48%)	0·79
Gonad failure	27/80 (34%)	13/27 (48%)	25/53 (47%)	>0·99

*Calculated by use of Fisher's test.

Table 2: **Clinical disorders and tryptophan-hydroxylase antibodies in 80 patients with APS1**

Statistical analysis

Fisher's exact test was used to compare the frequencies of reactivity to tryptophan hydroxylase in the patients with and without intestinal and other symptoms.

Results

Immunoscreening of the cDNA library with serum samples from seven APS1 patients identified 13 positive clones, which were partly sequenced. When the clones were screened again with serum samples from nine APS1 patients, two clones showed immunoreactivity with eight of the nine serum samples. These two clones, identified as tryptophan hydroxylase and aromatic aminoacid decarboxylase, were roughly 1·5 kb and 1·4 kb in size. The clone encoding tryptophan hydroxylase was fully sequenced, and comparison with the published sequence[17] showed no variation or mutations.

After in-vitro transcription and translation of the tryptophan hydroxylase gene, we showed that 6–7% of sulphur-35-labelled methionine was incorporated into the protein. On denaturing polyacrylamide-gel electrophoresis a band with the expected size of about 58 kDa was seen.

38 (48%) of the 80 patients had a tryptophan hydroxylase antibody index of more than 14, indicating the presence of autoantibodies (figure 1). However, the frequency of reactivity varied between patients from different countries. All eight of the Swedish APS1 patients showed reactivity against tryptophan hydroxylase, compared with only 28 of the 63 Finnish patients and two of the nine Norwegian patients. There was no significant difference in frequency of reactivity between men (17 [46%] of 37) and women (21 [48%] of 43). 17 (89%) of 19 patients with intestinal symptoms showed reactivity, compared with 21 (34%) of 61 patients without intestinal symptoms ($p<0·0001$). No significant associations were shown between the presence of tryptophan hydroxylase autoantibodies and other components of the syndrome (table 2).

All eight of the serum samples from Swedish patients with autoantibodies to tryptophan hydroxylase also caused cytoplasmic staining of enterochromaffin cells. These cells were identified by staining of consecutive duodenal sections with a specific antibody against serotonin (figure 2). Some samples also stained secretory granules in Paneth cells (three) and goblet cells (three). Serum samples from blood donors and APS1 patients without

Figure 2: **Immunostaining of consecutive sections of normal human small intestine with serum from an APS1 patient (A) and a specific serotonin antibody (B)**
Reduced by 33% from ×281. Immunostains diluted 1 in 100. Cells stained by the patients' serum are the same as the enterochromaffin cells stained by the serotonin antibody (arrows).

Figure 3: **Immunostaining of normal duodenum (A) and duodenal biopsy sample from an APS1 patient with gastrointestinal dysfunction (B) with monoclonal antibody to serotonin**
Reduced by 50% from ×62·5. Immunostains diluted 1 in 100.

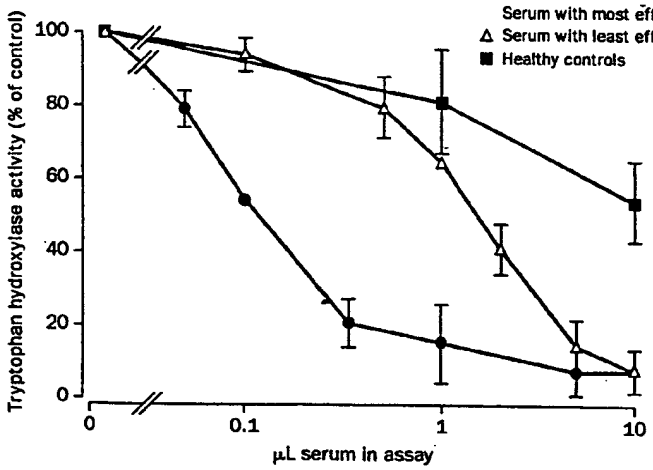

Figure 4: **Effect of serum from two APS1 patients and blood donors on activity of human tryptophan hydroxylase**
Activity without serum added 0·13 nmol min^{-1} mL^{-1}. Representative results for the patients with the greatest and the least effect are shown; values are mean of three or four separate assays (patients) or single assay (controls); error bars indicate SD.

antibodies to tryptophan hydroxylase did not cause any specific immunostaining. Immunostaining of duodenal biopsy samples from two APS1 patients showed no serotonin-containing enterochromaffin cells, unlike normal duodenum (figure 3).

To assess whether the presence of serum from APS1 patients affected the activity of tryptophan hydroxylase, we produced the enzyme by in-vitro translation and transcription, and assayed its activity in the presence of serum samples from 16 APS1 patients and 11 healthy blood donors. Addition of serum from blood donors at a final dilution of one in ten resulted in a non-specific decrease in activity to about 50–60% of that of control experiments without any serum (figure 4). The decrease was possibly due to high concentrations of protein and free aminoacids in the serum. By contrast, serum samples at a similar dilution from APS1 patients almost completely inhibited the enzyme activity; also there was partial inhibition of enzyme activity with patients' serum at a dilution at which the blood-donor serum samples had no significant effect (figure 4). At a final dilution of 1 in 100, addition of serum samples with reactivity to tryptophan hydroxylase caused 35–98% inhibition of the enzyme activity.

Discussion

Our findings suggest that tryptophan hydroxylase, the rate-limiting enzyme in the synthesis of serotonin,[18] is an important intestinal autoantigen in patients with APS1. Tryptophan hydroxylase is a 230 kDa tetramer made up of identical subunits each with a molecular mass of 58 kDa. It is expressed in serotonin-producing cells in the central nervous system and the intestine.[19] In the intestine, tryptophan hydroxylase and serotonin are present in enterochromaffin cells in the mucosa, and in neuronal cells in the submucosal and myenteric plexus. The specific staining of enterochromaffin cells in the mucosa of normal duodenum by serum from APS1 patients and the complete absence of enterochromaffin cells from duodenal biopsy samples from APS1 patients suggest that tryptophan hydroxylase is an antigen linked to intestinal dysfunction in APS1. The staining of Paneth and goblet cells suggests that there are additional intestinal autoantigens linked to APS1. These findings also support the hypothesis that autoimmune mechanisms, rather than mechanisms secondary to other components of APS1 such as candidosis or hypocalcaemia, may cause the intestinal symptoms.

Polyclonal and monoclonal antibodies to the pteridine-dependent aminoacid hydroxylases tryptophan hydroxylase, tyrosine hydroxylase, and phenylalanine hydroxylase have been generated experimentally.[20,21] Some of these antibodies are enzyme-specific, and others recognise all three enzymes. Although the mouse and rabbit antibodies can either stimulate or inhibit the enzymes, all the tryptophan hydroxylase antibodies that we found in APS1 patients are inhibitory. The inhibitory autoantibodies in APS1 patients were specific for tryptophan hydroxylase; there was no significant inhibition of human tyrosine hydroxylase (isoform 1) or human phenylalanine hydroxylase under similar experimental conditions (data not shown). Although the inhibition of tryptophan hydroxylase activity by APS1 serum in vitro shows that the autoantibody reaction is highly specific, we cannot assume that the same is true in vivo without further experimental evidence.[22]

Serotonin is generally believed to upregulate intestinal motility.[23] However, we cannot rule out the possibility that the complete loss of serotonin-producing enterochromaffin cells observed in our patients may affect other regulatory systems; this hypothesis would explain why both diarrhoea and constipation occur in APS1 patients. In our study, 17 (89%) of 19 APS1 patients with gastrointestinal problems were positive for antibodies to tryptophan hydroxylase, which suggests that these antibodies are a marker for gastrointestinal dysfunction in APS1. The absence of these antibodies from patients with other autoimmune diseases and healthy blood donors shows that these antibodies are highly specific. The finding that 34% (21 of 61) APS1 patients without gastrointestinal symptoms were positive for antibodies to tryptophan hydroxylase may be explained by under-reporting of gastrointestinal symptoms, subclinical disease, or the appearance of antibodies before the onset of clinical symptoms. The differences in frequency of autoantibodies in APS1 patients from Sweden, Finland, and Norway may perhaps be explained by the occurrence of different mutations of the *AIRE* gene in the three populations.

Our findings may lead to the identification of autoantigens in other autoimmune diseases.[24] Antibodies to tryptophan hydroxylase should be sought in people with other gastrointestinal diseases, such as Crohn's disease, ulcerative colitis, and irritable-bowel syndrome. Autoimmune enteropathy[25,26] and pseudo-obstruction in connection with small-cell carcinoma[27] are two disorders in which immunoreactivity against mucosal cells or submucosal neurons has been shown, but no autoantigen has yet been identified. Immunotherapy of malignant melanoma with tyrosinase has been proposed,[28] and tyrosinase has also been identified as an autoantigen in autoimmune vitiligo.[29] Immunisation with tryptophan hydroxylase, or with fragments of this protein, may be a suitable treatment for malignant gut carcinoids that

originate from serotonin-producing enterochromaffin cells.

The identification of tryptophan hydroxylase as an intestinal autoantigen raises the question of why many autoantigens, such as glutamic acid decarboxylase in insulin-dependent diabetes mellitus and aminoacid decarboxylase in APS1, are key enzymes in the synthetic pathways of neurotransmitters. These enzymes may share properties that make them potent triggers of the immune system. Alternatively, the presentation of these enzymes in the thymus may be incomplete, since they are expressed rather late during fetal development.

We identified tryptophan hydroxylase through immunoscreening of an intestinal cDNA library despite the fact that initial immunoblotting experiments did not show any consistent reactivity against whole intestinal tissue. In retrospect, this was probably because tryptophan hydroxylase is only present in a small fraction of intestinal cells and in concentrations below the detection level for immunoblotting. This may be of relevance when trying to identify other autoantigens in tissues containing different cell types. Further showing the specificity of the approach to immunoscreen cDNA libraries, a clone coding for aminoacid decarboxylase—a known autoantigen in APS1[8] with a much broader tissue-distribution—was identified by several serum samples.[30]

The identification of antibodies to tryptophan hydroxylase in APS1 may be a useful diagnostic marker to predict and monitor intestinal disorders associated with this autoimmune disease. It may also add to our understanding of the pathogenesis of these intestinal disorders in APS1, and lead to more effective treatment.

Contributors

Olov Ekwall was the main investigator, supervised by Fredrik Rorsman and Olle Kämpe. Håkan Hedstrand contributed to the cloning of tryptophan hydroxylase. Lars Grimelius did the immunostainings and interpreted the results. Jan Haavik designed and ran the assays for tryptophan hydroxylase. Jaakko Perheentupa in Finland, Jan Gustafsson in Sweden, and Eystein Husebye in Norway supplied serum samples from APS1 patients and information on their clinical characteristics. All investigators contributed to writing of the paper.

Acknowledgments

This study was supported by grants from the Swedish Medical Research Council, the Swedish Cancer Society, the Torsten and Ragnar Söderberg Fund, the Swedish Diabetes Association, the Swedish Society of Medicine, the Torsten Nilsson Fund, the Åke Wiberg Foundation, the Lennander Fund, and the Ernfors Family Fund. We thank Katrin Österlund and Majlis Book for technical assistance, Lars Berglund for help with statistical analysis, Mona Landin-Olsson for insulin-dependent diabetes mellitus serum samples, and Tiinamaija Tuomi for help with the Finnish APS1 serum samples.

References

1 The Finnish-German APECED Consortium. An autoimmune disease, APECED, caused by mutations in a novel gene featuring two PHD-type zinc-finger domains. *Nat Genet* 1997; 17: 399–403.

2 Nagamine K, Peterson P, Scott HS, et al. Positional cloning of the APECED gene. *Nat Genet* 1997; 17: 393–98.

3 Neufeld M, Maclaren N, Blizzard R. Autoimmune polyglandular syndromes. *Pediatr Ann* 1980; 9: 154–62.

4 Ahonen P, Myllarniemi S, Sipila I, Perheentupa J. Clinical variation of autoimmune polyendocrinopathy-candidiasis-ectodermal dystrophy (APECED) in a series of 68 patients. *N Engl J Med* 1990; 322: 1829–36.

5 Chen S, Sawicka J, Betterle C, et al. Autoantibodies to steroidogenic enzymes in autoimmune polyglandular syndrome, Addison's disease, and premature ovarian failure. *J Clin Endocrinol Metab* 1996; 81: 1871–76.

6 Peterson P, Uibo R, Peranen J, Krohn K. Immunoprecipitation of steroidogenic enzyme autoantigens with autoimmune polyglandular syndrome type I (APS I) sera; further evidence for independent humoral immunity to P450c17 and P450c21. *Clin Exp Immunol* 1997; 107: 335–40.

7 Winqvist O, Karlsson FA, Kämpe O. 21-Hydroxylase, a major autoantigen in idiopathic Addison's disease. *Lancet* 1992; 339: 1559–62.

8 Rorsman F, Husebye ES, Winqvist O, Björk E, Karlsson FA, Kämpe O. Aromatic-L-amino-acid decarboxylase, a pyridoxal phosphate-dependent enzyme, is a beta-cell autoantigen. *Proc Natl Acad Sci USA* 1995; 92: 8626–29.

9 Tuomi T, Björses P, Falorni A, et al. Antibodies to glutamic acid decarboxylase and insulin-dependent diabetes in patients with autoimmune polyendocrine syndrome type I. *J Clin Endocrinol Metab* 1996; 81: 1488–94.

10 Gebre-Medhin G, Husebye ES, Gustafsson J, et al. Cytochrome P450IA2 and aromatic L-amino acid decarboxylase are hepatic autoantigens in autoimmune polyendocrine syndrome type I. *FEBS Lett* 1997; 412: 439–45.

11 Heubi JE, Partin JC, Schubert WK. Hypocalcemia and steatorrhea—clues to etiology. *Dig Dis Sci* 1983; 28: 124–28.

12 Scire G, Magliocca FM, Cianfarani S, Scalamandre A, Petrozza V, Bonamico M. Autoimmune polyendocrine candidiasis syndrome with associated chronic diarrhea caused by intestinal infection and pancreas insufficiency. *J Pediatr Gastroenterol Nutr* 1991; 13: 224–27.

13 Bereket A, Lowenheim M, Blethen SL, Kane P, Wilson TA. Intestinal lymphangiectasia in a patient with autoimmune polyglandular disease type I and steatorrhea. *J Clin Endocrinol Metab* 1995; 80: 933–35.

14 Husebye ES, Gebre-Medhin G, Tuomi T, et al. Autoantibodies against aromatic L-amino acid decarboxylase in autoimmune polyendocrine syndrome type I. *J Clin Endocrinol Metab* 1997; 82: 147–50.

15 Portela-Gomes GM, Stridsberg M, Johansson H, Grimelius L. Complex co-localization of chromogranins and neurohormones in the human gastrointestinal tract. *J Histochem Cytochem* 1997; 45: 815–22.

16 Vrana SL, Dworkin SI, Vrana KE. Radioenzymatic assay for tryptophan hydroxylase: [^{3}H]H_2O release assessed by charcoal adsorption. *J Neurosci Methods* 1993; 48: 123–29.

17 Boularand S, Darmon MC, Ganem Y, Launay JM, Mallet J. Complete coding sequence of human tryptophan hydroxylase. *Nucleic Acids Res* 1990; 18: 4257.

18 Boadle-Biber MC. Regulation of serotonin synthesis. *Prog Biophys Mol Biol* 1993; 60: 1–15.

19 Hufton SE, Jennings IG, Cotton RG. Structure and function of the aromatic amino acid hydroxylases. *Biochem J* 1995; 311: 353–66.

20 Friedman PA, Lloyd T, Kaufman S. Production of antibodies to rat liver phenylalanine hydroxylase: cross-reactivity with other pterin-dependent hydroxylases. *Mol Pharmacol* 1972; 8: 501–10.

21 Haan EA, Jennings IG, Cuello AC, et al. Identification of serotonergic neurons in human brain by a monoclonal antibody binding to all three aromatic amino acid hydroxylases. *Brain Res* 1987; 426: 19–27.

22 Manns MP, Zanger U, Gerken G, et al. Patients with type II autoimmune hepatitis express functionally intact cytochrome P-450 db1 that is inhibited by LKM-1 autoantibodies in vitro but not in vivo. *Hepatology* 1990; 12: 127–32.

23 Kobayashi T, Hasegawa H, Kaneko E, Ichiyama A. Gastrointestinal serotonin: depletion due to tetrahydrobiopterin deficiency induced by 2,4-diamino-6-hydroxypyrimidine administration. *J Pharmacol Exp Ther* 1991; 256: 773–79.

24 Winqvist O, Gebre-Medhin G, Gustafsson J, et al. Identification of the main gonadal autoantigens in patients with adrenal insufficiency and associated ovarian failure. *J Clin Endocrinol Metab* 1995; 80: 1717–23.

25 Mirakian R, Richardson A, Milla PJ, et al. Protracted diarrhoea of infancy: evidence in support of an autoimmune variant. *BMJ* 1986; 293: 1132–36.

26 Corazza GR, Biagi F, Volta U, Andreani ML, De Franceschi L, Gasbarrini G. Autoimmune enteropathy and villous atrophy in adults. *Lancet* 1997; 350: 106–09.

27 Lennon VA, Sas DF, Busk MF, et al. Enteric neuronal autoantibodies in pseudo-obstruction with small-cell lung carcinoma. *Gastroenterology* 1991; 100: 137–42.

28 Yee C, Gilbert MJ, Riddell SR, et al. Isolation of tyrosinase-specific CD8+ and CD4+ T cell clones from the peripheral blood of melanoma patients following in vitro stimulation with recombinant vaccinia virus. *J Immunol* 1996; 157: 4079–86.

29 Song YH, Connor E, Li Y, Zorovich B, Balducci P, Maclaren N. The role of tyrosinase in autoimmune vitiligo. *Lancet* 1994; 344: 1049–52.

30 Rahman MK, Nagatsu T, Kato T. Aromatic L-amino acid decarboxylase activity in central and peripheral tissues and serum of rats with L-DOPA and L-5-hydroxytryptophan as substrates. *Biochem Pharmacol* 1981; 30: 645–49.

Identification of tissue transglutaminase as the autoantigen of celiac disease

WALBURGA DIETERICH[1], TOBIAS EHNIS[1], MICHAEL BAUER[1], PETER DONNER, UMBERTO VOLTA, ERNST OTTO RIECKEN[1] & DETLEF SCHUPPAN[1]

[1]*Department of Gastroenterology, Klinikum Benjamin Franklin, Free University of Berlin, Hindenburgdamm 30, 12200 Berlin, Germany*
[2]*Research Laboratories of Schering AG, 13342 Berlin, Germany*
[3]*Istituto di Clinical Medical generale e Terapia Medica, Policlinico S.Orsola, via Massarenti 9, 40138 Bologna, Italy*
Correspondence should be addressed to D.S.

Celiac disease is characterized by small intestinal damage with loss of absorptive villi and hyperplasia of the crypts, typically leading to malabsorption[1]. In addition to nutrient deficiencies, prolonged celiac disease is associated with an increased risk for malignancy, especially intestinal T-cell lymphoma[2,3]. Celiac disease is precipitated by ingestion of the protein gliadin, a component of wheat gluten, and usually resolves on its withdrawal. Gliadin initiates mucosal damage which involves an immunological process in individuals with a genetic predisposition. However, the mechanism responsible for the small intestinal damage characteristic of celiac disease is still under debate[4-6]. Small intestinal biopsy with the demonstration of a flat mucosa which is reversed on a gluten-free diet is considered the main approach for diagnosis of classical celiac disease[7]. In addition, IgA antibodies against gliadin and endomysium, a structure of the smooth muscle connective tissue, are valuable tools for the detection of patients with celiac disease and for therapy control[7-9]. Incidence rates of childhood celiac disease range from 1:300 in Western Ireland to 1:4700 in other European countries[10-12], and subclinical cases detected by serological screening revealed prevalences of 3.3 and 4 per 1000 in Italy and the USA, respectively[13,14]. IgA antibodies to endomysium are particularly specific indicators of celiac disease[8,15], suggesting that this structure contains one or more target autoantigens that play a role in the pathogenesis of the disease[16,17]. However, the identification of the endomysial autoantigen(s) has remained elusive. We identified tissue transglutaminase as the unknown endomysial autoantigen. Interestingly, gliadin is a preferred substrate for this enzyme, giving rise to novel antigenic epitopes.

Western blotting with serum samples from active celiac disease patients containing high-titer antiendomysial IgA antibodies did not allow us to identify specific protein bands in extracts from placenta, uterus, liver or gut, possibly because of loss of antigenicity of the partially denatured protein preparations. Therefore, we used immunoprecipitation from cell cultures, a method that can be used for target antigens susceptible to denaturation.

Cell cultures were screened by immunohistochemistry for the expression of the autoantigen with high-titer sera of patients with celiac disease and the alkaline phosphatase/monoclonal anti-alkaline phosphatase (APAAP) technique[18]. This method revealed that cytoplasmic vesicles of HT1080 (human fibrosarcoma) cells, WI38 (human embryonal fibroblasts) as well as Hep1 and HepG2 (human hepatocarcinoma) cells were specifically stained by the patients' IgA antibodies. We then immunoprecipitated both supernatant and cell lysate of HT1080 cells metabolically labeled with [^{35}S]methionine, using the IgA fraction from celiac disease sera bound to Sepharose. After separation by SDS–polyacrylamide gel electrophoresis (SDS–PAGE) and autoradiography, immunoprecipitation of the supernatant yielded varying amounts of a high-molecular-weight protein that was identified as fibronectin by western blotting and by the characteristic peptide pattern after protease V8 digest (data not shown). When the cell lysate was analyzed in a similar way, a single protein band with an apparent relative molecular weight (M_r) of 85,000 before and after disulfide reduction was immunoprecipitated exclusively with 25 celiac disease serum samples, but with none of 25 control serum samples (from healthy adults, patients with ulcerous colitis or Crohn's disease, or patients with Sjögren's syndrome, an autoimmune disease characterized by high-titer serum autoantibodies) (Fig. 1, *a* and *b*). As before, varying quantities of fibronectin could be precipitated in celiac disease, but also small amounts were precipitated in some control sera, suggesting that this large adhesive glycoprotein was not the primary target of the celiac disease autoimmune response. Instead, fibronectin may have precipitated nonspecifically or in association with the 85-kDa autoantigen (see below).

In order to further characterize the putative 85-kDa autoantigen, larger quantities of the protein were isolated by immunoprecipitation, SDS–PAGE and electrophoretic elution, followed by cleavage with endoproteinase Asp-N. The resultant fragments were separated in a 10% tricine gel (Fig. 2*a*) and transferred to a polyvinylidene-difluoride membrane. Three major cleavage products with M_r 10,000, 14,000 and 16,000 were excised and subjected to amino-terminal sequence analysis. All three peptides yielded sequences that could be clearly assigned to tissue transglutaminase (EC 2.3.2.13, tTG)[19] (Fig. 2*b*). An interaction of tTG with fibronectin has been described[20], which might explain the occasional coprecipitation of fibronectin with tTG in our immunoprecipitation experiments.

Tissue transglutaminase (synonymous with erythrocyte, cellular, endothelial, cytoplasmic, type II or liver TG)[21] belongs to a family of calcium-dependent enzymes that catalyze the crosslinking of proteins resulting in the formation of an ε-(γ-glutamyl)-lysine bond. Whereas several proteins can serve as acceptor substrates, only a limited number of donor substrates exists. The physiological role of the tTG has only been partly explored. Although the enzyme is normally localized in the cytoplasm, tTG can be released during wounding, where it associ-

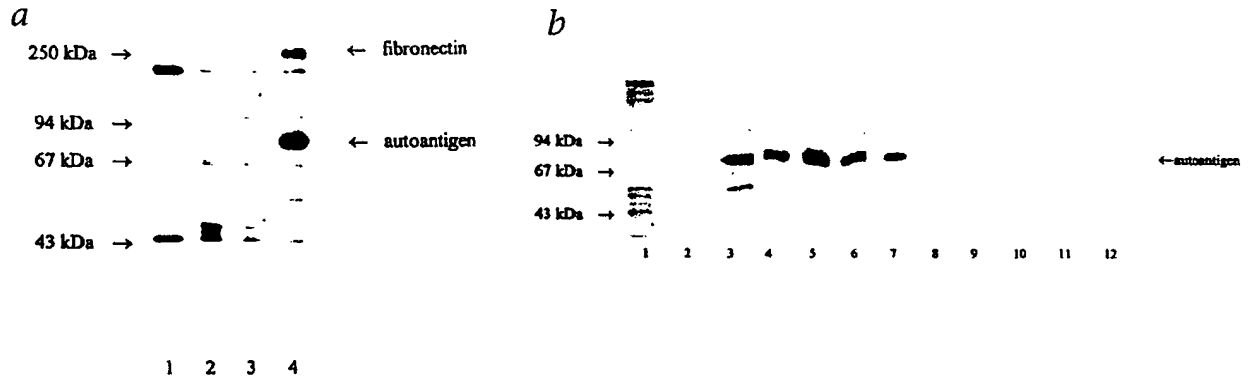

Fig. 1 IgA antibodies of celiac disease sera precipitate a characteristic protein species from cell cultures. Autoradiography of the immunoprecipitated cell lysate from HT1080 cells after separation by SDS–PAGE under reducing conditions. *a* (lane 1), Preadsorption on plain Sepharose CL-4B shows nonspecific binding of two major proteins; (lanes 2 and 3), immunoprecipitates with serum IgA from healthy controls and (lane 4), precipitation of the 85-kDa autoantigen by serum IgA from a patient with celiac disease. Note high-molecular-mass material that was identified as fibronectin, which coprecipitated from samples from patients with celiac disease as well as some with non-celiac disease. *b*, Immunoprecipitates with serum IgA from celiac disease patients and controls: (lane 1), material preadsorbed on plain Sepharose; (lane 2), healthy control; (lanes 3–7), patients with celiac disease; (lane 8), Crohn's disease; (lane 9), ulcerative colitis; (lanes 10–12), patients with Sjögren's syndrome.

ates with cell surfaces or certain extracellular matrix molecules[23]. tTG can crosslink fibronectin[20,23], osteonectin[24], collagen II[24], V and XI[25], procollagen III[26] and nidogen[27]. Thus, secreted tTG is thought to stabilize the provisional extracellular matrix in granulation tissue[22]. Furthermore, its expression is enhanced during apoptosis, leading to irreversible crosslinking of intracellular proteins, and may be deranged during growth of some tumors[28–30]. The commercially available enzyme from guinea pig liver shows a high-protein sequence identity with human tTG (>80%)[19], with a high probability of conserved antigenic epitopes, which allowed us to carry out further experiments with this preparation.

Gliadin, the dietary factor incriminated in the initial pathogenesis of celiac disease, contains numerous glutamines amounting to approximately 40% of its amino acids[4]. In order to test whether gliadin could serve as a substrate for tTG, we used an *in vitro* assay with radiolabeled putrescine as acceptor substrate[27]. Gliadin proved to be an excellent substrate and was quantitatively crosslinked by tTG, whereas the control proteins (chicken albumin, bovine serum albumin, α-lactalbumin, β-lactoglobulin) were essentially unaltered (data not shown). These results are in accord with previous reports that showed preferential incorporation of putrescine in gliadin by a transglutaminase extract from intestinal tissue[31] and also crosslinking of gliadin by a lysate of human red blood cells that contain tTG (ref. 31).

The celiac disease-specific IgA autoantibodies to endomysium are detected and semiquantified by performing indirect im-

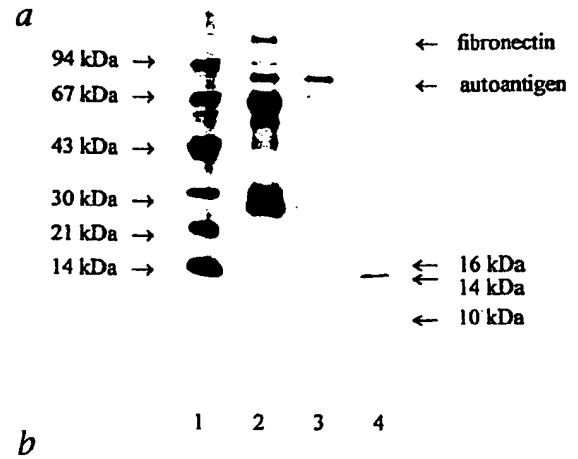

b

tissue transglutaminase: 28′ Arg Glu Lys Leu Val Val Arg Arg Gly Gln Pro Phe Trp

10 kDa fragment: Arg Glu Lys Leu Val Val Arg Arg Gly Gln Pro Phe (Ser)

tissue transglutaminase: 581′ Asp Leu Tyr Leu Glu Asn Pro Glu Ile Lys Ile Arg Ile Leu Gly

14 kDa fragment: Asp Leu Tyr Leu Glu Asn Pro Glu Ile -X- Ile -X- Ile Leu Gly

tissue transglutaminase: 438′ Asp Ile Thr His Thr Tyr Lys Tyr Pro Glu

16 kDa fragment: Asp Ile Thr Leu Thr Tyr Gln Tyr Pro (Val)

Fig. 2 Purification and amino-terminal sequence analysis of the 85-kDa autoantigen. *a*, Separation of the unlabeled immunoprecipitated 85-kDa autoantigen by SDS–PAGE under reducing conditions; proteins revealed by silver staining. (lane 1), Molecular weight standard (as mass); (lane 2), immunoprecipitate of the 85-kDa autoantigen; additional major bands are fibronectin, and light and heavy immunoglobulin chains (25–30 kDa and 60–65 kDa, respectively); (lane 3), 85-kDa autoantigen purified by electrophoretic elution; (lane 4), fragments of the purified autoantigen after digestion with endoproteinase Asp-N; the three peptides subjected to N-terminal sequence analysis are marked. *b*, The N-terminal sequence data of the three fragments of the 85-kDa autoantigen generated by endoproteinase Asp-N were compared with the Swiss-Prot 31 data base (PC/GENE, IntelliGenetics) and found compatible with human tissue transglutaminase (EC 2.3.2.13). The identity of residue X is unknown, residues in parentheses are uncertain.

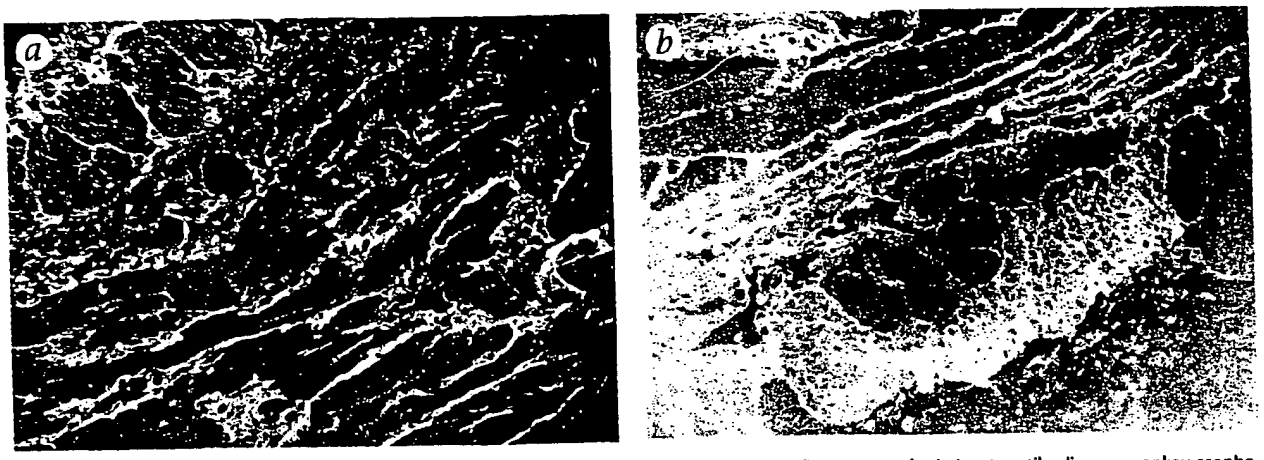

Fig. 3 Tissue transglutaminase as the prominent autoantigen of celiac disease. Indirect immunofluorescence for IgA autoantibodies on monkey esophagus (×62.5). *a*, The characteristic staining of endomysial structures by high-titer celiac disease serum (dilution 1:320). *b*, Loss of specific staining after preincubation of the same serum dilution with tTG, suggesting that the identified tTG is the prominent, if not sole, autoantigen in celiac disease.

munofluorescence on muscular sections of monkey esophagus or umbilical cord[9,15,22]. In order to further confirm tTG as the autoantigen in celiac disease, we performed indirect immunofluorescence with high-titer celiac disease serum samples on monkey esophagus with or without prior preincubation of the sera with tTG. Whereas untreated celiac disease serum samples showed the characteristic feature of endomysial labeling, pretreatment with tTG nearly completely abolished endomysial immunofluorescence (Fig. 3, *a* and *b*). This demonstrated that tTG represents the predominant, if not sole, endomysial autoantigen considered characteristic for celiac disease.

On the basis of these data, we established an enzyme-linked immunosorbent assay (ELISA) for the detection of IgA anti-tTG antibodies. Serum samples either from celiac disease patients with well-known anti-endomysium titers (as determined by immunofluorescence) or from controls were analyzed. In this ELISA only celiac disease patients displayed elevated levels of IgA anti-tTG, whereas none of the controls showed significant reactivity (Table 1). Furthermore, two of the high-titer sera were retested at higher dilutions. Even at 1:3200 these sera exhibited extinctions of $A = 1.02 \pm 0.09$ (celiac disease A) and 0.84 ± 0.12 (celiac disease C), thus demonstrating the high sensitivity of the ELISA test (data not shown). In addition, there was a good correlation between decreasing titers of anti-endomysium IgA and the IgA antibodies to tTG as measured by ELISA once patients were on a gluten-free diet (Table 2). We also measured IgG autoantibodies to tTG using the same ELISA system, in which the anti-IgA antibody was replaced by an anti-IgG antibody. Even though the high-titer celiac disease sera showed elevated anti-tTG IgG levels, this system was not comparable in sensitivity and specificity to the IgA-based ELISA (Table 2). In addition, some control sera, especially those of patients with chronic inflammatory disorders, showed raised titers of IgG anti-tTG (data not shown). The high sensitivity and specificity for celiac disease of IgA class autoantibodies to tTG is most plausibly explained by the prominent production of IgA by mucous membranes, especially those of the intestinal tract, with the IgA anti-tTG response thus reflecting the active phase of intestinal mucosal injury.

The identification of tTG as the autoantigen in celiac disease should fuel novel concepts about the insufficiently understood pathogenesis of celiac disease. The usually intracellular enzyme is released from cells during wounding[22]. One of its roles is the irreversible crosslinking of a small set of extracellular matrix and some cytoplasmic proteins, including cytoskeletal elements. This crosslinking might stabilize the wound area and protect the surrounding tissue from further damage. In addition, cytoskeletal crosslinking has been reported in apoptosis, leading to the noninflammatory elimination of potentially dangerous infected cells[23].

The finding that gliadin is a preferred substrate for the otherwise highly substrate-specific enzyme is of particular interest.

Table 1 Enzyme-linked immunosorbent assay (ELISA) based on tTG for the celiac disease (CD) autoantigen

Serum sample	EmA titer	Serum IgA anti-tTG dilution (1:400)
CD A	(1:640)	>3.500
CD B	(1:320)	>3.500
CD C	(1:320)	3.114 ± 0.024
CD D	(1:320)	1.257 ± 0.024
CD E	(1:320)	1.977 ± 0.018
CD F	(1:320)	1.525 ± 0.085
CD G	(1:160)	1.208 ± 0.019
CD H	(1:160)	0.747 ± 0.048
CD I	(1:160)	2.174 ± 0.291
CD K	(1:80)	0.667 ± 0.037
CD L	(1:80)	1.372 ± 0.093
CD M	(1:40)	0.286 ± 0.009
Ulcerative colitis	(ND)	0.119 ± 0.014
Indeterminate colitis	(ND)	0.092 ± 0.016
Crohn's disease	(ND)	0.090 ± 0.001
Sjögren's syndrome	(ND)	0.137 ± 0.004
Sjögren's syndrome	(ND)	0.082 ± 0.003
Alcoholic liver fibrosis	(ND)	0.059 ± 0.001
Healthy control	(ND)	0.070 ± 0.001

An ELISA for IgA antibodies against tTG was established. Shown are the optical densities of twelve different celiac disease serum samples with varying anti-endomysium antibody (EmA) titers as well as seven control sera. Sera were diluted 1:400 and listed according to their EmA titer (in parentheses). All celiac disease sera with high EmA-titers (>1:80) show high anti-tTG IgA titers, whereas the control sera display background levels. Celiac disease sera with low EmA-titer (<1:80) show only slightly raised ELISA titers, but are highly elevated above controls when diluted 1:100 (0.67 ± 0.02 versus 0.12 ± 0.01; celiac disease M, not shown). Values are means (±s.d.) of three parallel determinations. ND, not determined.

Table 2 IgA and IgG anti-tTG antibodies in celiac disease (CD) patients before and after a gluten-free diet

Serum sample	EmA titer	IgA anti-tTG dilution (1:400)	IgG anti-tTG dilution (1:100)
CD A	(1:640)	>3.500	1.267 ± 0.030
CD A gfd	(neg)	0.321 ± 0.013	1.055 ± 0.055
CD B	(1:320)	>3.500	3.116 ± 0.058
CD B gfd	(1:40)	0.286 ± 0.009	0.569 ± 0.009
CD C	(1:320)	3.114 ± 0.024	1.360 ± 0.009
CD C gfd	(neg.)	0.162 ± 0.002	0.959 ± 0.024
CD E	(1:320)	1.977 ± 0.018	0.827 ± 0.032
CD E gfd	(neg.)	0.186 ± 0.041	0.504 ± 0.045
CD F	(1:320)	1.525 ± 0.085	0.555 ± 0.016
CD F gfd	(1:80)	1.372 ± 0.093	3.186 ± 0.069
CD G	(1:160)	1.208 ± 0.019	1.154 ± 0.011
CD G gfd	(1:20)	0.066 ± 0.010	0.370 ± 0.008
CD H	(1:160)	0.747 ± 0.048	0.563 ± 0.014
CD H gfd	(1:80)	0.667 ± 0.037	1.632 ± 0.016

ELISA data for IgA (1:400) and IgG (1:100) class antibodies against tTG of seven different CD serum samples before and after a gluten-free diet (gfd). EmA-titers are given in parentheses. IgA anti-tTG antibodies decline in most patients kept on a gfd. Compared with IgA anti-tTG antibodies, IgG anti-tTG antibodies appear less sensitive markers for the active phase of CD; titers are means (±s.d.) of three parallel determinations.

Bruce *et al.*[30] already demonstrated that gliadin efficiently incorporates putrescine in the presence of intestinal extracts containing transglutaminase. However, these researchers did not differentiate the responsible enzyme nor implicate tTG as the endomysial autoantigen of celiac disease. Furthermore, localization of the intestinal TG within the lamina propria mucosae, with only 1% in the epithelial layer[30], is in agreement with the site of immunological damage in celiac disease.

We hypothesize that damage or hyperpermeability of the intestinal epithelium, either owing to toxic gluten fractions or to other (minor) irritants, triggers the abundant extracellular release of cytosolic tTG, mainly by lamina propria mononuclear or mesenchymal cells. Subsequent crosslinking of dietary gliadin results in gliadin–gliadin or gliadin–tTG complexes and thus creates antigenic neoepitopes. These neoepitopes could then initiate an immune response in genetically susceptible individuals, finally directed both to gliadin and tTG. In fact, a genetic predisposition has been found in celiac disease patients, who often bear the major histocompatibility complex antigens HLA-DQ(α1*0501,β1*0201)[4,33]. Further support comes from our preliminary data showing that a proportion of the IgA autoantibodies of celiac disease patients are directed to such neoepitopes (data not shown). Taken together, these data are well in line with the suggested importance of the celiac disease autoantigen in the pathogenesis of the disease as suggested by others[14,17]. Nevertheless, it must be borne in mind that celiac disease is not a classical autoimmune disease, since IgA antibodies to tTG disappear when gliadin is strictly removed from the diet, and the mucosal damage is reversed without residual fibrosis or scarring.

Our findings further suggest that the immunological detection of IgA autoantibodies to tTG, the newly discovered autoantigen of celiac disease, is a useful tool in the diagnosis and follow-up of the disease. Because of its simplicity, the ELISA for the identified autoantigen now allows an economical and rapid screening of large portions of the general population for the presence of latent or subclinical celiac disease. Therefore, the too-long intervals from early symptoms to diagnosis and finally treatment of celiac disease (median 5.4 years in Germany)[34] could be shortened decisively, leading to a decreased morbidity from this intestinal disease.

We cannot completely exclude IgA autoantibodies to tTG in diseases with mucosal lesions that are similar to celiac disease lesions, for example, tropical sprue, giardiasis, cow milk enteropathy or postenteritis syndrome. However, we think that it is quite unlikely to find these tTG autoantibodies in sera of these patients, because no IgA EmA were found in serum samples from patients with cow milk enteropathy, giardiasis or postenteritis syndrome[9]. Furthermore, no association of these diseases to the celiac disease-associated HLA-DQ genes is described.

By assuming a yet unproven potential of tTG, which is released during wound healing to serve as a further trigger for celiac disease, a novel treatment based on oral feeding of the autoantigen and induction of an oral tolerance may be envisaged[35]. tTG apparently elicits autoantibodies of the IgG class in various other chronic inflammatory conditions and might play a role in the initiation and perpetuation of certain autoimmune diseases.

Methods

Cell culture and immunoprecipitation. HT1080 cells were cultured in Dulbecco's modified Eagle's medium containing 10% fetal calf serum (Gibco, Eggenstein, Germany). For radioactive labeling 10^5 cells were incubated with 0.2 mCi [^{35}S]methionine (Expre^{35}S^{35}S, Du Pont-NEN, Bad Hamburg, Germany) and cultivated for further 16–20 h. For immunoprecipitation (IP) the cells were lysed in 3 ml 50 mM Tris-HCl, 150 mM NaCl, 1% nonionic detergent, protease inhibitors, pH 7.5, for 10 min at 4 °C. Cell fragments were removed by centrifugation. 1 ml lysate was incubated with 50 µl Sepharose CL-4B (Pharmacia, Freiburg, Germany) for 30 min at room temperature to remove nonspecifically binding proteins. The thus pretreated lysate was incubated with CNBr-activated Sepharose 4B (Pharmacia) preadsorbed with serum IgA either from celiac disease patients or from controls via an anti-human IgA bridging antibody from rabbit (2.4 mg antibody/ml Sepharose; Dianova, Hamburg, Germany) for 16 h at 4 °C. After several washes the precipitated proteins were dissolved in 50 µl SDS sample buffer under reducing conditions and separated by SDS–PAGE (ref. 36).

Isolation, cleavage and sequencing of the autoantigen. For isolation of the autoantigen by electrophoretic elution (Prep Cell 491, Bio-Rad, Krefeld, Germany) the discontinuous buffer system of Laemmli[36] was used. A 7.5% resolving gel (acrylamide, bisacrylamide 30:0.4, Pharmacia) was preceded by a 4% stacking gel. The immunoprecipitated sample was reduced and heated in sample buffer and then separated by a constant voltage of 225 V. Elution was performed in 25 mM Tris-HCl, 0.1 M glycin, 0.01% sodium laurylsulfate and fractions of 1.5 ml (0.8 ml/min) were collected. Fractions of interest were analyzed by tricine-SDS–PAGE (ref. 37) and further concentrated with Centriprep-50 (Amicon, Witten, Germany). Cleavage with endoproteinase Asp-N (Boehringer Mannheim, Germany) was performed in the elution buffer for 30 min at 37 °C, with an enzyme-to-substrate ratio of 1:100. Protein fragments were transferred to a polyvinylidene-difluoride membrane (Immobilon, Millipore, Eschborn, Germany) in a semi-dry-fast-blot apparatus (Fastblot B32/33 Biometra, Göttingen, Germany) and excised. Amino-terminal sequences were determined by Edman-degradation in an Applied Biosystems 477A sequencer (Foster City, CA).

Inhibition of endomysial staining. Preincubation of celiac disease sera (10 µl, diluted 1:320 in phosphate-buffered saline, pH 7.3, PBS) with 1 µg or 10 µg tTG from guinea pig liver (Sigma, Deisenhofer, Germany) or with 10 µg bovine serum albumin (Sigma) was performed for 1 h at room temperature. Monkey esophagus tissue slides (Euroimmun, Lübeck, Germany) were then incubated with the pretreated celiac disease sera, their untreated controls or non-celiac disease control sera in a humidified chamber for 1 h

at room temperature and washed 3× in PBS containing 0.2% bovine serum albumin. Bound IgA was detected with TRITC-labeled antihuman IgA from rabbit (1:50 in PBS; Dianova) for 30 min at room temperature.

Enzyme linked immunosorbent assay. For the ELISA 1 µg tTG (Sigma) in 100 µl PBS was coated per well on 96-well microtiter plates (Nunc, Wiesbaden, Germany) for 2 h at 37 °C, and unreacted sites were blocked with PBS containing 1% bovine serum albumin at 4 °C overnight. Patient and control sera were diluted in 100 µl PBS, 0.1% Tween-20 (Sigma), added to the wells and incubated for 1 h at room temperature. Three washes with PBS, 0.1% Tween-20 were followed by incubation with 100 µl peroxidase-conjugated antibody to human IgA (Dianova) diluted 1:1000 in PBS, 0.1% Tween-20, for 1 h at room temperature. Unbound antibodies were removed by three washes and color was developed by addition of 200 µl 0.1 M sodium citrate, 1 mg/ml o-phenylenediamine-hydrochloride, 0.06% H_2O_2, pH 4.2, for 30 min at room temperature. The absorbance was read on an ELISA reader (MRX, Dynatech Laboratories/Dynex Technologies, Denkendorf, Germany) at 450 nm.

Acknowledgments

We thank M. Becker, B. Gerling and S. Daum for making available some of the celiac disease sera, P.C. Fox for the kind gift of the Sjögren's syndrome sera, N. Otto for performing amino-terminal sequence analysis and J. Atkinson for valuable suggestions. The study was supported in part by project DFG Schu 646/10-1 and SFB366 C5. D.S. is the recipient of a Hermann and Lilly Schilling professorship.

RECEIVED 11 FEBRUARY; ACCEPTED 12 MAY 1997

1. Trier, J.S. Celiac sprue. *N. Engl. J. Med.* 325, 1709–1719 (1991).
2. Holmes, G.K.T., Prior, P., Lane, M.R., Pope, D. & Allan, R.N. Malignancy in coeliac disease — effect of a gluten-free diet. *Gut* 30, 333–338 (1989).
3. Logan, R.F.A., Rifkin, E.A., Turner, I.D. & Ferguson, A. Mortality in celiac disease. *Gastroenterology* 97, 265–271 (1989).
4. Marsh, M.N. Gluten, major histocompatibility complex, and the small intestine: A molecular and immunobiologic approach to the spectrum of gluten sensitivity ('celiac sprue'). *Gastroenterology* 102, 330–354 (1992).
5. Sturgess, R. *et al.* Wheat peptide challenge in coeliac disease. *Lancet* 343, 758–761 (1994).
6. Ferguson, A., Arranz, E. & Kingstone, K. Clinical and pathological spectrum of coeliac disease. in: *Malignancy and Chronic Inflammation in the Gastraintestinal Tract — New Concepts.* (eds. Riecken, E.O., Zeitz, M., Stallmach, A. & Heise, W.) 51–63 (Kluwer Acad. Press, Dordrecht, the Netherlands, 1995).
7. Walker-Smith, J.A., Guandalini, S., Schmitz, J., Shmerling, D.H. & Visakorpi, J.K. Revised criteria for diagnosis of coeliac disease. *Arch. Dis. Child.* 65, 909–911 (1990).
8. Bürgin-Wolff, A. *et al.* Antigliadin and antiendomysium antibody determination for coeliac disease. *Arch. Dis. Child.* 66, 941–947 (1991).
9. Volta, U., Molinaro, N., Fusconi, M., Cassani, F. & Bianchi, F.B. IgA antiendomysial antibody test: A step forward in celiac disease screening. *Dig. Dis. Sci.* 36, 752–756 (1991).
10. Mylotte, A., Egan-Mitchell, B., McCarthy, C.F. & McNicholl, B. Incidence of coeliac disease in the west of Ireland. *Br. Med. J.* 1, 703–705 (1973).
11. Greco, L., Mäki, M., Di Donato, F. & Visakorpi, J.K. Epidemiology of coeliac disease in Europe and the Mediterranean Area. in: *Common Food Intolerances*, Vol. I, *Epidemiology of Coeliac Disease.* (eds. Auricchio, S. & Visakorpi, J.K.) 25–44 (Karger, Basel, Switzerland, 1992).
12. Sandforth, F. *et al.* Inzidenz der einheimischen Sprue/Zöliakie in Berlin (West): Eine prospektive Untersuchung mit kurzer Falldiskussion. *Z. Gastroenterol.* 29, 327–332 (1991).
13. Catassi, C. *et al.* Coeliac disease in the year 2000: Exploring the iceberg. *Lancet* 343, 200–203 (1994).
14. Not, T. *et al.* Endomysium antibodies in blood donors predicts a high prevalence of celiac disease in the USA. *Gastroenterology* 110, A351 (1996).
15. Lerner, A., Kumar, V. & Iancu, T.C. Immunological diagnosis of childhood coeliac disease: comparison between antigliadin, antireticulin and antiendomysial antibodies. *Clin. Exp. Immunol.* 95, 78–82 (1994).
16. Picarelli, A. *et al.* Production of antiendomysial antibodies after in-vitro gliadin challenge of small intestine biopsy samples from patients with coeliac disease. *Lancet* 348, 1065–1067 (1996).
17. Mäki, M. Coeliac disease and autoimmunity due to unmasking of cryptic epitopes? *Lancet* 348, 1046–1047 (1996)
18. Cordell, J.L. *et al.* Immunoenzymatic labeling of monoclonal antibodies using immune complexes of alkaline phosphatase and monoclonal anti-alkaline phosphatase (APAAP) complexes. *J. Histochem. Cytochem.* 32, 219–229 (1984).
19. Gentile, V. J. *et al.* Isolation and characterization of cDNA clones to mouse macrophage and human endothelial cell tissue transglutaminases. *J. Biol. Chem.* 266, 478–483 (1991).
20. Barsigian, C., Stern, A.M. & Martinez, J. Tissue (type II) transglutaminase covalently incorporates itself, fibrinogen, or fibronectin into high molecular weight complexes on the extracellular surface of isolated hepatocytes. *J. Biol. Chem.* 266, 22501–22509 (1991).
21. Greenberg, C.S., Birckbichler, P.J. & Rice, R.H. Transglutaminases: Multifunctional cross-linking enzymes that stabilize tissues. *FASEB J.* 5, 3071–3077 (1991).
22. Upchurch, H.F., Conway, E., Patterson, M.K. & Maxwell, M.D. Localization of cellular transglutaminase on the extracellular matrix after wounding: Characteristics of the matrix bound enzyme. *J. Cell Physiol.* 149, 375–382 (1991).
23. Martinez, J., Chalupowicz, D.G., Roush, R.K., Sheth, A. & Barsigian, C. Transglutaminase-mediated processing of fibronectin by endothelial cell monolayers. *Biochemistry* 33, 2538–2545 (1994).
24. Aeschlimann, D., Kaupp, O. & Paulsson, M. Transglutaminase-catalyzed matrix cross-linking in differentiating cartilage: Identification of osteonectin as a major glutaminyl substrate. *J. Cell Biol.* 129, 881–892 (1995).
25. Kleman, J., Aeschlimann, D., Paulsson, M. & van der Rest, M. Transglutaminase-catalyzed cross-linking of fibrils of collagen V/XI in A204 rhabdomyosarcoma cells. *Biochemistry* 34, 13768–13775 (1995).
26. Bowness, J.M., Folk, J.E. & Timpl, R.J. Identification of a substrate site for liver transglutaminase on the aminopropeptide of type III collagen. *J. Biol. Chem.* 262, 1022–1024 (1987).
27. Aeschlimann, D. & Paulsson, M. Cross-linking of laminin-nidogen complexes by tissue transglutaminase. *J. Biol. Chem.* 266, 15308–15317 (1991).
28. Piacentini, M. Tissue transglutaminase: A candidate effector element of physiological cell death. *Curr. Top. Microbiol. Immunol.* 200, 163–175 (1995).
29. Knight, C.R.L., Rees, R.C. & Griffin, M. Apoptosis: A potential role for cytosolic transglutaminase and its importance in tumour progression. *Biochim. Biophys. Acta* 1096, 312–318 (1991).
30. Bruce, S.E., Bjarnason, I. & Peters, T.J. Human jejunal transglutaminase: Demonstration of activity, enzyme kinetics and substrate specificity with special relation to gliadin and coeliac disease. *Clin. Sci.* 68, 573–579 (1985).
31. Szabolcs, M., Sipka, S. & Csorba, S. In vitro cross-linking of gluten into high-molecular-weight polymers with transglutaminase. *Acta Paediatr. Hung.* 28, 215–227 (1987).
32. Ladinser, B., Rossipal, E. & Pittschieler, K. Endomysium antibodies in coeliac disease: An improved method. *Gut* 35, 776–778 (1994).
33. Lundin, K.E.A. *et al.* Gliadin-specific, HLA-DQ(α1*0501,β1*0201) restricted T cells isolated from the small intestinal mucosa of celiac disease patients. *J. Exp. Med.* 178, 187–196 (1993).
34. Lankisch, P.G. *et al.* Diagnostic intervals for recognizing celiac disease. *Z. Gastroenterol.* 34, 473–477 (1996).
35. Sosroseno, W. A review of the mechanisms of oral tolerance and immunotherapy. *J. R. Soc. Med.* 88, 14–17 (1995).
36. Lämmli, U.K. Cleavage of structural proteins during the assembly of the head of bacteriophage T4. *Nature* 227, 680–685 (1970).
37. Schägger, H. & von Jagow, G. Tricine-sodium dodecyl sulfate-polyacrylamide gel electrophoresis for the separation of proteins in the range from 1 to 10 kDa. *Anal. Biochem.* 166, 368–379 (1987).

Molecular Characterization of the Ro/SS-A Autoantigens

Daniel P. McCauliffe and Richard D. Sontheimer

Department of Dermatology (DPM), University of North Carolina, Chapel Hill, North Carolina; and Department of Dermatology and Internal Medicine (RDS), University of Texas Southwestern Medical Center, Dallas Texas, U.S.A.

Molecular techniques have recently revealed that there are several immunologically distinct Ro/SS-A antigens. Three genes encoding putative Ro/SS-A protein antigens with calculated masses of 46, 52, and 60 kD have been isolated. The encoded amino acid sequence of each is quite dissimilar. The 46-kD antigen is calreticulin (CR), a highly conserved calcium-binding protein that resides predominately in the endoplasmic reticulum where it may be involved in protein assembly. Although CR has recently been confirmed to be a new human rheumatic disease-associated autoantigen, its relationship to the other components of the Ro/SS-A ribonucleoprotein has become somewhat controversial owing predominately to the fact that recombinant forms of calreticulin have not displayed the same pattern of autoantibody reactivity possessed by the native form of this protein.

The 52-kD antigen most likely resides in the nucleus and may be involved in the regulation of gene expression. The cellular location and function of the 60-kD antigen is uncertain but studies indicate that it is a RNA-binding protein.

The 46- and 60-kD antigens share homology with foreign polypeptides, suggesting that an immune response initially directed against a foreign protein may give rise to the autoimmune response directed at cross-reacting self proteins.
J Invest Dermatol 100:73S–79S, 1993

In 1969 Clark *et al* first demonstrated a novel antigen in human tissue extracts that by immunodiffusion analysis reacted with sera from patients with systemic lupus erythematosus and Sjögren's syndrome [1]. This antigen and its reactive autoantibodies were called Ro (auto)antigen and Ro (auto)antibodies, respectively. In 1975 Alspaugh and Tan similarly demonstrated the presence of three different autoantibodies in sera from patients with Sjögren's syndrome that they designated SS-A, SS-B, and SS-C [2]. Later it was demonstrated that SS-A autoantibodies were immunologically equivalent to the Ro autoantibodies [3], and thus we now commonly preface these autoantibodies and their respective antigens with the term Ro/SS-A. SS-B autoantibodies were also shown to be identical to La autoantibodies, a specificity that frequently accompanies Ro/SS-A autoantibodies [3].

Reprint requests to: Dr. Daniel P. McCauliffe, Department of Dermatology, CB 7600, Room 137 North Carolina Memorial Hospital, Chapel Hill, 27514.

Abbreviations:
ANA: anti-nuclear antibody
cDNA: complementary DNA
CMV: cytomegalovirus
CR: calreticulin
ELISA: enzyme-linked immunosorbent assay
ER: endoplasmic reticulum
GRP: glucose-regulated protein
hY RNA: human cytoplasmic RNA
LE: lupus erythematosus
NLE: neonatal lupus erythematosus
PDI: protein disulfide isomerase
RNP: ribonucleoprotein
SCLE: subacute cutaneous lupus erythematosus
SDS-PAGE: sodium dodecyl sulfate polyacrylamide gel electrophoresis
UV: ultraviolet
VSV: vesicular stomatitis virus

CLINICAL SIGNIFICANCE OF THE Ro/SS-A ANTIGENS AND ANTIBODIES

The Ro/SS-A antigens are of clinical interest in that antibodies directed against them are found in the majority of patients with primary Sjögren's syndrome, subacute cutaneous lupus erythematosus (SCLE), neonatal lupus erythematosus (NLE), anti-nuclear antibody (ANA) negative lupus erythematosus (LE), and systemic LE-like disease secondary to homozygous C2 or C4 complement deficiency [4–9]. Substantial evidence indicates that they play a major role in the pathogenesis of disease [10,11]. The strongest evidence comes from observations in patients with NLE. Pregnant mothers with circulating Ro/SS-A autoantibodies can pass them across the placenta to their fetus. The fetus can develop congenital heart block, hepatic inflammation, and thrombocytopenia from tissue injury presumably caused by these antibodies [12,13]. Additionally, shortly after birth and perhaps triggered by ultraviolet (UV) light exposure, these infants can develop skin lesions clinically and histopathologically similar to those of SCLE [12]. In several months, as the maternally acquired antibodies are cleared from the infant's circulation, the skin lesions resolve [12].

Investigative work has provided additional evidence that Ro/SS-A antibodies may be pathogenic. Ro/SS-A antibodies administered intravenously to immunodeficient mice engrafted with human skin bind preferentially in and about the human basal keratinocytes [14]. This binding is augmented by UV light exposure. This pattern of immunoglobulin deposition is identical to that found in biopsies from NLE and SCLE skin lesions.

CHARACTERIZATION OF THE Ro/SS-A ANTIGENS

Since Clark *et al* first demonstrated the presence of Ro/SS-A autoantibodies by immunodiffusion studies in 1969[1], we have learned a great deal more about their target antigens.

In 1981 Lerner *et al* demonstrated that human Ro/SS-A autoimmune sera immunoprecipitated a novel class of small RNAs that they designated the human (h) cYtoplasmic (Y) RNAs or hY RNA

0022-202X/93/$06.00

[15]. In 1984 Wolin and Steitz showed that this hY RNA immunoprecipitation resulted from the binding of Ro/SS-A autoantibodies to a 60-kD protein to which the hY RNAs were apparently linked [16]. From 1984 until 1988 it was generally thought that Ro/SS-A autoantibodies were directed at a single 60-kD protein. However, in 1988 Ben-Chetrit *et al* demonstrated a novel 52-kD Ro/SS-A antigen by immunoblot analysis that was immunologically distinct from the 60-kD antigen [17]. In 1989 Rader *et al* demonstrated four immunologically distinct antigens that react with monospecific Ro/SS-A autoimmune sera [18]. Over the past four years genes encoding 60-, 46-, and 52-kD autoantigens have been isolated.

60-kD Ro/SS-A In 1988 Deutscher *et al* reported the cloning of a 60-kD Ro/SS-A antigen from a human placental complementary (cDNA) library [19]. In 1989 Ben-Chetrit *et al* [20] reported the cDNA sequence cloned from a human T-cell leukemia cDNA library that appeared to be a homologous gene or a differentially spliced version of the gene characterized by Deutscher *et al*. Deutscher's and Ben-Chetrit's sequences both encoded a 60-kD protein that was identical except for several amino acids at the carboxy-terminus. Both amino acid sequences contain a zinc finger motif and a sequence motif common to RNA binding proteins [19,20]. Zinc fingers are thought to serve as a site of nucleic acid binding or protein binding [21].

There is no extensive sequence homology between the 60-kD protein and other published protein sequences; however, six segments of this protein have limited homology to different portions of a vesicular stomatitis virus (VSV) nucleocapsid protein [22]. Five of these homologous regions have significant reactivity to human Ro/SS-A autoimmune sera by enzyme-linked immunosorbent assay (ELISA), which suggests that an immune response initially directed at the VSV protein or a similar viral protein might cross-react with the 60-kD Ro/SS-A protein by way of its cross-reacting epitopes. VSV is not known to be particularly pathogenic in humans, but the data suggest that this VSV protein or a similar viral protein might elicit the Ro/SS-A autoimmune response. This is an example of "molecular mimicry" where a microbial protein is thought to trigger an immune response that cross-reacts with a self-antigen [23].

46-kD Ro/SS-A Our group isolated a cDNA from an Epstein-Barr virus transformed human B-cell line that encodes a protein reactive with human Ro/SS-A autoimmune sera [24]. The encoded 46-kD protein migrates aberrantly at 60 kD by sodium dodecylsulfate–polyacrylamide gel electrophoresis (SDS-PAGE). The amino acid sequence of this 46-kD molecule reveals a hydrophobic leader sequence at its amino terminal typical of molecules transported into the endoplasmic reticulum (ER), and a KDEL carboxy terminal sequence that is classic for proteins that are retained in the ER [24,27]. This sequence is extremely homologous to murine and rabbit CR (94% and 92%, respectively) [28]. CR is a calcium-binding protein that resides in the endoplasmic and sarcoplasmic reticulum [29]. From this high degree of sequence homology and other data it has been concluded that the 46-kD molecule is human CR [28,30].

Recent evidence indicates that CR may be coordinately expressed with the glucose-regulated protein (GRP)78, GRP94, and protein disulfide isomerase (PDI) genes [31]. The protein products of all four of these genes are highly acidic, localize to the ER, and bind calcium [32]. GRP78 and GRP94 are highly homologous to heat-shock proteins [33,34]. Both of these proteins and PDI are thought to play a major role in protein assembly within the ER [33–35]. Thus, by implication, CR may also play a role in protein assembly.

It is also interesting to note that patients infected with *Onchocerca volvulus*, a filarial nematode that causes river blindness, sclerosing lymphadenitis, and dermatologic disease in humans residing in parts of Africa and Central America, have antibodies directed against the Ral-1 antigen, which is highly homologous to CR [28,36]. Although patients with this nematode are not at increased risk for developing Sjögren's syndrome or LE, this homology between CR and a filarial protein raises the possibility that a foreign Ro/SS-A protein equivalent might trigger the autoimmune Ro/SS-A antibody response seen in some patients with Sjögren's syndrome and several LE-related disorders. *Drosophila melanogaster* and the marine snail *Aplysia californica* have molecules similar to CR [28].

Work recently presented by other laboratories has now confirmed our initial suggestion that calreticulin is a rheumatic disease–associated autoantigen [37,38]. One group has found that an *Escherichia coli* recombinant form of human calreticulin reacted by ELISA with 40% of the serum samples from unselected SLE patients [37], whereas another group found 33% of their SLE sera to react with the same form of recombinant CR by Western blot [38]. Curiously, neither group found a significant correlation between anti-CR and anti-Ro/SS-A autoantibody levels in their SLE patient sera.

We have reason to believe that post-translational modification such as phosphorylation, perhaps through the augmentation of hY RNA binding, could also be relevant to the configuration of CR that is recognized by Ro/SS-A autoantibodies. Non-mammalian forms of recombinant CR are unlikely to possess the same pattern of RNA binding or phosphorylation that is displayed by the native configuration of CR present in mammalian cells. The concern that CR may not be a component of the Ro/SS-A RNP complex stems from the fact that *recombinant* forms of CR both in our laboratory (personal unpublished observation) and in others [37,38] do not display the same degree of reactivity with Ro/SS-A autoantibodies that has previously been demonstrated with *native* human CR purified from human Wil-2 cells. We now have evidence that the protein-RNA binding site present on a subpopulation of CR molecules that bind hY RNA contributes to the structure that is being recognized by human anti-Ro/SS-A autoantibodies [39].

52-kD Ro/SS-A Chan *et al* and Itoh *et al* independently isolated the same cDNA sequence from two different human T-cell cDNA libraries that encodes a 52-kD protein reactive with human Ro/SS-A autoimmune sera [40,41]. The amino acid sequence predicted by this cDNA contained leucine zipper and zinc finger binding motifs and also had significant homology with the human ret transforming protein and the murine T-cell regulatory protein rpt-1, which are thought to play a role in gene regulation[40,41]. These sequence motifs and homologies suggest that the 52-kD Ro/SS-A molecule may be involved in gene regulation and thus probably resides in the nucleus.

There are no significant sequence homologies between the 60-, 46-, or 52-kD antigens (Table I). Despite the knowledge gained from analyzing the encoded amino acid sequences of each Ro/SS-A cDNA, there still remain a number of unanswered questions that several investigators have started to address.

Are These Antigens Structurally Associated and What Are Their Relationships to the hY RNAs? Ro/SS-A autoimmune sera from patients with LE and Sjögren's syndrome immunoprecipitate four hY RNAs (hY1,3,4, and 5) from human cell extracts [15] (see Fig 1). Antisera specific for either a 52-kD or a 60-kD protein have been shown to immunoprecipitate the hY RNAs from cellular extracts. However, in one study whenever 52-kD specific antibodies (not reactive to the 60-kD antigen by immunoblot analysis) were used, the hY RNAs and 52-kD protein were precipitated along with a small amount of 60-kD protein [17]. Thus it is not certain whether 1) the 52-kD species binds the hY RNAs directly; 2) the 52-kD protein is indirectly associated with the hY RNA through a direct association with a 60-kD hY RNA binding protein; or 3) the antibodies that appeared specific for the 52-kD antigen by immunoblot may recognize a cross-reactive epitope on the native Ro/SS-A ribonucleoprotein (RNP) particle.

Deutscher *et al* have demonstrated that the 60-kD Ro/SS-A protein directly associates with hY RNAs in reconstitution studies [19]. There is some evidence that CR associates with the hY RNA as suggested by UV cross-linking studies [24], immunoprecipitation of hY RNA by affinity-purified CR antisera [24], and the fact that onchocerciasis patient sera with CR reactive antibodies can immunoprecipitate hY RNA [42]. Additionally, preliminary data indicate that rabbit antisera raised against two synthetic peptides corre-

Table I. Characteristics of Three Ro/SS-A cDNA-Encoded Products

Protein	Location	Function	Homology	Pathogenic Role
60 kD	Nuclear? Cytoplasmic?	RNA binding	VSV nucleocapsid protein	Molecular mimicry?
46 kD	Predominantly cytoplasmic ± nuclear	Ca^{++} binding Protein folding?	Calreticulin Ral-1	Translocation Parasite homology
52 kD	Predominantly nuclear ± cytoplasmic	Gene regulation?	rfp, rpt-1	?

sponding to different portions of the CR amino acid sequence can precipitate hYRNA [39]. However, the relationships that exist between CR and the other molecular constituents of the Ro/SS-A RNP particle continue to be debated [38,43,44].

Earlier data suggested that Ro/SS-A autoimmune sera precipitated a 60-kD protein along with the hY RNA and this immunoprecipitation was dependent on the presence of protein [15]. More recently Boire and Craft have identified Ro/SS-A antibodies that specifically immunoprecipitate hY5 RNA and a 60-kD protein, but not the other types of hY RNA [45]. They concluded that some Ro/SS-A autoimmune sera contain autoantibodies directed at a conformational epitope that is expressed only on Ro/SS-A-hY5 RNA particles but absent on hY1,2,3, and 4 containing particles.

The 60-kD protein immunoprecipitated in the above studies most probably represents the authentic 60-kD protein as its amino acid sequence contains a sequence motif typically found in RNA-binding proteins, although it is clear that proteins without the classic RNA-binding consensus sequence can also bind RNA molecules [46,47]. The hY RNAs and Ro/SS-A proteins might exist in a RNP multimeric complex similar to the U1 RNPs. One could hypothesize that the zinc finger motif in the 60-kD Ro/SS-A molecule might serve as a site for this protein to bind one or more of the other Ro/SS-A molecules, whereas the RNA binding motif would serve as a site of hY RNA binding.

Several different investigators have reported different masses for the Ro/SS-A RNP particle. Three groups have reported a mass of approximately 100–150 kD for the Ro/SS-A particle as determined by gel filtration [1,48,49]. Wolin and Steitz determined that the particle sediments in sucrose at approximately 7S [16]. This is equivalent to ~93 kD, which could be accounted for by the mass of one 60-kD protein and the average mass of one hY RNA molecule. Boire and Craft biochemically purified Ro/SS-A particles and found them to partition into three different groups by sucrose sedimentation gradients [50]. The particles in two of these groups have a mass of approximately 300–350 kD by gel filtration and the other has a mass of approximately 230 kD. These investigators concluded that Ro/SS-A RNP particles are heterogeneous and may exist as multimeric units consisting of hY RNA, a 60-kD protein, and perhaps other polypeptides including the La/SS-B protein [50] (see Fig 2).

Some investigators argue that if a particular protein reactive with Ro/SS-A autoantibodies is not part of the hY RNA-bearing RNP complex, then perhaps it should not be called a Ro/SS-A antigen. Although this is a matter of semantics, there is a clear need to

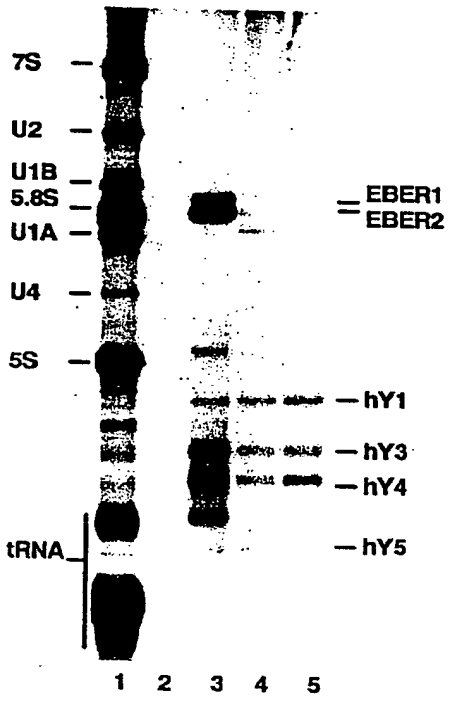

Figure 1. hY RNA immunoprecipitation. Wil-2 cells, an EBV transformed B-cell line, were radiolabeled with ^{32}P-orthophosphoric acid and sonicated. The resulting cell extract was incubated with sera and the immunoprecipitated material was harvested and subjected to gel electrophoresis according to previously established protocols [15]. *Lane 1* contains total radiolabeled RNA from the extract and serves to provide molecular weight standards as indicated to the left of this lane. *Lane 2* demonstrates that no RNA was immunoprecipitated with normal human serum. *Lane 3* is RNA immunoprecipitated with human autoimmune sera containing both Ro/SS-A and La/SS-B autoantibodies. *Lanes 4* and *5* are sera from two different patients with Ro/SS-A autoantibodies as defined by double immunodiffusion. All three sera with Ro/SS-A autoantibodies immunoprecipitated the four major types of hY RNA. The very faint unlabeled band in *lane 3* between hY1 and hY3 is hY2, a breakdown product of hY1. The Epstein-Barr virus encoded EBER 1 and 2 immunoprecipitate with La/SS-B antibodies as previously described [56].

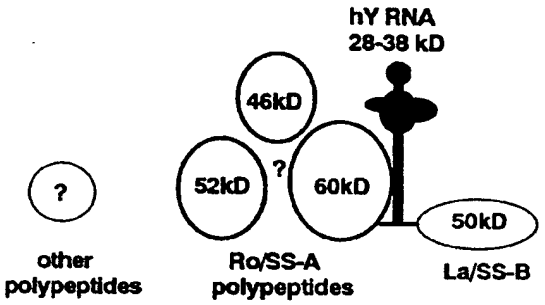

Figure 2. One model of the Ro/SS-A RNP particle. The proposed relationship between hY RNA and the Ro/SS-A and La/SS-B proteins is indicated. The hY RNA are RNA polymerase III transcripts and are thought to be at least transiently associated with the La/SS-B protein through binding of its uridine rich 3′ end. The 60-kD Ro/SS-A protein contains an RNA binding motif believed to be the site of hY RNA binding. It is uncertain if the 46- and/or 52-kD proteins reactive with Ro/SS-A autoimmune sera or other polypeptides are a part of this particle, although there is some evidence that the 46-kD protein is associated with hY RNA.

develop a more precise designation for each of these antigens. However, it should be remembered that Ro/SS-A antigens were initially defined by immunodiffusion assays, not by hY RNA association. It has not yet been determined which of the molecules reactive with Ro/SS-A autoimmune sera are responsible for the immunoprecipitate seen in immunodiffusion assays. Rader *et al*, however, observed that non-reducing SDS-PAGE of eluted precipitins from counter-immunoelectrophoresis showed the precipitins to be composed of a 60-kD protein [18].

What Is the Cellular Distribution of Each Ro/SS-A Molecule? Some investigators have reported predominantly intranuclear localization of the Ro/SS-A antigens by indirect immunofluorescence [51–54] whereas others have reported cytoplasmic [55–57] or both cytoplasmic and nuclear localization [58,59]. Whether this discrepancy in subcellular localization is related to the method of cell fixation, cell substrate, or the specificity of the Ro/SS-A autoimmune sera used has not been fully investigated.

Koch *et al* have demonstrated that conventional cell fixation for ANA testing does not allow full visualization of proteins, such as CR, that reside in the ER [60]. They demonstrated that ER proteins can be better visualized by immunofluorescence techniques with detergent permeabilization of fixed cells or of unfixed cells that have been equilibrated in 9% sucrose [60].

Isolation of antibodies specific for each Ro/SS-A antigenic polypeptide has allowed more precise cellular localization of the Ro/SS-A polypeptides and these results have helped explain the discrepancies encountered previously with immunofluorescence staining using whole Ro/SS-A patient sera.

Ben-Chetrit *et al* demonstrated strong punctate nuclear and slight cytoplasmic staining of cells with Ro/SS-A autoimmune serum immunoaffinity purified from a 52-kD protein and also with monospecific anti–52-kD serum (as determined by immunoblot analysis) [17]. They reported an indistinguishable pattern with Ro/SS-A autoimmune serum immunoaffinity purified from a 60-kD protein [17]. There is some evidence that there may be Ro/SS-A antibodies that react with an epitope on the native 60-kD RNP antigen that cross-react with an epitope on the 52-kD protein [61]. Thus one might speculate that the 60-kD protein resides primarily in the cytoplasm and that nuclear staining results from antibodies that recognize a cross-reactive epitope on the 52-kD protein. Preliminary ELISA data have revealed that all Ro/SS-A autoimmune sera with high-titer antibodies directed against a recombinant 52-kD Ro/SS-A protein have given a speckled nuclear ANA pattern of fluorescence (personal unpublished observation). The 52-kD Ro/SS-A amino acid sequence reveals motifs and homologies that indicate that it may be involved in gene regulation and thus would likely reside in the nucleus [40,41]. Antiserum specific for CR has revealed predominantly perinuclear cytoplasmic staining with lesser amounts of nuclear staining [62,63].

Kato *et al* have reported that the majority of the hY5 RNA is found in the cytoplasmic fraction of HeLa cells [64]. More recently Boire and Craft have demonstrated that more than 90% of the Ro/SS-A particles were recovered from the cytoplasmic fraction of HeLa cells [50]. One should recall that Ro/SS-A antigen was originally described as a saline-soluble, "cytoplasmic" autoantigen [1].

Is There Any Correlation Between the Type of Ro/SS-A Autoantibodies Patients Produce and Their Diagnosis, Disease Course, and/or Response to Therapy? Preliminary data suggest that patients with Ro/SS-A autoantibodies might be clinically categorized according to the Ro/SS-A proteins or epitopes their sera recognize. The specificity of the maternally acquired Ro/SS-A autoantibodies may determine which infants develop NLE. Buyon *et al* have shown that the predominant antibody response in the NLE patient group with acquired heart block was directed against the 52-kD Ro/SS-A protein, although some patients also had antibodies directed against a 60-kD protein [65]. Ben-Chetrit *et al* have demonstrated that of 51 SLE patients who were Ro/SS-A positive by immunodiffusion, 47% had antibodies that recognized both a 60-kD and a 52-kD protein, 18% had antibodies that recognized a 60-kD protein only, and 35% were nonreactive to both [66]. Similarly, they demonstrated that of 47 Ro/SS-A–positive Sjögren's syndrome patients, 47% had antibodies reactive to both a 60-kD and a 52-kD protein, 40% reacted only with a 52-kD protein only, and 13% were non-reactive. Unfortunately the results obtained by both Buyon *et al* and Ben-Chetrit *et al* were obtained by immunoblot analysis and might not detect conformational epitopes, including epitopes that might be present on a multimeric complex.

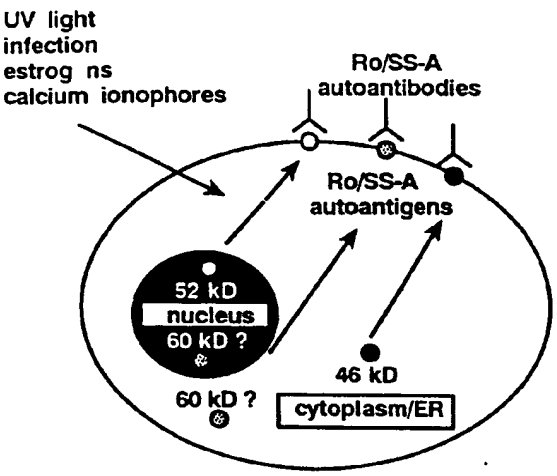

Figure 3. Ro/SS-A translocation. Agents that may translocate Ro/SS-A antigens to the cell surface where they are available to bind circulating Ro/SS-A autoantibodies are listed. The likely predominant location of the 46- and 52-kD antigens are indicated. The location of the 60-kD antigen is more uncertain.

Work is currently in progress in several laboratories, including our own, to determine those portions of each Ro/SS-A molecule to which Ro/SS-A autoantibodies bind and to define further the nature of conformational epitopes that may exist on an individual Ro/SS-A protein or as part of a multimeric structure. Epitope mapping should determine if subsets of Ro/SS-A autoantibody-associated disease can be based on antigenic site-recognition patterns. Such subclassification may have clinical use regarding the pathogenesis, diagnosis, and treatment of the Ro/SS-A autoantibody–associated diseases.

What Role Do the Ro/SS-A Autoantigens Play in the Pathogenesis of SCLE and NLE Skin Disease and How Might Their Cellular Expression Be Affected by Factors that May Influence These Two Skin Diseases? A number of agents have been shown to influence SCLE and NLE disease expression. Some of these agents have been shown to displace Ro/SS-A antigens to the surface of cells (Fig 3).

UV light SCLE and NLE skin diseases are frequently exacerbated by UV light exposure, primarily of the UVB type (290–320 nM) [67,68]. Investigators have demonstrated that UVB light can displace Ro/SS-A antigen from within keratinocytes to the cell surface [69,70]. Similar results have recently been reported for the La/SS-B antigen [71]. Such displacement would allow the autoantigen to have access to the Ro/SS-A autoantibody binding that could result in tissue injury through complement-mediated lysis or antibody-dependent cell-mediated cytotoxicity. At this time it is uncertain which of the various molecular components of the Ro/SS-A autoantigen complex are affected by UV light exposure. Recent preliminary studies have indicated that physiologically relevant doses of UVB induce both CR gene transcription [72] (personal observation) and translation [73]. However, similar doses of UVB did not increase cellular levels of the 60-kD Ro/SS-A protein [73]. No evidence has yet been presented regarding the displacement of the various Ro/SS-A proteins to the cell surface by UV light.

Estrogens The hormonal milieu may also play an important role in Ro/SS-A–associated disease, as approximately 75% of SCLE patients and infants with NLE skin disease are female. Estrogen treatment of cultured keratinocytes results in increased expression of Ro/SS-A antigens on the cell surface, but it is uncertain which of the Ro/SS-A molecules are so displaced [74].

Heat Some SCLE patients have noted that heat can exacerbate their skin disease [67]. The similarities that CR shares with the heat shock–like proteins GRP78 and GRP94 is of interest in this regard. There is recent evidence that heat shock–like proteins can be translocated to the cell surface, where they may participate in antigen presentation or may be a target for gamma/delta T-cell–directed cytotoxicity [75,76].

State of keratinocyte differentiation and proliferation Studies have shown that human keratinocytes grown in low-calcium–containing culture media have greater amounts of cytoplasmic Ro/SS-A antigen as detected by immunofluorescence staining with Ro/SS-A autoimmune sera [59]. It is uncertain which of the Ro/SS-A antigens are expressed in greater amounts, however. At lower calcium concentrations, cultured keratinocytes are in a less-differentiated, more rapidly proliferating state, more like the basal layer keratinocytes [77]. This might explain why the more rapidly proliferating basal keratinocytes appear to be preferentially targeted in SCLE and NLE [11,78]. Preliminary evidence indicates that CR is expressed at higher levels in rapidly proliferating cells (personal unpublished observation).

There is some evidence that CR can be transiently secreted from cells after treatment with calcium ionophores [79], although this has not been fully substantiated by others [80]. Recent studies in our laboratory employing calreticulin reporter gene constructs have indicated that calreticulin transcription is markedly augmented in A431 cells following treatment with the calcium ionophore ionomycin [72] (personal unpublished observation). Additionally, it has been suggested that calcium ionophore treatment of cultured human keratinocytes displaces Ro/SS-A antigen to the cell membrane, although it is uncertain which of the Ro/SS-A antigens is (are) so displaced [81].

Infection There is considerable evidence that viral infections can precipitate or exacerbate autoimmune disease [82]. Some work has suggested that virally infected cells in culture displace Ro/SS-A antigens to the cell surface, similar to the effects caused by UV light [83]. Jianhui and Newkirk have recently presented evidence that suggests that human cytomegalovirus (CMV) infection increases the expression of CR in MRC-5, a human embryonic lung fibroblast line [84]. These studies found that total cellular CR levels increased following CMV infection, but the greatest increase in CR antigenicity was associated with the plasma membrane. CMV infection also resulted in increased intracellular levels of the 60-kD Ro/SS-A antigen, but similar increases were not observed in the plasma membrane. Viral infection has also been shown to displace the La/SS-B antigen from the nucleus [85].

Polymorphism It is not known whether Ro/SS-A proteins are polymorphic. Preliminary studies have indicated, however, that the CR encoding gene is not highly polymorphic in normal individuals by restriction fragment length polymorphism analysis [24]. There is evidence of at least two forms of the 60-kD Ro/SS-A encoding gene [18–20]. Kutsch *et al* have recently reported variability in Ro/SS-A displacement to keratinocyte membranes after treatment with calcium ionophore or tumor necrosis factor alpha, which they suggest might arise from genetic differences in the keratinocyte donors [81]. It is possible that certain forms of a Ro/SS-A molecule may be more immunogenic, expressed at higher levels, or more easily displaced to the cell surface where it could participate in immune-mediated injury.

SUMMARY

With molecular techniques, we have recently learned that there are several immunologically distinct Ro/SS-A antigens. Three putative Ro/SS-A genes have been isolated and the encoded proteins from these three genes have been found to be quite dissimilar. CR, the 46-kD protein, appears to reside predominately in the endoplasmic reticulum/cytoplasm, whereas the 52-kD protein most likely resides in the nucleus. The structure of the 60-kD protein and at least one immunofluorescence study suggest that it may also reside predominantly in the nucleus, although if it is the authentic hY RNA binding protein, it should also reside in the cytoplasm. The Ro/SS-A RNP particles are heterogeneous multimeric complexes that may include more than one Ro/SS-A molecule, hY RNA, La/SS-B, and perhaps other currently undefined molecules.

Two of the putative Ro/SS-A proteins share significant homology with foreign proteins, suggesting that an immune response initially directed against a foreign protein, such as a viral protein, may give rise to the autoimmune response directed at cross-reacting self Ro/SS-A protein. This, plus the possibility that viral infection can alter the normal cellular distribution of Ro/SS-A antigens, presents the intriguing paradigm illustrated in Fig 4 where virus infection might have a dual impact on the Ro/SS-A autoimmune response.

Work is in progress to determine if there is an association between which Ro/SS-A molecules and/or epitopes are targeted by patient autoimmune sera and patient diagnosis, clinical course, and/or response to therapy. We are hopeful that efforts to characterize the structures and functions of the Ro/SS-A antigens will further elucidate the pathogenesis of the Ro/SS-A autoantibody-associated diseases and aid in the development of better diagnostic and therapeutic modalities for those afflicted.

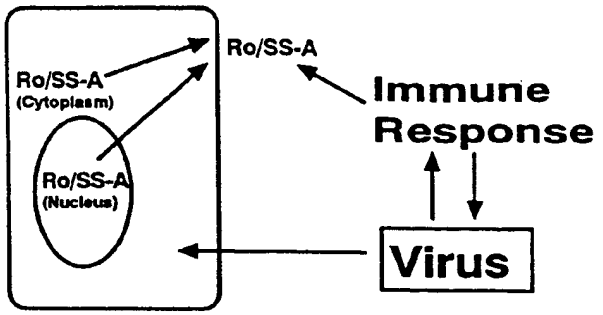

Figure 4. Model for a dual effect of virus infection on the Ro/SS-A autoimmune response. Infection with viruses that express molecules structurally associated with Ro/SS-A molecular subunits could result in translocation of Ro/SS-A antigens to the surface of cells. The immune response generated by the virus could then recognize the translocated Ro/SS-A antigens at the cell surface and mediate cellular damage through mechanisms such as complement-mediated lysis or antibody-dependent cell-mediated cytotoxicity.

Dr. McCauliffe is the recipient of a Dermatology Foundation Career Development Award sponsored by Sandoz Pharmaceuticals and Dr. Sontheimer is the recipient of an NIH Research Career Development Award (ARO1784). This work was supported by NIH grant AR19101.

REFERENCES

1. Clark G, Reichlin M, Tomasi TB: Characterization of a soluble cytoplasmic antigen reactive with sera from patients with systemic lupus erythematosus. J Immunol 102:117–122, 1969
2. Alspaugh MA, Tan EM: Antibodies to cellular antigens in Sjögren's syndrome. J Clin Invest 55:1067–1073, 1975
3. Alspaugh MA, Maddison P: Relation of the identity of certain antigen-antibody systems in systemic lupus erythematosus and Sjögren's syndrome: an interlaboratory collaboration. Arthritis Rheum 22:796–798, 1979
4. Martinez-Lavin M, Vaughan JH, Tan EM: Autoantibodies and the

spectrum of Sjögren's syndrome. Ann Intern Med 91:185–190, 1979

5. Sontheimer RD, Maddison PJ, Reichlin M, Jordon RE, Stastny P, Gilliam JN: Serologic and HLA associations in subacute cutaneous lupus erythematosus, a clinical subset of lupus erythematosus. Ann Intern Med 97:664–671, 1982
6. Maddison PJ, Provost TT, Reichlin M: ANA negative systemic lupus erythematosus: serological analysis. Medicine (Baltimore) 60:87–94, 1981
7. Kephart D, Hood AF, Provost TT: Neonatal lupus: serologic findings. J Invest Dermatol 77:331–333, 1981
8. Provost TT, Arnett FC, Reichlin M: Homozygous C2 deficiency, lupus erythematosus and anti-Ro(SSA) antibodies. Arthritis Rheum 26:1279–1282, 1983
9. Meyer O, Hauptmann G, Tuppeiner G, Ochs HD, Mascart-Lemone F: Genetic deficiency of C4, C2 or C1q and lupus syndromes: association with anti-Ro(SS-A) antibodies. Clin Exp Immunol 62:678–684, 1985
10. McCauliffe DP, Lux F, Lieu TS, Sanz I, Hanke J, Newkirk M, Siciliano MJ, Sontheimer RD, Capra JD: Ro/SS-A and the pathogenic significance of its antibodies. J Autoimmun 2:375–381, 1989
11. Sontheimer RD, McCauliffe DP: Pathogenesis of anti-Ro/SS-A autoantibody-associated cutaneous lupus erythematosus. Dermatol Clin 8:751–758, 1990
12. Lee LA, Weston WL: New findings in neonatal lupus syndrome. Am J Dis Child 138:233–236, 1984
13. Laxer RM, Roberts EA, Gross KR, Britton JR, Cutz E, Dimmick J, Petty RE, Silverman ED: Liver disease in neonatal lupus erythematosus. J Pediatr 116:238–242, 1990
14. Lee LA, Gaither KK, Coulter SN, Norris DA, Harley JB: Pattern of cutaneous immunoglobulin G deposition in subacute cutaneous lupus erythematosus is reproduced by infusing purified anti-Ro(SSA) autoantibodies into human skin-grafted mice. J Clin Invest 83:1556–1562, 1989
15. Lerner MR, Boyle J, Hardin JA, Steitz JA: Two novel classes of small ribonucleoproteins detected by antibodies associated with lupus erythematosus. Science 211:400–402, 1981
16. Wolin SL, Steitz JA: The Ro small cytoplasmic ribonucleoproteins: identification of the antigenic protein and its binding site on the Ro RNA's. Proc Natl Acad Sci USA 81:1996–2000, 1984
17. Ben-Chetrit E, Chan EK, Sullivan KF, Tan EM: A 52-kD protein is a novel component of the SS-A/Ro antigenic particle. J Exp Med 167:1560–1571, 1988
18. Rader MD, O'Brien C, Liu Y, Harley JB, Reichlin M: The heterogeneity of the Ro/SSA antigen: different molecular forms in lymphocytes and red blood cells. J Clin Invest 83:1293–1298, 1989
19. Deutscher SL, Harley JB, Keene JD: Molecular analysis of the 60-kDa human Ro ribonucleoprotein. Proc Natl Acad Sci USA 85:9479–9483, 1988
20. Ben-Chetrit E, Gandy BJ, Tan EM, Sullivan KF: Isolation and characterization of a cDNA clone encoding the 60-kD component of the human SS-A/Ro ribonucleo-protein autoantigen. J Clin Invest 83:1284–1292, 1989
21. Frankel AD, Pabo C: Fingering too many proteins. Cell 53:675, 1988
22. Scofield RH, Harley JB: Autoantigenicity of a Ro/SSA is related to a nucleocapsid protein of vesicular stomatitis virus. Proc Natl Acad Sci USA 88:3343–3347, 1991
23. Oldstone MBA: Molecular mimicry and autoimmune disease. Cell 50:819–820, 1987
24. McCauliffe DP, Lux FA, Lieu TS, Sanz I, Hanke J, Newkirk MM, Bachinski LL, Itoh Y, Siciliano MJ, Reichlin M, Sontheimer RD, Capra JD: Molecular cloning, expression, and chromosome 19 localization of a human Ro/SS-A autoantigen. J Clin Invest 85:1379–1391, 1990
25. Lingappa VR: Intracellular traffic of newly synthesized proteins. Current understanding and future prospects. J Clin Invest 83:739–751, 1989
26. Fliegel L, Burns K, Wlasichuk K, Michalak M: Peripheral membrane proteins of the sarcoplasmic and endoplasmic reticulum. Comparison of carboxy-terminal amino acid sequences. Biochem Cell Biol 67:696–702, 1989
27. Andres DA, Dickerson IM, Dixon JE: Variants of the carboxyl-terminal KDEL sequence direct intracellular retention. J Bio Chem 265:5952–5955, 1990
28. McCauliffe DP, Lieu T-S, Michalak M, Sontheimer RD, Capra JD: A human Ro/SS-A autoantigen is the homologue of calreticulin and is highly homologous with onchocercal Ral-1 antigen and an aplysia memory molecule. J Clin Invest 86:332–335, 1990
29. Smith MJ, Koch GL: Multiple zones in the sequence of calreticulin, a major calcium binding ER/SR protein. EMBO 8:3581–3586, 1989
30. Lieu T-S, McCauliffe DP, Volpe P, Alderson-Lang BH, Michalak M, Capra JD, Sontheimer RD: Structural and functional homology between a human Ro/SS-A autoantigen and the calcium-binding protein, calreticulin (abstr). Clin Res 38:408A, 1990
31. McCauliffe DP, Yang YS, Wilson J, Sontheimer RD, Capra JD: The 5′ flanking region of the human calreticulin gene is highly homologous with the human GRP78, GRP94 and protein disulfide isomerase promoters. J Biol Chem 267:2557–2562, 1992
32. Sambrook JF: The involvement of calcium in transport of secretory proteins from the endoplasmic reticulum. Cell 61:197–199, 1990
33. Munro S, Pelham HRB: An hsp70-like protein in the ER: identity with the 78 kD glucose-regulated protein and immunoglobulin heavy chain binding protein. Cell 46:291–300, 1986
34. Sorger PK, Pelham HRB: The glucose-regulated protein grp94 is related to heat shock protein hsp90. J Mol Biol 194:341–344, 1987
35. Freedman RB: Protein disulfide isomerase: multiple roles in the modification of nascent secretory proteins. Cell 57:1069–1072, 1989
36. Lux FA, McCauliffe DP, Buttner DW, Capra JD, Sontheimer RD, Lieu TS: Antibodies to *Onchocerca volvulus* cross-react with a human Ro/SS-A autoantigen (abstr). Clin Res 38:626A, 1990
37. Hunter FA, Barger BD, Schrohenloher R, Koopman WJ, Dohlman JG: Autoantibodies to calreticulin in the sera of systemic lupus erythematosus (abstr). Arthritis Rheumat 34 (suppl 9):S75, 1991
38. Rokeach LA, Haselby JA, Meilof JF, Smeenk RJT, Unnasch TR, Greene BM, Hoch SO: Characterization of the autoantigen calreticulin. J Immunol 147:3031–3039, 1991
39. Lieu TS, Capra JD, Sontheimer RD: Calreticulin is a component of the human Wil-2 cell Ro/SS-A autoantigen complex (abstr). Clin Res 40:508A, 1992
40. Edward K, Chan L, Hamel JC, Buyon JP, Jan EM: Molecular definition and sequence motifs of the 52-kD component of human SS-A/Ro autoantigen. J Clin Invest 87:68–76, 1991
41. Itoh K, Itoh Y, Frank MB: Protein heterogeneity in the human Ro/SSA ribonucleoproteins. The 52- and 60-kD Ro/SSA autoantigens are encoded by separate genes. J Clin Invest 87:117–186, 1991
42. Lux FA, McCauliffe DP, Buttner DW, Capra JD, Sontheimer RD, Lieu TS: Serologic cross-reactivity between a human Ro/SS-A autoantigen (calreticulin) and the Ral-1 antigen of *Onchocerca volvulus*. J Clin Invest 89:1945–1951, 1992
43. Lieu TS, McCauliffe DP, Volpe P, Alderson-Lang BH, Heilman C, Leberer E, Michalak M, Fliegel L, Capra JD, Sontheimer RD: Further evidence supporting the identity of a native human Wil-2 cell 46 kD Ro/SS-A autoantigen with the highly conserved calcium binding protein, calreticulin (submitted for publication)
44. Sontheimer RD, Lieu TS, McCauliffe DP: Molecular characterization of the Ro/SS-A autoimmune response. Semin Dermatol 10:199–205, 1991
45. Boire G, Craft J: Biochemical and immunological heterogeneity of the Ro ribonucleoprotein particles. Analysis with sera specific for the RohY5 particle. J Clin Invest 84:270–279, 1989
46. Swanson MS, Nakagawa TY, LeVan, Dreyfuss G: Primary structure of human nuclear ribonuclear particle C proteins: conservation of sequence and domain structures in heterogeneous nuclear RNA, mRNA and pre-rRNA-binding proteins. Mol Cell Biol 7:1731–1739, 1987
47. Rokeach LA, Haselby JA, Hoch SO: Molecular cloning of a cDNA encoding the human Sm-D autoantigen. Proc Natl Acad Sci USA 85:4832–4836, 1988
48. Yamagata H, Harley JB, Reichlin, M: Molecular properties of the Ro/SS-A antigen and enzyme-linked immunosorbent assay for quantitation of antibody. J Clin Invest 74:625–633, 1984
49. Scopelitis E, Biundo JJ, Alspaugh MA: Anti-SS-A antibody and other antinuclear antibodies in systemic lupus erythematosus. Arthritis Rheum 23:287–293, 1980
50. Boire G, Craft J: Human Ro ribonucleoprotein particles: characterization of native structure and stable association with the La polypeptide. J Clin Invest 85:1182–1190, 1990
51. Harmon CE, Deng JS, Peebles CL, Tan EM: The importance of tissue

substrate in the SS-A/Ro antigen-antibody system. Arthritis Rheum 27:166–173, 1984

52. Wermuth DJ, Geoghegan WD, Jordon RE: Anti-Ro/SS-A antibodies. Association with a particulate. (large, speckled-like thread) immunofluorescent nuclear staining pattern. Arch Dermatol 121:335–338, 1985
53. Elenitsas R, Bair LW, Medsger TA, Deng JS: Discordance of SS-A/Ro and SS-B/La cellular antigens in synchronized cells. J Invest Dermatol 87:504–509, 1986
54. Gaither KK, Fox OF, Yamagata H, Mamula MJ, Reichlin M, Harley JB: Implications of anti-Ro/Sjögren's syndrome A antigen autoantibody in normal sera for autoimmunity. J Clin Invest 79:841–846, 1987
55. Maddison PJ: ANA-negative SLE. Clin Rheum Dis 8:105–119, 1982
56. Hendrick JP, Wolin SL, Rinke J, Lerner MR, Steitz JA: Ro small cytoplasmic ribonucleoproteins are a subclass of La ribonucleoproteins: further characterization of the Ro and La small ribonucleoproteins from uninfected mammalian cells. Mol Cell Biol 12:1138–1149, 1981
57. Bachmann M, Mayet WJ, Schroder HC, Pfeifer K, Neyer Zum Buschenfelde KH, Muller WEG: Association of La and Ro antigens with intracellular structures in HEp-2 carcinoma cells. Proc Natl Acad Sci USA 83:7770–7774, 1986
58. Wollina U, Beensen H, Kittler L, Schaarschmidt H, Knopf B: PUVA treatment of human cultured fiberglass from sclerotic skin enhances the binding of antibodies to SS-A (Ro). Arch Dermatol Res 279:206–208, 1987
59. Miyagawa S, Okada N, Inagaki Y, Kitano Y, Ueki H, Sakamoto K, Steinberg ML: SSA/Ro antigen expression in simian virus 40-transformed human keratinocytes. J Invest Dermatol 90:342–345, 1988
60. Koch GLE, Macer DRJ, Smith MJ: Visualization of the intact endoplasmic reticulum by immunofluorescence with antibodies to the major ER glycoprotein, endoplasmin. J Cell Sci 87:535–542, 1987
61. Itoh Y, Reichlin M: Molecular conformation and autoantibodies to the Ro/SSA particle. Arthritis Rheum 34(suppl):S101, 1991
62. Sontheimer RD, McCauliffe DP, Michalak M, Capra JD, Lieu TS: Cytoplasmic localization of a calcium-binding 46 kD human Ro/SS-A antigen. Arthritis Rheum 33S:B15, 1990
63. Milner RE, Baksh S, Shemanko C, Carpenter MR, Smillie L, Vance JE, Opas M, Michalak M: Calreticulin, and not calsequestrin, is the major calcium binding protein of smooth muscle sarcoplasmic reticulum and liver endoplasmic reticulum. J Biol Chem 266:7155–7165, 1991
64. Kato N, Hoshimo H, Harada F: Nucleotide sequence of 4.5S RNA (C8 or hY5) from HeLa cells. Biochem Biophys Res Commun 108:363–370, 1982
65. Buyon JP, Ben-Chetrit E, Karp S, Roubey RAS, Pompeo L, Reeves WH, Tan EM, Winchester R: Acquired congenital heart block. Pattern of maternal antibody responses to biochemically defined antigens of the SSA/Ro-SSB/La system in neonatal lupus. J Clin Invest 84:627–634, 1989
66. Ben-Chetrit E, Fox RI, Tan EM: Dissociation of immune responses to the SS-A (Ro) 52-kD and 60-kD polypeptides in systemic lupus erythematosus and Sjögrens syndrome. Arthritis Rheum 33:349–355, 1990
67. Sontheimer RD: Subacute cutaneous lupus erythematosus. Clin Dermatol 3:58–68, 1985
68. Lee LA, David KM: Cutaneous Lupus erythematosus. Curr Probl Dermatol 1:161–200, 1989
69. LeFeber WP, Norris DA, Ryan SR, Huff JC, Lee LA, Kubo M, Boyce ST, Kotzin BL, Weston WL: Ultraviolet light induces binding of antibodies to selected nuclear antigens on cultured human keratinocytes. J Clin Invest 74:1545–1551, 1984
70. Furukawa F, Kashihara-Sawami M, Lyons MB, Norris DA: Binding of antibodies to ENA SS-A/Ro and SS-B/La is induced on the surface of human keratinocytes by UVL: implications for the pathogenesis of photosensitive cutaneous lupus. J Invest Dermatol 94:77–85, 1990
71. Bachmann M, Chang SH, Slor H, Kukulies J, Muller WEG: Shuttling of the autoantigen La between nucleus and cell surface after UV irradiation of human keratinocytes. Exp Cell Res 191:171–180, 1990
72. Sontheimer RD, McCauliffe DP, Wilson JL, Capra JD: Transcriptional regulation of human calreticulin. Clin Res 40:493A, 1992
73. Kawashima T, Lieu TS, Capra JD, Sontheimer RD: Ultraviolet irradiation preferentially upregulated expression of the 46 kD Ro/SS-A autoantigen (calreticulin) in transformed human epidermal keratinocytes (abstr). Clin Res 40:508A, 1992
74. Furukawa F, Lyons MB, Lee LA, Coulter SN, Norris DA: Estradiol enhances binding to cultured human keratinocytes of antibodies specific for SS-A/Ro and SS-B/La. J Immunol 141:1480–1488, 1988
75. Vanbruskirk A, Crump BL, Margoliash E, Pierce SK: A peptide binding protein having a role in antigen presentation is a member of the HSP70 heat shock family. J Exp Med 170:1799–1809, 1989
76. Fisch P, Malkovsky M, Kovats S, Strum E, Braakman E, Klein BS, Voss SD, Morrissey LW, DeMars R, Welch WJ, Bolhuis RLH, Sondel PM: Recognition by human Vgamma9/Vdelta2 T cells of a GroEL homolog on Daudi Burkitt's lymphoma cells. Science 250:1269–1273, 1990
77. Hennungs H, Michael D, Cheng C, Steinert P, Holbrook K, Yuspa SH: Calcium regulation of growth and differentiation of mouse epidermal cells in culture. Cell 19:245–254, 1980
78. Lee LA, Gaither KK, Coulter SN, Norris DA, Harley JB: Pattern of cutaneous immunoglobulin G deposition in subacute cutaneous lupus erythematosus is reproduced by infusing purified anti-Ro (SS-A) autoantibodies in human skin-grafted mice. J Clin Invest 83:1556–1562, 1989
79. Booth C, Koch GLE: Perturbation of cellular calcium induces secretion of luminal ER proteins. Cell 59:729–737, 1989
80. Lodish HF, Kong N: Perturbation of cellular calcium blocks exit of secretory proteins from rough endoplasmic reticulum. J Biol Chem 265:10893–10899, 1990
81. Kutsch CL, Norris DA, Middleton MH, Lee LA: Induction of anti-Ro/SS-A antibody binding to human keratinocytes stimulated by either calcium ionophore A23187 or by TNF-alpha (abstr). J Invest Dermatol 96:610, 478, 1991
82. Schattner A, Rager-Zisman B: Virus-induced autoimmunity. Rev Infect Dis 12:204–222, 1990
83. Tesar TT, Armstrong J: Expression of Ro/SSA and La/SSB on epithelial cell surface following *in vitro* adenovirus infection (abstr). Arthritis Rheum S74, C20, 1986
84. Jianhui Z, Newkirk MM: Viral induction of the human autoantigen calregulin Ro/SS-A (abstr). Arthritis Rheumat 34(suppl):S102, 1991
85. Bachmann M, Falke D, Shroder HC, Muller WEG: Intranuclear distribution of the La antigen in CV-1 cells after herpes simplex virus type I infection compared with the localization of U small nuclear ribonucleoprotein particles. J Gen Virol 70:881–891, 1989

Islet Cell Autoantigen 69 kD (ICA69)

Molecular Cloning and Characterization of a Novel Diabetes-associated Autoantigen

Massimo Pietropaolo,* Luis Castaño,* Sunanda Babu,* Roland Buelow,‡ Yu-Ling S. Kuo,‡ Stephan Martin,§ Andrea Martin,§ Alvin C. Powers,|| Michal Prochazka,¶ Jurgen Naggert,¶ Edward H. Leiter,¶ and George S. Eisenbarth*

*Barbara Davis Center for Childhood Diabetes, University of Colorado Health Sciences Center, Denver, Colorado 80262; and Elliot P. Joslin Research Laboratory, Joslin Diabetes Center, Brigham and Women's Hospital, New England Deaconess Hospital, Harvard Medical School, Boston, Massachusetts 02215 ‡ImmuLogic Pharmaceutical Corporation, Palo Alto, California 94394; §Diabetes Forschungsinstitut, D-4000 Düsseldorf, Germany; ||Division of Endocrinology, Nashville Veterans Affairs Medical Center, Vanderbilt University, Nashville, Tennessee 37232; and ¶The Jackson Laboratory, Bar Harbor, Maine 04609

Abstract

We have identified a novel 69-kD peptide autoantigen (ICA69) associated with insulin-dependent diabetes mellitus (IDDM) by screening a human islet λgt11 cDNA expression library with cytoplasmic islet cell antibody positive sera from relatives of IDDM patients who progressed to the overt disease. The deduced open reading frame of the ICA69 cDNA predicts a 483–amino acid protein. ICA69 shows no nucleotide or amino acid sequence relation to any known sequence in GenBank, except for two short regions of similarity with BSA. The ICA69 cDNA probe hybridizes with a 2-kb mRNA in poly(A^+) RNA from human pancreas, brain, heart, thyroid, and kidney, but not with skeletal muscle, placenta, spleen, or ovary. Expression of ICA69 was also detected in β cells and cell lines, as well as in tumoral tissue of islet cell origin. The native ICA69 molecule migrates to 69 kD in SDS-PAGE as detected with specific antibodies. Serum samples from relatives of IDDM patients specifically reacted with affinity-purified recombinant ICA69 on Western blotting. The structural gene for ICA69 was designated *ICA1*. A homologue in the mouse, designated *Ica-1* was mapped to the proximal end of chromosome 6 (within 6 cM of the Met protooncogene). ICA69 adds a novel autoantigen to the family of identified islet target molecules, and by the manner of its identification and characterization large amounts of antigen are available for development of quantitative, convenient predictive assays for autoantibodies and analysis of the role of this molecule in diabetes autoimmunity, as well as its physiologic function. (*J. Clin. Invest.* 1993. 92:359–371.) Key words: autoantigens • preclinical diabetes • molecular cloning • autoimmunity • ICA69

Introduction

There is evidence that insulin-dependent diabetes mellitus (IDDM)[1] is a chronic autoimmune disease in which the presence of autoantibodies, such as cytoplasmic islet cell antibodies or insulin autoantibodies, can be present years before the clinical onset of the disease (1). A common feature of type I diabetes and other autoimmune diseases is a humoral immune response characterized by the appearance of autoantibodies against cellular proteins, including islet peptides (2–4). Although all the target antigens in type I diabetes have not been identified, several autoantigens associated with the disease have been molecularly characterized using different experimental approaches, namely insulin (5), glutamic acid decarboxylase (GAD) (6), carboxypeptidase H (7), as well as the glycolipids GT3 (8) and GM2-1 (9). Recently, cDNA encoding for a fragment of carboxypeptidase H (7), a granule-associated enzyme, has been reported to react with sera from prediabetic patients and another peptide expressed in a λgt11 phage from a human islet library appears to be recognized by IDDM sera (10). Cellular proteins of unknown sequence whose molecular masses are 38 (11), 52 (12), and 69 kD (13), have also been reported to be recognized by a humoral and/or a cellular immune response. It is of interest that almost all patients with type I diabetes have elevated levels of IgG anti-BSA antibodies related to a 69,000-M_r islet peptide, which may represent a target antigen for cow milk–induced islet autoimmunity (14, 15).

The present study was undertaken to isolate clones that code for some of these or other unidentified autoantigens and characterize their molecular structure. Isolation of cDNA clones expressing antigenic determinants has been extensively used to identify clones coding for autoantigens in different autoimmune diseases (16). This approach offers the possibility of identifying and characterizing novel autoantigens that may be of restricted cellular distribution as well as low cellular expression (17). Such proteins may not be detected by routine screening tests such as immunofluorescence or immunoprecipitation.

We have used this approach to immunoscreen a human islet λgt11 expression library with a pool of sera from prediabetic relatives of IDDM patients, identify, sequence the clones, and characterize the expressed proteins. In this report, we describe the cloning of a cDNA that encodes a novel islet autoantigen, whose apparent migration is 69 kD on SDS-polyacrylamide gel chromatography.

Methods

Serum samples. Sera were obtained from first degree relatives of patients with type I diabetes. All of them were at high risk of developing IDDM, and some have already progressed to the overt disease on prospective follow-up. Clinical studies were performed with informed consent, as well as approval from the Joslin Clinic and University of Colorado institutional review boards. All the sera used for the screening of the human islet λgt11 library expressed high titer of islet cell antibodies (> 80 Juvenile Diabetes Foundation units). The sera were repeatedly absorbed with a protein lysate of a wild λgt11 phage–infected *Esche-*

Address correspondence and reprint requests to Dr. George S. Eisenbarth, The Barbara Davis Center for Childhood Diabetes, University of Colorado Health Sciences Center, 4200 East 9th Ave., Box B140, Denver, CO 80262.

Received for publication 6 October 1992 and in revised form 3 February 1993.

1. *Abbreviations used in this paper:* APAAP, alkaline phosphatase–antialkaline phosphatase; GAD, glutamic acid decarboxylase; ICA, islet cell antibodies; IDDM, insulin-dependent diabetes mellitus; IPTG, isopropyl-β-D-thiogalactopyranoside; LB, Luria-Bertani; PAP, peroxidase antiperoxidase; pfu, plaque-forming units; RFLV, restriction length fragment variation.

J. Clin. Invest.

0021-9738/93/07/359/13 $2.00
Volume 92, July 1993, 359–371

richia coli strain Y1090 (18) to remove anti-*E. coli* antibodies. Absorbed antibodies were stored at −20°C in the presence of 0.05% sodium azide until used for immunological screening. Originally, a pool of three sera was used to identify positive clones, and subsequently sera of three other relatives were studied for reactivity with the positive clone. 10 sera of normal individuals were also tested for reactivity with the positive clone. Sera from additional prediabetic relatives (subjects followed to diabetes onset) (n = 23), autoantibody positive but currently nondiabetic relatives (n = 31), and normal controls (n = 70) were tested for reactivity to the expressed molecule on Western blots.

λgt11 expression libraries. Two λgt11 libraries were used, a human islet library provided by Dr. Alan Permutt (Washington University, St. Louis, MO) and a human insulinoma library generated by Alvin C. Powers (Vanderbilt University, Nashville, TN). A human λgt11 islet library was constructed from human islet poly(A$^+$) mRNA by Clontech (Palo Alto, CA), with ~ 1×10^9 plaque-forming units (pfu)/ml and 85% being recombinants. A human insulinoma library was generated from insulinoma poly(A$^+$) mRNA and then cDNA was produced and packaged into the λgt11 phage (19), with ~ 1.3×10^9 pfu/ml and a recombinant rate of more than 80%.

Screening of λgt11 expression libraries with antibody and cDNA probes. A phage human islet λgt11 expression library was screened with a pool of sera from preclinical IDDM relatives (20). Isolated recombinant phages were plated on Luria-Bertani (LB) agar plates (150 mm diameter) with *E. coli* strain Y1090 at ~ $0.5–1 \times 10^4$ pfu/plate. After a 3-h incubation at 42°C, a nitrocellulose filter (Schleicher & Schuell, Keene, NH) saturated with 10 mM isopropyl-β-D-thiogalactopyranoside (IPTG) (BRL, Grand Island, NY) was overlaid on the agar overnight at 37°C to induce the expression of β-galactosidase fusion proteins. After that, the filters were blocked with 1% BSA (Sigma Immunochemicals, St Louis, MO) in Tris-buffered saline (TBS), incubated containing 0.05% Tween, incubated for 2 h at room temperature), and then incubated with 1/500 diluted sera overnight at 4°C. After several washes with TBS, the bound antibodies were detected by incubation with anti-human IgG alkaline phosphatase (Cappel Laboratories, Durham, NC) diluted 1/100 (2 h at room temperature). A phage human islet λgt11 expression library was initially screened with pooled sera from three prediabetics. The original positive plaque was replated and rescreened sequentially until all progeny of plaques were recognized by the sera. To determine whether prediabetic sera or controls reacted with the product of the clone and to reduce the possibilities of false positivity, plaque-purified recombinant bacteriophage was mixed ~ 1:1 with a wild-type λgt11 and plated with *E. coli* Y1090 as for screening. Pieces of nitrocellulose carrying plaque proteins were then incubated with individual sera. Reactions were considered positive if significant staining of ~ 50% of the plaques was observed. Intensity of staining was estimated to score reactivity of individual sera on a 0 (negative) to 4+ (strongest) scale. The cDNA insert of the original positive clone, termed PM1/1 (Fig. 1 *B*), was used as probe to further screen the human islet library and a human insulinoma library by plaque hybridization (21) to obtain several longer and overlapping cDNA clones. The probe was labeled with [α^{32}P]dCTP by random priming (21, 22) using Klenow fragment (Amersham Corp., Arlington Heights, IL) and used to rescreen the libraries.

Amplification of λgt11 cDNA insert and cloning. The λgt11 cDNA insert from the positive clones was amplified by PCR (23, 24) using λgt11 primers complementary to the β-galactosidase portion of the λgt11 template (primer 1218: 5′-GGTGGCGACGACTCCTGGAGCCCG-3′; primer 1222: 5′-TTGACACCAGACCAACTGGTAATG-3′, New England Biolabs, Beverly, MA). Reaction mixtures for PCR (0.1 ml) contained cDNA template, 100 pmol each of the primers, and 2.5 U of *Taq* I DNA polymerase (Perkin-Elmer Cetus Instruments, Norwalk, CT) in 10 mM Tris/HCl, pH 8.3, 50 mM KCl, 1.5 mM $MgCl_2$ containing dNTPs at 0.2 mM each and 0.01% gelatin. Reactions were carried out in a thermal cycler (Perkin-Elmer Cetus) for 30 cycles of denaturation (92°C, 1 min), annealing (60°C, 1.5 min), and elongation (72°C, 1 min). After *Eco* RI digestion and fractionation on 1% agarose gel stained with ethidium bromide to visualize the PCR products, the product of interest was excised, purified, and subcloned into the *Eco* RI site of pBluescript II vector. This vector was used to transform *E. Coli* strain XL1 Blue, and to sequence the PCR products across its polylinker arms (Stratagene, La Jolla, CA). cDNA samples for PCR were obtained from phage suspension.

DNA sequencing and computer analysis of nucleic acid and protein sequences. Nucleotide sequences were determined by using the dideoxynucleotide chain termination method of Sanger et al. (25), using T7 DNA polymerase (Sequenase; United States Biochemical Corp., Cleveland, OH). To avoid compression in G + C–rich sequences, additional sequencing reactions were performed with dITP alternating with dGTP (26).

Sequences were aligned and analyzed using the EUGENE, SAM, PIMA.SH, and PROSITE programs. The GenBank (DNA and Amino Acid Databank) was searched for similarities, and the PLSEARCH program analyzed for protein sequence patterns derived from the sequences of homologous protein families (Molecular Biology Computing Research Resource, Dana Farber Cancer Institute, and Harvard School of Public Health, Cambridge, MA). Hydropathy plots from the deduced amino acid sequence were prepared as described by Kyte and Doolittle (27, 28) and Klein et al. (29).

Cell lines. Cells were used at late log phase, when almost all were viable. RIN 1046-38, derived from a rat insulinoma (kindly provided by Christopher Newgard, Southwestern Medical Center, University of Texas, Dallas, TX), were cultured in DME supplemented with 10% FBS, and 5.6 mM glucose in a humidified atmosphere of 10% CO_2/90% air at 37°C (30). βTC-1 and αTC-1 were derived from progeny of transgenic mice expressing SV40 large T-antigen under control of the rat insulin II 5′-flanking region or rat preproglucagon 5′-flanking region respectively (31–33). The βTC-1 and αTC-6 cell lines were maintained in DME supplemented to a final concentration of 16.5 mM glucose and supplemented with Eagle's MEM, nonessential amino acids component, 44 mM sodium bicarbonate, 15 mM Hepes, 50 μg/liter gentamicin sulphate, and 10% heat-inactivated FBS in a humidified atmosphere of 5% CO_2/95% air. HIT cells, derived from a hamster insulin producing cell line (34), were grown in 5% CO_2/95% air in RPMI 1640 medium containing 10% FCS and 11.1 mM glucose. HeLa cells (ATCC CCL 2.2; American Type Culture Collection, Rockville, MD) (35), JEG cells (human choriocarcinoma; ATCC HTB 36) (36), and HepG2 cells (human hepatoma; ATCC HB 8065) (37) were maintained in RPMI 1640 supplemented with 10% FCS, 2 mM L-glutamine and 5 μg/ml gentamicine sulfate in 10% CO_2/90% air incubator. A human islet carcinoid cell line designated BON-1 (provided by Dr. Cortney Townsend, Department of Surgery, University of Texas Medical Branch, Galveston, TX) was maintained in DME with 10% heat-inactivated FCS and 5.6 mM glucose in a humidified atmosphere of 10% CO_2/90% air.

RNA isolation and Northern analysis. Total RNAs and poly(A$^+$) RNAs from various tissues and cell lines were prepared by the guanidinium isothiocyanate method, enriched for the polyadenylated (poly-A) fraction with an oligo(dT)-cellulose column and analyzed on Northern blots according to standard procedures (38). The hybridization was carried out for 18 h at 42°C in the prehybridization buffer (50% formamide, 5× SSPE [1× SSPE consists of 150 mM NaCl, 10 mM sodium phosphate, and 1 mM EDTA, pH 7.4]), 5× Denhardt's solution, 100 μg/ml denaturated salmon sperm DNA, and 0.1% SDS) (18) containing [α^{32}P]dCTP labeled cDNA purified probe. The probes consisted of either a 0.95-kb fragment from the original PM1/1 positive clone identified, or a 1.78-kb gt11 insert from an overlapping clone; 100 ng of each probe was labeled by the random priming method. 100 ng of a 2-kb human β-actin cDNA was used as control probe (39). The fresh hybridization solution contained the denatured radiolabeled DNA probes at a concentration of $2–4 \times 10^6$ cpm/ml with a specific activity ≥ 5×10^8 cpm/μg (18, 40). The nitrocellulose filters were washed in three changes of 2× SSC and 0.05% SDS at room temperature each time. The final three washes were carried out in 0.1× SSC and 0.1% SDS from room temperature to 65°C depending upon the stringency conditions required for each experiment. Filters were exposed to Kodak film at −80°C with intensifying screens. Ribosomal bands were used as size markers (41, 42).

Preparation of anti-ICA69 antibodies from synthetic peptides and from the purified molecule. Rabbit antibodies were produced using synthetic peptides from the deduced amino acid sequence as well as the ICA69 recombinant expressed molecule. Rabbits were immunized in order to generate antibodies against specific domains (28, 43). Two regions of the molecule, one corresponding to the COOH terminus, residues 471–483: GKTDKEHELLNA, and one to an internal polypeptide close to the COOH terminus, residues 458–470: ADLDPLSNPDAV, and the serum generated against the whole molecule, were used and found to yield antisera which reacted with the native ICA69 molecule on Western blots (44). The synthetic polypeptides were coupled to a carrier protein, keyhole limpet hemocyanin linked to bromoacetyl bromide. Five female New Zealand white rabbits were immunized with 1 mg of the keyhole limpet hemocyanin–peptide conjugate suspended in 1 ml of complete Freund's adjuvant. Rabbits were boosted three times with 1 mg of the specific polypeptide in incomplete Freund's adjuvant at 30-d intervals and serum samples were collected and stored in aliquots at −20°C. An ELISA was used to detect specific antipeptide antibodies.

Indirect ELISA. Indirect ELISA was performed for the detection of specific antibodies generated in rabbits against ICA69 polypeptides (45). 1 μg of specific polypeptide was used to coat each well of a microtiter plate (Immulon; Dymatech Laboratories, Inc., Chantilly, VA) (46), and after blocking residual binding of the plate with a PBS solution containing 1% BSA for 2 h, appropriate dilutions of rabbit pre- and postimmune sera were added to each well (1:100–1:32,000) and incubated overnight. All dilutions were tested in triplicate. After washing away unbound antibodies, a solution containing anti–rabbit IgG (whole molecule) peroxidase conjugate (Sigma Immunochemicals) as developing reagent was added to the wells. After 2 h incubation, unbound conjugate was washed away and a substrate solution (*o*-phenylenediamine dihydrochloride) (Sigma Immunochemicals), was added. A specific hyperimmune serum raised to another polypeptide (PEP-80, of the IRS-1 molecule kindly provided by Dr. M. White, Joslin Diabetes Center) (47) and preimmune sera from normal rabbits were used in each assay as positive and negative controls respectively. The optical density of the solutions in the wells was measured with a spectrophotometer through a 405-nm filter.

SDS-PAGE and immunoblotting. Cell line extracts and total homogenates of rat brain tissues were prepared as described by Laemmli (48). Cell line extracts and total-homogenate proteins were separated by SDS-PAGE using a constant voltage of 180 V for 4 h through stacking and the resolving gel. Bromophenol blue was included in the sample buffer to visualize buffer front. A mixture of individually colored and purified proteins were used as protein standards (Rainbow® Protein Molecular Weight Markers, Amersham Corp.): myosin, mol wt 200,000, blue; phosphorylase b, mol wt 97,400, brown; BSA, mol wt 69,000, red; ovalbumin, mol wt 46,000, yellow; carbonic anhydrase, mol wt 30,000, orange; trypsin inhibitor, mol wt 21,000, green; and lysozyme, mol wt 14,300, magenta. Homogenate protein concentrations were determined by Lowry's method (Pierce Chemical Co., Rockford, IL) and 4–50 μg of proteins per lane (depending on the size of the PAGE) were run on a 10% SDS-PAGE under reducing conditions. Proteins were then transferred onto nitrocellulose according to Towbin et al. (49) in transfer buffer (12.5 mM Tris, 96 mM glycine, 20% methanol) for 1 h on a semi-dry electrophoretic transfer cell at 15 V. The nitrocellulose was cut into strips, and incubated for 2 h at 37°C in 5% (wt/vol) nonfat dried milk diluted in PBS (Blotto buffer) to block the nonspecific binding sites. The nitrocellulose strips were then incubated with a 1:100 dilution of a rabbit anti-ICA69 antiserum and then washed in 5% (wt/vol) nonfat dried milk diluted in PBS adding Tween 20 to a final concentration of 0.01%. After incubation of the filters at room temperature for 2 h with ^{125}I-Protein A (Amersham Corp.) to detect the rabbit anti-ICA69 antibodies, unbound ^{125}I-Protein A was removed by washing as described above. Blots were exposed to Kodak film at −80°C with intensifying screens for 12–24 h.

Expression of the recombinant ICA69. PM1/3 clone cDNA was amplified by PCR. The PCR product was generated using a primer spanning the PM1/3 start codon and encoding the first eight amino acids (5′-TCAGGACACAAATGCAGTTATCCC-3′), and a primer containing the codon sequence for the last seven amino acids, a translational stop codon and a HindIII restriction site (5′-TTTAAGCTTTCA-TGCATTGAGCAATTCGTGTTC-3′). The pMAL-c vector (50, 51), which encodes for maltose binding protein as product of the *malE* gene, was cut with StuI and HindIII restriction enzymes and ligated with the PM1/3 PCR product. The constructs were then transfected into the appropriate *E. coli*, strain TB1 (52). Ampicillin-resistant colonies were grown overnight in 3 ml LB medium containing 100 μg/ml ampicillin. 100 μl of TB1 pMAL-c-PM1/3 transformants were diluted in 1 ml LB/ampicillin medium and grown 1 h at 37°C followed by induction with 1 mM IPTG for 2 h. Lysates were prepared by centrifugation of 200 μl bacterial cultures for 1 min and boiling the cell pellet with 50 μl SDS sample buffer with 5% mercaptoethanol. After SDS-PAGE of lysates (10 μl) with and without IPTG induction, gels were stained with Coomassie blue. One colony expressing a protein whose molecular mass migrated ~ 105 kD was identified, and the correct size of the insert was confirmed by restriction analysis.

Another vector system was used to express the purified recombinant ICA69 protein without maltose binding protein. The coding region of the PM1/3 cDNA clone, was amplified by PCR using the primers 5′-GAAGGATCCATGTCAGGACACAAATGCAG-3′ and 5′-GGTCTCGAGTCATGCATTGAGCAATTCGTG-3′ and cloned into the BamHI and XhoI sites of the expression vector pTrc99A (His_6). This vector was constructed by insertion of a synthetic DNA fragment encoding six histidines ($[CAC]_6$) into the polylinker of pTrc 99A (53). Recombinant proteins were tagged with six histidine residues at the NH_2 terminus. The plasmid construct was transformed into *E. coli*–Tg1 and protein expression was induced by the addition of IPTG to the culture medium. After 2 h at 37°C, bacteria were lysed in 100 mM Tris pH 8.0, 6 M GuHCl, and 10 mM DTT, and insoluble material was removed by centrifugation at 40,000 *g* for 30 min. Recombinant $(His)_6$-ICA69 was purified using Ni-NTA-agarose (Qiagen, Chatsworth, CA) in the presence of 6 M GuHCl, 1 mM DTT buffer. The correct size of the ICA69 cDNA in the vector was confirmed by sequencing.

Lysates containing ICA69 and maltose binding protein fusion protein, as well as the purified recombinant ICA69, have been used as source for performing Western blots with control sera such as rabbit anti-ICA69 sera (pre- and postimmune), human control sera, and prediabetic sera at a dilution 1:100. Optical density of the bands corresponding to the ICA69 fusion protein and the affinity-purified ICA69 has been evaluated to quantitate the reactivity of the serum samples to ICA69 using a video densitometer (Bio Rad Laboratories, Hercules, CA), and the results were expressed as relative densitometric units.

Immunohistochemistry. Immunohistochemistry has been performed in formalin fixed rat pancreas paraffin embedded sections (4 μm thickness). A double immunoenzymatic labeling of rat islet cellular constituents has been performed (54, 55) using as detection system horseradish peroxidase antiperoxidase (PAP) and alkaline phosphatase–antialkaline phosphatase (APAAP). The PAP immune complex served for the identification of ICA69, whereas the APAAP complex for the identification of insulin, glucagon and somatostatin. After removal of paraffin and rehydratation of tissue, the pancreas sections were first treated with an hydrogen peroxidase solution to suppress possible endogenous peroxidase activity. This was followed by an incubation with normal serum to quench nonspecific protein binding to certain tissue elements, and then the sections were incubated with a primary antibody mixture (rabbit anti-ICA69 antibody generated to the whole molecule, and a mouse mAb generated insulin [HPI-005] to glucagon [GLU 001], or anti-ICA69 and a mouse mAb generated to somatostatin [SOM 018] [Novo Nordisk, Denmark]) for 30 min at room temperature. Unbound antibodies were washed with TBS. Antibody to target antigens (primary antibody), antibody to the primary antibody (link antibody: swine anti–rabbit for ICA69, or goat anti–mouse for antiinsulin, antiglucagon or antisomatostatin mAbs), APAAP and PAP reagents (Dako Corp., Santa Barbara, CA) were applied sequentially for simultaneous double staining. The color development was stopped by washing the slides thoroughly in deionized water.

a

```
     CGGGCGGGGGATACCCCAGGAGATGGGGGTCGAGGAGAGACCCCGGGGAGTAGAGAGAGAGAAACTCACTCCCCGAGTCCCCGACCCTCCCCAAG -178
CAAGGTTATAATATAACTTATCCTCTCATGCTTTTTTCCTGCCCCTTCTCCCCAAATCATCAACAATAGAAGAAGAAGAAAAC ATG TCA GGA CAC   12
                                                                                          Met Ser Gly His    4

AAA TGC AGT TAT CCC TGG GAC TTA CAG GAT CGA TAT GCT CAA GAT AAG TCA GTT GTA AAT AAG ATG CAA CAG AGA   87
Lys Cys Ser Tyr Pro Trp Asp Leu Gln Asp Arg Tyr Ala Gln Asp Lys Ser Val Val Asn Lys Met Gln Gln Arg   29
                                           AMD                                          CK2
TAT TGG GAG ACG AAG CAG GCC TTT ATT AAA GCC ACA GGG AAG AAG GAA GAT GAA CAT GTT GTT GCC TCT GAC GCG  162
Tyr Trp Glu Thr Lys Gln Ala Phe Ile Lys Ala Thr Gly Lys Lys Glu Asp Glu His Val Val Ala Ser Asp Ala   54

GAC CTG GAT GCC AAG CTA GAG CTG TTT CAT TCA ATT CAG AGA ACC TGT CTG GAC TTA TCG AAA GCA ATT GTA CTC  237
Asp Leu Asp Ala Lys Leu Glu Leu Phe His Ser Ile Gln Arg Thr Cys Leu Asp Leu Ser Lys Ala Ile Val Leu   79
                                CK2
TAT CAA AAG AGG ATA TGT TTC TTG TCT CAA GAA GAA AAC GAA CTG GGA AAA TTT CTT CGA TCC CAA GGT TTC CAA  312
Tyr Gln Lys Arg Ile Cys Phe Leu Ser Gln Glu Glu Asn Glu Leu Gly Lys Phe Leu Arg Ser Gln Gly Phe Gln  104
                                         PKC
GAT AAA ACC AGA GCA GGA AAG ATG ATG CAA GCG ACA GGA AAG GCC CTC TGC TTT TCT TCC CAG CAA AGG TTG GCC  387
Asp Lys Thr Arg Ala Gly Lys Met Met Gln Ala Thr Gly Lys Ala Leu Cys Phe Ser Ser Gln Gln Arg Leu Ala  129
                                         PKC
TTA CGA AAT CCT TTG TGT CGA TTT CAC CAA GAA GTG GAG ACT TTT CGG CAT CGG GCC ATC TCA GAT ACT TGG CTG  462
Leu Arg Asn Pro Leu Cys Arg Phe His Gln Glu Val Glu Thr Phe Arg His Arg Ala Ile Ser Asp Thr Trp Leu  154

ACG GTG AAC CGC ATG GAA CAG TGC AGG ACG GAA TAT AGA GGA GCA CTA TTA TGG ATG AAG GAC GTG TCT CAG GAG  537
Thr Val Asn Arg Met Glu Gln Cys Arg Thr Glu Tyr Arg Gly Ala Leu Leu Trp Met Lys Asp Val Ser Gln Glu  179

CTT GAT CCA GAC CTC TAC AAG CAA ATG GAG AAG TTC AGG AAG GTG CAA ACA CAA GTG CGC CTT GCA AAA AAA AAC  612
Leu Asp Pro Asp Leu Tyr Lys Gln Met Glu Lys Phe Arg Lys Val Gln Thr Gln Val Arg Leu Ala Lys Lys Asn  204

TTT GAC AAA TTG AAG ATG GAT GTG TGT CAA AAA GTG GAT CTT CTT GGA GCG AGC AGA TGC AAT CTC TTG TCT CAC  687
Phe Asp Lys Leu Lys Met Asp Val Cys Gln Lys Val Asp Leu Leu Gly Ala Ser Arg Cys Asn Leu Leu Ser His  229

ATG CTA GCA ACA TAC CAG ACC ACT CTG CTT CAT TTT TGG GAG AAA ACT TCT CAC ACT ATG GCA GCC ATC CAT GAG  762
Met Leu Ala Thr Tyr Gln Thr Thr Leu Leu His Phe Trp Glu Lys Thr Ser His Thr Met Ala Ala Ile His Glu  254
PKC                                      PKC      CK2
AGT TTC AAA GGT TAT CAA CCA TAT GAA TTT ACT ACT TTA AAG AGC TTA CAA GAC CCT ATG AAA AAA TTA GTT GAG  837
Ser Phe Lys Gly Tyr Gln Pro Tyr Glu Phe Thr Thr Leu Lys Ser Leu Gln Asp Pro Met Lys Lys Leu Val Glu  279
                                                                                          CK2
AAA GAA GAG AAG AAG AAA ATC AAC CAG CAG GAA AGT ACA GAT GCA GCC GTG CAG GAG CCG AGC CAA TTA ATT TCA  912
Lys Glu Glu Lys Lys Lys Ile Asn Gln Gln Glu Ser Thr Asp Ala Ala Val Gln Glu Pro Ser Gln Leu Ile Ser  304
                                AMP      PKC                                      CK2
TTA GAG GAA GAA AAC CAG CGC AAG GAA TCC TCT AGT TTT AAG ACT GAA GAT GGA AAA AGT ATT TTA TCT GCC TTA  987
Leu Glu Glu Glu Asn Gln Arg Lys Glu Ser Ser Ser Phe Lys Thr Glu Asp Gly Lys Ser Ile Leu Ser Ala Leu  329

GAC AAA GGC TCT ACA CAT ACT GCA TGC TCA GGA CCC ATA GAT GAA CTA TTA GAC ATG AAA TCT GAG GAA GGT GCT 1062
Asp Lys Gly Ser Thr His Thr Ala Cys Ser Gly Pro Ile Asp Glu Leu Leu Asp Met Lys Ser Glu Glu Gly Ala  354

TGC CTG GGA CCA GTG GCA GGG ACC CCG GAA CCT GAA GGT GCT GAC AAA GAT GAC CTG CTG CTG TTG AGT GAG ATC 1137
Cys Leu Gly Pro Val Ala Gly Thr Pro Glu Pro Glu Gly Ala Asp Lys Asp Asp Leu Leu Leu Leu Ser Glu Ile  379
          *  CK2
TTC AAT GCT TCC TCC TTG GAA GAG GGC GAG TTC AGC AAA GAG TGG GCC GCT GTG TTT GGA GAC GGC CAA GTG AAG 1212
Phe Asn Ala Ser Ser Leu Glu Glu Gly Glu Phe Ser Lys Glu Trp Ala Ala Val Phe Gly Asp Gly Gln Val Lys  404

GAG CCA GTG CCC ACT ATG GCC CTG GGA GAG CCA GAC CCC AAG GCC CAG ACA GGC TCA GGT TTC CTT CCT TCG CAG 1287
Glu Pro Val Pro Thr Met Ala Leu Gly Glu Pro Asp Pro Lys Ala Gln Thr Gly Ser Gly Phe Leu Pro Ser Gln  429
                                         CK2
CTT TTA GAC CAA AAT ATG AAA GAC TTA CAG GCC TCG CTA CAA GAA CCT GCT AAG GCT GCC TCA GAC CTG ACT GCC 1362
Leu Leu Asp Gln Asn Met Lys Asp Leu Gln Ala Ser Leu Gln Glu Pro Ala Lys Ala Ala Ser Asp Leu Thr Ala  454
                                CK2                      PKC
TGG TTC AGC CTC TTC GCT GAC CTC GAC CCA CTC TCA AAT CCT GAT GCT GTT GGG AAA ACC GAT AAA GAA CAC GAA 1437
Trp Phe Ser Leu Phe Ala Asp Leu Asp Pro Leu Ser Asn Pro Asp Ala Val Gly Lys Thr Asp Lys Glu His Glu  479

TTG CTC AAT GCA TGA ATCTGTACCCTTCGGAGGGCACTCACATGCCGCCCCCAGCAGCTCCCCTGGGGGCTAGCAGAAGTATAAAGTGATCAGT 1531
Leu Leu Asn Ala END                                                                                 483

ATGCTGTTTTAATAATTATGTGCCATTTTAATAAAATGAAAGGGTCAACGGCCCTGTTAAAAAAAAAAAAAAAAAAA                    1607
```

b

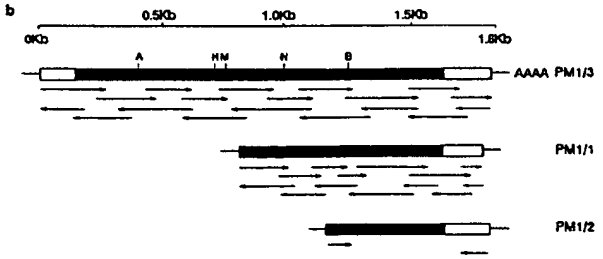

Figure 1. (*a*) Complete nucleotide and deduced amino acid sequence of the ICA69 molecule. Underlined are the first upstream in frame stop codon (*TAA*) at nucleotide −75 and the polyadenylation signal 29 bp upstream of the poly(A) tail. Homologous subunits with BSA are in boxes. A potential N-linked glycosylation site is indicated by an asterisk. Potential phosphorylation sites are as follows: PKC (protein kinase C), CK2 (casein kinase II), and AMP (cAMP/cGMP-dependent kinase). A potential amidation site is indicated as AMD. (*b*) Strategy for sequencing cDNA encoding ICA69 polypeptide and partial restriction map. Sequencing was performed with synthetic oligonucleotide primers, and the direction of sequencing is indicated by arrows. Restriction sites are: A, AccII; B, BglII; H, HgiAI; M, MaeII; and N, NdeI. The poly(A) tail (*AAAA*) was found in the PM1/3 clone. The coding region is indicated by solid bars and 5′ and 3′ untranslated regions are represented by empty bars. These sequence data are available from GenBank under accession number L01100.

The sections were then counterstained with Mayer's hematoxylin. Coverslips were mounted with an aqueous mounting medium without alcohol (Glicergel; Dako Corp.).

Mapping of the mouse homologue of Ica-1. Presence of a homologous locus in the mouse genome (*Ica-1*) was established by analysis of Southern blots of kidney DNA from the NOD (nonobese diabetic) mouse digested with a variety of restriction endonucleases and probed with the PM1/1 cDNA insert according to the procedure described in detail elsewhere (56). An XbaI restriction fragment length variation (RFLV) distinguishing the *Ica-1* locus in the diabetes-susceptible NOD/Lt (~ 8 kb fragment) from the related, but diabetes-resistant NON/Lt strain (~ 11 kb fragment), was used both to assign a chromosomal location and to assess whether a gene conferring susceptibility to IDDM was closely linked to the NOD/Lt allele of *Ica-1*. Segregation of this *Ica-1* RFLV was studied in a panel of kidney DNAs prepared from 19 first backcross diabetic mice from an NOD/Lt × NON/Lt outcross previously typed for other DNA markers (57), plus kidney DNAs from 40 diabetic F2 mice produced in an outcross between NOD/Lt and a diabetes-resistant NON/Lt stock congenic for the diabetogenic $H\text{-}2^{g7}$ haplotype of NOD (NON.NOD-H-2^{g7}) (58). A HindIII RFLV distinguished NOD/Lt (~ 8.5 kb fragment) from both NON/Lt and NON-NOD-H-2^{g7} (~ 7.8 kb fragment). Comparison of the *Ica-1* segregation pattern with previously typed markers indicated that this locus was linked to the *Met* protooncogene on proximal chromosome 6. To confirm this putative linkage, segregation of *D6Rck2*, *D6Mit1*, and *D6Mit16* was assessed by PCR using the oligonucleotide primer sequences described by Dietrich et al. (59). The recombination frequencies reported represent a weighted average using the information function (60).

Statistical analysis. Differences between groups of relatives and controls were analyzed by Wilcoxon rank sum test.

Results

Isolation of cDNA clones encoding the ICA69 molecule. A human islet λgt11 expression library was immunoscreened with a pool of sera from three prediabetic relatives of IDDM patients, which contained a high titer of cytoplasmic islet cell antibodies. Approximately 0.4×10^6 plaques were screened and a single, consistently positive 0.95 kb clone, designated PM1/1, was identified. Fusion protein from the purified clone induced by IPTG, reacted with three out of six ICA positive prediabetic subjects' sera (individually tested at 1:500 dilutions of the sera), whereas no reaction was obtained with 10 control individual sera. A labeled cDNA probe derived from the PM1/1 clone was used to screen both a human λgt11 islet library and a human insulinoma λgt11 library to obtain the full-length cDNA. Screening ~ 6.5×10^4 pfu, two additional hybridizing and overlapping clones were identified from the human islet λgt11 expression library, both of which retained specificity after secondary and tertiary screening to 100% purity. DNA sequence analysis (see below) confirmed that the clones contained fragments of the same gene.

DNA sequence. After PCR amplification and subcloning into pBluescript II vector, partial sequence indicates that the smallest overlapping clone (PM1/2), whose size is 0.6 kb, reveals sequence totally contained within the original sequenced PM1/1 insert (Fig. 1 *B*). The results of sequencing both cDNA strands of the longest clone (PM1/3), whose size is 1.78 kb, indicates complete identity in the region of the molecule overlapping with the two clones and sequence not contained within the previous clones.

Analysis of the nucleotide sequence 1,785 bp cDNA reveals a 1,449-bp open reading frame coding for 483 amino acids and ending in a poly(A) tail 29 bases downstream of the canonical polyadenylation signal (AATAAA). Translation of the ICA69 message putatively initiates from the first in frame ATG according to the criteria defined by Kozak (61). Upstream from the first ATG, there is an in frame stop codon (TAA) at −75 bp (Fig. 1 *A*). The predicted open reading frame from the deduced ATG start codon, codes for a protein with an estimated linear relative molecular mass of 54,600, which contains one potential N-linked glycosylation site.

Using computer programs to search databases of known nucleic acid or amino acid sequences, no significant similarities were found except for minimal homology with BSA, implying that our sequence was new and unique. Two short regions of bovine but not human serum albumin precursor appear to have similarities with the ICA69 molecule (Fig. 2).

A hydrophobicity plot generated from the ICA69 inferred amino acid sequence reveals a number of slightly hydrophobic regions, alternating with several very hydrophilic segments, which suggests that the molecule does not contain any membrane spanning domain, according to the criteria defined by both Kyte and Doolittle (27, 28) and Klein et al. (29). The segments of hydrophobicity appear not to be long enough to be potential transmembrane-spanning regions. The molecule is predominantly hydrophilic, with 27% of its amino acid residues positively or negatively charged.

Analysis of ICA69 transcripts in normal and tumor cells. The cDNA derived from two clones (PM1/1, PM1/3) was used to probe for transcripts in human and animal tissues and in several cell lines by Northern analysis (Figs. 3 and 4). Probes consisting of 0.95 kb (PM1/1) and 1.78 kb (PM1/3) hybridized with a 2-kb mRNA band in islet-derived cell lines, and in some tissues, with a 2.7-kb band. Fig. 3 shows a Northern blot of ICA69 transcripts in human tissues. A 2-kb poly(A^+) RNA band was detected in abundant amounts in both human pancreas and heart, and then in brain, and in small amounts in lung, liver and kidney, but not in placenta and skeletal muscle. In brain and heart, an additional 2.7-kb band is visible. A 2-kb poly(A^+) RNA band was also detected in human thyroid, but not in ovary and spleen (not shown). The β-actin control probe hybridized with a 2-kb band in all tissues with different intensity, and with a smaller band (1.6 kb) in both heart and

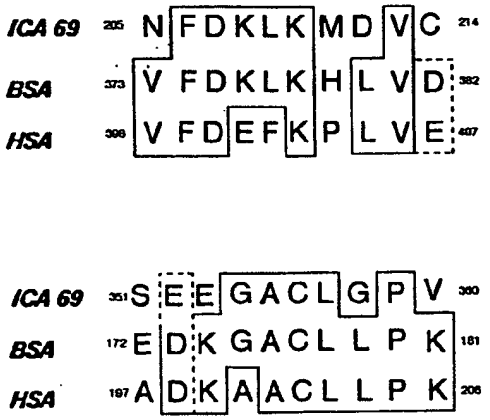

Figure 2. Regions of similarities between ICA69 molecule, BSA, and human serum albumin precursor (*HSA*). Solid line encloses identical amino acid residues. Dashed line encloses amino acid residues with similar charge. Numbers correspond to the amino acid residue numbers.

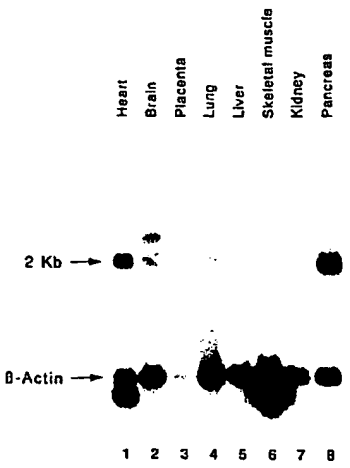

Figure 3. Northern blot analysis of poly(A$^+$) RNA from different human tissues hybridizing with the 0.95-kb cDNA insert of the PM 1/1 clone. The poly(A$^+$) RNA was obtained from Clontech. 2 μg of pure poly(A$^+$) RNA from each tissue was applied and resolved on denaturating gel as described under Methods. Lane *1*, human heart; lane *2*, human brain; lane *3*, human placenta; lane *4*, human liver; lane *5*, human lung; lane *6*, human skeletal muscle; lane *7*, human kidney; and lane *8*, human pancreas. The same blot was rehybridized with a human β-actin cDNA control probe to show that the mRNA was not degraded. Hybridization and washing were performed with identical conditions in the two different experiments. The blot was exposed for 4 h (β-actin cDNA probe) and 24 h (PM1/1 cDNA probe) at −80°C with intensifying screen.

skeletal muscle. This is because β-actin is not expressed in equal amount in all tissues and because there are two forms of β-actin mRNA in both heart and skeletal muscle (2 and 1.6 kb) (40). The labeled cDNA PM1/1 insert hybridizes with a 2-kb mRNA band in total RNA from rat pancreas, brain, and cerebellum and kidney (in the last three tissues, also with a 5-kb band). In contrast, no ICA69 transcripts were detectable in rat spleen, thymus, bowel, lymph nodes, and salivary gland (not shown). The heterogeneity of mRNA size among tissues may be caused by an alternative splicing of the *ICA1* gene. As shown in Fig. 4, the 2-kb *ICA1* transcript was detected in total RNA from human insulinoma and from a variety of endocrine cell lines, such as a human islet carcinoid cell line (BON-1), a hamster insulin-producing cell line (HIT), and three rodent islet cell lines, namely the rat RIN 1046-38 insulinoma cell line, the mouse βTC-1 (producing primarily insulin, but also some glucagon, and which shows a transcript after longer exposure than shown in Fig. 4), and the mouse αTC-6 (glucagon-producing clonal line). No *ICA1* transcripts were detected in total RNA from three human nonislet cell lines, namely HepG2-hepatoma, HeLa-cells, and JEG-choriocarcinoma (Fig. 4).

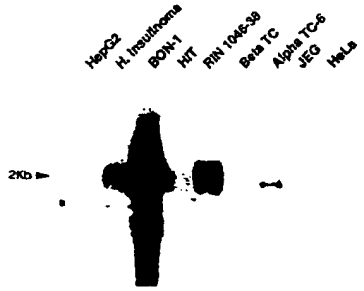

Figure 4. Northern blot analysis of ICA69 expression in human insulinoma, and rat, hamster, and mouse transformed cell lines. A 2-kb mRNA is detected in total RNA from human (*H*) insulinoma, a human islet carcinoid cell line (*BON-1*), a hamster insulin-producing cell line (*HIT*), RIN 1046-38, and the mouse islet lines βTC-1 (which is visible after longer exposure), and αTC-6 (a clonal line producing glucagon). No detectable mRNA was found in total RNA from three human nonislet cell lines: HepG2-hepatoma, HeLa-fibroblast, and JEG-choriocarcinoma. Autoradiograph exposure time was 2–7 d.

Immunoblotting. Western blots of cell line extracts (RIN 1046-38, BON-1) and brain tissue homogenate revealed a specific band of 69 kD after incubation with rabbit antibodies raised to the COOH terminus of ICA69 and an internal polypeptide. Fig. 5 illustrates that rabbit antiserum (rabbit number 1) raised against the COOH terminus of the molecule specifically reacted with a protein of 69 kD in RIN 1046-38 and BON-1 (visible after longer exposure than shown in Fig. 5) total cell homogenate, but not with HeLa cell line homogenate. The specific 69-kD band disappears after absorption with the polypeptide against which specific antibodies were produced. The control serum from the same rabbit before the polypeptide immunization does not show any 69-kD reactivity. The same specific 69-kD reactivity was also detectable in rat brain total homogenate (not shown), and also using hyperimmune sera generated to an internal polypeptide as well as antiserum produced against the whole ICA69 molecule (see Methods). Since the deduced amino acid sequence of ICA69 is 483 residues with an estimated relative molecular mass of 54,600, the difference between the Western blot size of the protein fractionated in the SDS-PAGE and the estimated size based on the deduced amino acid sequence is likely caused by an aberrant migration of the RIN and the brain tissue proteins in SDS-PAGE as a result of detergent solubilization, as previously observed for a brain protein of approximately the same sequence deduced molecular mass and a similarly discrepant migration on SDS-PAGE (62, 63).

Reactivity of recombinant ICA69 with serum of first degree relatives of IDDM patients on Western blotting. To determine whether sera from prediabetic subjects reacted with the recombinant ICA69 fusion protein, and then with the purified ICA69 recombinant molecule, further testing of Western blots was

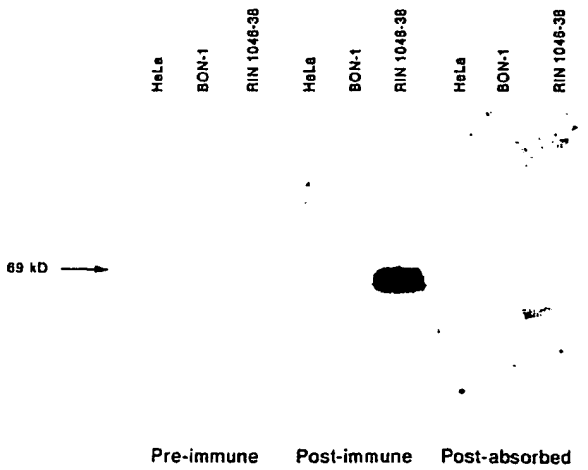

Figure 5. Rabbit antiserum raised against a COOH-terminal ICA69 peptide sequence specifically reacted with a protein of 69 kD in RIN 1046-38 and BON-1 (visible after longer exposure) cell total homogenate but not with homogenate from HeLa cells. The specific 69-kD band disappears after absorption with the polypeptide against which specific antibodies were produced. The serum from the same rabbit (rabbit number 1) before the polypeptide immunization does not react with the 69-kD band.

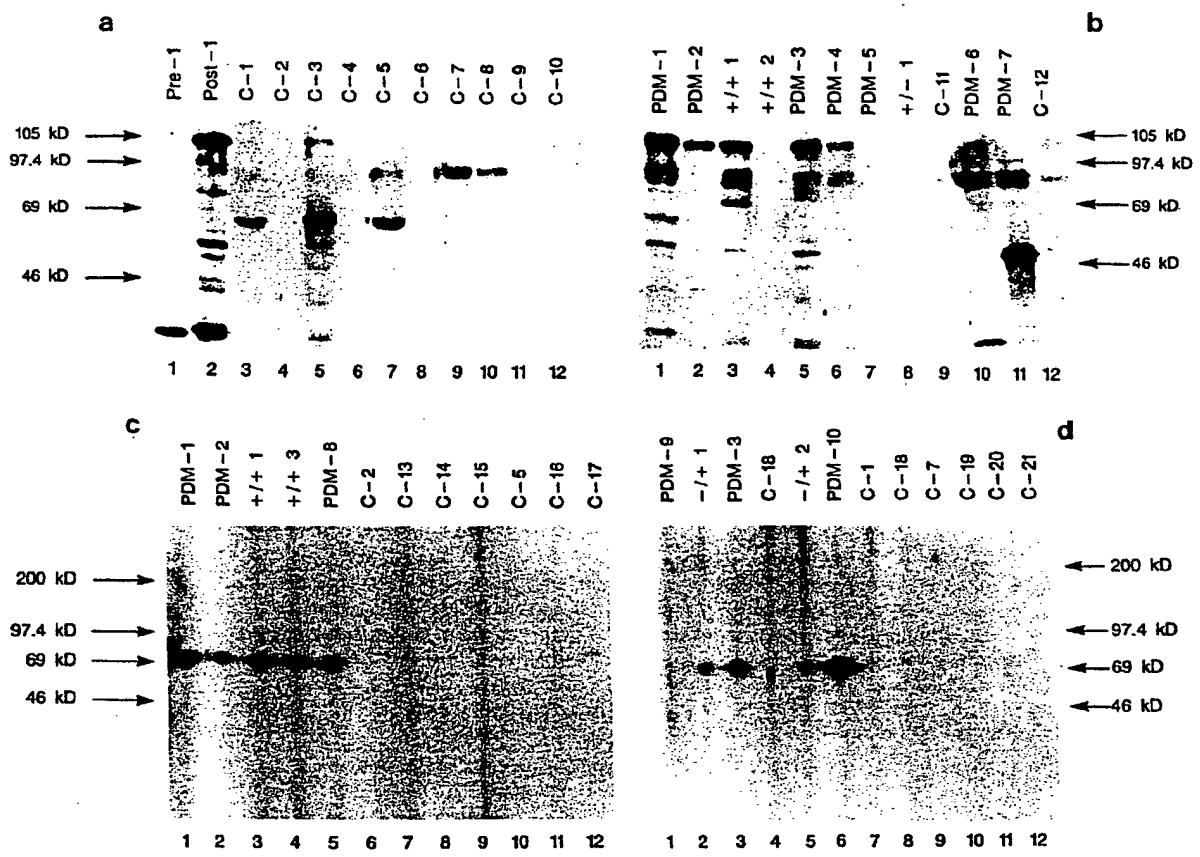

Figure 6. Anti-ICA69 sera from relatives of IDDM patients recognize a maltose binding protein-ICA69 fusion protein (*a* and *b*) and affinity-purified recombinant ICA69 without fusion protein (*c* and *d*) on Western blots. Fluorograms of 10% SDS-PAGE showing reactivity of normal control (C), prediabetic relatives' sera (PDM) from preclinical IDDM subjects (at dilution 1:100) and reactivity of serum samples from autoantibody positive relatives (citoplasmic islet cell antibody/insulin autoantibody +/+, +/−) who have not yet developed diabetes. Bands at ~ 105 kD (*arrows*) represent the PM1/3 clone fusion protein as indicated by reactivity with rabbit-anti ICA69 peptide antibody. The ~ 105 kD bands correspond to the SDS-PAGE migration of the whole fusion protein. Lanes *1–2* (*a*), samples from the same rabbit (rabbit number 1) before (*Pre-1*) and after (*Post-1*) the immunization with the deduced COOH terminus polypeptide of ICA69 (see Methods). Lanes *3–12*, serum samples from 10 healthy individuals. In *b*, sera from seven prediabetics (PDM-1 to 7), from two cytoplasmic islet cell antibody+/insulin autoantibody+ relatives who have not developed diabetes (+/+), from one cytoplasmic islet cell antibody+/insulin autoantibody negative (+/−) and two additional human control sera (C-11, C-12). Immunoblots showing reactivity of preclinical IDDM relatives cytoplasmic islet cell antibody–positive serum samples (PDM) with Ni-NTA-agarose purified recombinant $(His)_6$-ICA69 (*c* and *d*). The purified ICA69 was separated by a 10% SDS-PAGE, and probed with sera from relatives of IDDM patients, and from controls (at 1:100 dilution). Lanes *1*, *2*, and *5* (*c*) and lanes *3* and *6* (*d*) show reactivity of sera from relatives of IDDM patients followed to the overt disease (PDM) with the 69-kD band. Cytoplasmic islet cell antibody/insulin autoantibodies (+/+ and −/+), serum samples from relatives of IDDM patients that have not developed the disease, show also reactivity with ICA69. Note the absence of detectable reactivity with control sera (lanes *6–12* in *c*; lanes *4* and *7–12* in *d*). All the sera from both prediabetics and controls used in the preliminary MBP/PM1/3 clone fusion protein Western blot assay gave consistent results using the affinity-purified recombinant ICA69 as source of antigen for performing Western blots (some of the same serum samples, used in the immunoblots in *a* and *b*, are indicated with the same label in the two sets of immunoblots [Fig. 6, *a*, *b*, *c* and *d*]). Rabbit hyperimmune sera produced against the whole ICA69 and the COOH terminus of the molecule specifically reacted also with the Ni-NTA-agarose purified $(His)_6$-ICA69 (not shown). Positions of molecular mass markers ($M_r \times 10^{-3}$), and ~ 105 kD bands are indicated at right and left edges. The gels were exposed for 6–12 h.

performed. We first assessed whether antiserum raised against the COOH terminus and the whole ICA69 molecule, as well as the three sera from prediabetics previously reacting with the λgt11 IPTG-induced PM1/1 insert, could react on a Western blot with the PM1/3 clone expressed as a fusion protein with maltose binding protein. The rabbit hyperimmune serum and 6 out of 10 sera from relatives with IDDM specifically reacted with a ~ 105 kD band (Fig. 6, *a* and *b*) which corresponds to the SDS-PAGE migration of the whole fusion protein, whereas none of the 12 control sera reacted significantly (quantitating the sera reactivity to the ~ 105 kD band by scanning densitometry).

Sera from first degree relatives from patients with insulin-dependent diabetes mellitus demonstrated specific binding to the affinity purified recombinant ICA69 on Western blotting (Fig. 6, *c* and *d*, and Fig. 7). Serum samples from 23 relatives of IDDM patients who were initially found to be ICA positive and then followed to the clinical onset of the disease (*Pre-DM*: Fig. 7), 70 healthy volunteers, serum samples from 13 ICA+/IAA+ (cytoplasmic islet cell antibody+/insulin autoanti-

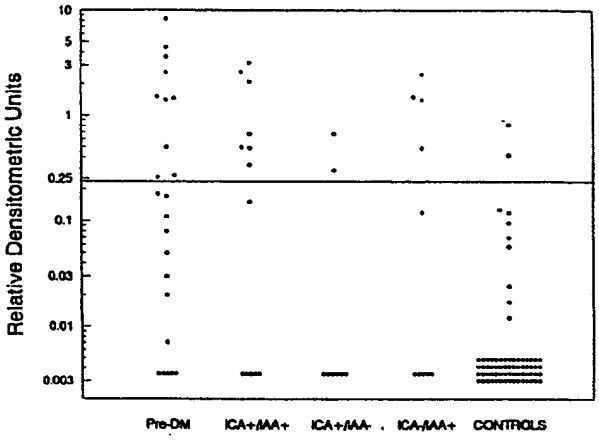

Figure 7. Quantitative comparison of serum binding to recombinant affinity-purified ICA69. Results of Western blots for individual serum samples (dilution 1:100) assayed against purified islet cell autoantigen 69 kD (ICA69) are shown. Levels of antibody to ICA69 in Pre-DM (preclinical IDDM relatives followed up to the overt disease [n = 23]); in relatives that have not developed diabetes, but with evidence of humoral antiislet autoimmunity, namely (cytoplasmic islet cell antibody/antiinsulin autoantibody) ICA+/IAA+ (n = 13), ICA+/IAA− (n = 8), and ICA−/IAA+ (n = 10); and in normal control subjects (n = 70). The horizontal line represents the value 2 SD above the pooled mean control values. Anti-ICA69 antibody levels are expressed as relative densitometric units.

body+), 8 ICA+/IAA−, and 10 ICA−/IAA+ who have not developed type I diabetes to date were assayed to determine their reactivity to highly purified ICA69. Most serum samples from the control group reacted minimally with the purified ICA69 in this assay format. When significant antigen binding was defined as an optical density of > 2 SD above the mean values for the control group (Fig. 7), serum from 10 of the 23 Pre-DM group, exceeded 2 SD of normal binding to ICA69 (43%), as well as serum samples from 7 of the 13 ICA+/IAA+ (54%), from 2 of the 8 ICA+/IAA− (25%), and from 4 of the 10 ICA−/IAA+ (40%). It is of interest that in the ICA+/IAA− group all the serum samples from relatives of IDDM patients that are considered negative, detected by our Western blot assay format, are restricted ICA, who rarely progress to the overt IDDM.

ICA69 islet immunohystochemistry. Staining of formalin-fixed sections of rat pancreas with antibodies raised to the human recombinant ICA69 revealed selective β cell reactivity (Fig. 8). In islets double immuno-enzymatically labeled with a polyclonal antibody to ICA69 and with mAbs to glucagon or somatostatin, antibodies to ICA69 reacted with the β cell core (Fig. 8 *a*) but not with either glucagon or somatostatin containing cells (Fig. 8, *b* and *c*).

Chromosome localization of Ica-1, the mouse homologue, to chromosome 6. Linkage data summarized in Fig. 9 indicate that *Ica-1* (*Ica-1* is the mouse gene symbol for the gene coding for ICA69; ICA1 is the human gene symbol for the gene coding for ICA69) is linked to the *Met* protooncogene (located 6 cM proximal on chromosome 6). Linkage to two other proximal *Met*-linked markers (*D6Mit1*, *D6Rck2*, 5 cM proximal) was demonstrated. The weighted average of the interval between *Met* and *Ica-1* was estimated to be 6.23±2.5 cM based on 1/17 recombinant in the backcross panel and 5/40 obligate recombinant in the F2 panel (total of 97 informative meioses). The proximal *D6Mit1* and *D6Rck2* markers were separable by the finding of three recombinations in 101 informative meioses between *Ica-1* and *D6Mit1* versus six recombinations in 94 informative meioses between *Ica-1* and *D6Rck2*. The weighted average of the interval between *Met* and *D6Mit1* was estimated to be 3.05±2.29 cM and the interval between *D6Mit1* and *Ica-1* to be 3.85±2.20 cM. The finding of 22 recombinations in 74 informative meiosis between *Ica-1* and the more distal marker *D6Mit16* confirms that *Ica-1* is proximal to *Met*. Collectively, these data would suggest a gene order of centromere-*Ica1-D6Mit1-D6Rck2-Met-D6Mit16* as indicated in Fig. 9. Though a polymorphism between NOD and NON exists for the *Ica-1* gene, and segregation of the NOD-derived *Ica-1* allele was not significantly associated with diabetes in either the backcross or the F2 generation ($P > 0.05$ by chi square analysis), indicating that it was not closely linked to a locus at the proximal end of chromosome 6 conferring susceptibility to insulin dependent diabetes (*Idd* gene) of NOD mice.

In the human, *MET* has been mapped to chromosome 7q21-7q31 (65). The localization of the mouse *Ica-1* gene within 6 cM of the *Met* protooncogene on chromosome 6, suggests that the human *ICA1* gene may be found close to the *MET* protooncogene protein-tyrosine kinase locus in a conserved region around 7q31.

Discussion

Recent findings have indicated that the range of autoantigens related to type I diabetes is more diverse than was originally thought. Sera from IDDM patients, as well as from stiff-man syndrome patients, appear to recognize one or both forms of the neuroendocrine-associated enzyme GAD (6, 66), namely GAD 65 (67), and GAD 67 (68), and one portion of the antibody response to islet cells, termed "restricted ICA," has been reported to recognize GAD (69, 70). In the present study, we have cloned, sequenced, and characterized a novel 69-kD diabetes-related autoantigen.

In an attempt to identify molecular targets for antiislet autoimmunity in IDDM, we have used sera from preclinical IDDM subjects as probe to isolate cDNA clones from a human islet λgt11 expression library. We have obtained a cDNA of a novel protein that codes for a full-length amino acid sequence 54.6 kD with an apparent mobility of 69 kD on SDS-PAGE. The detection of mRNA in neural tissues studied such as brain, the presence of ICA69 transcripts in islet-derived cell lines, namely, RIN 1046-38, BON-1, HIT, βTC-1, αTC-6, and in human insulinoma tissue, in contrast to nonneuroendocrine cell lines such as HeLa cells, JEG-choriocarcinoma, and HepG2-hepatoma likely reflect the sharing of many molecules between islets and neurons. A low level of ICA69 mRNA was also found in human lung, liver, and kidney. It is of interest that a high level of ICA69 mRNA is present in heart, whereas mRNA is undetectable in skeletal muscle and this could be related to the presence of selective cells expressing high levels of this molecule. Islets and neuronal cells both contain secretory granules and microvesicular bodies; for instance, GAD has been localized to microvesicular structures in both pancreatic β cells, as well as in synaptic nerve microvesicular structures (71). Many of the molecules of both of these shared structures appear to be prominent targets of the autoimmunity related to

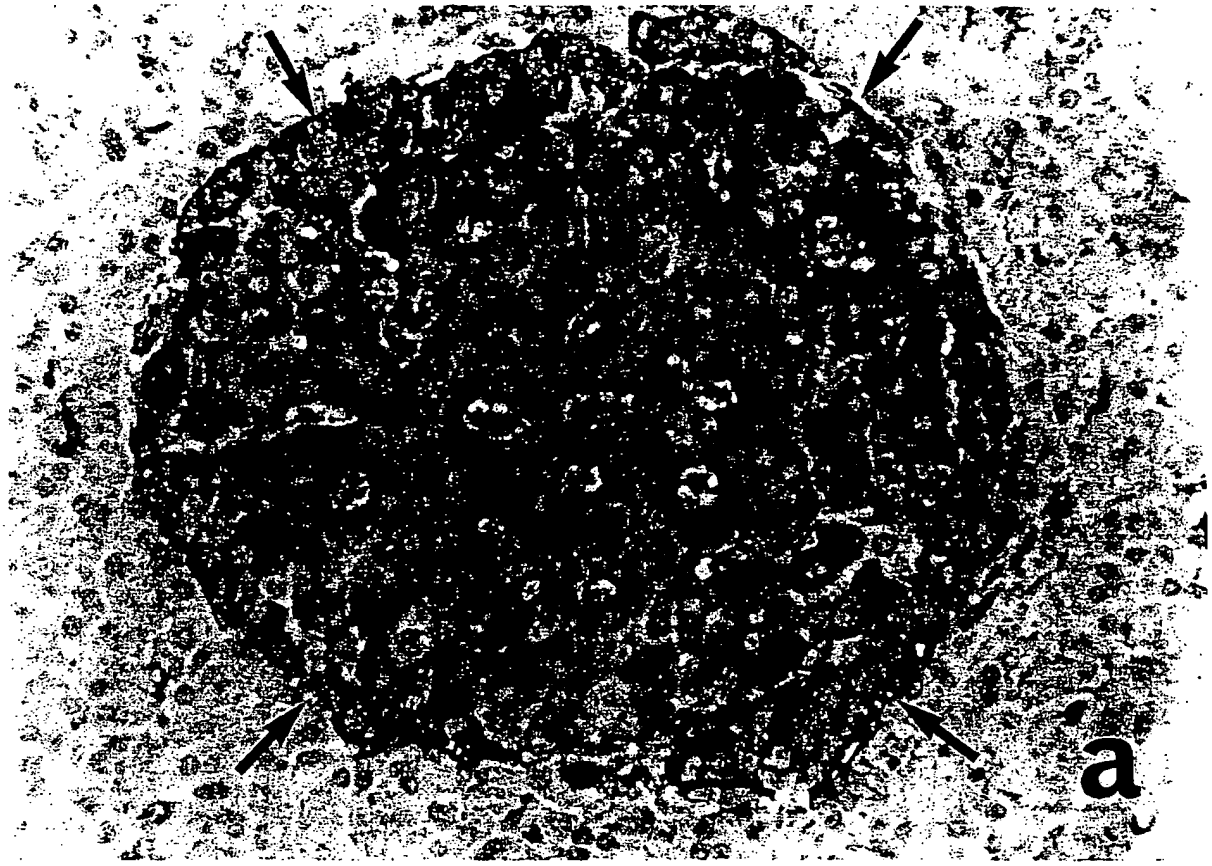

Figure 8. Microphotographs of peroxidase and alkaline phosphatase double immunoenzymatic rat islets labeling using anti-ICA69, antiinsulin, antiglucagon, and antisomatostatin antibodies. (*a*) The islet was double-labeled for ICA69 and glucagon. Anti-ICA69 antiserum reacted with the β cell core of the islet (*brown*), whereas the glucagon containing cells are stained with an antiglucagon mAb (*red, arrows*) and are not reactive with ICA69 (×350). (*b*) The islet was double-labeled for ICA69 and somatostatin. Anti-ICA69 antiserum (*brown*) reacted with the β cell core, whereas the somatostatin containing cells reacted with an antisomatostatin mAb (*red*); additional peripheral cells (*arrows*), negative for both ICA69 and somatostatin, are apparently non-β cells (×315). (*c*) An islet was double-labeled with mAb anti-insulin (*brown*) and antiglucagon (*red, arrows*), showing a pattern identical to that of (*a*) (anti-ICA69 and antiglucagon) (×350).

type I diabetes. The fact that ICA69 mRNA is detected mostly in endocrine cell lines of islet cell origin, and that ICA69 mRNA is also detected in brain, thyroid and heart, but not skeletal muscle, suggests that ICA69 may be in fact related to the neuroendocrine system. A 2-kb mRNA band is visible in total RNA a glucagon producing cell line, namely αTC-6, whereas no staining is visible on normal rat glucagon containing cells detecting by immunohystochemistry.

The putative polypeptide encoded by the longest open reading frame of ICA69 clones has a molecular mass of 54,600 D. On Western blots, immunoreactive ICA69 has a molecular mass of 69 kD suggesting aberrant migration on SDS-PAGE. A molecular mass discrepancy between that calculated from the deduced amino acid sequence and that measured by SDS-PAGE, has been reported in the cloning of a number of proteins (62, 63, 72–74). These proteins have highly charged regions that appear to be related to retarded SDS-PAGE gel migration, resulting thus in an overestimation of the true molecular mass. Our protein has several strongly charged regions, such as the segment of the molecule between residues 307 and 320. The fact that cDNA encoding the full length of the molecule produces a 69-kD protein when expressed in bacteria whose molecular mass is higher than the one inferred by the relative molecular mass of the deduced sequence (54.6 kD), supports aberrant gel migration as the likely cause of the relative molecular mass disparity.

Environmental factors are potential triggers of autoimmunity in type I diabetes (13). There is evidence in animal models of IDDM such as BB rats that the elimination of cow milk proteins from the diet significantly reduces the incidence of the clinical onset of diabetes in these animals (75). Sera from patients with type I diabetes as well as BB rats are reported to have high titer of IgG anti–BSA antibodies (but not of antibodies to other milk proteins) or IgG anti–ABBOS (a region of the BSA molecule extending from 152 to 158 amino acid residues) antibodies (13–15). It has been reported that antibodies raised to one short BSA unique peptide region (ABBOS) or serum from a newly diagnosed IDDM child react on a Western blot format

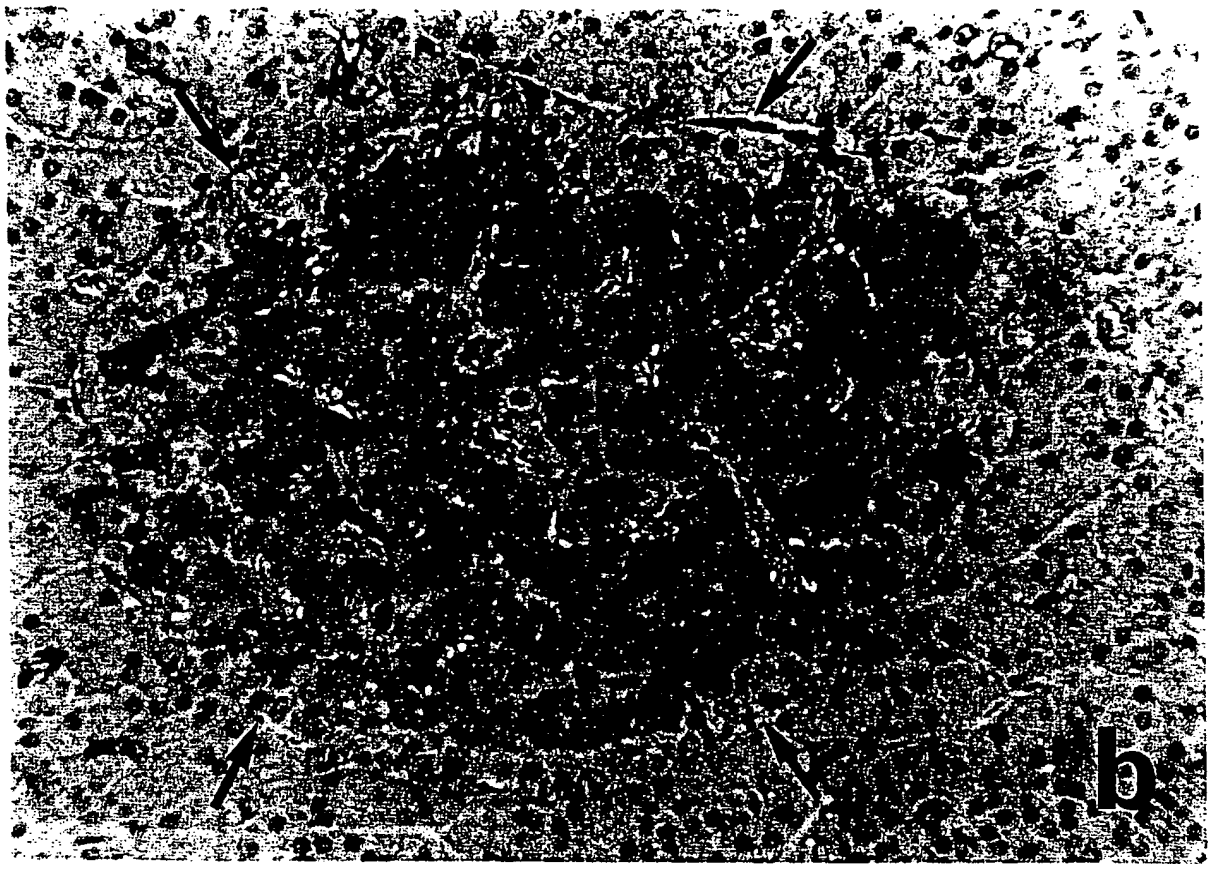

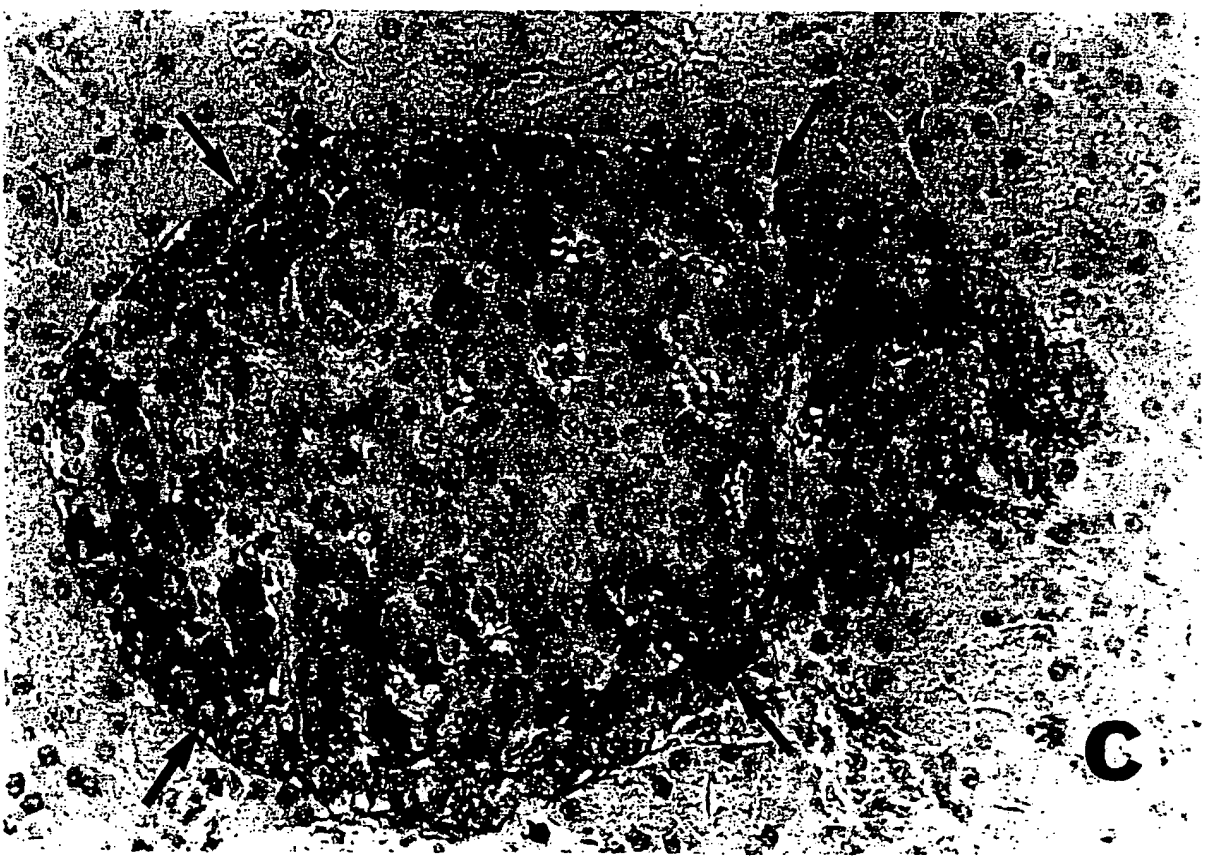

Figure 8 (Continued)

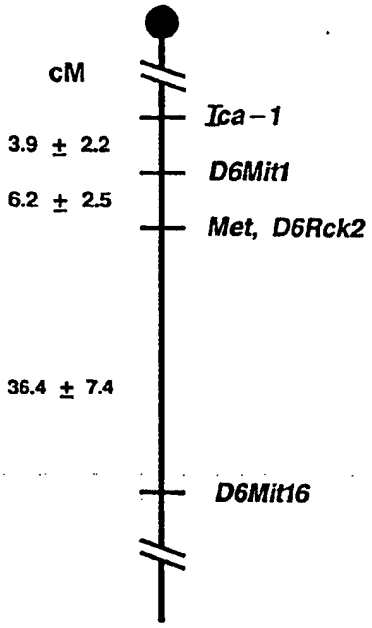

Figure 9. Localization of *Ica-1* on proximal chromosome 6 of the mouse. The recombination frequencies between linked loci are expressed in cM±SEM (shown at the left) and were estimated using a weighted average for backcross and F2 data. Multipoint linkage map constructed using MAPMAKER 1.9 (64) gave maximum likelihood estimates for the best three gene orders as follows: order 1, *Ica-1-D6Mit1-D6Rck2-Met* log likelihood −79.10; order 2, *D6Rck2-Met-Ica-1-D6Mit14* log likelihood −82.85; and order 3, *D6Rck2-Met-D6Mit1-Ica-1* log likelihood −86.88. *Recombination frequency estimated from F2 data only.

with γ-interferon–induced RIN 69-kD protein or with islet proteins with a similar mobility (60–70 kD), respectively (13).

It is of interest that our 69-kD molecule shares two short regions of similarity with bovine serum albumin (not with human serum albumin precursor). These two antigenic determinants perhaps could play a role in the induction of cow milk–induced autoimmunity based upon the hypothesis of pathogenesis related to molecular mimicry, or may be simply a cause of a cross-reactivity with anti-ICA69 antibodies and with anti-BSA antibodies. To prove one of these two hypotheses, further studies are required. We have just learned that a partial peptide sequence available from a p69 BSA-related molecule studied by Dosch and co-workers is identical to amino acids 262 to 325 of ICA69 (H.-M. Dosch, personal communication).

Our study shows that first degree relatives of patients with IDDM who developed the disease carry antibodies reacting with ICA69. Antibodies to ICA69 are detected also in relatives who have not yet developed the disease. Such antibodies are found in 43% of the serum samples from preclinical IDDM relatives assayed so far, and we believe that with the optimization of a more sensitive assay (such as a radioassay or an ELISA), the percentage of reactivity with ICA69 among IDDM relatives will increase.

Detecting by Western blotting, the percentage of anti-ICA69 reactivity among sera from relatives of IDDM patients that developed the disease and in from ICA+/IAA+ group appears to be higher than the ICA+/IAA− group (25%) (Fig. 7), seemingly because all the anti-ICA69 negative sera from ICA+/IAA− relatives assayed thus far, show a β cell–selective ICA pattern (termed "restricted"), that includes recognition of GAD, which is associated with the lack of progression to overt diabetes (69, 70). Therefore, the low percentage of anti-ICA69 positive sera in the ICA+/IAA− group as compared to the other groups appears to be related to the fact that most of the ICA+/IAA− IDDM serum samples from IDDM relatives assayed so far are restricted ICA and rarely progress to the overt IDDM. In light of these observations, we believe that with the combination of different assays for the detection of autoantibodies in IDDM, such as anti-IAA, anti-GAD, anti-ICA69, and in the future against other islet autoantigens, combinatorial algorithms for improving the prediction of type I diabetes will be designed.

The identification, the characterization of the molecular structure and the availability of the ICA69 molecule will help to add this autoantigen to a battery of markers for the prediction of diabetes risk, and will enhance our understanding of islet biochemistry. A family of islet antigen specific therapies are considered for the suppression of insulin-dependent diabetes; e.g., oral tolerance to insulin (76). ICA69 with its β cell expression and autoantigenicity becomes an additional candidate molecule for manipulation of β cell autoimmunity.

Acknowledgments

We are grateful to Dr. Mary Loeken for helpful technical suggestions on the cloning, Dr. Temple Smith for the computer-based sequence analysis, and in particular, Dr. Alan Permutt for provision of the human islet library, Dr. Christopher Newgard for providing the RIN 1046-38 cell line and for valuable discussions, and Dr. Cortney Townsend for providing the BON-1 cell line. Drs. Linda Wicker and Larry Peterson (Merck Research Laboratories, Rahway, NJ) are thanked for providing kidneys from diabetic F2 mice. Drs. Ben Taylor and Don Doolittle (The Jackson Laboratory, Bar Harbor, ME) are thanked for their assistance in establishing mouse genetic map distances. We thank Dr. Filippo Calcinaro and Dr. Francisco G. La Rosa for assisting with the microphotography, and David Stenger for careful review of the manuscript.

Dr. Pietropaolo was the recipient of a Juvenile Diabetes Foundation International postdoctoral fellowship and was supported by a postdoctoral fellowship from the Italian Ministero della Pubblica Istruzione. Dr. Prochazka was the recipient of a Juvenile Diabetes Foundation International postdoctoral fellowship.

Supported by grants from the Greenwall Foundation, the Blum-Kovler Foundation, the Juvenile Diabetes Foundation, the American Diabetes Association, ImmuLogic Pharmaceutical Corporation, the National Institutes of Health (DK 32083, DK 36175, and DK 27722), the Veterans Administration Research Service, and the Italian Ministero della Pubblica Istruzione.

References

1. Eisenbarth, G. S. 1986. Type I diabetes mellitus: a chronic autoimmune disease. *N. Engl. J. Med.* 314:1360–1368.

2. Bottazzo, G. F., S. Genovese, E. Bosi, B. M. Dean, M. R. Christie, and E. Bonifacio. 1991. Novel considerations on the antibody/autoantigen system in type I (insulin-dependent) diabetes mellitus. *Ann. Med.* 23:453–461.

3. Pietropaolo M., and G. S. Eisenbarth. 1992. Prediction of type I diabetes mellitus. *Diabetes Nutr. Metab.* 5(Suppl. 1):105–110.

4. Tan, E. M. 1991. Autoantibodies in pathology and cell biology. *Cell.* 67:841–842.

5. Palmer, J. P., C. M. Asplin, P. Clemons, K. Lyen, O. Tatpati, P. K. Raghu, and T. L. Paquette. 1983. Insulin antibodies in insulin-dependent diabetics before insulin treatment. *Science (Wash. DC).* 222:1337–1339.

6. Baekkeskov, S., H. Aanstoot, S. Christgau, A. Reetz, M. S. Solimena, M. Cascalho, F. Folli, H. Richter-Olsen, and P. De Camilli. 1990. Identification of the 64K autoantigen in insulin dependent diabetes as the GABA-synthesizing enzyme glutamic acid decarboxylase. *Nature (Lond.).* 347:151–156.

7. Castaño, L., E. Russo, L. Zhou, M. A. Lipes, and G. S. Eisenbarth. 1991. Identification and cloning of a granule autoantigen (carboxypeptidase H) associated with type I diabetes. *J. Clin. Endocrinol. & Metab.* 73:1197–1201.

8. Gillard, B. K., J. W. Thomas, L. J. Nell, and D. M. Marcus. 1989. Antibodies against ganglioside GT3 in the sera of patients with type I diabetes mellitus. *J. Immunol. Methods.* 142:3826–3832.

9. Dotta, F., P. G. Colman, D. Lombardi, D. W. Scharp, D. Andreani, G. M. Pontieri, U. Di Mario, L. Lenti, G. S. Eisenbarth, and R. C. Nayak. 1989. Ganglioside expression in human pancreatic islets. *Diabetes.* 38:1478–1483.

10. Rabin, D. U., S. Pleasic, R. Palmer-Crocker, and J. A. Shapiro. 1992. Cloning and expression of IDDM-specific human autoantigens. *Diabetes.* 41:183–186.

11. Roep, B. O., A. A. Kallan, W. L. W. Hazenbos, G. J. Bruining, E. M. Bailyes, S. Arden, J. C. Hutton, and R. R. P. DeVries. 1991. T-cell reactivity to 38 kD insulin-secretory-granule protein in patients with recent-onset type 1 diabetes. *Lancet.* 337:1439–1441.

12. Karounos, D. G., and J. W. Thomas. 1990. Recognition of common islet antigen by autoantibodies from NOD mice and humans with IDDM. *Diabetes.* 39:1085–1090.

13. Martin, J. M., B. Trink, D. Daneman, H.-M. Dosch, and B. Robinson. 1991. Milk proteins in the etiology of insulin-dependent diabetes mellitus (IDDM). *Ann. Med.* 23:447–452.

14. Karjalainen, J., J. M. Martin, M. Knip, J. Ilonen, B. H. Robinson, E. Savilahti, H. K. Akerblom, and H.-M. Dosch. 1992. A bovine albumin peptide as a possible trigger of insulin-dependent diabetes mellitus. *N. Engl. J. Med.* 327:302–307.

15. Karjalainen, J., T. Saukkonen, E. Savilahti, and H.-M. Dosch. 1992. Disease-associated anti-bovine serum albumin antibodies in type 1 (insulin-dependent) diabetes mellitus are detected by particle concentration fluoroimmunoassay and not by enzyme linked immunoassay. *Diabetologia.* 35:985–990.

16. Coppel, R. L., M. E. Gershwin, and A. D. Sturgess. 1989. Cloned autoantigens in the study and diagnosis of autoimmune diseases. *Mol. Biol. Med.* 6:27–34.

17. Dropcho, E. J., Y.-T. Chen, J. B. Posner, and L. J. Old. 1987. Cloning of a brain protein identified by autoantibodies from a patient with a paraneoplastic cerebellar degeneration. *Proc. Natl. Acad. Sci. USA.* 84:4552–4556.

18. Sambrook, J., E. F. Fritsch, and T. Maniatis. 1989. Molecular Cloning: A Laboratory Manual. Cold Spring Harbor Laboratory Press, Cold Spring Harbor, NY.

19. Huynh, T. V., R. A. Young, and R. W. Davis. 1985. *In* Constructing and Screening cDNA libraries λgt10 and λgt11. D. M. Glover, editor. JRL Press, Oxford. 49–78.

20. Young, R. A., and R. W. Davis. 1984. Yeast RNA polymerase II genes: isolation with antibody probes. *Science (Wash. DC).* 222:778–782.

21. Feinberg, A. P., and B. Vogelstein. 1983. A technique for radiolabeling DNA restriction endonuclease fragments to high specific activity. *Anal. Biochem.* 132:6–13.

22. Wallace, R. B., M. J. Johnson, T. Hirose, T. Miyake, E. H. Kawashima, and K. Itakura. 1981. The use of synthetic oligonucleotides as hybridization probes. Hybridization of oligonucleotides of mixed sequence to rabbit β-globin DNA. *Nucleic Acids Res.* 9:879–894.

23. Friedman, K. D., N. L. Rosen, P. J. Newman, and R. R. Montgomery. 1988. Enzymatic amplification of specific cDNA from λgt11 libraries. *Nucleic Acids Res.* 16:8718.

24. Innis, M., D. Gelfand, J. Sninsky, and T. White. 1990. PCR Protocols: a Guide to Methods and Applications. Academic Press, Inc., San Diego, CA 253–258.

25. Sanger, F., S. Nickel, and A. R. Consoln. 1977. DNA sequencing with chain terminating inhibitors. *Proc. Natl. Acad. Sci. USA.* 74:5463–5467.

26. Tabor, S., and C. C. Richardson. 1975. DNA sequence analysis with a modified bacteriophage T7 DNA polymerase. *Proc. Natl. Acad. Sci. USA.* 84:4767–4771.

27. Kyte, J., and R. F. Doolittle. 1982. A simple method for displaying hydrophobic character of a protein. *J. Mol. Biol.* 157:105–132.

28. Doolittle, R. F. 1987. Of URSF and ORFS. A Primer on How to Analyze Derived Amino Acid Sequences. University Sciences Books, Mill Valley, CA.

29. Klein, P., M. Kanehisa, and C. DeLisi. 1985. The detection and classification of membrane-spanning proteins. *Biochim. Biophys. Acta.* 815:468–476.

30. Clark, S. A., B. Burnham, and W. L. Chick. 1990. Modulation of glucose-induced insulin secretion from a rat clonal beta-cell line. *Endocrinology.* 127, 6:2779–2788.

31. Hamaguchi, K., and E. H. Leiter. 1990. Comparison of cytokine effects on mouse pancreatic alpha cell and beta cell lines. Viability, secretory function, and MHC antigen expression. *Diabetes.* 39:415–425.

32. Powers, A. C., S. Efrat, S. Mojsov, D. Spector, J. F. Habener, and D. Hanahan. 1990. Proglucagon processing similar to normal islets in pancreatic alpha-like cell line derived from transgenic mouse tumor. *Diabetes.* 39:406–414.

33. Breant, B., C. Lavergne, and G. Rosselin. 1990. Cell cycle and gene expression in the insulin producing pancreatic cell line βTC-1. *Diabetologia.* 33:586–592.

34. Purrello, F., M. Buscema, M. Vetri, C. Vinci, C. Gatta, F. Forte, A. M. Rabuazzo, and R. Vigneri. 1991. Glucose regulates both glucose transport and the glucose transporter gene expression in a hamster-derived pancreatic beta-cell line (HIT). *Diabetologia.* 21:366–369.

35. Contreras, G., D. F. Summers, J. Maizel, and E. Ehrenfeld. 1973. HeLa cell nucleolar RNA synthesis after poliovirus infection. *Virology.* 53:120–129.

36. Kohler, P. O., W. E. Bridson, J. M. Hammond, B. Weintraub, M. A. Kirschner, and D. M. Van Thiel. 1971. Clonal lines of human choriocarcinoma cells in culture. *Acta Endocrinol.* 153(Suppl.):137–150.

37. Broze, G. J., and J. P. Miletich. 1987. Isolation of the tissue factor inhibitor produced by HepG2 hepatoma cells. *Proc. Natl. Acad. Sci. USA.* 84:1886–1890.

38. Thomas, P. S. 1980. Hybridization of denatured RNA and small DNA fragments transferred to nitrocellulose. *Proc. Natl. Acad. Sci. USA.* 77:5201–5205.

39. Cleveland, D. W., M. A. Lopata, R. J. MacDonald, N. J. Cowan, W. J. Rutter, and M. W. Kirschner. 1980. Number and evolutionary conservation of alpha- and beta-tubulin and cytoplasmic beta- and gamma-actin genes using specific cloned cDNA probes. *Cell.* 20:95–105.

40. Pari, G., K. Jardine, and M. W. McBurney. 1991. Multiple CArG boxes in the human cardiac actine gene promoter required for expression in embryonic cardiac muscle cells developing in vitro from embryonal carcinoma cells. *Mol. Cell. Biol.* 11:4796–4803.

41. Hassouna, N., B. Michot, and J.-P. Bachellerie. 1984. The complete nucleotide sequence of mouse 28 S RNA gene. Implications for the process of size increase of the large subunit rRNA in higher eukaryotes. *Nucleic Acids Res.* 12:3563.

42. Raynal, F., B. Michot, and J.-P. Bachellerie. 1984. Complete nucleotide sequence of mouse 18 S rRNA gene: comparisons with other available homologs. *FEBS (Fed. Eur. Biochem. Soc.) Lett.* 167:263.

43. Van Regenmortel, M. H. V., J. P. Briand, S. Muller, and S. Plaue. 1988. Syntetic polypeptides antigens. *In* Laboratory Techniques in Biochemistry and Molecular Biology. R. H. Burdon and P. H. von Knippenberg, editors. Elsevier Science Publishing Co., Inc., New York.

44. Walter, G. 1986. Production and use of antibodies against synthetic peptides. *J. Immunol. Methods.* 88:149–161.

45. Kurstak, E. 1986. Enzyme Immunodiagnostic. Academic Press, San Diego, CA.

46. Jitsukawa, T., S. Nakajima, I. Sugawara, and H. Watanabe. 1989. Increased coating efficiency of antigens and preservation of original antigenic structure after coating in ELISA. *J. Immunol. Methods.* 116:251–257.

47. Sun, X. J., P. Rothenberg, C. R. Kahn, J. M. Backer, E. Araki, P. A. Wilden, D. A. Cahill, B. J. Goldstein, and M. F. White. 1991. Structure of the insulin receptor substrate IRS-1 defines a unique signal transduction protein. *Nature (Lond.).* 352:73–77.

48. Laemmli, U. K. 1970. Cleavage of structural proteins during the assembly of the head of bacteriophage T4. *Nature (Lond.).* 227:680–685.

49. Towbin, H., T. Staehelin, and J. Gordon. 1979. Electrophoretic transfer of proteins from polyacrylamide gels to nitrocellulose sheets: procedure and some applications. *Proc. Natl. Acad. Sci. USA.* 76:4350.

50. Maina, C. V., P. D. Riggs, A. G. Grandea III, B. E. Slatko, L. S. Moran, J. A. Tagliamonte, L. A. McReynolds, and C. di Guan. 1988. An *Escherichia coli* vector to express and purify foreign proteins by fusion to and separation from maltose-binding protein. *Gene (Amst.).* 74:365–373.

51. di Guan, C., P. Li, P. D. Riggs, and H. Inouye. 1988. Vectors that facilitate the expression and purification of foreign peptides in *Escherichia coli* by fusion to maltose-binding protein. *Gene (Amst.).* 67:21–20.

52. Johnston, T. C., R. B. Thompson, and T. O. Baldman. 1986. Nucleotide sequence of the luxB gene of vibrio harveyi and the complete amino acid sequence of the beta subunit of bacterial luciferase. *J. Biol. Chem.* 261:4805–4811.

53. Aman, E. B., B. Ocfis, and K. J. Abel. 1988. Tightly regulated *tac* promoter useful for the expression of unfused and fused proteins in *Escherichia coli*. *Gene (Amst.).* 69:301–315.

54. Mason, D., and Y. R. Sammons. 1978. Alkaline phosphatase and peroxidase for double immunoenzimatic labelling of cellular constituents. *J. Clin. Pathol.* 31:454.

55. Mason, D. Y., B. F. Abdulaziz, and H. Stein. 1983. Double immunoenzimatic labelling. *In* Immunocytochemestry. Practical Application in Pathology and Biology. J. M. Polak and S. Van Noorden, editors. Wright PSG, Boston.

56. Prochazka, M., D. V. Serreze, S. M. Worthen, and E. H. Leiter. 1989. Genetic control of diabetogenesis in NOD/Lt mice: development and analysis of congenic stocks. *Diabetes.* 38:1446–1455.

57. Prochazka, M., E. H. Leiter, D. V. Serreze, and D. L. Coleman. 1987. Three recessive loci required for insulin-dependent diabetes in NOD mice. *Science (Wash. DC).* 237:286–289.

58. Leiter, E. H., and D. V. Serreze 1992. Antigen presenting cells and the immunogenetics of autoimmune diabetes in NOD mice. *Reg. Immunol.* 4:263–273.

59. Dietrich, W., H. Katz, S. Lincoln, H.-S. Shin, J. Friedman, N. Dracopoli, and E. S. Lander. 1992. A genetic map of the mouse suitable for typing intraspecific crosses. *Genetics.* 131:423–447.

60. Green, E. L. 1985. Tables and a computer program for analyzing linkage data. *Mouse News Let.* 73:20–21.

61. Kozak, M. 1987. An analysis of 5'-noncoding sequences from 699 vertebrate messenger RNAs. *Nucleic Acids Res.* 20:8125–8132.

62. Krumar, K. N., N. Tilakaratne, P. S. Johnson, A. E. Allen, and E. K.

Michaelis. 1991. Cloning of cDNA for the glutamate-binding subunit of the NMDA receptor complex. *Nature (Lond.)*. 354:70–73.

63. Krumar, K. N., K. T. Eggman, J. L. Adams, and E. K. Michaelis. 1991. Hydrodynamic proterties of the purified glutamate-binding protein subunit of the *N*-methyl-D-aspartate receptor. *J. Biol. Chem.* 23:14947–14952.

64. Lander, E. S., P. Green, J. Abrahamson, A. Barlow, M. J., Daly, S. E. Daly, and L. Newberg. 1987. MAPMAKER: an interactive computer package for constructing primary genetic linkage maps for experimental and natural populations. *Genomics*. 1:174–181.

65. Dean, M., M. Park, M. M. LeBeau, T. S. Robins, M. O. Diaz, J. D. Rowley, D. G. Blair, and G. F. Vande Woude. 1985. The human met oncogene is related to the tyrosine kinase oncogenes. *Nature (Lond.)*. 318:385–388.

66. Thivolet, C. H., M. Tappaz, A. Durand, J. Petersen, A. Stefanutti, P. Chaelain, B. Bialettes, W. Scherbaum, and J. Orgiazzi. 1992. Glutamic acid decarboxylase (GAD) autoantibodies are additional predictive markers of type 1 (insulin-dependent) diabetes mellitus in high risk individuals. *Diabetologia*. 35:570–576.

67. Hagopian W. A., B. Michelsen, A. E. Karlsen, F. Larsen, A. Moody, C. E. Grubin, R. Rowe, J. Petersen, R. McEvoy, and Å. Lernmark. 1993. Autoantibodies in IDDM primarily recognize the 65,000-M_r rather than 67,000-M_r isoform of glutamic acid decarboxylase. *Diabetes*. 42:631–636.

68. Kaufman, D. L., M. G. Erlander, M. Clare-Salzer, M. A. Atkinson, N. K. Maclaren, and A. J. Tobin. 1992. Autoimmunity to two forms of glutamate decarboxylase in insulin-dependent diabetes mellitus. *J. Clin. Invest.* 89:283–292.

69. Gianani, R., A. Pugliese, S. Bonner-Weir, A. J. Shiffrin, J. S. Soeldner, H. Erlich, Z. L. Awdeh, C., A. Alper, R., A. Jackson, and G. S. Eisenbarth. 1992. Prognostically significant heterogeneity of cytoplasmic islet cell antibodies in relatives of patients with type 1 diabetes. *Diabetes*. 41:347–353.

70. Genovese, S., E. Bonifacio, J. M. McNally, B. M. Dean, R. Wagner, E. Bosi, E. A. M. Gale, and G. F. Bottazzo. 1992. Distinct cytoplasmic islet cell antibodies with different risks for type 1 (insulin-dependent) diabetes mellitus. *Diabetologia*. 35:385–388.

71. Christgau, S., H. J. Aanstoot, H. Schierbeck, K. Begley, T. Tullin, K. Hejnaes, and S. Baekkeskov. 1992. Membrane anchoring of the autoantigen GAD65 to microvesicles in pancreatic beta-cells by palmitoylation in the NH_2-terminal domain. *J. Cell Biol.* 118(2):309–320.

72. McCauliffe, D. P., F. A. Lux, T.-S. Lieu, I. Sanz, J. Hanke, M. M. Newkirk, L. L. Bachinski, Y. Itoh, M. J. Siciliano, M. Reichlin, R. D. Sontheimer, and J. D. Capra. 1990. Molecular cloning, expression, and chromosome 19 localization of a human Ro/SS-A autoantigen. *J. Clin. Invest.* 85:1379–1391.

73. Benedum, U. M., D. S. Baeuerle, D. S. Konecki, R. Frank, J. Powell, J. Mallet, and W. B. Huttner. 1986. The primary structure of bovine chromogranin A: a representative of a class of acidic secretory proteins common to a variety of peptidergic cells. *EMBO (Eur. Mol. Biol. Organ.) J.* 5:1495–1502.

74. Spritz, R. A., K. Strunk, C. S. Surowy, S. O. Hoch, D. E. Barton, and U. Francke. 1987. The human U1-70K snRNP protein: cDNA cloning, chromosomal localization, expression, alternative splicing and RNA-binding. *Nucleic Acids Res.* 15:10373–10391.

75. Elliot, R. B., and J. M. Martin. Dietary protein: a trigger of insulin-dependent diabetes in rat? 1984. *Diabetologia*. 26:297–299.

76. Zhang, Z. J., L. Davidson, G. S. Eisenbarth, and H. L. Weiner. 1991. Suppression of diabetes in NOD mice by oral administration of porcine insulin. *Proc. Natl. Acad. Sci. USA*. 88:10252–10256.

Proc. Natl. Acad. Sci. USA
Vol. 93, pp. 6367–6370, June 1996
Medical Sciences

IA-2, a transmembrane protein of the protein tyrosine phosphatase family, is a major autoantigen in insulin-dependent diabetes mellitus

(autoantibodies)

MICHAEL S. LAN†‡, CLIVE WASSERFALL§, NOEL K. MACLAREN§, AND ABNER LOUIS NOTKINS†

†Laboratory of Oral Medicine, National Institute of Dental Research, National Institutes of Health, Bethesda, MD 20892-4322; and §Department of Pathology and Laboratory Medicine, University of Florida College of Medicine, Gainesville, FL 32610

Communicated by Hugh McDevitt, Stanford University School of Medicine, Stanford, CA, February 27, 1996 (received for review November 20, 1995)

ABSTRACT **IA-2 is a 105,847 Da transmembrane protein that belongs to the protein tyrosine phosphatase family. Immunoperoxidase staining with antibody raised against IA-2 showed that this protein is expressed in human pancreatic islet cells. In this study, we expressed the full-length cDNA clone of IA-2 in a rabbit reticulocyte transcription/translation system and used the recombinant radiolabeled IA-2 protein to detect autoantibodies by immunoprecipitation. Coded sera (100) were tested: 50 from patients with newly diagnosed insulin-dependent diabetes mellitus (IDDM) and 50 from age-matched normal controls. Sixty-six percent of the sera from patients, but none of the sera from controls, reacted with IA-2. The same diabetic sera tested for autoantibodies to islet cells (ICA) by indirect immunofluorescence and glutamic acid decarboxylase (GAD_{65}Ab) by depletion ELISA showed 68% and 52% positivity, respectively. Up to 86% of the IDDM patients had autoantibodies to IA-2 and/or GAD_{65}. Moreover, greater than 90% (14 of 15) of the ICA-positive but GAD_{65} Ab-negative sera had autoantibodies to IA-2. Absorption experiments showed that the immunofluorescence reactivity of ICA-positive sera was greatly reduced by prior incubation with recombinant IA-2 or GAD_{65} when the respective antibody was present. A little over one-half (9 of 16) of the IDDM sera that were negative for ICA were found to be positive for autoantibodies to IA-2 and/or GAD_{65}, arguing that the immunofluorescence test for ICA is less sensitive than the recombinant tests for autoantibodies to IA-2 and GAD_{65}. It is concluded that IA-2 is a major islet cell autoantigen in IDDM, and, together with GAD_{65}, is responsible for much of the reactivity of ICA with pancreatic islets. Tests for the detection of autoantibodies to recombinant IA-2 and GAD_{65} may eventually replace ICA immunofluorescence for IDDM population screening.**

Autoantibodies that react with pancreatic islets were first detected by immunofluorescent techniques over 20 years ago (1). It is now clear that these antibodies recognize several different antigens in the islets (2–7). In recent years, extensive efforts have been made to identify and characterize the antigens with which these islet cell autoantibodies (ICA) react. Autoantibodies to one of these antigens, now known to be the lower molecular weight isoform of glutamic acid decarboxylase (GAD_{65}), have been widely used as a marker for identifying individuals with insulin-dependent diabetes mellitus (IDDM) and in predicting the risk of developing IDDM in nondiabetic individuals (8–12). GAD_{65} is primarily an intracellular antigen. Recently, we described a new member of the protein tyrosine phosphatase family, IA-2, (13, 14). IA-2 cDNA predicts a transmembrane protein of 979 amino acids in length and has a molecular mass of 105,847 Da. The extracellular domain extends from amino acid 1 to 576, the transmembrane domain from amino acid 577 to 601, and the intracellular domain from amino acid 602 to 979. The gene is expressed in human, mouse, and rat insulinoma cells as well as enriched normal islets (13). It also is found in human brain and neuroendocrine cells.

In the present report, we describe the expression of the full-length of IA-2 in a eukaryotic reticulocyte transcription/translation system and a sensitive radioimmunoprecipitation assay for detecting autoantibodies to IA-2 in the sera of IDDM patients. For comparison, the same sera were tested for ICA and GAD_{65} antibody (GAD_{65}Ab). The relationship of IA-2 antibody (IA-2Ab) to GAD_{65}Ab and ICA also was assessed.

MATERIALS AND METHODS

Human Subjects. New-onset IDDM patients (50) who had been diagnosed within a week of their blood sampling and 50 age-matched controls with no history of autoimmune disease were studied (15). Blood samples were collected under informed consent as approved by the University of Florida Institutional Review Board. Some IDDM patients were selected for the study because they had ICA but not GAD_{65}Ab.

Radioimmunoprecipitation of *in Vitro* Translated Full-Length IA-2 Autoantigen. The full-length human IA-2 cDNA without the leader sequence (13) was cloned into a pCRII cloning vector (Invitrogen) with a perfect Kozak translational start sequence (GCCGCCACCATGG) (16). Plasmid DNA (1 μg) was added to TNT coupled rabbit reticulocyte lysate system (Promega) in the presence of [^{35}S]methionine (Amersham) at 30°C for 2 hr. Radiolabeled protein was determined by 10% trichloroacetic acid precipitation. Immunoprecipitation was performed as described (17). Briefly, translated reticulocyte lysate (approximately 50,000–75,000 cpm) and 5 μl of tested serum were mixed in 100 μl of immunoprecipitation buffer (20 mM Tris (pH 7.4), 150 mM NaCl, 1% Triton X-100). The reaction mixture was incubated at 4°C overnight and 50 μl of 50% (vol/vol) protein A-Agarose (Life Technologies) was added to the solution at 4°C for 1 hr. The immunoprecipitation mixture was washed four times with immunoprecipitation buffer, boiled in sample buffer, and applied to an 8% SDS/PAGE gel. The gels were fixed with acetic acid/methanol (12.5%:12.5%), then exposed to film overnight. The intensity of the IA-2 bands (≈106 kDa) was scored from 1+ to 4+ by two independent investigators and corresponded very

The publication costs of this article were defrayed in part by page charge payment. This article must therefore be hereby marked "*advertisement*" in accordance with 18 U.S.C. §1734 solely to indicate this fact.

Abbreviations: ICA, islet cell autoantibodies; IDDM, insulin-dependent diabetes mellitus; GAD_{65}, glutamic acid decarboxylase; GAD_{65}Ab, GAD_{65} antibody; IA-2Ab, IA-2 antibody; JDF, juvenile diabetes foundation.

‡To whom reprint requests should be addressed.

closely to counts in the immunoprecipitate as determined by liquid scintillation (unpublished data).

ICA and GAD_{65}Ab. ICA and GAD_{65}Ab were determined as described (15, 18). Recombinant baculovirus-expressed GAD_{65} was kindly supplied by Syra (Palo Alto, CA), and used in an antigen depletion ELISA (D-ELISA) assay (19, 20). The results obtained closely parallel those by our previously published radioimmunoassay (21).

ICA Absorption. Tests were performed to see if the reactivity of ICA with pancreatic islets could be removed by absorption with recombinant GAD_{65} and/or IA-2. Serum (200 μl) was incubated overnight with an equal volume of biotinylated GAD_{65} bound to streptavidin-Sepharose beads. The slurry then was centrifuged and the supernatants tested in the usual way for ICA reactivity. Similarly, the intracellular domain of IA-2, expressed as a fusion protein with glutathione *S*-transferase and bound to glutathione-sepharose beads, was used to absorb serum antibody to IA-2. Sepharose beads, bound to neither GAD_{65} nor IA-2, served as controls.

RESULTS

Radiolabeled IA-2 was immunoprecipitated with serum from IDDM patients and the immunoprecipitate was separated on an 8% SDS/PAGE gel. As seen in Fig. 1, seven representative sera from IDDM patients identified a band with a relative molecular mass of 106 kDa. The intensity of the bands ranged from 1+ to 4+. No bands were seen when control sera were used.

Coded sera (50) from diabetic patients and 50 sera from controls were tested by this assay for autoantibodies to IA-2. As seen in Fig. 2, 66% of the sera from IDDM patients, but none of the sera from controls, reacted with IA-2. The intensity of the bands varied from 1+ to 4+ with 21 of the 33 positive sera being in the strongly positive (3+ to 4+) range. Equivocal bands (±) were scored as negative.

The sera used in Fig. 2 also were tested by D-ELISA for antibodies that reacted with GAD_{65}. As seen in Figs. 3 and 4, 52% of the sera from IDDM patients, but none of the sera from controls, reacted with GAD_{65}. Up to 86% of the IDDM patients developed autoantibodies to IA-2 and/or GAD_{65}. Some of the patients (34%) developed antibodies to both antigens, 12% to only GAD_{65}, and 4% to only IA-2. The current data, together with data from other studies (15), suggest that the age of the onset of IDDM may influence the nature of the immune response. Of 60 patients diagnosed with IDDM before age 20, 68% had antibodies to IA-2 and 60% had antibodies to GAD_{65}. However, of 15 patients diagnosed with IDDM after age 20, only 46% had antibodies to IA-2, whereas 86% had antibodies to GAD_{65}.

Detection of autoantibodies to islet cells by indirect immunofluorescence on human blood group O pancreatic sections has been widely used as a marker for IDDM. One of the antigens recognized by the immunofluorescence assay is GAD_{65} (18). However, it is known that at least 20% of sera that

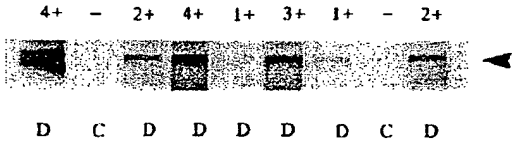

FIG. 1. Autoantibodies to IA-2 in patients with IDDM as measured by radioimmunoprecipitation. Sera were incubated with recombinant IA-2 expressed in a reticulocyte system. The dissociated precipitates were run on an 8% SDS/PAGE gel. Bands with a molecular mass of 106 kDa were scored on an intensity scale of 1+ to 4+. Representative sera with different band-intensities are illustrated. D, diabetic sera; C, control sera.

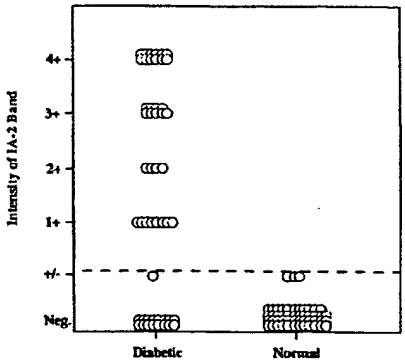

FIG. 2. Sera from 50 patients with clinically documented IDDM and 50 normal controls were tested for autoantibodies to IA-2 by radioimmunoprecipitation. The intensity of bands were scored as illustrated in Fig. 1. Equivocal bands (±) were considered negative for autoantibodies.

are positive for ICA by immunofluorescence do not react with GAD_{65}, indicating that the immunofluorescence assay is recognizing a still unidentified antigen(s). In the present study (Fig. 3), 68% of the sera were positive for ICA, but only 52% had autoantibodies to GAD_{65}. Remarkably, of the 15 ICA-positive sera that did not react with GAD_{65}, 14 reacted unambiguously with IA-2, arguing that IA-2 is one of the islet antigens that is routinely recognized by ICA in the immunofluorescence test. Moreover, of the 34 ICA-positive sera, 33 reacted with IA-2 and/or GAD_{65}.

Absorption experiments (Table 1) showed that the immunofluorescence reactivity of IA-2Ab-positive, but GAD_{65}Ab-negative, sera with islet cells was greatly reduced by absorption with IA-2, but not by absorption with GAD_{65}. Conversely, the immunofluorescence reactivity of IA-2Ab-negative but GAD_{65}Ab-positive sera with islet cells was greatly reduced by absorption with GAD_{65}, but not by absorption with IA-2. Taken together, our studies strongly argue that IA-2 and GAD_{65} are two of the major autoantigens recognized by ICA immunofluorescence. In one case (serum 4), however, islet cell reactivity was not substantially reduced by absorption with either IA-2 or GAD_{65}, suggesting that another still unidentified islet cell autoantigen(s) is being recognized by some ICA-positive sera. Preliminary experiments suggest that this autoantigen is closely related to IA-2.

DISCUSSION

In the present experiments, using full-length IA-2 cDNA and a eukaryotic expression system, we developed a radioimmunoassay for detecting autoantibodies to IA-2. Two-thirds of our IDDM patients had autoantibodies to IA-2 as compared with none of the controls. This radioimmunoassay is considerably more sensitive and specific than the ELISA used in our laboratory (unpublished data) or the one described by Rabin *et al.* (22), with a truncated form of IA-2 lacking the first 389 amino acids, designated ICA512. Moreover, the radioimmunoassay used here is a liquid phase assay and therefore is more likely to detect conformational epitopes than the solid phase ELISA.

Autoantibodies to GAD_{65} have been widely used as a marker for IDDM. At least 20% or more of newly diagnosed IDDM patients, however, are known to be negative for antibodies to GAD_{65} (23). In the present report, the patient population we studied was somewhat biased because a higher than expected percentage of patients were GAD_{65}Ab-negative (48%). However, of particular interest is the finding that of 15 ICA-positive

Sera	IA-2	GAD	ICA (JDF)
3	neg.	8	160
8	3+	8	320
9	neg.	neg.	neg.
10	4+	neg.	1280
13	2+	neg.	160
16	3+	6	320
19	neg.	>16	neg.
20	4+	10	320
25	2+	neg.	neg.
27	neg.	2	320
28	3+	16	320
30	neg.	neg.	neg.
32	3+	neg.	160
34	1+	4	neg.
35	3+	6	2560
38	4+	neg.	320
41	4+	>16	160
42	4+	neg.	320
43	3+	neg.	neg.
44	1+	neg.	160
47	2+	8	320
48	neg.	16	neg.
50	neg.	neg.	20
52	neg.	neg.	neg.
53	3+	>16	1280
54	neg.	16	neg.
57	neg.	>16	neg.
59	1+	16	80
60	neg.	neg.	neg.
61	1+	neg.	20
62	neg.	>16	neg.
63	4+	neg.	640
65	3+	12	320
67	3+	4	1280
69	neg.	3	80
73	4+	>16	640
74	neg.	12	neg.
75	4+	>16	320
77	4+	neg.	640
78	neg.	neg.	neg.
79	1+	neg.	80
80	neg.	neg.	neg.
85	4+	>16	1280
87	1+	neg.	160
88	2+	>16	320
91	4+	neg.	320
92	3+	neg.	160
93	3+	>16	320
95	1+	neg.	40
97	neg.	neg.	neg.

FIG. 3. Sera from patients and controls were tested for: IA-2Ab by radioimmunoassay; GAD_{65}Ab by D-ELISA; and ICA by immunofluorescence. Numbers in the ICA column represent JDF units. Patients (coded numbers) are indicated in the serum column. Fifty normal controls (not shown) were negative in all three autoantibody tests.

patients who showed no reactivity to GAD_{65}, 14 had autoantibodies to IA-2, arguing that IA-2 is one of the major autoantigens recognized by ICA in the indirect immunofluorescence test using human pancreas as tissue substrate. Additional support for this contention comes from our absorption studies (Table 1), which showed that a major portion of the reactivity of ICA could be absorbed by IA-2 or GAD_{65} when the respective antibody was present.

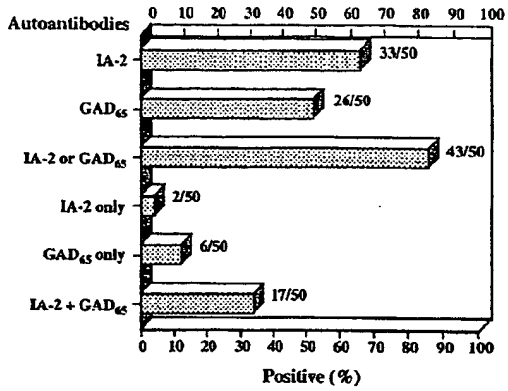

FIG. 4. Comparison of autoantibody response to IA-2 and GAD_{65} in 50 patients with IDDM.

The data further show that measurements of antibodies to both IA-2 and GAD_{65} detect a higher percentage of IDDM patients than measurement of either antibody alone. In the current study (Fig. 3), autoantibodies to IA-2 were identified in 66% (33/50) of the IDDM patients, whereas autoantibodies to GAD_{65} were detected in 52% (26/50) of the IDDM patients. Of the patients in this series, 34% (17/50) showed antibodies to both GAD_{65} and IA-2, with 65% (17/26) of the GAD_{65}Ab-positive patients also having antibodies to IA-2 and 52% (17/33) of the IA-2Ab-positive patients also having antibodies to GAD_{65}. However, up to 86% of the IDDM patients had antibodies to one or the other antigens or both. Thus, some IDDM patients will be missed if detection relies on only one autoantibody test. Of particular interest, 33 of the 34 ICA-positive patients showed autoantibodies to IA-2 and/or GAD_{65}. Moreover, of the 16 patients who were negative for ICA, nine were positive for autoantibodies to IA-2 and/or GAD_{65} demonstrating that, in some cases, these latter two assays detect autoantibodies when the ICA immunofluorescence assay is negative. Thus, the measurement of autoantibodies to both IA-2 and GAD_{65} seems to have advantages over the immunofluorescence assay for ICA in terms of sensitivity and specificity. The assays for IA-2 and GAD_{65} use molecularly expressed proteins and do not rely on the more subjective readings of tissue immunofluorescence and the inherent variations of human pancreatic sections. Prospective studies involving large number of subjects are ongoing in our laboratories and the preliminary data indicates that the positive predictive value of IA-2Ab, in identifying subjects likely to develop IDDM, is over 90% (unpublished data). Based on our present findings, IDDM patients diagnosed before age 20 are more likely to have IA-2Ab than patients diagnosed after age 20, but further studies are needed to settle whether IA-2Ab generally appears before or after GAD_{65}Ab in the natural history of the preclinical disease. Although autoantibodies to IA-2 and GAD_{65} seem to account for much and perhaps most of the immunofluorescence reactivity of ICA, the fact that some ICA reactivity remains after absorption with IA-2 or GAD_{65} argues for the existence of still another autoantigen. In this connection, we recently identified a novel cDNA from beta cells that encodes a protein, designated IA-2β, that is closely related to IA-2 (24). Moreover, these studies showed that IA-2β is the precursor of the 37-kDa tryptic fragment isolated from pancreatic islets, whereas IA-2 is the precursor of the 40-kDa tryptic fragment also isolated from pancreatic islets (24, 25).

Whether autoantibodies to IA-2 and GAD_{65} are a cause or a result of the immunologically mediated destruction of pan-

Table 1. Absorption of ICA-positive sera with IA-2 and GAD_{65}

Patient serum	Reactivity of sera with			Absorption of ICA-positive sera with	
				IA-2	GAD_{65}
	Islet cells	IA-2	GAD_{65}	Reactivity of absorbed sera with islet cells	
1	Pos	Pos	Neg	⇊	—
2	Pos	Pos	Neg	⇊	—
3	Pos	Pos	Neg	↓	—
4	Pos	Pos	Neg	↓	↓
5	Pos	Neg	Pos	—	⇊
6	Pos	Neg	Pos	—	⇊

Reactivity of ICA-positive sera with islet cells as measured by intensity of immunofluorescence: ⇊, greatly reduced; ↓, moderately reduced; ↓, slightly reduced; —, not reduced. Pos, positive; Neg, negative.

creatic beta cells underlying IDDM, is still not clear. However, what is clear is that these autoantibodies serve as markers of the underlying disease process, and thus have strong predictive power. In ongoing studies, we found that antibodies to GAD_{65} (26) and now IA-2 occur at highest frequencies among nondiabetic relatives who have the highest risk HLA phenotypes, especially DRB1*03/DQB1*0201; DRB1*04/DQB1*0302 heterozygotes. Why the host should make an immune response to two such seemingly unrelated antigens as GAD_{65} and IA-2 is unknown. While both are expressed in neuroendocrine cells (i.e., pancreatic islets and brain), IA-2 is particularly interesting because, in contrast to GAD_{65}, it has an extracellular domain. The possibility that the extracellular domain of IA-2 serves as a target for an autoimmune attack and/or is the site for deleterious transmembrane signaling is currently under investigation.

We thank Drs. Hersh Mehta and Barbara Vold for their assistance with the assay for autoantibodies to GAD_{65}. We gratefully acknowledge the editorial help of Janice Solomon. This study was supported by Grants R01 HD 19469, P01 DK39079, and GCRC MO1 RR00082 from the National Institutes of Health.

1. Bottazzo, G. F., Florin-Christensen, A. & Doniach, D. (1974) *Lancet* 2, 1279–1282.
2. Nayak, R. C., Omar, M. A., Rabizadeh, A., Srikanta, S. & Eisenbarth, G. S. (1985) *Diabetes* 34, 617–619.
3. Christie, M. R., Tun, R. Y., Lo, S. S., Cassidy, D., Brown, T. J., Hollands, J., Shattock, M., Bottazzo, G. F. & Leslie, D. G. (1992) *Diabetes* 41, 782–787.
4. Castano, L., Russo, E., Zhou, L., Lipes, M. H. & Eisenbarth, G. S. (1991) *J. Clin. Endocrinol. Metab.* 73, 1197–1201.
5. Atkinson, M. A. & Maclaren, N. K. (1994) *N. Engl. J. Med.* 331, 1428–1436.
6. Baekkeskov, S., Aanstoot, H. J., Christgau, S., Reetz, A., Solimena, M., Cascalho, M., Folli, F. & Richter-Oleson, H. (1990) *Nature (London)* 347, 151–156.
7. Inman, L. R., McAllister, C. T., Chen, L., Hughes, S., Newgard, C. B., Kettman, J. R., Unger, R. H. & Johnson, J. H. (1993) *Proc. Natl. Acad. Sci. USA* 90, 1281–1284.
8. Baekkeskov, S., Landin, M., Kristensen, J. K., Srikanta, S., Bruining, G. J., Mandrup-Poulsen, T., deBeaufort, C., Soeldner, J. S., Eisenbarth, G., Lindgren, F., Sundkvuist, G. & Lernmark, Å. (1987) *J. Clin. Invest.* 79, 926–934.
9. Christie, M., Landin-Olsson, M., Sundkvist, G., Dahlquist, G., Lernmark, Å. & Baekkeskov, S. (1988) *Diabetologia* 31, 597–602.
10. Atkinson, M. A., Maclaren, N. K., Scharp, D. W., Lacy, P. E. & Riley, W. J. (1990) *Lancet* 335, 1357–1360.
11. DeAizpurua, H. J., Wilson, Y. M. & Harrison, L. C. (1992) *Proc. Natl. Acad. Sci. USA* 89, 9841–9845.
12. Tuomilehto, J., Zimmet, P., Mackay, I. R., Koskela, P., Vidgren, G., Toivanen, L., Tuomilehto-Wolf, E., Kohtamäki, K., Stengård, J. & Rowley, M. J. (1994) *Lancet* 343, 1383–1385.
13. Lan, M. S., Lu, J., Goto, Y. & Notkins, A. L. (1994) *DNA Cell Biol.* 13, 505–514.
14. Lu, J., Notkins, A. L. & Lan, M. S. (1994) *Biochem. Biophys. Res. Commun.* 204, 930–936.
15. Riley, W. J., Maclaren, N. K., Krischer, J., Spillar, R. P., Silverstein, J. H., Schatz, D. A., Schwartz, S., Malone, J., Shah, S., Vadheim, C. & Rotter, J. I. (1990) *N. Engl. J. Med.* 323, 1167–1172.
16. Kozak, M. (1987) *Nucleic Acids Res.* 15, 8125–8148.
17. Grubin, C. E., Daniels, T., Toivola, B., Landin-Olsson, M., Hagopian, W. A., Karlsen, A. E., Boel, E., Michelsen, B. & Lernmark, Å. (1994) *Diabetologia* 37, 344–350.
18. Atkinson, M. A., Kaufman, D. L., Newman, D., Tobin, A. J. & Maclaren, N. K. (1993) *J. Clin. Invest.* 91, 350–356.
19. Wasserfall, C., Schatz, D., Mehta, H., Vold, B., Krischer, J., Atkinson, M. & Maclaren, N. (1995) *Diabetes* 44, Suppl. 77A (abstr. 287).
20. Mehta, H., Vold, B., Minkin, S., & Ullman, E. (1996) *Clin. Chem.* 42, 263–269.
21. Scott, M., Schatz, D., Atkinson, M., Krischer, J., Mehta, H., Vold, B. & Maclaren, N. (1994) *J. Autoimmun.* 7, 865–872.
22. Rabin, D. U., Pleasic, S. M., Shapiro, J. A., Yoo-Warren, H., Oles, J., Hicks, J. M., Goldstein, D. E. & Rae, P. M. M. (1994) *J. Immunol.* 152, 3183–3188.
23. Verge, C. F., Howard, N. J., Rowley, M. J., Mackay, I. R., Zimmet, P. Z., Egan, M., Hulinska, H., Hulinsky, I., Silvestrini, R. A., Kamath, S., Sharp, A., Arundel, T. & Silink, M. (1994) *Diabetologia* 37, 1113–1120.
24. Lu, J., Li, Q., Xie, H., Chen, Z. J., Borovitskaya, A. E., Maclaren, N. K., Notkins, A. L. & Lan, M. S. (1996) *Proc. Natl. Acad. Sci. USA* 93, 2307–2311.
25. Payton, M. A., Hawkes, C. J. & Christie, M. R. (1995) *J. Clin. Invest.* 96, 1506–1511.
26. Huang, W., She, J., Muir, A., Laskowska, D., Zorovich, B., Schatz, D. & Maclaren, N. (1994) *J. Autoimmun.* 7, 889–897.

Autoimmunity to Two Forms of Glutamate Decarboxylase in Insulin-dependent Diabetes Mellitus

Daniel L. Kaufman,* Mark G. Erlander,‡ Michael Clare-Salzler,§ Mark A. Atkinson,‖ Noel K. Maclaren,‖ and Allan J. Tobin¶**‡‡
*Department of Psychiatry and Behavioral Sciences; ‡Program for Neuroscience; §Department of Medicine; ¶Department of Biology; **Molecular Biology Institute; and ‡‡Brain Research Institute, University of California Los Angeles, Los Angeles, California 90024; and ‖Department of Pathology and Laboratory Medicine, College of Medicine, University of Florida, Gainesville, Florida 32610

Abstract

Insulin-dependent diabetes mellitus (IDDM) is thought to result from the autoimmune destruction of the insulin-producing β cells of the pancreas. Years before IDDM symptoms appear, we can detect autoantibodies to one or both forms of glutamate decarboxylase (GAD_{65} and GAD_{67}), synthesized from their respective cDNAs in a bacterial expression system. Individual IDDM sera show distinctive profiles of epitope recognition, suggesting different humoral immune responses. Although the level of GAD autoantibodies generally decline after IDDM onset, patients with IDDM-associated neuropathies have high levels of antibodies to GAD, years after the appearance of clinical IDDM. We note a striking sequence similarity between the two GADs and Coxsackievirus, a virus that has been associated with IDDM both in humans and in experimental animals. This similarity suggests that molecular mimicry may play a role in the pathogenesis of IDDM. (*J. Clin. Invest.* 1992. 89:283–292.) Key words: insulin-dependent diabetes mellitus • glutamate decarboxylase • diabetic neuropathy

Introduction

Insulin-dependent diabetes (IDDM;[1] type I diabetes) is one of the most serious and common of metabolic disorders, affecting approximately 1 person in 300 in the U.S., while epidemiological studies in Europe suggest that its incidence is increasing (reviewed in 1–3). The disease is thought to result from the autoimmune destruction of the insulin-producing β cells of the pancreas and the subsequent metabolic derangements. Although insulin therapy allows most patients to lead active lives, this replacement is imperfect since it does not restore normal metabolic homeostasis. Metabolic abnormalities are thought to be important in the subsequent development of common complications, which include retinopathy, cataract formation, nephropathy, neuropathy, and heart disease.

While the initiating agent of IDDM autoimmunity is not known, it ultimately provokes a loss of immunological tolerance to self-antigens present in insulin-secreting β cells within the pancreatic islets (4–6). IDDM begins with an asymptomatic stage, characterized by a chronic inflammatory infiltrate of the islets (insulitis), which selectively destroys the β cells. Only after the destruction of the majority of the β cells, often occurring over several years, do hyperglycemia and ketosis appear.

The pathogenesis of IDDM involves both genetic and environmental factors. One or more susceptibility factors are encoded by the major histocompatibility complex on chromosome 6, probably by the DQ A1 and B1 loci (7, 8). Studies of monozygotic twins, however, show a concordance for IDDM of < 40%, suggesting that environmental factors play an important role (9). Long suspected environmental causes of IDDM include a number of viruses, such as rubella, encephalomyocarditis virus, and especially Coxsackie virus B_4 (reviewed in 10–12).

Autoantibodies to a 64,000 M_r islet cell protein are associated with IDDM and have been detected years before the onset of symptoms (13–15). Other IDDM-associated autoantibodies, such as those against insulin and cytoplasmic gangliosides of islet cells (ICA), appear later, possibly as a consequence of the release of these antigens (or their precursors) from the damaged islet cells (16, 17). Antibodies to the 64,000 M_r proteins are, however, the earliest and most reliable predictive marker of IDDM in humans and are also present in the two animal models for IDDM, the nonobese diabetic (NOD) mouse and the Biobreeding rat (14, 15, 18, 19).

Baekkeskov et al. (20) reported that the 64,000 M_r islet cell autoantigen is a form of glutamate decarboxylase (GAD; E.C. 4.1.1.15), the enzyme responsible for the synthesis of γ-aminobutyric acid (GABA) in brain, peripheral neurons, pancreas, and other organs (21). We have recently shown that the brain contains two forms of GAD, which are encoded by two separate genes (22). The two GADs (GAD_{65} and GAD_{67}) differ in molecular size (with M_rs = 65,000 and 67,000) and amino acid sequence (with ~ 30% sequence divergence), as well as in their intracellular distributions and interactions with the GAD cofactor pyridoxal phosphate (22–25). In brain neurons, GAD_{65} is preferentially associated with axon terminals, while GAD_{67} is present in both terminals and cell bodies (25).

Previous studies of the 64,000 M_r IDDM autoantigen have used pancreatic extracts enriched for membrane-associated

Dr. Erlander's present address is Department of Molecular Biology, Scripps Clinic, La Jolla, CA 92037. Address correspondence to Daniel L. Kaufman, Ph.D., Department of Psychiatry and Behavioral Sciences, UCLA, Los Angeles, CA 90024-1759, or to Allan J. Tobin, Ph.D., Department of Biology, UCLA, Los Angeles, CA 90024-1606.

Received for publication 22 March 1991 and in revised form 20 September 1991.

1. *Abbreviations used in this paper:* GAD, glutamate decarboxylase; ICA, islet cell antibodies; IDDM, insulin-dependent diabetes mellitus; JDF, Juvenile Diabetes Foundation; NIDDM, non-IDDM; NOD, nonobese diabetic; PAS, protein A-Sepharose; PCR, polymerase chain reaction.

J. Clin. Invest.

0021-9738/92/01/0283/10 $2.00
Volume 89, January 1992, 283–292

proteins. In view of our demonstration that the brain contains two GADs, we set out to determine the molecular identity of islet cell GAD by immunohistochemistry with monospecific antibodies. We then used GAD_{65} and GAD_{67} produced in genetically engineered bacteria from our GAD cDNAs to examine the specificity of IDDM autoantibodies for the two GADs and for restricted sets of GAD epitopes.

Our results lead to two new suggestions concerning the pathogenesis of IDDM and its complications: (*a*) GAD autoimmunity may play a role in the pathogenesis of IDDM-associated neuropathies; and (*b*) IDDM autoimmunity may result from molecular mimicry of GAD and a Coxsackievirus peptide.

Methods

Patient sera. IDDM patients and individuals at high risk for later developing IDDM were selected from a previous study at the University of Florida Diabetes Clinics (15, 26). IDDM patients with peripheral neuropathies were selected from the University of Florida Diabetes Clinics and the UCLA Diabetes Clinic.

Nondiabetic controls and the individuals studied before the documented clinical onset were ascertained through ongoing prospective screening for islet cell antibodies of more than 5,000 first-degree relatives of IDDM probands, and 8,200 individuals from the general population, of whom 4,813 were school children. These studies were approved by the University of Florida's Institutional Review Board. All participating individuals first gave their written informed consent. Individuals at high risk for the development of IDDM were identified by the presence of high titers of ICAs, assayed by indirect immunofluorescence on cryostat sections of blood group O human pancreas. All results were interpreted on coded samples, with control negative and positive sera in each batch. The ICA levels were estimated as Juvenile Diabetes Foundation units, according to the standardization guidelines established by the Immunology Diabetes Workshop (IDW), as previously described. M. Atkinson and N. Maclaren subscribe to the IDW's ICA proficiency testing program, which they currently supervise.

GAD assays. Patient sera were assayed blind for their ability to bind GAD enzymatic activity from a cleared homogenate of human cerebellar cortex in "GAD buffer," which contained 60 mM potassium phosphate, pH 7.1, 0.5% Triton X-100, 1 mM PMSF, 1 mM 2-aminoethylisothiouronium bromide, and 0.1 mM pyridoxal phosphate. IgG from each serum was bound to protein A-Sepharose (PAS) by adding 40 μl of serum to 80 μl of a 1:1 slurry of preswollen PAS in GAD buffer, incubating for 30 min at 4°C with gentle rocking, isolated by centrifugation, and then washing four times in the same buffer. 100 μl of brain extract was then added to each sample and incubated for 1 h at 4°C with gentle rocking, washed four times, resuspended in buffer, and assayed for GAD activity as previously described (25). Values shown are means of three determinations.

Immunohistochemistry. Immunochemical detection of the two forms of GAD was performed as previously described for rat cerebellum (25).

Antigen preparation and immunoadsorption. Rat GAD_{65} and GAD_{67} cDNAs were subcloned in the NcoI site of pET 8C and the Nhe I site of pET-5C respectively and transformed into *Escherichia coli* BL21 (DE3) (20, 27). Control and GAD-producing *E. coli* were grown and induced with isopropyl-thio-β-D-galactoside, harvested by centrifugation, resuspended in GAD buffer, sonicated, and cleared by centrifugation at 55,000 *g* for 15 min. For immunocompetition, 30 μl of each patient serum was incubated with 100 μl of extract from control bacteria or from bacteria that produced either GAD_{65} or GAD_{67} for 1 h at 4°C. Human pancreatic islets were labeled with ^{35}S-methionine as previously described (15). A detergent extract (300 μl) was first precleared with human control serum. The material that bound to the control IgG was removed with protein A-Sepharose. The precleared islet cell detergent extract was then split into three fractions and then incubated (2 h on ice) with serum that had been absorbed with each of the *E. coli* lysates. IgG-bound material was isolated with protein A-Sepharose as described above, and the bound material was analyzed by polyacrylamide gel electrophoresis in SDS (SDS-PAGE), followed by fluorography.

Detection of GAD autoantibodies. E. coli expressing rat GAD_{65} and GAD_{67} cDNAs were grown in minimal medium and induced with isopropyl-thio-β-D-galactoside in the presence of a mixture of ^{35}S-labeled amino acids (Tran-^{35}S; ICN Pharmaceuticals, Inc., Irvine, CA). The bacteria were harvested, sonicated in GAD buffer, and centrifuged to remove debris. Sera were preadsorbed with extracts of unlabeled host bacteria and then added to a mixture of ^{35}S-labeled extracts of GAD_{65}- and GAD_{67}-producing bacteria. IgG-bound polypeptides were isolated with PAS and analyzed by SDS-PAGE. Initial experiments analyzed sera for their ability to precipitate GAD_{65} and GAD_{67} separately (data not shown). Using a mixture of the two extracts simplified the assay. A number of *E. coli* polypeptides were also immunoadsorbed by some patient and some control sera. One such band, with M_r ~ 70,000, is apparent in many samples.

Epitope mapping. Portions of GAD_{65} cDNA were amplified by the polymerase chain reaction (PCR; 28) to produce DNA segments encoding three polypeptide segments: amino acid residues 1–224 (segment A); 224–398 (segment B); and 398–585 (segment C). Each construct also contained a T_7 promoter, a consensus sequence for the initiation of translation and an initiating methionine codon (29). Each PCR product was then transcribed in vitro with T_7 RNA polymerase and translated in vitro in a rabbit reticulocyte cell-free system in the presence of ^{35}S-methionine, using conditions recommended by the supplier (Amersham Corp., Arlington Heights, IL). Each test serum (30 μl) was incubated with the resulting ^{35}S-polypeptides. The bound peptides were isolated with PAS and analyzed by SDS-PAGE in 15% polyacrylamide and fluorography.

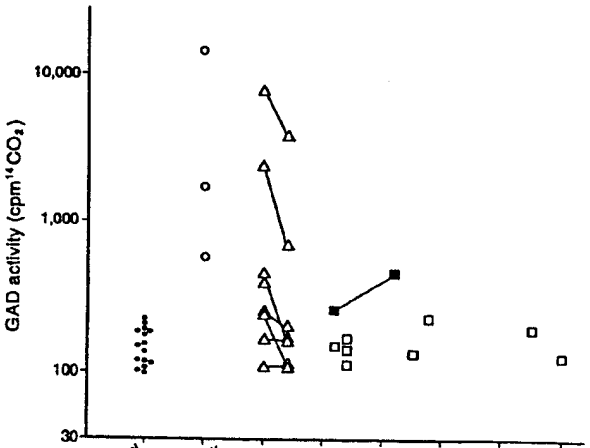

Figure 1. Immunoprecipitation of GAD activity by IDDM sera. GAD activity in brain extracts was immunoprecipitated with sera from healthy controls (●); individuals at high risk for IDDM (○); IDDM patients at diagnosis and two years later (△); and unrelated patients more than six years after diagnosis (□); one patient (■) developed a sensory neuropathy.

Results

IDDM patients have autoantibodies to GAD. We initially performed a blind trial to test for the presence of GAD autoantibodies in IDDM sera. We tested IDDM sera for the presence of GAD autoantibodies by assaying their ability to immunoprecipitate GAD activity from human brain homogenates (Fig. 1). We included sera from 35 individuals, which included 3 people judged to be at high risk for IDDM on the basis of their previously determined ICA titers, reduced responses to intravenous glucose, and their HLA DR/DQ haplotypes (15, 26), 8 IDDM patients studied at onset and 7 of these same patients two years later, 9 unrelated patients six or more years after IDDM onset, and 15 normal controls. Our results parallel those independently reported by Baekkeskov et al. (20).

The three high-risk individuals whose sera we examined had high anti-GAD titers, in one case comparable to those raised against purified brain GAD in experimental animals (data not shown). The levels of antibodies to GAD in five of eight newly diagnosed patients exceeded the mean + 1 SD of the control sera. Levels in these patients decreased by ~ 50% during the subsequent two years, with only two of seven sera having levels more than the mean + 1 SD of the control sera. In most patients ≥ 6 years after diagnosis, the concentrations of antibodies to GAD were indistinguishable from controls. In one patient in this series, however, anti-GAD levels actually rose between 6 and 11 years after onset, during which time the patient developed a sensory neuropathy.

Levels of anti-GAD antibodies in these patients generally parallel the previously determined titers of autoantibodies to the 64,000 M_r antigen. Our assays of immunoprecipitated GAD enzymatic activity easily identified individuals with high titers of autoantibodies to the 64,000 M_r antigen, but did not often distinguish individuals with low titers from controls.

This study established that autoantibodies to GAD are present at and before the clinical diagnosis of IDDM and decline within a few years after diagnosis. We next addressed the question of the molecular identity of the GAD autoantigen.

Islet cells contain both GAD_{65} and GAD_{67}. Immunohistochemical experiments with the GAD-6 monoclonal antibody, which recognizes only GAD_{65}, show the presence of GAD_{65} in pancreatic islets (Fig. 2; references 20, 25, 30). Using our recently described K-2 antiserum, which recognizes only GAD_{67}, we show that islet cells also contain GAD_{67} (Fig. 2; reference 25). Since both GAD_{65} and GAD_{67} are present in islets, either or both could be the autoantigen recognized by the IDDM sera surveyed in Fig. 1 and by Baekkeskov et al. (20).

The 64,000 M_r islet cell autoantigen is GAD_{65}. To define further the molecular identity of the IDDM autoantigen, we performed two sets of experiments. In the first experiment we used GAD-6 (the GAD_{65}-specific monoclonal antibody) to immunoadsorb GAD_{65} both from detergent extracts of ^{35}S-labeled islet cells and from soluble extracts of ^{35}S-labeled GAD-producing bacteria. GAD-6 specifically recognized a 65,000 M_r immunoreactive polypeptide in both islet cells and GAD_{65}-producing bacteria with identical electrophoretic mobilities, which were distinct from bacterially produced GAD_{67}. Prior immunoadsorption with an IDDM serum removes immunoreactive GAD_{65} (i.e., "64K") from both islet cell and bacterial extracts (data not shown).

In the second set of experiments, we examined the ability of bacterially produced GAD_{65} and GAD_{67} to compete with the immunoadsorption of islet cell autoantigens by IDDM sera. Sera taken from two patients (patient 052 and 496 which recognize both GADs; see Table I) specifically precipitate a polypeptide of M_r 64–65,000 from detergent-phase extracts of ^{35}S-labeled islets in the presence of extracts of host bacteria (i.e., bacteria not engineered to produce GAD), containing 400 μg of protein (Fig. 3, lanes *1* and *2*). When we added extracts (also containing 400 μg of total protein) of genetically engineered bacteria that produce either GAD_{65} or GAD_{67}, we found that an extract containing 100 μg of GAD_{67} partially blocked the binding of the islet cell antigen, as would be expected if GAD_{67} adsorbs some of the antibodies that recognize epitopes common to GAD_{65} and GAD_{67} (Fig. 3, lanes *5* and *6*). In contrast, an extract containing only 10 μg of GAD_{65} completely blocked immunoadsorption of the 64K autoantigen (Fig. 3, lanes *9* and *10*). These data show that the previously identified 64,000 M_r autoantigen is immunologically indistinguishable from GAD_{65}. A serum (patient 476) that predominantly recognizes GAD_{67} (which does not partition into the detergent phase of the islet cell extracts used in these studies) precipitated a very faint 64K band. The healthy control serum did not precipitate a 64K antigen.

IDDM sera differ in the recognition of GAD_{65} and GAD_{67}. Antisera raised in experimental animals against purified brain GAD vary in their recognition of GAD_{65} and GAD_{67}. With this in mind, we determined the specificity of individual IDDM sera for each species of GAD. We examined their ability to immunoprecipitate ^{35}S-labeled GAD_{65} and GAD_{67}, produced from GAD cDNAs in a bacterial expression system. We examined sera from 59 individuals (to whose IDDM status we were blind), including 8 people at high risk for IDDM, 12 people who later (3–64 months) developed IDDM, 3 newly diagnosed IDDM patients, 12 patients 2–22 years after onset who had no neurological symptoms, and 9 patients 10–48 years after onset who developed sensory or autonomic neuropathies (Table I; Fig. 4). None of the control sera from 15 healthy individuals had detectable ICA, antibodies to the 64,000 M_r pancreatic antigen, or antibodies to either form of GAD.

Levels of GAD autoantibodies were generally highest in the sera of individuals who were likely to have been in the process of developing the disease; those who were known to develop IDDM some time after their sera were drawn and those thought to be at high risk for IDDM on the basis of their previously determined ICA levels and autoantibodies to 64K. Levels were much lower in the sera of patients examined a few years after IDDM onset. None of the nine patients without neuropathies tested long after onset (≥ 5 years) had detectable antibodies to GAD. The intensity of the ^{35}S-labeled GAD_{65} immunoprecipitated by the IDDM sera generally paralleled the previously determined titers of autoantibodies to the 64,000 M_r islet cell polypeptide (15, 26), again supporting the latter's identification as GAD_{65}. There was no obvious correlation between ICA titers and the levels of autoantibodies to either GAD form.

Among IDDM sera, the ability to precipitate each of the two GADs varied among individuals. Of the 23 individuals tested whom we thought to be at early stages of IDDM (8 at high risk, 12 tested before subsequent onset, and 3 newly diagnosed), 15 recognized both GADs, 3 recognized only GAD_{65}, and 4 recognized only GAD_{67}. We found no obvious correlation between the time before or after diagnosis and the specific-

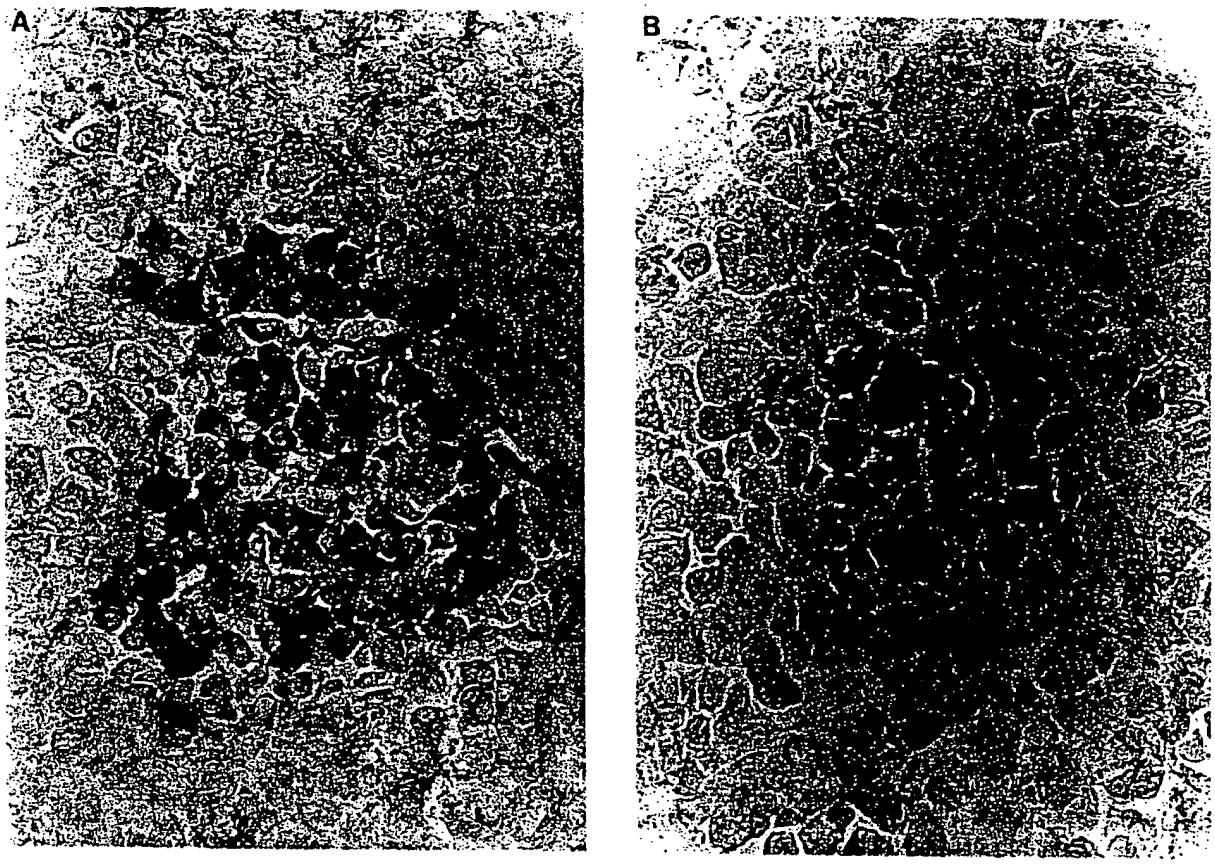

Figure 2. Pancreatic islets contain both GAD_{65} and GAD_{67}. (*A*) Immunohistochemistry with the GAD-6 monoclonal antibody specific for GAD_{65}, and (*B*) with the K-2 antiserum specific for GAD_{67}.

ity of autoantibodies for either form of GAD. A more sensitive assay (for example, one using human rather than rat GADs) might in fact reveal antibodies to both forms of GAD.

Altogether 78% (18/23) of sera from early stage IDDM individuals recognized GAD_{65}, a frequency similar to that reported in previous studies of 64,000 M_r autoantibodies (reviewed in 15, 20). When we tested for both GADs, however, we could detect autoantibodies to either or both in 96% (22/23) of the early stage individuals tested.

The sera of NOD mice also show immunoreactivity both to GAD_{65} and to GAD_{67} (Fig. 4, lane *22*). This finding further underscores the similarity of the disease processes in human IDDM and in NOD mice.

Individual sera vary in epitope recognition. To examine the individual variability in epitope recognition of IDDM autoantibodies, we determined the ability of sera from four individuals to recognize three polypeptide segments of GAD_{65} (Fig. 5). Each of these individuals was at a different stage in the progression of the disease: 052 (high risk), 723 (a patient who subsequently developed IDDM), 705 (at diagnosis), and UC2 (advanced neuropathy). We used PCR amplification followed by in vitro transcription and translation of the PCR products to produce ^{35}S-labeled polypeptides that represented the amino-terminal (A), middle (B), and carboxy-terminal (C) thirds of GAD_{65}. None of the four sera reacted with the segment A, two (052 and UC2) reacted with segments B and C, one (705) with the carboxy-terminal segment C only, and one (723) with none of the GAD_{65} segments. Our inability to immunoprecipitate polypeptides with serum 723 (which, as shown in Fig. 4, does precipitate both GAD_{65} and GAD_{67} as intact molecules) may have resulted from a lack of sensitivity of the assay or from the inability of any of the utilized peptides to fold into the recognized epitope. While the three peptides that we investigated are unlikely to have formed all their native epitopes, our epitope mapping data, like our studies of the differential recognition of GAD_{65} and GAD_{67}, suggest that each of the tested sera has a distinctive profile of anti-GAD antibodies. Although IDDM autoantibodies recognize different GAD epitopes, we do not know which epitopes are recognized by the self-reactive T lymphocytes, which contribute to both humoral and cellular autoimmunity.

Persistent autoimmunity to GAD is often associated with peripheral and autonomic neuropathy. The occurrence of antibodies to GAD (and to the previously determined 64,000 M_r antigen), is unusual in patients many years after onset (Fig. 1, Table I, and M. Atkinson, unpublished data). Autoantibodies to GAD were, however, present in 8 of 9 IDDM patients with sensory or autonomic neuropathies, long (10–41 years) after

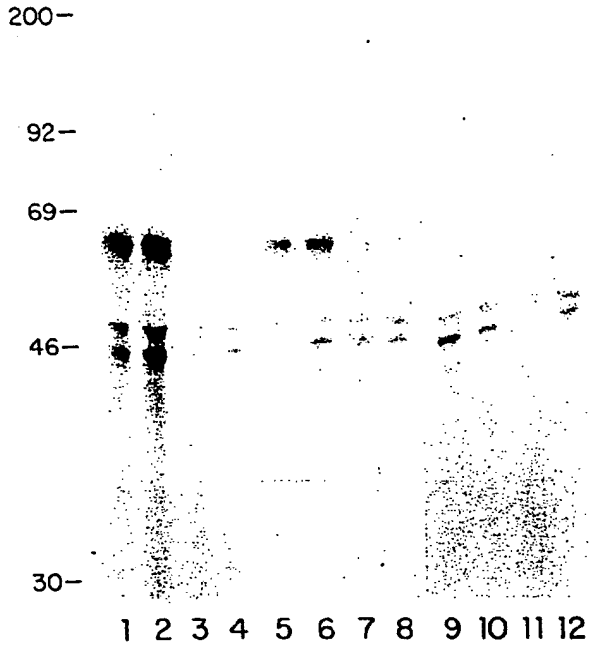

Figure 3. The 64,000 M_r autoantigen is GAD_{65}. The ability of sera which recognize both GADs (patients 052 and 496) to bind the previously described 64,000 M_r islet cell autoantigen was not blocked by preadsorption with an extract of wild-type BL21 (DE3) *E. coli*. Preadsorption with an extract of GAD_{67}-producing bacteria produced only partial blocking of these sera's ability to bind the pancreatic antigen. In contrast, preadsorption with extracts of GAD_{65}-producing bacteria, abolished the serum's ability to bind 64K antigen. Lanes *1–4* preadsorbed with 400 μg of a wild-type *E. coli* extract. Lanes *5–8* preadsorbed with a 400-μg extract containing 100 μg of GAD_{67}. Lanes *9–12* preadsorbed with a 400-μg extract containing 10 μg of GAD_{65}. Lanes *1, 5, 9;* patient 052. Lanes *2, 6, 10;* patient 496. Lanes *3, 7, 11;* healthy control. Lanes *4, 8, 12;* patient 476, whose serum predominantly recognizes GAD_{67} (Table I), does bind the 64K antigen very weakly which is not apparent in the photograph.

the onset of diabetic symptoms (Table I; Fig. 4, lanes *18–21*). Six of the sera examined had detectable levels of autoantibodies to both GAD_{65} and GAD_{67}, while two had detectable autoantibodies only to GAD_{67}. Two patients with rapidly progressing autonomic neuropathies (UC1 and UC2) had especially high levels of autoantibodies to GAD. In contrast, none of the nine patients who were free of IDDM-associated complications examined at or more than five years after onset had detectable antibodies to GAD. The GAD autoantibodies in neuropathy patients may result from the restimulation of the immune system by GAD released from damaged neurons, or they may be involved in the actual pathogenesis of this complication. In either case, GAD autoantibodies may serve as a useful marker of an ongoing degenerative process.

Sequence similarities between GAD and Coxsackievirus. Although we observe high levels of autoantibodies to GAD before IDDM onset, their presence may merely reflect an immune reaction to the exposure of previously sequestered antigens following β cell damage. Indeed, the initiating agent of the autoimmune response in IDDM is completely unknown, though the increasing incidence of IDDM and its frequent discordance in monozygotic twins has led to the suggestion that an environmental agent triggers autoimmunity (31, reviewed in 3, 12). In other autoimmune diseases, pathogenesis is thought to involve "molecular mimicry," in which a bacterial or viral antigen triggers an immune response that then reacts with a similar self antigen (reviewed 4, 32, 33).

Analysis of the deduced amino acid sequences of GAD_{65} and GAD_{67} shows an extensive and surprising sequence similarity to the P2-C protein of Coxsackievirus B_4. Coxsackievirus B_4 is a picornavirus with a worldwide distribution. It causes a mild upper respiratory infection and can also infect β cells (reviewed in 10–12). It has a small genome (7,395 bases), and its P2-C protein appears to contribute to the membrane-bound replication complex (34). A core polypeptide segment of six amino acid residues is identical in sequence between GAD_{65} and P2-C (Fig. 6; 22, 34). The immediately adjacent polypeptide segments also share a high level of similarity both in sequence and

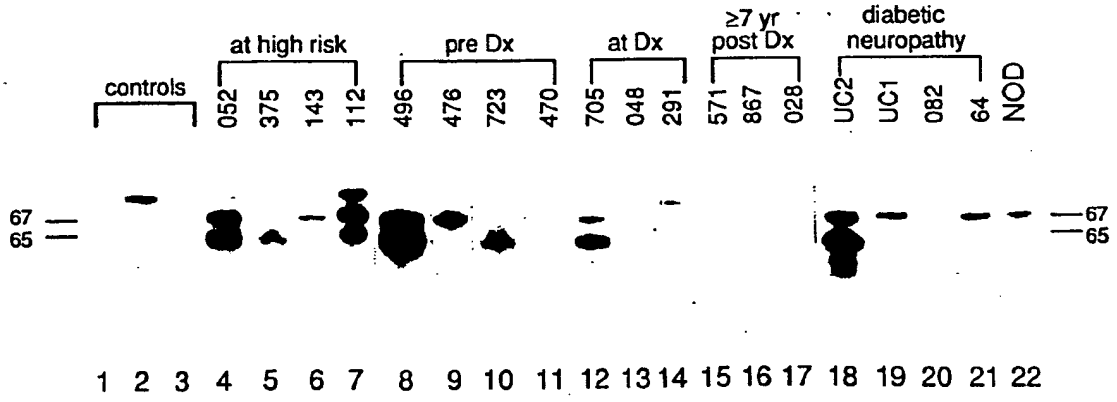

Figure 4. Detection of autoantibodies against GAD_{65} and GAD_{67} in IDDM sera. Sera were incubated with a mixture of ^{35}S-labeled lysates of GAD_{65}- and GAD_{67}-producing *E. coli*, and IgG-bound polypeptides were analyzed by SDS-PAGE. The composite photo shows representative data from controls and from individuals at different stages of IDDM: three controls (lanes *1–3*), four people at high risk for IDDM (lanes *4–7*), four who later developed IDDM (lanes *8–11*), three patients at diagnosis (lanes *12–14*), three IDDM patients more than seven years after diagnosis (lanes *15–17*), four IDDM patients with neuropathies (lanes *18–21*), and NOD mice (lane *22*).

Table I. Analysis of Characterized Sera for GAD_{65} and GAD_{67} Immunoreactivity

Patient ID				ICA	Anti-64K	Anti-GAD_{65}	Anti-GAD_{67}
				JDF units			
Individuals at high risk for IDDM							
052				160	+++	+++	+++
825				20	+++	++	0
375				0	+++	++	+
143				40	++	0	++
692				ND	++	0	+++
356				160	+++	++	+++
112				80	ND	+++	+++
410				0	++	++	++
Individuals who later developed IDDM							
	Months before IDDM diagnosis						
624	12			20	++	0	++
UF1	4			ND	+	+	++
584	24			0	++	+	0
035	64			40	+	+	0
496	6			160	+++	+++	+++
171	3			40	+	0	+
470	13			0	+++	+	+
055	8			40	+	0	0
438	42			320	++	+	+
840	9			0	+	+	+
723	14			ND	+++	+++	+
476	11			ND	+	+	+++
At onset of clinical symptoms							
048				320	+++	+	++
705				160	+++	+++	++
291				0	+++	++	++
IDDM patients without neuropathies							
	Years after diagnosis						
147	2			ND	+	0	0
476	3			0	ND	0	+
604	3			0	ND	+	0
113	5			160	ND	0	0
238	6			0	ND	0	0
997	6			80	ND	0	0
867	7			ND	ND	0	0
382	7			0	ND	0	0
052	12			0	ND	0	0
571	13			0	ND	0	0
M31	15			0	ND	0	0
025	22			0	ND	0	0
IDDM patients with neuropathies							
	Years after diagnosis	Autonomic neuropathy	Peripheral neuropathy				
UC1	35	+	+	0	ND	0	++
UC2	10	+	+	0	ND	+++	+++
UC3	13	+	+	0	ND	+	+
082	11	+	−	0	+	+	+

Table I. (Continued)

Patient ID				ICA	Anti-64K	Anti-GAD_{65}	Anti-GAD_{67}
038	21	+	+	ND	ND	+++	+++
344	33	–	+	0	ND	0	+
194	41	–	+	0	ND	+	+
310	48	–	+	0	ND	0	0
64	29	–	+	-0	ND	+	++

Patient sera were obtained and assayed for ICA and autoantibodies to the 64,000 M_r protein as part of a previous study (15, 26) or from the UCLA Diabetes Clinic. Patients that are part of the University of Florida's database are identified by three digit numbers. Other patients are identified by sequential numbers, with UF numbers representing patients seen in Gainesville and UC patients seen in Los Angeles. ICA titers are expressed in JDF units. +++, high titers; ++, intermediate; +, detectable; ND, not determined. Patients UC1, UC2, and UC3 had rapidly progressing sympathetic neuropathies. None of the sera from 15 healthy controls had detectable ICA, antibodies to the 64,000 M_r protein, or antibodies to either form of GAD.

in the positions of charged residues. In the 24 residue segments of GAD_{65} and P2-C that are illustrated in Fig. 6, 19 residues are either identical or conservative differences. The three peptides shown in Fig. 6 have nearly identical hydrophobicity profiles (data not shown). The high charge density and the presence of a proline residue in the shared core suggest that the segments are highly antigenic. No other significant similarities were found between GAD and other viruses implicated in IDDM, such as rubella, mumps, encephalomyocarditis virus, and cytomegalovirus. A generally similar sequence similarity is also present in the P2-C region of other members of the Coxsackievirus family. If specific members of the Coxsackievirus family (such as B_4 and B_5) are indeed involved in the etiology of IDDM, their pathogenicity may involve factors such as their particular amino acid sequences, virulence, and cell trophism, as well as the host immune repertoire.

Discussion

In a blind clinical study, we tested IDDM sera for the presence of GAD autoantibodies by their ability to immunoprecipitate

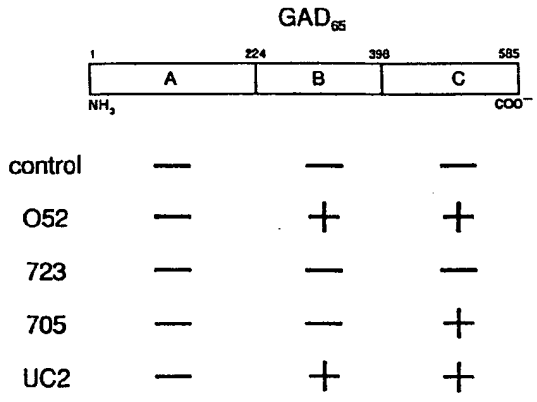

Figure 5. Epitope mapping of GAD_{65}. Three labeled segments containing the amino-terminal (*A*), middle (*B*), and carboxy-terminal (*C*) portions of GAD_{65} were immunoprecipitated with four IDDM sera that were initially characterized in the experiment shown in Fig. 4.

GAD enzymatic activity from brain homogenates. We found the highest levels of GAD autoantibodies in individuals at high risk for IDDM and in newly diagnosed IDDM patients. Levels of GAD autoantibodies decreased by ~ 50% within two years after diagnosis. Six years after IDDM onset, the patients whose sera we examined had GAD autoantibody levels indistinguishable from controls. One patient, however, displayed increased GAD antibodies years after onset, during which time the patient developed a sensory neuropathy.

Our studies of GADs in the brain have shown that neurons express two forms of GAD, which derive from separate genes (22). Pancreatic β cells also express GAD and use GABA to regulate glucagon secretion by α cells (35). Our immunohistochemical data, using antibodies monospecific for GAD_{65} and GAD_{67}, show that β cells, like most GABA neurons, contain both GAD_{65} and GAD_{67}. Although our enzymatic studies, and those of Baekkeskov et al. (20), demonstrated GAD autoimmunity in IDDM, they did not distinguish the two forms of GAD.

We used GAD_{65} and GAD_{67} cDNAs to express large amounts of each GAD in a bacterial expression system and tested the ability of each form to compete with the immunoadsorption of the 64,000 M_r autoantigen from ^{35}S-labeled islet cells. Only GAD_{65}-containing lysates effectively competed, suggesting that the 64,000 M_r autoantigen corresponds to GAD_{65}.

The islet cell homogenates previously used to characterize IDDM autoantigens were enriched for membrane-associated molecules and may preferentially have included GAD_{65}. In contrast, both our studies of the soluble fraction and those of Christie et al. (36) show a complex pattern of antigens recognized by IDDM autoantibodies (data not shown). Since islet cells contain both GAD_{65} and GAD_{67}, (Fig. 2) we sought to characterize the GAD autoantibodies by testing the ability of IDDM sera to recognize bacterially produced GAD_{65} and GAD_{67}.

We could detect autoantibodies to either GAD_{65} or GAD_{67} or both in almost all people who later developed IDDM, in some cases years before the onset of clinical symptoms. Of 23 early stage IDDM individuals tested, we found antibodies to both GADs in 15, to GAD_{65} alone in 3, and to GAD_{67} alone in 4. By testing for antibodies to both forms of GAD we were able to detect GAD antibodies in 96% of the individuals tested.

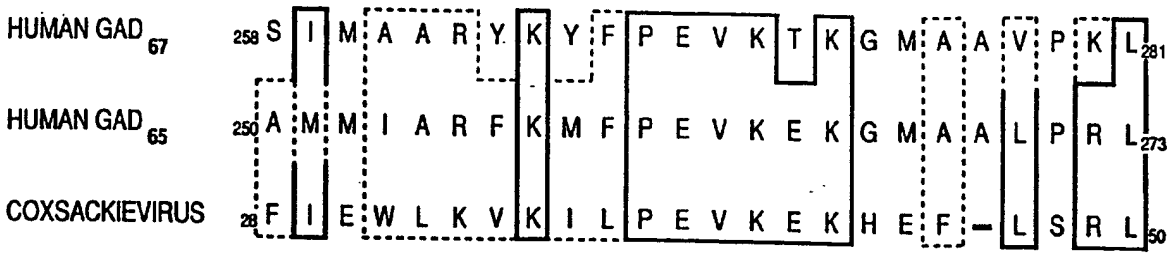

Figure 6. GAD and Coxsackievirus P2-C share common sequences. Solid line encloses identical amino acid residues. Dashed line encloses amino acid residues with similar charge, polarity, or hydrophobicity. Numbers refer to the amino acid residues in GAD_{65}, GAD_{67}, and Coxsackievirus protein P2-C. The human GAD amino acid sequences, which are almost identical to the rat GAD sequences, were determined by Bu Dingfang et al. (manuscript submitted for publication).

Levels of GAD autoantibodies were usually highest before IDDM onset and, in our patient sample, appeared as early as five years before onset of symptoms. GAD antibody levels declined after onset, presumably in parallel with the loss of GAD-containing β cells and the extinction of antigen-driven autoimmunity.

Patients showed varying immunoreactivity to GAD_{65} and GAD_{67}, which share ~ 70% amino acid similarity and are most divergent at their amino termini (22). They also varied in their ability to recognize individual polypeptide segments of GAD_{65}. These data suggest a diverse B lymphocyte response to different epitopes of GAD. While not all IDDM sera recognize the GAD_{65} polypeptide that contains the sequence shared with Coxsackievirus (segment B in Fig. 5), the antibodies may recognize GAD epitopes different from those that originally activated T lymphocytes.

Because our initial survey of IDDM patients detected increased levels of GAD autoantibodies in a patient who developed a sensory neuropathy long after the onset of diabetes itself, we further studied GAD autoimmunity in patients with IDDM-associated neuropathies. We found that 8/9 patients who had developed clinical IDDM symptoms 10–41 years earlier, showed significant levels of autoantibodies to GAD_{65}, GAD_{67}, or both. Of the eight patients in this group for whom we had ICA data, none had detectable ICA, and their low basal C-peptide did not respond to intravenous glucagon, suggesting that the continued high levels of anti-GAD autoantibodies did not result from the persistence of GAD-containing β cells.

The production of anti-GAD autoantibodies in patients with diabetic neuropathy may reflect continued stimulation of the immune system by GAD in the peripheral nervous system. Consistent with this hypothesis, Rabinowe et al. (37) have shown that, in some IDDM patients, autoantibodies to sympathetic ganglia are present at the diagnosis of IDDM, before the onset of clinical neuropathy. In addition, postmortem examination has revealed lymphocytic infiltration of sympathetic ganglia in IDDM patients with autonomic neuropathy (38). Our data suggest that autoimmunity to GAD, together with the metabolic effects of hyperglycemia, may play an important pathogenic role in diabetic neuropathy in IDDM.

The surprising similarity of the amino acid sequences of GAD_{65} and GAD_{67} to the P2-C protein of Coxsackievirus suggests that IDDM autoimmunity may arise by molecular mimicry, as a consequence of infection by Coxsackievirus. Epidemiological studies have shown that 39% of newly diagnosed IDDM patients have IgM responses to Coxsackievirus, compared to 6% of controls (39, 40). The molecular mimicry hypothesis suggests a mechanism to explain both the epidemiological association of Coxsackievirus B_4 with human IDDM and its ability (in contrast to other viruses epidemiologically associated with IDDM) to produce diabetes in mice and primates (31, 41–44). Direct association of Coxsackie B_4 infection and subsequent onset of human IDDM has been documented in a few cases (45, 46).

Coxsackievirus infection (perhaps of β cells themselves) may, in genetically susceptible individuals, initiate the characteristic autoimmune attack on pancreatic β cells. Viral peptides would then be presented to T lymphocytes, probably on the surface of antigen-presenting cells in the context of class II molecules. Although the sequences of both GADs suggest that they are cytosolic molecules, GAD polypeptides may be presented on the cell surface in the context of MHC molecules (as discussed in 47 and 48). Christie et al. (36), moreover, have demonstrated the association of the molecule we now know to be GAD_{65} with β cell membranes. GAD epitopes on the surface of β cells, in the context of either class I or class II molecules, could thus become the targets of immune responses initially directed against a Coxsackievirus epitope. The resultant destruction of β cells would then release more GAD_{65} and GAD_{67}, including GADs from the cytoplasm. The released GAD could then continue to stimulate lymphocytes already primed to the Coxsackievirus peptide, thus perpetuating the immune response long after the termination of the viral infection. This molecular mimicry would then lead to the continued autoimmune destruction of β cells and eventually to the development of clinical diabetes.

Assays for antibodies to recombinant GADs should allow a straightforward means of distinguishing IDDM from other forms of diabetes mellitus. This should be especially useful for evaluating adult patients presenting with the more common type II, non-insulin-dependent diabetes mellitus (NIDDM). Patients with true NIDDM do not have ICAs or autoantibodies to the 64,000 M_r protein or to insulin. Of adult onset patients initially diagnosed as having NIDDM, however, 10–15% are true type I (IDDM) diabetics and will eventually require insulin therapy.

Clinical trials are now under way to test the effectiveness of general immunosuppressive agents (such as cyclosporin and azathioprine) in delaying the onset of IDDM in individuals at high risk, that is, who already have islet cell autoantibodies

(49). Autoantibodies to GAD are the earliest indication of autoimmunity in IDDM and the two GADs are therefore excellent candidates for the initial targets for autoimmunity. Future experiments will determine whether the epitope shared by GAD and Coxsackievirus contributes to IDDM pathogenesis. If GAD is indeed involved in the etiology of IDDM, it may be possible to devise specific, rather than nonspecific, immunosuppressive strategies to block the function of specific MHC and T cell receptor molecules.

Acknowledgments

We thank the following people for helpful discussions and support: Bu Dingfang, Cheryl Craft, Chris Evans, Ken Pischel, Christian Ruppert, Richard Spielman, Niranjala Tillakaratne, Robert Weatherwax, Leslie Weiner, and Janis Young. We are especially grateful for the support and advice of Glen Evans.

This work was supported by grants from the National Institutes of Health to A. Tobin, M. Clare-Salzler, and N. Maclaren, and from the American Diabetes Association to N. Maclaren and M. Atkinson.

References

1. LaPorte, R., and K. Cruickshanks. 1988. Incidence and risk factors for insulin dependent diabetes mellitus. *In* Diabetes in America, National Diabetes Data Group. NIH Publication No. 85-1468. Chapter III, pp. 1–12.

2. Krolewski, A. S., J. H. Warram, L. I. Rand, and C. R. Kahn. 1987. Epidemiologic approach to the etiology of type I diabetes mellitus and its complications. *N. Engl. J. Med.* 317:1390–1398.

3. Castaño, L., and G. S. Eisenbarth. 1990. Type I-diabetes: a chronic autoimmune disease of human, mouse, and rat. *Annu. Rev. Immunol.* 8:647–679.

4. Sinha, A. A., M. T. Lopez, and H. O. McDevitt. 1990. Autoimmune diseases: the failure of self tolerance. *Science (Wash. DC).* 248:1380–1393.

5. Bottazzo, G. F., R. Pujol-Borrell, T. Hanafusa, and M. Feldman. 1983. Role of aberrant HLA-DR expression and antigen presentation in induction of endocrine autoimmunity. *Lancet.* ii:1115–1118.

6. Maclaren, N., D. Schatz, A. Drash, and G. Grave. 1989. The initial pathogenic events in insulin-dependent diabetes. *Diabetes.* 38:534–538.

7. Todd, J. A., H. Acha-Orbea, J. I. Bell, N. Chao, Z. Fronek, C. O. Jacob, M. McDermott, A. A. Sinha, L. Timmerman, L. Steinman, and H. O. McDevitt. 1988. A molecular basis for MHC class II autoimmunity. *Science (Wash. DC).* 240:1003–1009.

8. Todd, J. A. 1990. Genetic control of autoimmunity in type 1 diabetes. *Immunol. Today.* 11:122–129.

9. Olmos, P., R. A'Hern, D. A. Heaton, B. A. Millward, D. Risley, D. A. Pyke, and R. D. G. Leslie. 1988. The significance of the concordance rate for type 1 (insulin-dependent) diabetes in identical twins. *Diabetologia.* 31:747–750.

10. Gamble, D. R. 1980. The epidemiology of insulin dependent diabetes, with particular reference to the relationship of virus infection to its etiology. *Epidemiol. Rev.* 2:49–69.

11. Barrett-Connor, E. 1985. Is insulin-dependent diabetes mellitus caused by coxsackievirus B infection? a review of the epidemiologic evidence. *Rev. Infect. Dis.* 7:207–215.

12. Banatvala, J. E. 1987. Insulin-dependent (juvenile-onset, type 1) diabetes mellitus coxsackie B viruses revisited. *Prog. Med. Virol.* 34:33–54.

13. Baekkeskov, S., J. H. Nielsen, B. Marner, T. Bilde, J. Ludvigsson, and Å. Lernmark. 1982. Autoantibodies in newly diagnosed diabetic children immunoprecipitate human pancreatic islet cell proteins. *Nature (Lond.).* 298:167–169.

14. Baekkeskov, S., M. Landin, J. K. Kristensen, S. Srikanta, G. J. Bruining, T. Mandrup-Pousen, C. de Beaufort, J. S. Soeldner, G. Eisenbarth, F. Lindgren, et al. 1987. Antibodies to a 64,000 M_r human islet cell antigen precede the clinical onset of insulin-dependent diabetes. *J. Clin. Invest.* 79:926–934.

15. Atkinson, M. A., N. K. Maclaren, D. W. Scharp, P. E. Lacy, and W. J. Riley. 1990. 64,000 M_r autoantibodies as predictors of insulin-dependent diabetes. *Lancet.* 335:1357–1360.

16. Maclaren, N. K. 1988. How, when, and why to predict IDDM. *Diabetes.* 37:1591–1594.

17. Ziegler, A. G., R. D. Herskowitz, R. A. Jackson, J. S. Soeldner, and G. Eisenbarth. 1990. Predicting type I diabetes. *Diabetes Care.* 13:762–775.

18. Baekkeskov, S., T. Dyrberg, and Å. Lernmark. 1984. Autoantibodies to a 64-kilodalton islet cell protein precede the onset of spontaneous diabetes in the BB rat. *Science (Wash. DC).* 224:1348–1350.

19. Atkinson, M. A., and N. K. Maclaren. 1988. Autoantibodies in nonobese diabetic mice immunoprecipitate 64,000-M_r islet antigen. *Diabetes.* 37:1587–1590.

20. Baekkeskov, S., H.-J. Aanstoot, S. Christgau, A. Reetz, M. Solimena, M. Cascalho, F. Folli, H. Richter-Olesen, and P. De Camilli. 1990. Identification of the 64K autoantigen in insulin-dependent diabetes as the GABA-synthesizing enzyme glutamic acid decarboxylase. *Nature (Lond.).* 347:151–156.

21. Erdö, S. L., and J. R. Wolff. 1990. γ-Aminobutyric acid outside the mammalian brain. *J. Neurochem.* 54:363–372.

22. Erlander, M. G., N. J. K. Tillakaratne, S. Feldblum, N. Patel, and A. J. Tobin. 1991. Two genes encode distinct glutamate decarboxylases with different responses to pyridoxal phosphate. *Neuron.* 7:91–100.

23. Kaufman, D. L., J. F. McGinnis, N. R. Krieger, and A. J. Tobin. 1986. Brain glutamate decarboxylase cloned in λ-gt-11: fusion protein produces γ-aminobutyric acid. *Science (Wash. DC).* 232:1138–1140.

24. Kobayashi, Y., D. L. Kaufman, and A. J. Tobin. 1987. Glutamic acid decarboxylase cDNA: nucleotide sequence encoding an enzymatically active fusion protein. *J. Neurosci.* 7:2768–2772.

25. Kaufman, D. L., C. R. Houser, and A. J. Tobin. 1991. Two forms of the γ-aminobutyric acid synthetic enzyme glutamate decarboxylase have distinct intraneuronal distributions and cofactor interactions. *J. Neurochem.* 56:720–723.

26. Riley, W. J., N. K. Maclaren, J. Krischer, R. P. Spillar, J. H. Silverstein, D. A. Schatz, S. Schwartz, J. Malone, S. Shah, C. Vadheim, and J. I. Rotter. 1990. A prospective study of the development of diabetes in relatives of patients with insulin-dependent diabetes. *N. Engl. J. Med.* 323:1167–1172.

27. Studier, F. W., and B. A. Moffatt. 1986. Use of bacteriophage T7 RNA polymerase to direct selective high-level expression of cloned genes. *J. Mol. Biol.* 189:113–130.

28. Saiki, R. K., D. H. Gelfand, S. Stoffel, S. J. Scharf, R. Higuchi, G. T. Horn, K. B. Mullis, and H. A. Erlich. 1988. Primer-directed enzymatic amplification of DNA with a thermostable DNA polymerase. *Science (Wash. DC).* 239:487–491.

29. Kozak, M. 1989. The scanning model for translation: an update. *J. Cell Biol.* 108:229–241.

30. Chang, Y. C., and D. I. Gottlieb. 1988. Characterization of the proteins purified with monoclonal antibodies to glutamic acid decarboxylase. *J. Neurosci.* 8:2123–2130.

31. Toniolo, A., T. Onodera, J.-W. Yoon, and A. L. Notkins. 1980. Induction of diabetes by cumulative environmental insults from viruses and chemicals. *Nature (Lond.).* 288:383–385.

32. Oldstone, M. B. A. 1987. Molecular mimicry and autoimmune disease. *Cell.* 50:819–820.

33. Oldstone, M. B. A. 1989. Molecular mimicry as a mechanism for the cause and as a probe uncovering etiologic agent(s) of autoimmune disease. *Curr. Top. Microbiol. Immunol.* 145:126–135.

34. Jenkins, O., J. D. Booth, P. D. Minor, and J. W. Almond. 1987. The complete nucleotide sequence of coxsackievirus B4 and its comparison to other members of the picornaviridae. *J. Gen. Virol.* 68:1835–1848.

35. Rorsman, P., P.-O. Berggren, K. Bokvist, H. Ericson, H. Möhler, C.-G. Östenson, and P. A. Smith. 1989. Glucose-inhibition of glucagon secretion involves activation of $GABA_A$-receptor chloride channels. *Nature (Lond.).* 341:233–236.

36. Christie, M. R., D. G. Pipeleers, Å. Lernmark, and S. Baekkeskov. 1990. Cellular and subcellular localization of an M_r 64,000 protein autoantigen in insulin-dependent diabetes. *J. Biol. Chem.* 265:376–381.

37. Rabinowe, S. L., F. M. Brown, M. Watts, M. M. Kadrofske, and A. I. Vinik. 1989. Anti-sympathetic ganglia antibodies and postural blood pressure in IDDM subjects of varying duration and patients at high risk of developing IDDM. *Diabetes Care.* 12:1–6.

38. Duchen, L. W., N. A. Anjorin, P. J. Watkins, and J. D. Mackay. 1980. Pathology of autonomic neuropathy in diabetes mellitus. *Ann. Intern. Med.* 92:301–303.

39. King, M. L., A. Shaikh, D. Birdwell, A. Voller, and J. E. Banatvala. 1983. Coxsackie-B-virus-specific IgM responses in children with insulin-dependent (juvenile-onset; type 1) diabetes mellitus. *Lancet.* i:1397–1399.

40. Banatvala, J. E., G. Schernthaner, E. Schober, L. M. DeSilva, J. Byrant, M. Borkenstein, D. Brown, and M. A. Menser. 1985. Coxsackie B, mumps, rubella, and cytomegalovirus specific IgM responses in patients with juvenile-onset insulin-dependent diabetes mellitus in Britain, Austria and Australia. *Lancet.* i:1409–1412.

41. Toniolo, A., T. Onodera, G. Jordan, J.-W. Yoon, and A. L. Notkins. 1982. Glucose abnormalities produced in mice by the six members of the coxsackie B virus group. *Diabetes.* 31:496–499.

42. Yoon, J.-W., W. T. London, B. L. Curfman, R. L. Brown, and A. L. Notkins. 1986. Coxsackie Virus B_4 produces transient diabetes in nonhuman primates. *Diabetes.* 35:712–716.

43. Chatterjee, N. K., C. Nejman, and I. Gerling. 1988. Purification and characterization of a strain of coxsackievirus B4 of human origin that induces diabetes in mice. *J. Med. Virol.* 26:57–69.

44. Gerling, I., C. Nejman, and N. K. Chatterjee. 1988. Effect of Coxsackievirus B4 infection in mice on expression of 64,000-*M*, autoantigen and glucose sensitivity of islets before development of hyperglycemia. *Diabetes.* 37:1419–1425.

45. Yoon, J.-W., M. Austin, T. Onodera, and A. L. Notkins. 1979. Virus induced diabetes mellitus. Isolation of a virus from the pancreas of a child with diabetic ketoacidosis. *N. Engl. J. Med.* 300:1173–1179.

46. Gladish, R., W. Hofmann, and R. Waldherr. 1976. Myokarditis und insulinitis nach coxsackie virus infect. *Z. Kardiol.* 65:835–849.

47. Germain, R. N. 1986. The ins and outs of antigen processing and presentation. *Nature (Lond.).* 322:687–689.

48. Nuchtern, J. G., J. S. Bonifacino, W. E. Biddision, and R. D. Klausner. 1989. Befeldin A implicates egress from endoplasmic reticulum in class I restricted antigen presentation. *Nature (Lond.).* 339:223–226.

49. Skyler, J. S., O. B. Crofford, J. Dupre, G. S. Eisenbarth, G. C. Sathman, E. A. M. Gale, D. Goldstein, J. T. Harmon, M. W. Haymond, R. A. Jackson, et al. 1990. Prevention of type I diabetes mellitus. *Diabetes.* 39:1151–1152.

Human Desmocollin 1 (Dsc1) Is an Autoantigen for the Subcorneal Pustular Dermatosis Type of IgA Pemphigus

Takashi Hashimoto,* Chie Kiyokawa,* Osamu Mori,* Minoru Miyasato,* Martyn A. J. Chidgey,† David R. Garrod,† Yasushi Kobayashi,‡ Koji Komori,‡ Ken Ishii,‡ Masayuki Amagai,‡ and Takeji Nishikawa‡

*Department of Dermatology, Kurume University School of Medicine, Fukuoka, Japan, †Epithelial Morphogenesis Research Group, University of Manchester, Manchester, U.K.; and ‡Department of Dermatology, Keio University School of Medicine, Tokyo, Japan

IgA pemphigus showing IgA anti-keratinocyte cell surface autoantibodies is divided into subcorneal pustular dermatosis (SPD) and intraepidermal neutrophilic IgA dermatosis (IEN) types. We previously showed by immunoblotting that IgA from some IgA pemphigus patients reacted with bovine desmocollins (Dsc), but not human Dsc. To determine the antigen for IgA pemphigus, we focused on conformation-dependent epitopes of Dsc, because sera of patients with classical pemphigus recognize conformation-sensitive epitopes of desmogleins. We constructed mammalian expression vectors containing the entire coding sequences of human Dsc1, Dsc2, and Dsc3 and transiently transfected them into COS7 cells by lipofection. Immunofluorescence of COS7 cells transfected with single human Dscs showed that IgA antibodies of all six SPD-type IgA pemphigus cases reacted with the surface of cells expressing Dsc1, but not with cells expressing Dsc2 or Dsc3. In contrast, none of seven IEN-type IgA pemphigus cases reacted with cells transfected with any Dscs. These results convincingly indicate that human Dsc1 is an autoantigen for SPD-type IgA pemphigus, suggesting the possibility of an important role for Dsc1 in the pathogenesis of this disease. This study shows that a Dsc can be an autoimmune target in human skin disease. ***Key words: autoimmune bullous disease/desmosome/keratinocyte/mammalian cell transfection. J Invest Dermatol 109:127–131, 1997***

Desmosomal cadherins are of two types, desmoglein (Dsg) and desmocollin (Dsc), both of which occur as three isoforms, Dsg1, 2, and 3 and Dsc1, 2, and 3, derived from different genes (Buxton *et al*, 1993; Amagai *et al*, 1995). Each Dsc gene produces two alternatively spliced products, the longer "a" form and the shorter "b" form, i.e., Dsc1a and Dsc1b.

Classical pemphigus, characterized by the presence of IgG anti-keratinocyte cell surface autoantibodies in the sera, consists of two major subtypes, pemphigus vulgaris (PV) and pemphigus foliaceus (PF). Brazilian PF is endemic in South America and shows features similar to PF. Extensive studies of these diseases have revealed that the autoantigen for PF and Brazilian PF is Dsg1 (Stanley *et al*, 1986; Hashimoto *et al*, 1990; Koch *et al*, 1990; Amagai *et al*, 1995) and for PV is Dsg3 (Hashimoto *et al*, 1990, Stanley *et al*, 1982; Amagai *et al*, 1991). Recently, a number of cases with anti-cell surface antibodies of the IgA class and showing distinct clinical features have been reported (Ebihara *et al*, 1991; Iwatsuki *et al*, 1991). Although various terms have been used for these conditions, we will use the most simple term, IgA pemphigus, throughout this report. IgA pemphigus is divided into two subtypes, intraepidermal neutrophilic IgA dermatosis (IEN) type, showing pustule formation through the entire depth of the epidermis (Huff *et al*, 1985; Teraki *et al*, 1991), and subcorneal pustular dermatosis (SPD) type, showing pustules in the upper epidermis (Tagami *et al*, 1983, Hashimoto *et al*, 1987).

We have sought the target antigens for the IgA anti-keratinocyte cell surface autoantibodies of IgA pemphigus and found that certain IgA pemphigus sera recognized bovine Dsc (Ebihara *et al*, 1991; Iwatsuki *et al*, 1991). The significance of this finding, however, was unclear, because no IgA pemphigus sera reacted human Dsc by immunoblotting. We speculated that the cause of this failure may be that the IgA pemphigus sera react with conformation-dependent epitopes on Dsc because most pathogenic autoantibodies recognize conformation-sensitive epitopes of desmogleins in PV and PF (Amagai *et al*, 1994, 1995; Emery *et al*, 1995). The widely used technique of immunoprecipitation is able to detect such conformation-dependent epitopes on IgG antibodies. A technique for immunoprecipitation with IgA antibodies, however, has not been established.

In the current study, to detect antibodies to native Dsc molecules, we constructed mammalian expression vectors containing the entire coding sequence of human Dsc1, Dsc2, or Dsc3 and transfected them into COS7 cells by lipofection. We found that IgA in the sera of SPD type, but not IEN type, reacted with Dsc1. This study shows that human Dsc can be a target autoantigen in human

Manuscript received February 26, 1997; revised May 14, 1997; accepted for publication May 22, 1997.

Reprint requests to: Dr. Takashi Hashimoto, Department of Dermatology, Kurume University School of Medicine, 67 Asahimachi, Kurume, Fukuoka 830, Japan.

Abbreviations: Dsg, desmoglein; Dsc, desmocollin; PV, pemphigus vulgaris; PF, pemphigus foliaceus; IEN, intraepidermal neutrophilic IgA dermatosis; SPD, subcorneal pustular dermatosis; mAb, monoclonal antibody; pAb, polyclonal antibody

0022-202X/97/$10.50

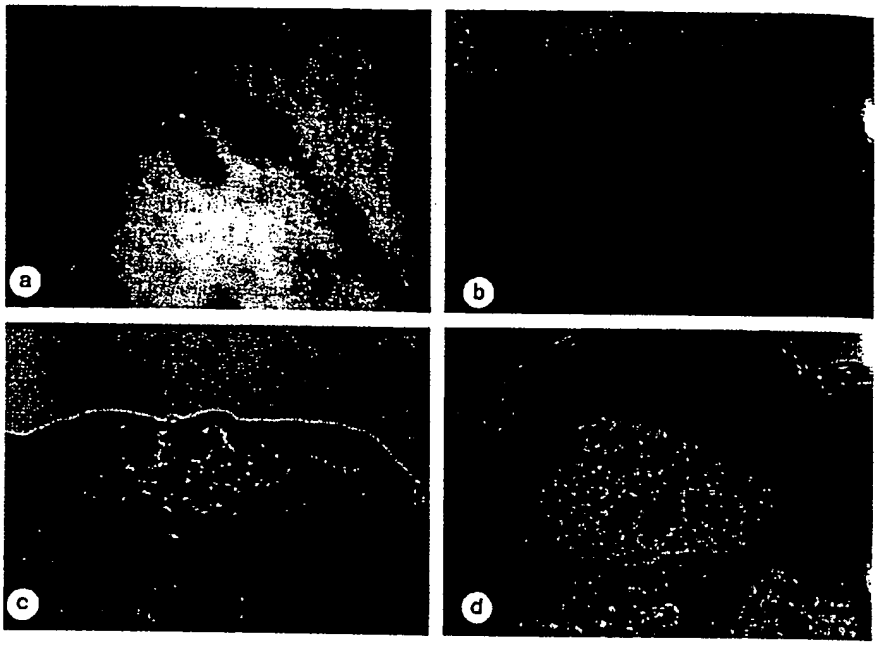

Figure 1. Clinical and histopathologic features are distinct between SPD and IEN types of IgA pemphigus. A patient of SPD type IgA pemphigus clinically showed superficial pustules *(a)*. A patient of IEN type showed different cutaneous lesions with deeper pustules *(b)*. A patient of SPD type histopathologically showed subcorneal pustule formation *(c)*. A patient of IEN type showed pustule formation in the entire epidermis *(d)*. *Scale bar*, 30 μm.

skin disease and also suggests an important insight into the pathogenesis of IgA pemphigus.

MATERIALS AND METHODS

Sera We selected 13 typical cases with IgA pemphigus (six SPD type and seven IEN type). All the patients of SPD type showed SPD-like clinical features of superficial pustules (Fig 1*a*) and histopathologically subcorneal pustule formation in the upper epidermis (Fig 1*c*). In contrast, all the patients of IEN type showed deeper vesiculo-pustular skin lesions, occasionally characterized by sunflower-like arrangement (Fig 1*b*), and pustule formation in the entire epidermis (Fig 1*d*).

Sera obtained from three patients each with PV and PF as well as from five normal volunteers were used as controls. All sera were stored at −30°C or −80°C as aliquots and used immediately after thawing because IgA may be less stable than IgG.

Antibodies Anti-Dsg monoclonal antibody (mAb) 32–2B (Vilela *et al*, 1987) and anti-Dsc mAb 52–3D (Collins *et al*, 1991) were characterized previously. Polyclonal antibody (pAb) JCMC was obtained by immunizing a rabbit with a recombinant bovine Dsc1-specific peptide (North *et al*, 1996). pAbs D1K2 and C+DGII were obtained by immunizing rabbits with peptides specific to human Dsc1 and Dsc2, respectively (Suzuki *et al*, manuscript in preparation).

Kawamura *et al* (1994) have recently isolated a novel human Dsc cDNA, which was tentatively designated human Dsc4. By comparison of human Dsc sequences with bovine Dsc sequences that are taken as standards (Collins *et al*, 1991; Parker *et al*, 1992; King *et al*, 1993; Theis *et al*, 1993; Troyanovsky *et al*, 1993; Kawamura *et al*, 1994; Legan *et al*, 1994; Yue *et al*, 1995), this is now re-designated human Dsc3. pAb LNCF3 was obtained by immunizing a rabbit with a human Dsc3-specific peptide (Suzuki *et al*, manuscript in preparation). The pAbs D1K2, C+DGII, and LNCF3 were generous gifts from Tadaaki Suzuki, Kazuo Kawamura, and Susumu Tsurufuji (Institute of Cytosignal Research, Inc.).

Preparation of Mammalian Cell Expression Constructs of Human Dsc1, 2, and 3 and Transfection into COS7 Cells To prepare a construct of human Dsc1, we used cDNA clones K24 (King *et al*, 1993) and K55 (King, 1994) (generous gifts from Dr. R.S. Buxton and Dr. I.A. King, Laboratory of Eukaryotic Molecular Genetics, National Institute for Medical Research, Mill Hill, London, U.K.). K24 contains almost the entire coding sequence except for the N-terminal end, and K55 contains the N-terminal region including the ATG initiation codon. To obtain cDNA covering the entire coding sequence, we utilized the *Acc*I sites at nucleotide 1494 in human Dsc1 and within the multiple cloning site of pBluescript II SK −. The 3.0-kbp fragment excised from K24 by *Acc*I digestion, which contains the C-terminal region of Dsc1, was subcloned into *Acc*I-digested K55, and a clone with the proper orientation, designated K24/K55, was selected. The *Bam*HI/*Xba*I-digested fragment of K24/K55 containing the entire coding sequence of human Dsc1 was subcloned into the eukaryotic expression vector pcDNAI/Amp (Invitrogen Corp., San Diego, CA) previously digested with *Bam*HI/*Xba*I. A clone designated pcDNAI-hDsc1 was selected and propagated.

To prepare a construct of human Dsc2, the entire coding sequence was obtain by *Eco*RI digestion from pPB192 (a generous gift from Dr. R.S. Buxton and Dr. I.A. King), which is a pBluescript vector carrying the L5 clone (Parker *et al*, 1992). This cDNA fragment was subcloned into *Eco*RI-digested pcDNAI/Amp, and a clone with the proper orientation, designated pcDNAI-hDsc2, was selected.

pcDNAI-hDsc1 and pcDNAI-hDsc2 allow the expression of full-length cDNA inserts of human Dsc1 and Dsc2 under the control of the cytomegalovirus promoter.

Preparation of human Dsc3 cDNA (a generous gift from Tadaaki Suzuki, Kazuo Kawamura, and Susumu Tsurufuji) subcloned into the eukaryotic expression vector, pcDL-SRa296, was previously described (Kawamura *et al*, 1994). This clone allows the expression of a full-length human Dsc3 cDNA insert under the control of the simian virus early promoter, SRa (Kawamura *et al*, 1994; Takabe *et al*, 1988). All three clones produced "a" form (longer form) of each Dsc species.

Transient transfection of COS7 cells using lipofectAMIN reagent (Life Technologies, Gaithersburg, MD) was carried out according to the manufacturer's recommendations.

Immunofluorescence Immunofluorescence of normal human skin sections was performed by a standard method (Beutner *et al*, 1968) using fluorescein-conjugated anti-human IgG (specific to γ-chains), anti-human IgA (specific to α-chains), anti-mouse Igs, and anti-rabbit Igs antisera (DAKO, Glostrup, Denmark) as secondary antibodies.

Immunofluorescence of unfixed COS7 cells transiently transfected with Dsc1, 2, or 3 cDNAs was performed by the method of Stanley *et al* (1982). The cells cultured on coverglasses were first incubated at 4°C for 30 min in phosphate-buffered saline containing 1% bovine serum albumin and 0.1% NaN_3 to reduce background and membrane fluidity, respectively. The cells were incubated for 1 h at 4°C with patients' sera or specific antibodies diluted in the same buffer and subsequently with second antibodies conjugated with either FITC or rhodamine. For double labeling, the cells were incubated with a mixture of diluted sera and rabbit anti-Dsc pAb and subsequently with mixture of fluorescein-conjugated anti-human IgA antiserum and rhodamine-conjugated anti-rabbit Ig antiserum (DAKO). In some experiments, the cells were fixed and permeabilized by treatment with 100% methanol for 20 min at −20°C before immunostaining.

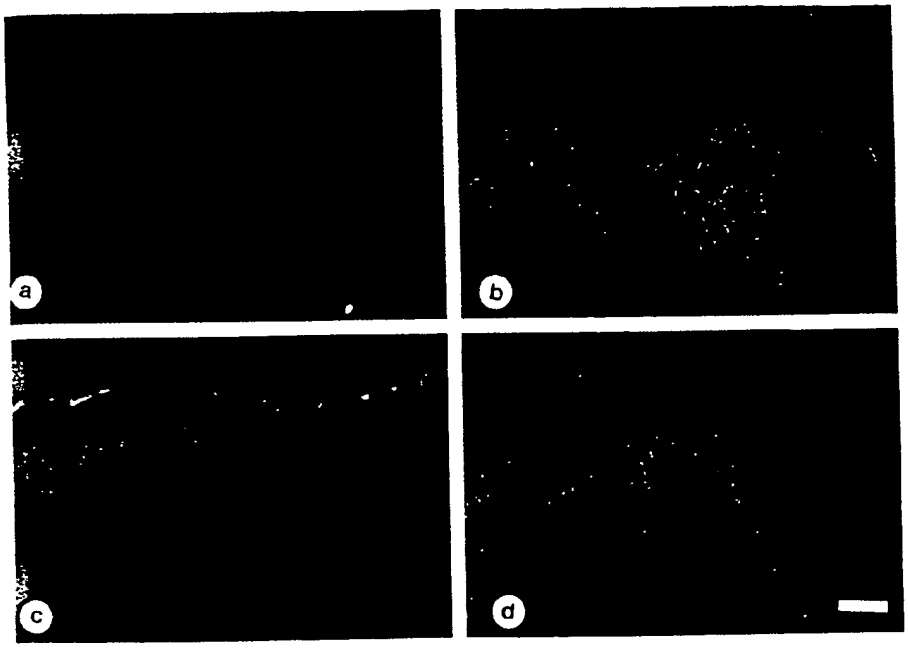

Figure 2. Immunofluorescence of normal human skin sections for anti-Dsc pAbs and IgA pemphigus sera suggested that SPD and IEN types may react with Dsc1 and Dsc3, respectively. Anti-Dsc1 peptide pAb JCMC stained keratinocyte cell surfaces in the upper epidermis *(a)*, whereas anti-Dsc3 peptide pAb LNCF3 stained cell surfaces in the entire epidermis *(b)*. A SPD type IgA pemphigus serum stained the uppermost epidermis *(c)*, and an IEN type IgA pemphigus serum stained the entire epidermis *(d)*. *Scale bar*, 30 μm.

Immunoblot Analysis of Normal Human Epidermal Extracts, Bovine Desmosome Preparations, and Extracts of COS7 Cells Transfected with Dsc1, 2, and 3 Preparation of extracts of normal human epidermis separated by dispase treatment, partial purification of desmosomes from bovine snout epidermis, and procedures for electrophoresis and immunoblotting were described previously (Hashimoto *et al*, 1990; Ebihara *et al*, 1991). All peroxidase-conjugated anti-human IgG (specific to γ-chains), anti-human IgA (specific to α-chains), anti-mouse Igs, and anti-rabbit Ig antisera used as secondary antibodies were obtained from DAKO.

COS7 cells transiently expressing Dsc1, 2, and 3 were lysed with Laemmli's sample buffer (Laemmli, 1970) and subjected to electrophoresis. Immunoblotting was performed by the same method as for epidermal extracts or desmosome preparations.

RESULTS

Immunofluorescence of Normal Human Skin Sections Suggested that SPD and IEN Types of IgA Pemphigus May React with Dsc1 and Dsc3, Respectively With immunofluorescence of normal human skin sections, anti-Dsc1 peptide pAbs (JCMC and D1K2) stained keratinocyte cell surfaces in the upper epidermis but not the keratinized layer (**Fig 2*a***). By contrast, pAb against Dsc3 peptides (LNCF3) stained cell surfaces at all levels in the epidermis except the keratinized layer (**Fig 2*b***). The reactivity of the anti-Dsc2 pAb C+DGII was very weak and stained cell surfaces of the spinous layer nearly down to the basal layer in normal skin, staining in the upper layers being much stronger. All

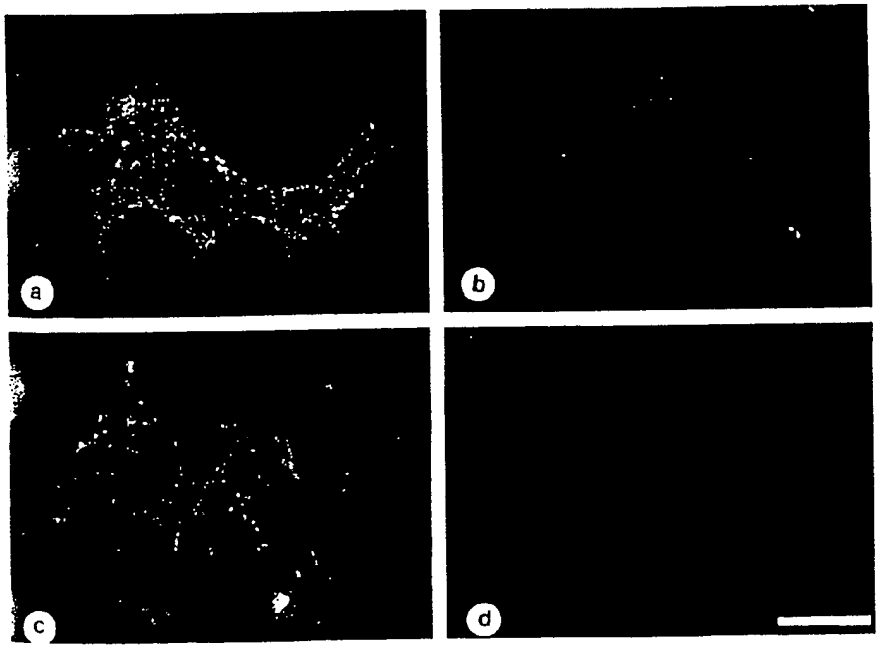

Figure 3. Immunofluorescence of COS7 cells transfected with human Dsc1, 2, or 3 indicated that the autoantigen for SPD type IgA pemphigus is Dsc1. A SPD type IgA pemphigus serum clearly stained cell surface of COS7 cells transfected with Dsc1 in a granular pattern *(a)*, whereas an IEN type IgA pemphigus serum showed no reactivity *(b)*. With double immunostaining, IgA antibodies in a SPD type of IgA pemphigus serum *(c)* and anti-Dsc1 pAb JCMC *(d)* showed exactly the same staining pattern. *Scale bar*, 30 μm.

Table I. Immunofluorescence of Various Antibodies and Sera with Normal Epidermal Sections and Dsc1-3-Transfected COS7 cells

Antibodies and Sera	(No.)	Section of Epidermis	COS7 Cells with Dsc1	Dsc2	Dsc3
mAB 52-3D		(+) all layers	+	+	+
pAb JCMC		(+) upper layers	+	−	−
pAb D1K2		(+) upper layers	+	−	−
pAb C+DGII		(+) upper-mid layers	−	+	−
pAb LNCF3		(+) all layers	−	−	+
SPD type IgA pemphigus	(6)	(+) upper layers	6	0	0
IEN type IgA pemphigus	(7)	(+) all layers	0	0	0
PV	(3)	(+) lower layers	0	0	0
PF	(3)	(+) all layers	0	0	0
Normal	(5)	(−)	0	0	0

the sera of patients with SPD-type IgA pemphigus stained the upper epidermis (Fig 2*c*), resembling the pattern for Dsc1, whereas all the sera from patients with IEN-type IgA pemphigus stained the entire epidermis (Fig 2*d*), resembling staining for Dsc3. All the IgA pemphigus sera contained autoantibodies of IgA class, but not IgG class. All the results are summarized in Table I.

Immunoblotting of Epidermal Extracts and Desmosome Preparations Showed Controversial Results We first examined the reactivity of anti-Dsc autoantibodies of the IgA class by immunoblot analyses using both normal human epidermal extracts and bovine snout desmosome preparations and then compared their reactivities with those of anti-Dsc mAb or pAbs.

With immunoblotting of bovine desmosome preparations, the anti-Dsc mAb, 52–3D, and the rabbit pAbs against Dsc1, 2, and 3 peptides reacted with two protein bands of approximately 115 kDa and 105 kDa (data not shown, but see Ebihara *et al*, 1991). The IgA antibodies in the sera of three cases with SPD type and two cases with IEN type also reacted with a doublet of proteins showing similar mobilities to those recognized by the anti-Dsc antibodies. With immunoblotting of normal human epidermal extracts, none of the IgA pemphigus sera showed specific reactivity, whereas PV and PF sera reacted with the 130-kDa Dsg3 and the 160-kDa Dsg1 polypeptides, respectively, both of which were also recognized by the 32–2B anti-Dsg mAb. The 110-kDa and 100-kDa human Dscs were recognized by the 52–3D mAb (data not shown). The normal control sera showed no specific reactivity with immunoblotting of either antigen source.

Immunofluorescence of COS7 Cells Transfected with Human Dsc1, 2, or 3 Indicated That the Autoantigen for SPD-type IgA Pemphigus Is Dsc1 When COS7 cells transiently transfected with human Dsc1, 2, and 3 cDNAs were stained without fixation, the transfected cells reacted with pAbs specific to each Dsc: i.e., Dsc1 with JCMC and D1K2 pAbs, Dsc2 with C+DGII, and Dsc3 with LNCF3. No cross-reactivity was observed (data not shown). The positive cells, approximately 10% of the population, showed clear granular staining on the cell surface. Because 52–3D mAb reacts with the cytoplasmic domain of Dscs, the cells were permeabilized by treatment with 100% methanol. This mAb reacted with COS7 cells transfected with each of the three Dscs.

The IgA antibodies in all six sera of SPD-type IgA pemphigus reacted with COS7 cells expressing Dsc1 (Fig 3*a*), but none of the seven sera of the IEN type showed this reactivity (Fig 3*b*). The IgA antibodies in both types of IgA pemphigus did not react with either Dsc2 or Dsc3. IgG antibodies in three serum samples of SPD-type IgA pemphigus were examined, but no staining was observed in the Dsc-transfected cells. Neither IgG nor IgA in any control PV, PF, or normal sera showed reactivity. All the results are summarized in Table I.

When the COS7 cells were stained simultaneously with SPD-type IgA pemphigus serum and anti-Dsc1 pAb JCMC, the cell stained with the patient's IgA were also stained with the pAb (Fig 3*c,d*). The staining intensity of both the IgA pemphigus sera and anti-Dsc1 pAb, however, was considerably reduced, suggesting that the patient's IgA reacts with a region similar to that recognized by the pAb and interferes with the reactivity of the pAb by steric hindrance.

To examine the possibility that IgA of IEN-type IgA pemphigus may react with intracytoplasmic domain of Dsc3, the cells permeabilized by 100% methanol treatment were also examined. None of the seven IEN-type IgA pemphigus sera, however, stained cell surfaces of Dsc3-transfected COS7 cells, although considerable background staining made the staining a little obscure (data not shown).

Immunoblotting of Lysates of COS7 Cells Transfected with Human Dsc1, 2, or 3 Confirmed That All the Dsc1–3 cDNA Clones Expressed Each Molecule with a Proper Size With immunoblotting of the lysate of COS7 cells transfected with human Dsc1, 2, or 3 cDNAs, proteins of approximately 100 kDa were detected by pAb specific for each Dsc. In Fig 4, *lane 1* is for standard molecular weight markers. *Lane 2* shows the lysate of Dsc1-transfected cells stained with anti-Dsc1 pAb JCMC; *lane 3* shows the lysate of Dsc2-transfected cells stained with pAb C+DGII, and *lane 4* shows the lysate of Dsc3-transfected cells stained with mAb 52–3D. The pAb LNCF3 reacted with the same protein band in the Dsc3-transfected cell lysate. No Dsc protein was detected by pAb specific to other isoforms of Dsc, confirming the specificity of each pAb. Whereas a single protein band was recognized in Dsc2- and Dsc3-transfected COS7 cells, however, a doublet of protein bands as well as lower protein bands was detected in Dsc1-transfected cells *(lane 2)*. The reason for this reactivity is not known. These protein bands could be accounted for by unprocessed precursor or breakdown product. It is not likely that these bands represent "a" and "b" forms of Dsc, because the cells were transfected with cDNA. The same proteins were also recognized by the 52–3D mAb (data not shown). The Dscs expressed in COS7 cells, however, were not detected by IgA antibodies in any IgA pemphigus sera (data not shown).

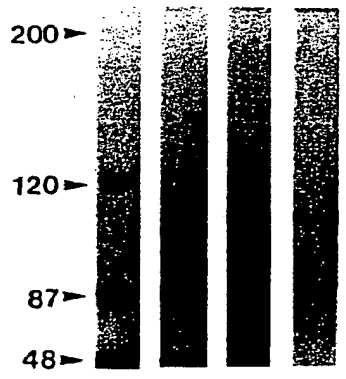

Figure 4. Immunoblotting of lysates of COS7 cells transiently transfected with human Dsc1, 2, or 3 confirmed that all the Dsc1–3 cDNA clones expressed each molecule with correct size. *Lane 1* is for standard molecular mass markers, indicating the positions of 200 kDa, 120 kDa, 87 kDa, and 48 kDa from top to bottom. *Lane 2* shows the lysate of Dsc1-transfected cells stained with anti-Dsc1 pAb JCMC; *lane 3* shows the lysate of a Dsc2-transfected cells stained with pAb C+DGII; and *lane 4* shows the lysate of a Dsc3-transfected cells stained with mAb 52–3D.

DISCUSSION

Immunofluorescence of normal human skin sections showed that IgA antibodies in sera of IEN-type IgA pemphigus bind to the keratinocyte cell surfaces at all levels in the epidermis, whereas IgA in sera of SPD-type IgA pemphigus bind only to the upper epidermis. The staining pattern of the SPD-type sera was very similar or identical to that shown by anti-Dsc1 pAbs. This suggested that sera of SPD-type IgA pemphigus might contain autoantibodies against Dsc1.

We have shown, with immunofluorescence of non-fixed COS7 cells expressing human Dsc1, 2, or 3, that all the sera of SPD-type IgA pemphigus reacted with Dsc1, but none of the sera of IEN type showed this reactivity. IgA antibodies in both types of IgA pemphigus reacted with neither Dsc2 nor Dsc3. The most likely reason, therefore, for the failure to detect human Dsc with immunoblotting of human epidermal extracts is that these epitopes on Dsc molecules may be altered by extraction, isolation, and immunoblotting procedures.

These results convincingly show that human Dsc1 is an autoantigen for SPD-type IgA pemphigus, which may therefore play an important role in the pathogenesis of this disease. This study also shows that a human Dsc can be a target antigen for an autoimmune blistering skin disease.

We initiated this study because we found that some IgA pemphigus sera react with bovine Dsc molecules in immunoblotting. It is still not clear, however, why some IgA pemphigus sera reacted with bovine, but not human, Dsc under these conditions. It may be that greater amounts of Dsc proteins were obtained in the bovine desmosome preparations than in extracts of human epidermis. Alternatively, it may be that bovine desmosomal glycoproteins retain more of their normal conformation on immunoblots because of some undefined species difference. The autoantibodies would then react with epitopes in the bovine desmosomes while similar epitopes disrupted in blotted human glycoproteins.

We anticipated that sera of IEN-type IgA pemphigus might react with Dsc3, because the staining pattern in human epidermis was similar to that of anti-Dsc3 pAb. This study does not indicate, however, that the target antigen for IEN-type IgA pemphigus is Dsc. Our previous immuno-electron microscopic study also indicated that the antigen for IEN type is not present in desmosomes (Akiyama *et al*, 1992). Therefore, it is plausible that the antigen for the IEN type is not a desmosomal protein. The results of this study reinforce the view that distinct antigen profiles are responsible for the clinico-pathologic differences between the IEN and SPD types of IgA pemphigus.

Although the target antigen of these IgA autoantibodies has been identified, their pathogenic role has not been directly confirmed. This question should now be resolved using the mouse model, as has been done for pemphigus autoantibodies. This study also shows that immunofluorescence using cells transfected with cDNA encoding possible antigen proteins is a useful method for defining antigens whose epitopes are conformation-dependent and so cannot be detected with conventional immunoblotting.

We are grateful to Dr. Roger S. Buxton and Dr. Ian A. King, Laboratory of Eukaryotic Molecular Genetics, National Institute for Medical Research, Mill Hill, London, U.K., for providing the cDNA clones of human Dsc1 and Dsc2. We also thank Tadaaki Suzuki, Kazuo Kawamura, and Susumu Tsurufuji, Institute of Cytosignal Research, Inc., Tokyo, Japan, for the cDNA clone for human Dsc3 and polyclonal antibodies to human Dsc1–3. This work was supported by Grant-in-Aid for Scientific Research from the Ministry of Education, Science and Culture of Japan (04454289), a grant from the Ministry of Health and Welfare of Japan, and a Collaboration Research Project of the British Council, Tokyo, Japan.

REFERENCES

Akiyama M, Hashimoto T, Sugiura M, Nishikawa T: Ultrastructural localization of autoantigens of intercellular IgA vesiculopustular dermatosis in cultured human squamous cell carcinoma cells. *Arch Dermatol Res* 284:371–3, 1992

Amagai M, Klaus-Kovtun V, Stanley JR: Autoantibodies against a novel epithelial cadherin in pemphigus vulgaris, a disease of cell adhesion. *Cell* 67:869–877, 1991

Amagai M, Hashimoto T, Shimizu T, Nishikawa T: Absorption of pathogenic autoantibodies by the extracellular domain of pemphigus vulgaris antigen (Dsg3) produced by baculovirus. *J Clin Invest* 94:59–67, 1994

Amagai M, Hashimoto T, Green K, Shimizu N, Nishikawa T: Antigen-specific immunoadsorption of pathogenic autoantibodies in pemphigus foliaceus. *J Invest Dermatol* 104:895–901, 1995

Amagai M: Adhesion molecules. I: Keratinocyte-keratinocyte interactions; Cadherins and pemphigus. *J Invest Dermatol* 104:146–152, 1995

Beutner EH, Jordon RE, Chorzelski TP: The immunopathology of pemphigus and bullous pemphigoid. *J Invest Dermatol* 51:63–80, 1968

Buxton RS, Cowin P, Franke WW, Garrod DR, Green KJ, King IA, Koch PJ, Magee AI, Rees DA, Stanley JR, Steinberg MS: Nomenclature of the desmosomal cadherins. *J Cell Biol* 121:481–483, 1993

Collins JE, Legan PK, Kenny TP, MacGarvie J, Holton JL, Garrod DR: Cloning and sequence analysis of desmosomal glycoproteins 2 and 3 (desmocollins): cadherin-like desmosomal adhesion molecules with heterogenous cytoplasmic domains. *J Cell Biol* 113:381–391, 1991

Ebihara T, Hashimoto T, Iwatsuki K, Takigawa M, Ando M, Ohkawara A, Nishikawa T: Autoantigens for IgA anti-intercellular antibodies of intercellular IgA vesiculopustular dermatosis. *J Invest Dermatol* 97:742–745, 1991

Emery DJ, Diaz LA, Fairley JA, Lopez A, Taylor AF, Giudice GJ: Pemphigus foliaceus and pemphigus vulgaris autoantibodies react with the extracellular domain of desmoglein-1. *J Invest Dermatol* 104:323–328, 1995

Hashimoto T, Inamoto N, Nakamura K, Nishikawa T: Intercellular IgA dermatosis with clinical features of subcorneal pustular dermatosis. *Arch Dermatol* 123:1062, 1987

Hashimoto T, Ogawa MM, Konohana A, Nishikawa T: Detection of pemphigus vulgaris and pemphigus foliaceus antigens by immunoblot analysis using different antigen sources. *J Invest Dermatol* 94:327–331, 1990

Huff JC, Golitz LE, Kunke KS: Intraepidermal neutrophilic IgA dermatosis. *N Engl J Med* 313:1643, 1985

Iwatsuki K, Hashimoto T, Ebihara T, Teraki Y, Nishikawa T, Kaneko F:Intercellular IgA vesiculo-pustular dermatosis and related disorders: diversity of IgA anti-intercellular autoantibodies. *Eur J Dermatol* 3:7–11, 1991

Kawamura K, Watanabe K, Suzuki T, Yamakawa T, Kamiyama T, Nakagawa H, Tsurufuji S: cDNA cloning and expression of novel human desmocollin. *J Biol Chem* 269:26295–26302, 1994

King IA, Arnemann J, Spurr NK, Buxton RS: Cloning of the cDNA (DSC1) coding for human type 1 desmocollin and its assignment to chromosome 18. *Genomics* 18:185–194, 1993

King IA: Identification of the ATG initiation codon in human type 1 desmocollin. *J Invest Dermatol* 102:822, 1994

Koch PJ, Walsh MJ, Schmelz M, Goldschmidt MD, Zimbelmann R, Franke WW: Identification of desmoglein, a constitutive desmosomal glycoprotein, as a member of the cadherin family of cell adhesion molecules. *Eur J Cell Biol* 53:1–12, 1990

Kowalczyk AP, Anderson JE, Borgwardt JE, Hashimoto T, Stanley JR, Green KJ: Pemphigus sera recognize conformationally sensitive epitopes in the amino-terminal region of desmoglein-1 (Dsg1). *J Invest Dermatol* 105:147–152, 1995

Laemmli UK: Cleavage of structural proteins during the assembly of the head of bacteriophage T4. *Nature* 227:680–685, 1970

Legan PK, Yue KKM, Chidgey MAJ, Holton JL, Wilkinson RW, Garrod DR: The bovine desmocollin family: a new gene and expression patterns reflecting cell proliferation and differentiation. *J Cell Biol* 126:507–518, 1994

North AJ, Chidgey MAJ, Clarke JP, Bardsley WG, Garrod DR: Distinct desmocollin isoforms occur in the same desmosomes and show reciprocally graded distributions in bovine nasal epidermis. *Proc Natl Acad Sci USA* 93:7701–7705, 1996

Parker AE, Wheeler GN, Arnemann J, Pidsley SC, Ataliotis P, Thomas CL, Rees DA, Magee AI, Buxton RS: Desmosomal glycoproteins II and III: cadherin-like junctional molecules generated by alternative splicing. *J Biol Chem* 266:10438–10445, 1992

Stanley JR, Yaar M, Hawley-Nelson P, Katz SI: Pemphigus antibodies identify a cell surface glycoprotein synthesized by human and mouse keratinocytes. *J Clin Invest* 70:281–288, 1982

Stanley JR, Koulu L, Klaus-Kovtun V, Teinberg MS: A monoclonal antibody to the desmosomal glycoprotein desmoglein I binds the same polypeptide as human autoantibodies in pemphigus foliaceus. *J Immunol* 136:1227–1230, 1986

Tagami H, Iwatsuki K, Iwase Y, Yamada M: Subcorneal pustular dermatosis with vesiculo-bullous eruption: demonstration of subcorneal IgA deposits and a leukocyte chemotactic factor. *Br J Dermatol* 109:581–587, 1983

Takabe Y, Seiki M, Fujisawa J, Hoy P, Yokota K, Arai K, Yoshida M, Arai N: SRa promoter: an efficient and versatile mammalian cDNA expression system composed of the simian virus 40 early promoter and the R-US segment of human T-cell leukemia virus type 1 long terminal repeat. *Mol Cell Biol* 8:466–472, 1988

Teraki Y, Amagai M, Hashimoto T, Kusunoki T, Nishikawa T: Intercellular IgA dermatosis of childhood. selective deposition of monomer IgA1 in the intercellular space of the epidermis. *Arch Dermatol* 127:221–224, 1991

Theis DG, Koch PJ, Franke WW: Differential synthesis of type 1 and type 2 desmocollin mRNA in human stratified epithelia. *Int J Dev Biol* 37:101–110, 1993

Troyanovsky SM, Eshkind LG, Troyanovsky RB, Leube RE, Franke WW: Contributions of cytoplasmic domains of desmosomal cadherins to desmosome assembly and intermediate filament anchorage. *Cell* 72:561–574, 1993

Vilela MJ, Parrish EP, Wright DH, Garrod DR: Monoclonal antibody to desmosomal glycoprotein 1—A new epithelial marker for diagnostic pathology. *J Pathol* 153:365–375, 1987

Yue KKM, Holton JL, Clarke JP, Hyam JLM, Hashimoto T, Chidgey MAJ, Garrod DR: Characterization of a desmocollin isoform (bovine Dsc3) exclusively expressed in lower layers of stratified epithelia. *J Cell Sci* 108:2163–2173, 1995

Brief Definitive Report

The Synaptic Vesicle-associated Protein Amphiphysin Is the 128-kD Autoantigen of Stiff-Man Syndrome with Breast Cancer

By Pietro De Camilli,*‡ Annette Thomas,*‡ Roxanne Cofiell,*‡ Franco Folli,* Beate Lichte,§ Giovanni Piccolo,‖ Hans-Michael Meinck,¶ Mario Austoni,** Giuliano Fassetta,‡‡ Gianfranco Bottazzo,§§ David Bates,‖‖ Niall Cartlidge,‖‖ Michele Solimena,*‡ and Manfred W. Kilimann§

*From the *Department of Cell Biology and ‡Howard Hughes Medical Institute, Yale University School of Medicine, New Haven, Connecticut 06510; the §Institüt für Physiologische Chemie, D-W-4630 Bochum 1, Germany; the **Istituto Neurologico Mondino, Universita' di Pavia, 27100 Pavia, Italy; the ¶Neurologische Klinik, University of Heidelberg, D44780 Heidelberg, Germany; the **Istituto di Semeiotica Medica, University of Padova, 35100 Padova, Italy; the ‡‡Divisione Neurologica, Ospedale di Belluno, 32100 Belluno, Italy; the §§Department of Immunology, London Hospital Medical College, London E1, 2AD, United Kingdom; and the ‖‖Department of Neurology, Royal Victoria Infirmary, Newcastle upon Tyne NE1, 4LP, United Kingdom*

Summary

Stiff-Man syndrome (SMS) is a rare disease of the central nervous system (CNS) characterized by progressive rigidity of the body musculature with superimposed painful spasms. An autoimmune origin of the disease has been proposed. In a caseload of more than 100 SMS patients, 60% were found positive for autoantibodies directed against the GABA-synthesizing enzyme glutamic acid decarboxylase (GAD). Few patients, all women affected by breast cancer, were negative for GAD autoantibodies but positive for autoantibodies directed against a 128-kD synaptic protein. We report here that this antigen is amphiphysin. GAD and amphiphysin are nonintrinsic membrane proteins that are concentrated in nerve terminals, where a pool of both proteins is associated with the cytoplasmic surface of synaptic vesicles. GAD and amphiphysin are the only two known targets of CNS autoimmunity with this distribution. This finding suggests a possible link between autoimmunity directed against cytoplasmic proteins associated with synaptic vesicles and SMS.

Stiff-Man syndrome (SMS) is a rare human central nervous system (CNS) disease, characterized by chronic rigidity of the body musculature with superimposed painful spasms (1). It is thought to result from an impairment of inhibitory pathways that control motor neuron activity (2–4). It was previously suggested that SMS may have an autoimmune pathogenesis. 60% of the patients affected by this condition are positive in their serum and cerebrospinal fluid (CSF) for autoantibodies directed against the GABA-synthesizing enzyme glutamic acid decarboxylase (GAD) (5–8). In our current caseload of 119 patients referred to us with a clinical diagnosis of SMS, 72 were found positive for these autoantibodies (Guarnaccia, J., M. Solimena, K. Marek, and P. De Camilli, unpublished observations). In the SMS patient subpopulation positive for GAD autoantibodies, a frequent occurrence of insulin-dependent diabetes mellitus and of other organ-specific autoimmune diseases is observed (6, 7).

We have recently described three female patients with SMS and breast cancer and no signs of organ-specific autoimmune diseases. These three patients (referred to henceforth as patients BC-SMS 1, 2, and 3, respectively) were negative for GAD autoantibodies but were positive for autoantibodies directed against a 128-kD neuronal antigen concentrated at synapses (9). We have now identified a fourth patient with both breast cancer and SMS syndrome. This patient (BC-SMS 4), as well, was positive for autoantibodies to the 128-kD protein (this study). The characterization of this autoantigen is crucial to the elucidation of pathogenetic mechanisms in SMS with breast cancer.

Recently, a novel synaptic vesicle-associated protein, amphiphysin, was described (10). This protein was identified by screening a chicken brain λgt11 library with antibodies raised against chicken brain synaptic proteins. Amphiphysin, an acidic protein present in chicken as well as in mammalian nervous tissue, was shown by immunocytochemistry to be concentrated in nerve terminals. A large fraction of am-

 J. Exp. Med. The Rockefeller University Press • 0022-1007/93/12/2219/05 $2.00
Volume 178 December 1993 2219–2223

phiphysin is present in cytosolic fractions of brain homogenates but a pool of the protein is recovered in a tightly bound form in highly purified synaptic vesicles, although the protein is not enriched on these organelles (10). Some of the properties of amphiphysin were reminiscent of the properties of the 128-kD antigen (10). Therefore, a detailed comparison of the characteristics of the two proteins was performed. We report here that the 128-kD antigen is amphiphysin.

Materials and Methods

Materials. Three sera of SMS patients affected by breast cancer were previously described (9). These sera, defined BC-SMS 1, 2, and 3, correspond to sera of patients 1, 2, and 3, respectively, of reference 9. Serum BC-SMS 4 is from a new patient with both conditions. A GAD autoantibody-positive human serum is from our caseload of SMS sera (6, 8). Rabbit polyclonal antibodies directed against a β-galactosidase chicken amphiphysin fusion protein were previously described (10). These antibodies were shown to recognize rat amphiphysin (10). Rabbit sera directed against synaptophysin (11) and GAD (serum no. 6799 (12)) were the kind gift of Dr. R. Jahn (Yale University, New Haven, CT), and Drs. Z. Katarova and G. Szabo (Hungarian Academy of Sciences, Szeged, Hungary), respectively. Small-scale lysates of bacteria expressing β-galactosidase fusion proteins were prepared according to reference 13. βTC3 and αTC9 cell lines were the kind gift of Drs. D. Hanahan (University of California, San Francisco, CA), S. Efrat (Albert Einstein College of Medicine, New York, New York), and E. Leiter (Jackson Laboratories, Bar Harbor, ME), and PC12 cells were the gift of Dr. L. Greene (Columbia University, New York).

Western Blotting of One- and Two-dimensional Gels. Total rat brain homogenate was prepared as described (6, 14). Postnuclear supernatants of rat tissues and of cell lines were prepared by homogenization in 10 vol of ice-cold 10 mM Hepes buffer, pH 7.4, containing freshly added protease inhibitors (0.1 mM PMSF, 1 μg/ml each of antipain, leupeptin, aprotinin, and pepstatin A) followed by centrifugation at 1,000 *g* for 10 min at 4°C. For two-dimensional gels, this supernatant (S1) was centrifuged at 170,000 *g* for 2 h at 4°C and the resulting supernatant was analyzed by the procedure described by O'Farrell et al. (15) and modified by Ames and Nikaico (16). Western blotting was performed as described (6, 14) using ^{125}I–protein A. Patient sera were used at the dilution of 1:250.

Cell Fractionation and Triton X-114 Phase Separation. A postnuclear supernatant of rat brain (S1) was prepared as described above. S1 was centrifuged at 36,000 *g* for 30 min at 4°C. The resulting supernatant (S2) was separated into particulate (P3) and cytosolic (S3) fractions by centrifugation at 170,000 *g* for 2 h at 4°C. P3 and S3 were extracted in 2% Triton X-114, and insoluble material was removed by centrifugation at 20,000 *g* for 30 min at 4°C. The soluble material was separated into detergent (D) and aqueous (A) phases as described (17). Volumes loaded in each lane were normalized so that corresponding aliquots of supernatants and pellets (or detergent and aqueous phases) were loaded for each pair of fractions.

Immunoprecipitation. A soluble fraction of rat brain (S3) prepared as described above was extracted in ice-cold 2% Triton X-100, 150 mM NaCl, 10 mM Hepes, pH 7.4, for 2 h. Insoluble material was removed by centrifugation at 20,000 *g* for 30 min at 4°C. The resulting supernatant was diluted with an equal volume of 150 mM NaCl, 10 mM Hepes, pH 7.4 (buffer A), to a final protein concentration of 1 mg/ml. 900-μl aliquots of extract were precleared as described (5) and used for each immunoprecipitation. For immunoprecipitation, the following additions were made in sequential order: (*a*) 25 μl human sera (16 h); (*b*) 20 μl rabbit anti-human IgGs (1.5 h); and (*c*) 125 μl 50% protein A-Sepharose in buffer A (1.5 h). All incubations were performed at 4°C with rotation. Immunoprecipitated material was recovered and analyzed by Western blotting as described (14).

Results and Discussion

Fig. 1 shows Western blots of total rat brain homogenate demonstrating that the 128-kD antigen, i.e., the protein recognized by the sera of BC-SMS patient (lanes *1–3*), has the same electrophoretic mobility in SDS-PAGE as the protein recognized by rabbit serum (lane *4*) and affinity-purified antibodies (lane *5*) raised against a chicken amphiphysin fusion protein. Chicken amphiphysin was calculated to have a molecular mass of 75,204 daltons, but in SDS-PAGE runs, it had an apparent molecular mass of 115–125 kD (10). This molecular mass is very similar to the one of 128 kD estimated here for the rat protein. Fig. 2 shows that the 128-kD antigen and amphiphysin have an identical isoelectric point of 4.7 in two-dimensional gels. This isoelectric point is similar to the predicted isoelectric point of 4.4, calculated on the basis of the amino acid composition of chicken amphiphysin (10).

The distribution of the 128-kD antigen and of amphiphysin were compared in the course of subcellular fractionation of brain homogenates. As shown in Fig. 3, *a* and *b*, both the autoantigen and amphiphysin were present in roughly equal amounts in a cytosolic fraction (S3) and in a particulate fraction (P3) obtained from rat brain. Synaptophysin, an intrinsic membrane protein of synaptic vesicles, was present exclusively in the particulate fraction (P3) (Fig. 3 *c*), demonstrating that the centrifugation conditions used were sufficient to sediment all membranes. Membrane-bound amphiphysin was previously shown to be recovered in the aqueous phase after Triton X-114 extraction and phase separation (10). As shown in Fig. 3, *a* and *b*, both the 128-kD antigen and amphiphysin were completely solubilized by Triton X-114 and were recovered exclusively in the aqueous phase irrespectively of whether the extraction was performed on P3 or S3 (Fig. 3, *a* and *b*). The effectiveness of phase separation conditions was confirmed by the presence of the bulk of synaptophysin (a protein with

Figure 1. The 128-kD antigen and amphiphysin have identical electrophoretic mobilities in SDS gels. Western blots of total rat brain homogenate probed with sera of three BC-SMS patients and rabbit antiamphiphysin antibodies (lane *4*, crude serum [*Amph-S*]; lane *5*, affinity-purified antibodies [*Amph-AP*]). The 128-kD antigen is indicated by an arrow. The single band of amphiphysin and of the 128-kD antigen visible in this gel can be resolved in a doublet of two closely spaced bands under different electrophoresis conditions (9, 10).

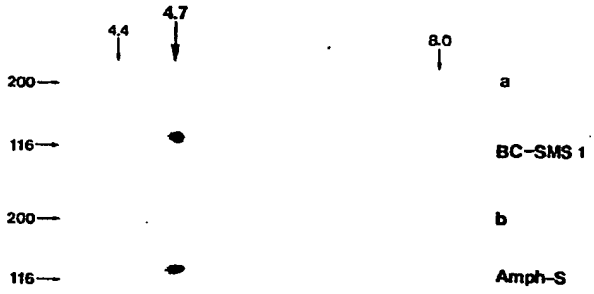

Figure 2. The 128-kD antigen and amphiphysin have identical electrophoretic mobilities in two-dimensional gels. Western blot of two-dimensional gels of a soluble rat brain fraction probed with BC-SMS 1 serum (*a*) and rabbit antiamphiphysin serum (*b*). Numbers at the top indicate isoelectric points, numbers at the left indicate molecular mass markers (in kD).

four transmembrane regions (18)) in the detergent phase obtained from P3 (Fig. 3 *c*).

The 128-kD antigen and amphiphysin were found to be immunologically cross-reactive. To prove that antiamphiphysin antibodies recognize the 128-kD antigen, BC-SMS patient sera were used to immunoprecipitate the 128-kD antigen from soluble extracts of rat brain. The presence of amphiphysin in the immunoprecipitate was then analyzed by Western blotting using antiamphiphysin serum. An immunoreactive band with electrophoretic mobility of 128 kD was detected (Fig. 4 *a*, lanes *1–3*) while no GAD was recovered in the same immunoprecipitates (Fig. 4 *b*, lanes *1–3*) confirming previous

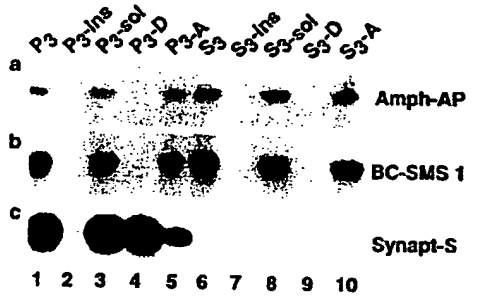

Figure 3. The 128-kD antigen and amphiphysin partition similarly in differential centrifugation and Triton X-114 phase separation. Particulate (P_3) and cytosolic (S_3) fractions of rat brain were extracted in Triton X-114 and centrifuged to obtain a soluble (*sol*) and an insoluble (*ins*) fraction. The Triton X-114–soluble material (lanes *3* and *8*) was separated into detergent (*D*; lanes *4* and *9*) and aqueous (*A*; lanes *5* and *10*) phases. The fractions were probed by immunoblotting with antiamphiphysin affinity-purified antibodies (*Amph-AP*), with BC-SMS 1 serum (*BC-SMS 1*), and with antisynaptophysin serum (*Synapt-S*). The 128-kD antigen and amphiphysin were recovered in both the cytosolic (S3) and in the particulate (P3) fractions, and exclusively in the Triton X-114 aqueous phase derived from these fractions. Synaptophysin, which is an integral membrane protein with four transmembrane spanning domains, is recovered only in P3 and primarily in the detergent phase derived from the Triton X-114–soluble material obtained from P3.

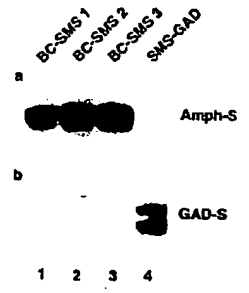

Figure 4. BC-SMS patient sera immunoprecipitate amphiphysin from rat brain extracts. Immunoprecipitates obtained with the sera of three BC-SMS patients (lanes *1–3*) and with the serum of a SMS patient positive for GAD autoantibodies (*SMS-GAD*) (lane *4*) were separated by SDS-PAGE. (*a*) Immunoblotted with rabbit antiamphiphysin serum (*Amph-S*); and (*b*) immunoblotted with the rabbit anti-GAD serum no. 6799 (*GAD-S*) (12).

results (9). As a control, immunoprecipitation was performed with a SMS patient serum that contained high-titer anti-GAD antibodies (6, 8), but no antibodies against the 128-kD autoantigen. This immunoprecipitate was positive for GAD (Fig. 4 *b*, lane *4*), but not for amphiphysin (Fig. 4 *a*, lane *4*). Conversely, a protein of 128 kD was detected when an immunoprecipitate obtained with antiamphiphysin serum was immunoblotted with BC-SMS patient sera (not shown). To

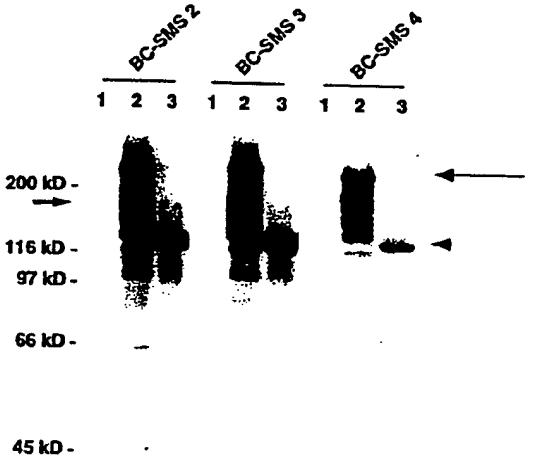

Figure 5. BC-SMS patient sera recognize recombinant amphiphysin. Western blots of three identical gel triplets reacted with sera BC-SMS 2, 3, and 4, as indicated. Lanes *1*, bacterial lysate expressing a 165-kD fusion protein of β-galactosidase with a yet unidentified synaptic protein (clone 10.12.1; B. Lichte, and M.W. Kilimann, unpublished observation). Lanes *2*, bacterial lysate expressing a β-galactosidase–chicken amphiphysin fusion protein (clone amphy-11.3; fusion protein size ~230 kD) (10). Lanes *3*, chicken brain total homogenate. Identical results were obtained with serum BC-SMS 1 (not shown). Long and short arrows indicate the mobilities of the chicken amphiphysin fusion protein and of the control fusion protein, respectively. Bands below the major immunopositive bands of lanes *2* most likely represent proteolytic fragments of the fusion protein. An arrowhead points to chicken brain amphiphysin.

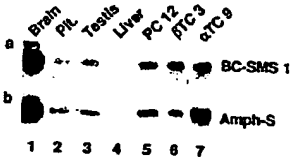

Figure 6. The 128-kD antigen and amphiphysin have the same tissue distribution. Western blot of postnuclear supernatants of rat tissues (brain, pituitary, testis, liver) and endocrine cell lines (PC12 cells [rat chromaffin cell line]; βTC3 cells [mouse insulinoma]; αTC9 [mouse glucagonoma]) probed with either BC-SMS patient serum (*BC-SMS 1*) or antiamphiphysin serum (*Amph-S*).

conclusively demonstrate that BC-SMS sera recognize amphiphysin, they were tested against bacterial lysates containing recombinant amphiphysin as shown in Fig. 5. BC-SMS sera labeled a β-galactosidase–chicken amphiphysin fusion protein (Fig. 5, lanes *2*) and chicken brain amphiphysin (Fig. 5, lanes *3*), but not a control fusion protein (Fig. 5, lanes *1*).

Amphiphysin was previously shown to have a restricted tissue distribution (10). Amphiphysin mRNA was detected at high levels in brain and at lower levels in adrenal gland. By immunoblotting amphiphysin was detected in the anterior and posterior pituitary as well (10). The expression of amphiphysin was compared with that of the 128-kD antigen in a variety of tissues and cell lines using Western blotting. Fig. 6 shows that the serum of a BC-SMS patient and the rabbit serum directed against amphiphysin label a similar protein in brain, pituitary, and cell lines derived from adrenal chromaffin cells (PC12 cells) and from pancreatic α and β cells (αTC9, βTC3) (19, 20) but not in liver. Presence of amphiphysin in all cells of pancreatic islets was confirmed by immunocytochemistry (not shown). Endocrine cells of the anterior pituitary, adrenal medulla, and pancreatic islets have many biochemical and functional similarities to neurons and contain organelles closely related to neuronal synaptic vesicles (21, 22). In addition, both amphiphysin and the 128-kD antigen were detected in the testis (Fig. 6). By immunocytochemistry with BC-SMS sera, amphiphysin immunoreactivity in the testis was found to be confined to germ cells. All germ cells expressed amphiphysin irrespective of their stage of differentiation (from spermatogonia to mature spermatozoa) (not shown). Previously, amphiphysin mRNA could not be detected in chicken testis (10), but this was probably so because the RNA had been purified from immature testis of 7-d-old animals. It should be noted that GAD as well is expressed in male germ cells (23).

These data convincingly demonstrate that the 128-kD antigen is amphiphysin. Amphiphysin contains in its sequence a hydrophobic 21–amino acid region that would be competent to form a transmembrane helix (10). However, the recovery of amphiphysin both in soluble and membrane fractions (10) as well as the presence of a pool of the protein detectable by immunocytochemistry throughout the neuronal cytoplasm (9) indicate that amphiphysin is not an intrinsic membrane protein. Like amphiphysin, GAD, the other major autoantigen of SMS, is concentrated in nerve terminals where it interacts with synaptic vesicles but is not an intrinsic membrane protein (14, 24–26). While GAD is expressed only by GABA-secreting neurons, amphiphysin is not restricted to these neurons (9, 10).

The similar subcellular localization of GAD and amphiphysin is intriguing if one considers that they are the only two known targets of CNS autoimmunity with this distribution. This observation raises the possibility that pathogenetic mechanisms in SMS may be linked to CNS autoimmunity directed against presynaptic components that interact with synaptic vesicles. Autoantibodies directed against GAD and amphiphysin are not likely to be directly pathogenetic because antibodies are not thought to have access to the cytoplasmic compartment. They may represent the dominant autoantibody species in the context of an autoimmune response directed against multiple antigens (27), including proteins exposed at the cell surface that may be the pathogenetic targets of the autoimmune response. Alternatively, these autoantibodies may reflect an autoimmune reaction in which T cells are the primary players. GAD and amphiphysin autoantibodies segregate with two SMS patient subpopulations, each characterized by different associated diseases. GAD autoantibody–positive SMS is often associated with organ-specific autoimmune diseases and primarily insulin-dependent diabetes mellitus (3–7). Amphiphysin autoantibody–positive SMS occurs only in association with cancer (9) and has the characteristics of an autoimmune paraneoplastic syndrome (28, 29). Therefore, the two patterns of autoimmunity are likely to be related to these different associated conditions. Further studies of antiamphiphysin autoimmunity and of the function of amphiphysin or amphiphysin-related molecules not only may shed some light on pathogenetic mechanisms in SMS, but may also help in the elucidation of the biology of at least some types of cancer. Although amphiphysin was not detected in breast cancer tissue (9), it will be of interest to determine whether amphiphysin-related proteins are expressed in breast cancer.

We thank Drs. J. Guarnaccia and K. Marek (New Haven, CT) for reviewing our case load of SMS patients; Drs. D. Hanahan (San Francisco, CA), S. Efrat (New York, NY), E. Leiter (Bar Harbor, ME), L. Greene (New York, NY), Z. Katarova, and G. Szabo (Szeged, Hungary) for the gift of cell lines and antibodies; and Dr. C. David (New Haven, CT) for critical reading of the manuscript.

This work was supported by grants from the National Institutes of Health and by a McKnight Research Project Award (P. De Camilli) and by the Fonds der Chemischen Industrie (M. W. Kilimann). F. Folli was supported by a Dottorato di Ricerca (University of Milano), M. Solimena by the Sydney Blackmer

Muscular Dystrophy Association fellowship and by a fellowship from the Juvenile Diabetes Foundation, and A. Thomas by a predoctoral National Institute for Mental Health fellowship. M. W. Kilimann is a Heisenberg Fellow of the Deutsche Forschungsgemeinschaft.

Address correspondence to Pietro De Camilli, Howard Hughes Medical Istitute, Department of Cell Biology, Boyer Center for Molecular Medicine, 295 Congress Avenue, New Haven, CT 06536-0812. F. Folli's permanent address is the Department of Medicine, Istituto Scientifico S. Raffaele, Via Olgettina 60, 20100 Milano, Italy, and his present address is the Joslin Diabetes Center, Harvard Medical School, 1 Joslin Place, Boston, MA 02215. B. Lichte's present address is the Institut für Biologie III, Universitat Freiburg, D-W-7800, Freiburg, Germany.

Received for publication 8 June 1993 and in revised form 4 August 1993.

References

1. Moersch, F.P., and H.W. Woltman. 1956. Progressive fluctuating muscular rigidity and spasm ("stiff-man" syndrome): report of a case and some observations in 13 other cases. *Mayo Clin. Proc.* 31:421.
2. Gordon, E.E., D.M. Januszko, and L. Kaufman. 1967. A critical survey of Stiff-man syndrome. *Am. J. Med.* 42:582.
3. McEvoy, K.M. Stiff-man syndrome. 1991. *Mayo Clin. Proc.* 66:300.
4. Blum, P., and J. Jankovic. 1991. Stiff-person syndrome: an autoimmune disease. *Movement Dis.* 6:12.
5. Solimena, M., F. Folli, S. Denis-Donini, G.C. Comi, G. Pozza, P. De Camilli, and A.M. Vicari. 1988. Autoantibodies to glutamic acid decarboxylase in a patient with Stiff-man syndrome, epilepsy, and type I diabetes mellitus. *N. Engl. J. Med.* 318:1012.
6. Solimena, M., F. Folli, R. Aparisi, G. Pozza, and P. De Camilli. 1990. Autoantibodies to GABA-ergic neurons and pancreatic beta-cells in Stiff-man syndrome. *N. Engl. J. Med.* 322:1555.
7. Solimena, M., and P. De Camilli. 1991. Autoimmunity to glutamic acid decarboxylase (GAD) in stiff-man syndrome and insulin-dependent diabetes mellitus. *Trends Neurosci.* 14:452.
8. Butler, M., M. Solimena, R. Dirkx, A. Hayday, and P. De Camilli. 1993. Identification of a dominant epitope of glutamic acid decarboxylase (GAD-65) recognized by autoantibodies in Stiff-Man syndrome. *J. Exp. Med.* 178:2097.
9. Folli, F., M. Solimena, R. Cofiell, M. Austoni, G. Tallini, G. Fassetta, D. Bates, N. Cartlidge, G.F. Bottazzo, G. Piccolo, and P. De Camilli. 1993. Autoantibodies to a 128kD synaptic protein in three women with the Stiff-man syndrome and breast cancer. *N. Engl. J. Med.* 328:546.
10. Lichte, B., R.W. Veh, H.E. Meyer, and M.W. Kilimann. 1992. Amphiphysin, a novel protein associated with synaptic vesicles. *EMBO (Eur. Mol. Biol. Organ.) J.* 11:2521.
11. Navone, F., R. Jahn, G. Di Gioia, H. Stukenbrok, P. Greengard, and P. De Camilli. 1986. Protein p38: an integral membrane protein specific for small vesicles of neurons and neuroendocrine cells. *J. Cell Biol.* 103:2511.
12. Katarova, Z., G. Szabo, E. Mugnaini, and R.J. Greenspan. 1989. Molecular identification of the 62 kD form of glutamic acid decarboxylase from the mouse. *Eur. J. Neurosci.* 2:190.
13. Carroll, S.B., and A. Laughon. 1987. DNA Cloning. Vol. III. D.M. Glover, editor. IRL Press Ltd., Eynsham, UK. 89–111.
14. Reetz, A., M. Solimena, M. Matteoli, F. Folli, K. Takei, and P. De Camilli. 1991. GABA and pancreatic β-cells: colocalization of glutamic acid decarboxylase (GAD) and GABA with synaptic-like microvesicles suggests their role in GABA storage and secretion. *EMBO (Eur. Mol. Biol. Organ.) J.* 10:1275.
15. O'Farrell, P.A., H. Goodman, and P.H. O'Farrell. 1977. Resolution of two dimensional electrophoresis of basic, as well as, acidic proteins. *Cell.* 12:1133.
16. Ames, B.F., and K. Nikaico. 1976. Two-dimensional gel electrophoresis of membrane proteins. *Biochemistry.* 15:616.
17. Bordier, C. 1981. Phase separation of integral membrane proteins in Triton X-114 solution. *J. Biol. Chem.* 256:1604.
18. Sudhof, T.C., F. Lottspeich, P. Greengard, E. Mehl, and R. Jahn. 1987. A synaptic vesicle protein with a novel cytoplasm domain and four transmembrane regions. *Science (Wash. DC).* 238:1142.
19. Efrat, S., S. Linde, H. Kofod, D. Spector, M. Delannoy, S. Grant, D. Hanahan, and S. Baekkeskov. 1988. Beta-cells derived from transgenic mice expressing a hybrid insulin gene-oncogene. *Proc. Natl. Acad. Sci. USA.* 85:9037.
20. Hamaguchi, K., and R.H. Leiter. 1990. Comparison of cytokine effects on mouse alpha-cell and beta-cell lines. *Diabetes.* 39:415.
21. De Camilli, P., and R. Jahn. 1990. Pathways to regulated exocytosis in neurons. *Annu. Rev. Physiol.* 52:625.
22. De Camilli, P. 1991. Co-secretion of multiple signal molecules from endocrine cells via distinct exocytotic pathways. *Trends Pharmacol. Sci.* 12:446.
23. Persson, H., M. Pelto-Huikko, and M. Metsis. 1990. Expression of the neurotransmitter synthesizing enzyme glutamic acid decarboxylase in male germ cells. *Mol. Cell. Biol.* 10:4701.
24. Erlander, M.G., N.J.K. Tillakaratne, S. Feldblum, N. Patel, and A.J. Tobin. 1991. Two genes encode distinct glutamate decarboxylases. *Neuron.* 7:91.
25. Christgau, S., H.-J. Aanstoot, H. Schierbeck, K. Begley, S. Tulin, K. Hejnaes, and S. Baekkeskov. 1992. Membrane anchoring of the autoantigen GAD 65 to microvesicles in pancreatic beta-cells by palmitoylation in the NH_2-terminal domain. *J. Cell Biol.* 118:309.
26. Solimena, M., D. Aggujaro, C. Muntzel, R. Dirkx, M. Butler, P. De Camilli, and A. Hayday. 1993. Association of GAD-65, but not of GAD-67, with the Golgi complex of transfected Chinese hamster ovary cells mediated by the N-terminal region. *Proc. Natl. Acad. Sci. USA.* 90:3073.
27. Tan, E. M. 1991. Autoantibodies in pathology and cell biology. *Cell.* 67:841.
28. Posner, J.B., and H.M. Furneaux. 1990. Paraneoplastic syndromes. *In* Immunologic Mechanisms in Neurologic and Psychiatric Disease. Research Publications: Association for Research in Nervous and Mental Disease. Vol. 68. B.H. Waksman, editor. Raven Press, Ltd., New York. 187–219.
29. Hetzel, D.J., C.R. Stanhope, O'Neill, and V.A. Lennon. 1990. Gynecologic cancer in patients with subacute cerebellar degeneration predicted by anti-Purkinje cell antibodies and limited in metastatic volume. *Mayo Clin. Proc.* 65:1558.

Autoantibodies to Glutamate Receptor GluR3 in Rasmussen's Encephalitis

Scott W. Rogers,* P. Ian Andrews, Lorise C. Gahring, Teri Whisenand, Keith Cauley, Barbara Crain, Thomas E. Hughes, Stephen F. Heinemann, James O. McNamara

Rasmussen's encephalitis is a progressive childhood disease of unknown cause characterized by severe epilepsy, hemiplegia, dementia, and inflammation of the brain. During efforts to raise antibodies to recombinant glutamate receptors (GluRs), behaviors typical of seizures and histopathologic features mimicking Rasmussen's encephalitis were found in two rabbits immunized with GluR3 protein. A correlation was found between the presence of Rasmussen's encephalitis and serum antibodies to GluR3 detected by protein immunoblot analysis and by immunoreactivity to transfected cells expressing GluR3. Repeated plasma exchanges in one seriously ill child transiently reduced serum titers of GluR3 antibodies, decreased seizure frequency, and improved neurologic function. Thus, GluR3 is an autoantigen in Rasmussen's encephalitis, and an autoimmune process may underlie this disease.

Rasmussen's encephalitis is a rare, progressive, catastrophic disease of unknown pathogenesis that begins in the first decade of life, affecting previously normal children (*1*). The disease affects the cortex of a single cerebral hemisphere, resulting in intractable seizures, hemiparesis, and dementia. The diagnosis is established by these typical clinical features, together with hemispheric atrophy and a characteristic inflammatory histopathology (*1*, *2*). Treatment of the incapacitating seizures with conventional anticonvulsants is of limited benefit. Surgical removal of the affected hemisphere is the standard therapy. Glutamate and related amino acids are the predominant excitatory neurotransmitters in the mammalian central nervous system (CNS) (*3*) and have been implicated in neurodegenerative diseases and epilepsy. To generate subtype-specific antibodies to recombinant GluR proteins, we immunized rabbits with bacterially expressed *trpE* gene fusion proteins that included a portion of the putative extracellular domain of GluR1, 2, 3, 5, or 6 or the putative cytoplasmic domain of subunits (β4) of the neuronal nicotinic acetylcholine receptor (nAChR) family (*4*).

After four immunizations with GluR3 fusion protein, two rabbits developed high titers of GluR3 antibodies, anorexia, and behaviors characteristic of seizures, consisting of brief periods of immobilization, unresponsiveness, and repetitive clonic movements. One rabbit had severely lacerated its tongue, suggestive of tongue biting during a seizure. By contrast, no behavioral abnormalities were seen in another rabbit immunized with GluR3 fusion protein or in any of more than 50 rabbits injected with fusion proteins containing GluR1, 2, 5, or 6 or neuronal nAChR subunits, although high titers of the appropriate antibodies were observed (*4*). Gross examination of the brains of the symptomatic, GluR3-immunized rabbits disclosed no abnormality. However, microscopic examination disclosed inflammatory changes consisting of microglial nodules and perivascular lymphocytic infiltration mainly, but not exclusively, in the cerebral cortex, together with lymphocytic infiltration of the meninges (Fig. 1). Microscopic examination of the brain of the asymptomatic rabbit immunized with GluR3 fusion protein disclosed no abnormality. We reasoned that the rabbits' symptoms and inflammatory CNS histopathology probably represented an autoimmune process directed against GluR3, on the basis of the immunization history, the occurrence of symptoms only in GluR3-immunized rabbits, and the similar distribution of inflammatory pathology in these animals and GluR3 mRNA in normal animals (*5*). The occurrence of disease in some, but not all, GluR3-immunized rabbits is similar to the incidence of autoimmune myasthenia gravis in mice immunized with nAChR (*6*).

These symptomatic rabbits resembled individuals with Rasmussen's encephalitis. Common features include (i) recurrent seizures (*1*); (ii) inflammatory histopathology, characterized by meningeal and perivascular lymphocytic infiltrates and microglial nodules (Fig. 1) (*2*); and (iii) predominant

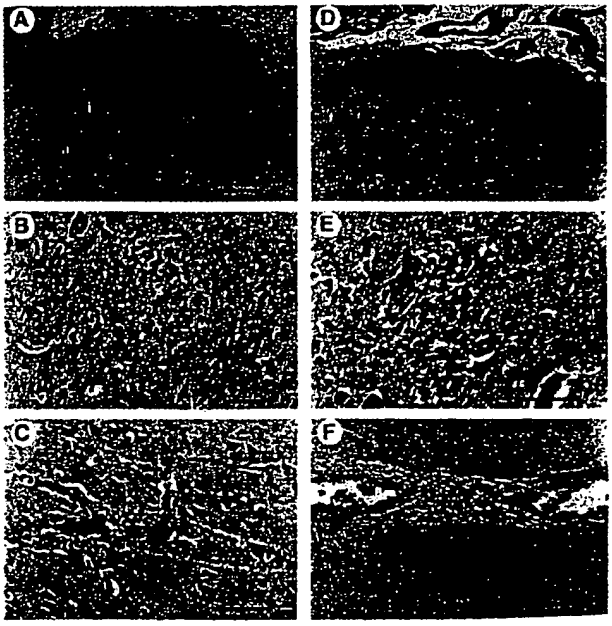

Fig. 1. Characteristic histopathology of neocortex of one symptomatic rabbit immunized with GluR3 (**A** through **C**) and comparable sections from resected temporal lobe of individual AI (**D** through **F**). (A) and (D) Neocortex with meningeal lymphocytic infiltrate (arrow) and a microglial nodule (double arrow). Bars are 200 μm. (B) and (E) Microglial nodules from (A) and (D). Bars are 50 μm. (C) and (F) Perivascular lymphocytic cuffing from entorhinal cortex in the rabbit and amygdala in individual AI. Bars are 100 μm.

S. W. Rogers, Salt Lake City Geriatric Research, Education, and Clinical Center, Veterans Affairs Medical Center; Human Molecular Biology and Genetics Program; and Department of Neurobiology and Anatomy; University of Utah, Salt Lake City, UT 84112, USA.
P. I. Andrews, Departments of Pediatrics and Medicine (Neurology), Duke University Medical Center, Durham, NC 27710, USA.
L. C. Gahring, Salt Lake City Geriatric Research, Education, and Clinical Center, Veterans Affairs Medical Center; Human Molecular Biology and Genetics Program; and Division of Human Development and Aging; University of Utah, Salt Lake City, UT 84112, USA.
K. Cauley and S. F. Heinemann, Salk Institute, La Jolla, CA 92307, USA.
B. Crain, Departments of Neurobiology and Medicine (Neurology), Duke University Medical Center, Durham, NC 27710, USA.
T. E. Hughes, Department of Ophthalmology, Yale University, New Haven, CT 06510, USA.
J. O. McNamara, Departments of Neurobiology, Medicine (Neurology), and Pharmacology, Duke University Medical Center, Durham, NC 27710, USA, and Department of Medicine (Neurology), Veterans Affairs Medical Center, Durham, NC 27705, USA.
*To whom correspondence should be addressed.

localization of this inflammatory process in the cerebral cortex with relative sparing of the basal ganglia, thalamus, deep white matter, brainstem, and cerebellum (2). We therefore hypothesized that Rasmussen's encephalitis is due to an autoimmune process directed at GluR3 protein.

To test this idea, we measured immunoreactivity toward GluR3 and other neural receptors in sera from four individuals with pathologically confirmed Rasmussen's encephalitis, four age- and sex-matched epileptic children, four age- and sex-matched children without CNS disease, five children with active CNS inflammation, four other epileptic children, and four other normal children. Protein immunoblot analysis was performed with *trpE* fusion proteins containing corresponding regions of the putative extracellular domains of GluR1, 2, 3, and 5 (Fig. 2 and Table 1) and a portion of the putative intracellular domain of nAChR subunit β4 (*4*, *7*, *8*); blots were interpreted by observers unaware of the sources of the sera. Immunoreactivity to GluR3 fusion protein was detected in multiple sera samples from two individuals with Rasmussen's encephalitis [CK in (*9*); AI in Fig. 2]. CK also exhibited weak immunoreactivity to GluR2 fusion protein. Serum from a third individual with Rasmussen's encephalitis (EM) exhibited weak immunoreactivity to GluR2 fusion protein but not to other antigens (*9*). The fourth individual with Rasmussen's encephalitis (GO) did not exhibit serum immunoreactivity to any tested antigen. Sera from 20 of 21 control individuals showed no immunoreactivity, and one control serum showed immunoreactivity to GluR3 (*10*) that was different from the serum GluR immunoreactivity exhibited by individuals with Rasmussen's encephalitis ($P = 0.006$; Fisher's exact test).

To obtain independent validation of GluR immunoreactivity in these sera, we examined immunoreactivity toward full-length GluR3 protein in its three-dimensional conformation. Human embryonic

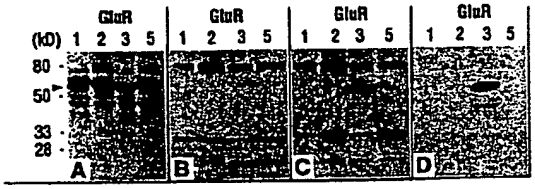

Fig. 2. Prominent serum reactivity toward GluR3-*trpE* fusion protein in an individual with active Rasmussen's encephalitis. Protein extracts enriched in fusion proteins were loaded on the designated lanes (GluR1, 2, 3, and 5) and visualized (*4*, *8*). The site at which GluR fusion proteins reside is denoted by the arrowhead in (**A**). (**A**) Serum immunoreactivity of a rabbit immunized with *trpE* protein devoid of GluR protein. Because each GluR fusion protein contains *trpE* protein, each GluR fusion protein exhibits immunoreactivity. The bands not marked by the arrowhead represent irrelevant immunoreactivity, principally to bacterial proteins or to fragments of GluR fusion protein. (**B**) No immunoreactivity to any GluR fusion protein is evident in serum from the individual (GO) without active disease. This blot was typical for sera of 20 of 21 controls. (**C**) Serum from individual AI shows immunoreactivity to GluR3, but not to any other GluR. (**D**) We first adsorbed serum from individual AI with lysate from *trpE*-expressing *E. coli* to remove immunoreactivity to bacterial antigens (*4*, *8*). The main GluR3 immunoreactivity is shown, with smaller faint bands presumably representing GluR3 fusion protein degradation products. Of the individuals tested, this serum exhibited the most prominent immunoreactivity to GluR3. Molecular size standards are shown at left (in kilodaltons).

Table 1. Summary of serum immunoreactivity to GluR in individuals with Rasmussen's encephalitis. Initials of all individuals were changed to protect their identity. Sz, seizures; GM Sz, generalized, tonic clonic seizures; R1, GluR1; and R6, GluR6 transiently expressed in transfected cells.

Diagnoses	Immunoreactivity	
	Immunoblot	In cells
	Rasmussen patients	
AI, progressive	GluR3	GluR3 (not R1 or R6)
CK, progressive	GluR3; weak GluR2	GluR3 (not R1 or R6)
EM, hemiparesis, Sz	Weak GluR2	GluR3 (not R1 or R6)
GO, stable, no Sz	None	None
	Age- and sex-matched epileptic controls	
Absence + GM Sz	None	None
Simple, partial Sz	None	None
Complex, partial Sz	None	None
Posttraumatic Sz	None	None
	Children with active CNS inflammation	
CNS lupus erythematosus	None	None
CNS lupus erythematosus	None	None
Multiple sclerosis	None	None
Varicella encephalitis	None	None
Tuberculous meningitis	None	None
	Age- and sex-matched normal controls	
Cardiac surgery	GluR3	None
Trauma	None	None
Trauma	None	None
Obesity	None	None
	Epileptic children	
Four children	None	None
	Normal children	
Four children	None	None

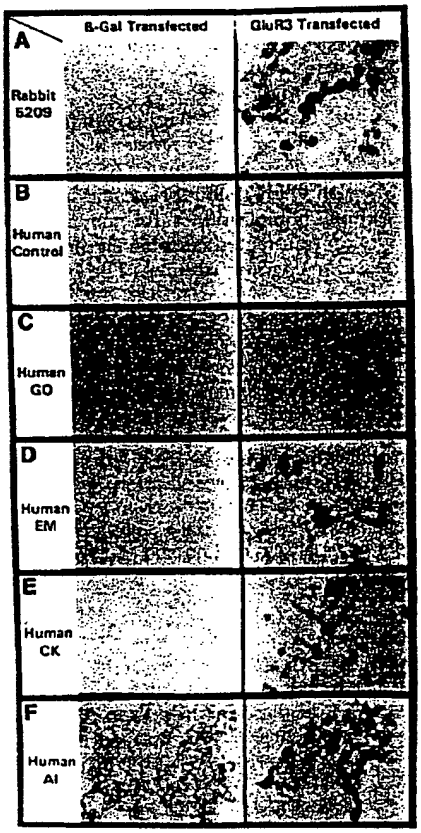

Fig. 3. Serum immunoreactivity toward transfected HEK 293 cells expressing either GluR3 or β-galactosidase (*11*). (**A**) Serum from one symptomatic, GluR3-immunized rabbit reacts with cells expressing GluR3. (**B**) Sera from control individuals exhibit no immunoreactivity. Immunoreactivity to transfected cells expressing GluR3 is present in sera of those individuals with active Rasmussen's encephalitis: EM (**D**), CK (**E**), and AI (**F**) but not in individual GO (**C**), who exhibits no active disease.

kidney (HEK) 293 cells were transiently transfected with expression plasmids containing the complementary DNA (cDNA) for GluR3 or β-galactosidase (*11*). Sera from the three individuals with Rasmussen's encephalitis that exhibited immunoreactivity to GluR3 or GluR2 on protein immunoblots also reacted with transfected cells expressing GluR3 (Fig. 3 and Table 1). Serum from the fourth individual with Rasmussen's encephalitis, which was negative by protein immunoblot analysis, did not react with transfected cells. None of the control sera reacted with transfected cells, including the single control serum that was positive on the protein immunoblot (*10*). The correlation between serum immunoreactivity to GluR3 and Rasmussen's encephalitis was significant ($P = 0.002$; Fisher's exact test). Sera from individuals with Rasmussen's encephalitis did not react with transfected cells expressing the closely related GluRs GluR1 or GluR6, demonstrating the specificity of the GluR3 immunoreactivity. All measurable immunoreactivity in these individuals was of the immunoglobulin G (IgG) class.

GluR immunoreactivity correlated with clinical findings of Rasmussen's encephalitis. The three individuals (AI, CK, and EM) with GluR immunoreactivity on protein immunoblot and GluR3 immunoreactivity on transfected cells have progressive disease or ongoing seizures. The only individual (GO) with Rasmussen's encephalitis without immunoreactivity to any GluR proteins by protein immunoblot or transfected cell analyses underwent hemispherectomy 2 years before data collection and has since remained clinically stable and seizure-free.

The correlation between GluR3 immunoreactivity and disease activity suggested that GluR3 antibodies could be pathogenic in Rasmussen's encephalitis. We therefore hypothesized that removal of GluR3 antibodies by recurrent plasma exchange (PEX) would be beneficial. CK, now 9 years old, was well until a minor, left forehead injury in 1990, following which she experienced increasingly frequent generalized and right body seizures with progressive cognitive decline, speech disability, right hemiparesis, and left cerebral atrophy. No remissions occurred. Pathologic examination of a left temporal cortex biopsy confirmed the diagnosis of Rasmussen's encephalitis. GluR3 immunoreactivity, monitored with an enzyme-linked immunosorbent assay (ELISA) (*4, 12*), was high. She was treated with recurrent, single-volume PEX and exhibited a beneficial response (Fig. 4). During the first 7 weeks of PEX, seizure frequency decreased by 80%. Cognition, speech, and hemiparesis improved, correlating in time with diminished GluR3 immunoreactivity. Over the ensuing 4 weeks, however, seizure frequency increased, and cognition, speech, and motor skills deteriorated in parallel with increased GluR3 immunoreactivity.

Molecular mimicry between self and foreign antigens expressed in microbes is one mechanism that has been proposed for the pathogenesis of autoimmune diseases (*13*). Structural similarities have been identified between the ligand-binding domains of multiple classes of GluRs and bacterial periplasmic amino acid–binding proteins (*14*). Infection with such microbes may induce an immune response that also targets GluRs.

The transient improvement after PEX in one seriously ill child suggests that circulating antibodies contribute to disease pathogenesis. The circulating autoantibodies would have to gain access to GluR3 in the brain, which is normally protected by the blood-brain-barrier (BBB). Focal disruption of the BBB can occur transiently with focal seizures (*15*) or as a consequence of head injury (*16*), an event that occasionally precedes Rasmussen's encephalitis (*2, 17*). After disruption of the BBB, we hypothesize that the ensuing immune-mediated neural injury could trigger focal seizures. Thus, a cycle could be set in motion whereby focal seizures disrupt the BBB and facilitate the local access of pathogenic antibodies to brain antigens; the subsequent immune response could cause more seizures; and a progressive disorder results. This cycle could also explain the localized cortical onset of disease and the gradual expansion throughout one hemisphere. The contralateral hemisphere would be spared because it would not be a source of focal seizures, and the BBB would be relatively preserved.

Our data establish a link between circulating antibodies to a ligand-gated ion channel receptor of the CNS and a progressive encephalopathy with epileptic seizures. A related process may be operative in other forms of epilepsy, because histopathology similar to that of Rasmussen's encephalitis has been identified in 5 to 10% of individuals undergoing temporal lobectomy for refractory epilepsy (*18*). Related processes may also contribute to other CNS disorders with inflammatory histopathology.

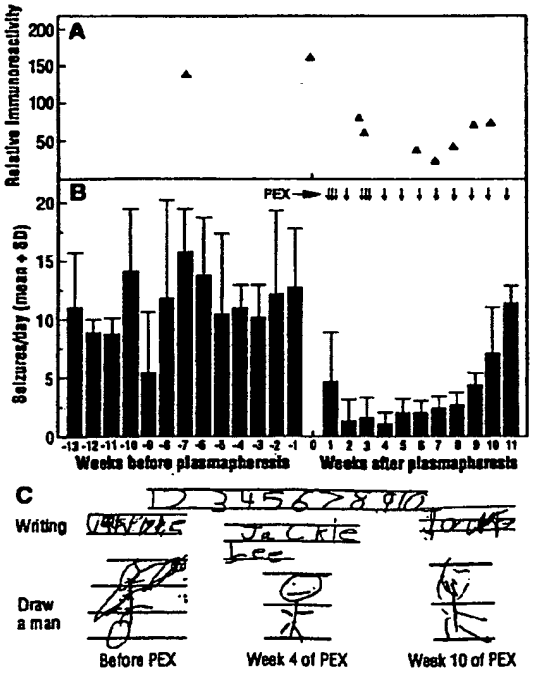

Fig. 4. Correlation of seizure frequency (**B**), neurologic function (**C**), and GluR3 immunoreactivity (**A**) in individual CK before and during 11 weeks of repeated PEX [indicated by arrows in (**B**)]. Before PEX, GluR3 antibody titer was high. She had 10 to 12 right body or generalized seizures daily, mild right hemiparesis, and no spontaneous speech. She was unable to read or solve simple math problems, and her writing and drawing were primitive. During the first 7 weeks of PEX, GluR3 antibody titer measured immediately before each PEX decreased, in temporal association with reduced seizure frequency. She spoke spontaneously in phrases and short sentences; her understanding, right hemiparesis, calculations, drawing, and writing improved. For the first time in 2 years, she resumed playing with dolls, riding a bicycle, and participating in household activities. During the last 4 weeks of PEX, GluR3 antibody titers gradually increased, seizure frequency increased, and cognitive skills declined. Numbers in (C) were written by the individual during week 4 of PEX. We omitted the individual's last name from her writing during week 4 of PEX to protect her identity. During PEX, other therapies were unchanged.

REFERENCES AND NOTES

1. T. Rasmussen, J. Olszewski, D. Lloyd-Smith, *Neurology* 8, 435 (1958); H. Oguni, F. Andermann, T. B. Rasmussen, in *Chronic Encephalitis and Epilepsy: Rasmussen's Syndrome*, F. Andermann, Ed. (Butterworth-Heinemann, Boston, 1991), pp. 7–36.
2. Y. Robitaille, in *Chronic Encephalitis and Epilepsy: Rasmussen's Syndrome*, F. Andermann, Ed. (Butterworth-Heinemann, Boston, 1991), pp. 79–110.
3. C. W. Cotman *et al.*, *Trends Neurosci.* 10, 273 (1987); C. Stevens, *Nature* 342, 620 (1989).

S. W. Rogers *et al.*, *J. Neurosci.* 11, 2713 (1991); *ibid.* 12, 4611 (1992).
J. Boulter *et al.*, *Science* 249, 1033 (1990); K. Keinanen *et al.*, *ibid.*, p. 556.
P. W. Berman *et al.*, *Ann. N.Y. Acad. Sci.* 377, 237 (1981).
G. W. Huntley *et al.*, *J. Neurosci.* 13, 2965 (1993).
Sera were numbered and frozen. GluR and β4-nAChR *trpE* fusion protein constructs were produced and analyzed as described (*4*, *7*), except we used 2% dry milk (Blotto) to block blots. Blots were incubated overnight at 4°C in primary serum diluted 1:1000 in Blotto, then in goat antibody to human IgG conjugated to alkaline phosphatase diluted at 1:750 in Blotto for 1 hour at 25°C, and then developed (*4*). We removed *Escherichia coli* background by incubating a suspension of lysed, *trpE*-expressing bacteria in the serum sample for 2 hours at 25°C and then centrifuging it. In another examination, each protein immunoblot was photographed, coded, and interpreted blindly by three investigators; interpretations were congruent in 73 of 76 samples (*9*).
S. W. Rogers *et al.*, unpublished data.
The single control individual whose serum exhibited immunoreactivity to GluR3 fusion protein by protein immunoblot analysis was sampled 1 week after open heart surgery. Cardiac bypass under hypothermic anesthesia may be a nonspecific activator of the immune system [J. R. Utley, *J. Cardiac Surg.* 5, 177 (1990)]. Her serum was not immunoreactive with GluR3 expressed in transfected cells, suggesting that the immunoreactivity detected by protein immunoblot analysis may not be to native GluR3.
HEK 293 cells were transfected with expression plasmids containing the cDNA for either GluR1, 3, or 6 or the bacterial protein β-galactosidase (*4*, *7*). The serum from individual AT exhibited nuclear immunoreactivity that we removed by adsorbing the serum samples with HEK 293 cells transfected with the parent expression plasmid without an insert (*4*). Sera were coded and tested in two laboratories independently (T.E.H. and S.W.R.). Sera from immunized rabbits served as the positive controls.
ELISA assays used either GluR3 or β4-nAChR fusion proteins that were solubilized and adsorbed to microtiter plates (Immulon) (*4*, *7*). Wells were blocked with Blotto for 2 hours at 25°C before we added sera at various dilutions for 1 hour at 25°C. We observed immunoreactivity using goat antibody to human IgG, conjugated with peroxidase, and 2,2′-azino-di-(3-ethylbenzthiazoline-6-sulfonic acid) (1 mg/ml) in McIlvain's buffer (pH 4.6) and 0.0005% hydrogen peroxide. Duplicate samples were scanned at 405 nM with an ELISA reader (Teritek). We determined GluR3-specific immunoreactivity by subtracting β4-nAChR reactivity from GluR3 reactivity.
R. T. Damian, *Am. Nat.* 98, 129 (1964); M. B. A. Oldstone, *Cell* 50, 819 (1987).
P. J. O'Hara *et al.*, *Neuron* 11, 41 (1993).
A. V. Lorenzo *et al.*, *Am. J. Physiol.* 223, 268 (1972); C. Nitsch and H. Hubauer, *Neurosci. Lett.* 64, 53 (1986).
J. C. Lee, in *Histology and Histopathology of the Nervous System*, W. Haymaker and R. D. Adams, Eds. (Thomas, Springfield, IL, 1982), pp. 798–870.
J. Peyser, J. Trevino, T. Resnick, *Int. Pediatr.* 7, 272 (1992).
K. D. Laxer, in *Chronic Encephalitis and Epilepsy: Rasmussen's Syndrome*, F. Andermann, Ed. (Butterworth-Heinemann, Boston, 1991), pp. 135–140.
We thank D. V. Lewis and G. R. DeLong for access to their patients and I. Verma for use of his cell culture laboratory. Supported by the National Institute of Neurological Disease and Stroke NS30990R29 (to S.W.R.), NS28709 (to S.F.H.), NS17771 and NS24448 (to J.O.M.), Research to Prevent Blindness and the National Eye Institute EY08362 (to T.E.H.), and the NIH General Clinical Research Centers Program to Duke University (MO1-RR-30).

28 December 1993; accepted 7 June 1994

Variable Gearing During Locomotion in the Human Musculoskeletal System

David R. Carrier,* Norman C. Heglund, Kathleen D. Earls

Human feet and toes provide a mechanism for changing the gear ratio of the ankle extensor muscles during a running step. A variable gear ratio could enhance muscle performance during constant-speed running by applying a more effective prestretch during landing, while maintaining the muscles near the high-efficiency or high-power portion of the force-velocity curve during takeoff. Furthermore, during acceleration, variable gearing may allow muscle contractil properties to remain optimized despite rapid changes in running speed. Force-plate and kinematic analyses of running steps show low gear ratios at touchdown that increas throughout the contact phase.

Toes were present in the earliest tetrapods (*1*) and occur in all modern tetrapods except those that are highly specialized for limbless or aquatic locomotion. Feet and toes form an adaptable interface between the animal and its environment. They provide traction and a means for grasping the substrate, function as various tools and weapons (*2*), and help to maintain balance (*3*). In this report, we suggest that feet and toes improve locomotor performance by varying the gear ratio (that is, the velocity ratio) between the ankle extensor muscles and the point of application of the force on the ground (the center of force) during the course of the contact phase of a running step.

The proposed mechanism is easily visualized during running at a steady speed (Fig. 1). The foot is analyzed as a simple Type 1 lever of zero mass with the fulcrum at the ankle by means of the equation $R \times F_r = r \times F_m$, where R is the ground force moment arm, F_r is the ground reaction force, r is the muscle force moment arm, and F_m is the muscle force. During the contact period of a step, the point at which force is applied to the ground (the center of force) moves from under the heel or middle portion of the foot at touchdown to the tips of the toes at takeoff. This forward translation could increase the length of the moment arm between the ankle and the force exerted on the ground (R) and, therefore, increase the gear ratio (R/r) of the ankle extensor muscles and tendons.

Variable gearing would be advantageous in running, as it is in the automobile, because in both cases the motors (cross-bridges in muscle and pistons in engines) have a limited speed range over which they operate at peak power or efficiency (*4*). In order to maintain a narrow range of optimal engine speeds despite varying drive speeds, the ratio of engine speed to drive speed must be changed by a variable gear ratio. Furthermore, muscles have unique properties that can benefit from variable gearing within the contact phase of a running step. Active muscles that are forcibly stretched just before shortening are able to do more work during the shortening. This nonelastic enhancement of the contractile properties of the muscle increases, within limits, with increasing stretch length (*5*) but is effective over relatively small shortening distances. If a runner were to land at a low gear ratio and take off at a higher gear ratio, both the prestretch and the subsequent shortening of the muscles could be optimized. Thus, variable gearing could reduce the need for locomotor specialization, allowing individuals to move about more efficiently, accelerate more quickly, run faster, and jump higher.

To test this hypothesis, five people (3 males and 2 females) ran over a Kistler 9281B force plate. Four of these people also accelerated maximally over the force plate, starting just off the plate so that the first step landed on the plate. A lateral view of limb position was recorded with a Peak high-speed video camera at 120 images per second (Fig. 1). Recordings of forces on the ground allowed calculation of the magnitude and orientation of the ground reaction force and the position of the center of force under the foot. For each video image taken during foot support (at 8.33-ms intervals), the ground force moment arm (R) was calculated by dividing the moment at the ankle by the resultant of the horizontal and vertical ground forces. Similarly, the mus-

D. R. Carrier and K. D. Earls, Department of Ecology and Evolutionary Biology, Brown University, Providence, RI 02912, USA.
N. C. Heglund, Pharos Systems, Inc., South Chelmsford, MA 01824, USA.
*To whom correspondence should be addressed.